

MODELING FIRE-INDUCED INSTABILITIES FOR TRACING PROGRESSIVE  
COLLAPSE IN STEEL FRAMED BUILDINGS

By

Svetha Venkatachari

A DISSERTATION

Submitted to  
Michigan State University  
in partial fulfillment of the requirements  
for the degree of

Civil Engineering – Doctor of Philosophy

2022

## **ABSTRACT**

### **MODELING FIRE-INDUCED INSTABILITIES FOR TRACING PROGRESSIVE COLLAPSE IN STEEL FRAMED BUILDINGS**

By

Svetha Venkatachari

Fire is one of the extreme loading events that a building may experience during its service life and can induce severe consequences on the safety of its occupants, first responders, and the structure. Recent fire incidents have clearly shown that steel framed buildings are vulnerable to progressive collapse under severe fire conditions, if not duly considered in the design. The progressive collapse in steel framed buildings initiates with the onset of temperature-induced instabilities at a local or global level, which in turn can lead to the partial or complete collapse of the structure. Despite fire being a severe hazard, the current practice does not have specific recommendations or guidance to evaluate the fire-induced progressive collapse in critical buildings. This is unlike other loading events such as blasts, earthquakes, etc. Further, the current fire design philosophy of steel structures is primarily based on a member (or section) level behavior and does not account for several critical factors, including some of the temperature-induced instabilities.

To overcome some of the knowledge gaps, a series of advanced simulations are carried out for tracing the fire-induced collapse in steel framed buildings. To establish the connection between evacuation strategies (times) and structural stability under fire, a set of evacuation simulations is undertaken to evaluate the effect of varying egress parameters on the emergency evacuation process in a high-rise building. In addition, the influence of incorporating situational awareness during an emergency evacuation is quantified. These evacuation strategies and times are to be considered, together with the fire-induced progressive collapse timelines, for achieving the required fire safety in critical buildings.

Furthermore, for facilitating complete evacuation and efficient firefighting operations, stability of the structure is to be maintained and any chance of fire-induced collapse is to be minimized. Evaluating progressive collapse under fire conditions is highly complex and requires advanced analysis. For this purpose, a comprehensive finite element-based model is developed in ABAQUS to trace the overall response of a steel framed building under fire exposure, including the onset of instabilities leading to the progressive collapse. The developed model specifically accounts for high-temperature material properties and creep effects, geometric nonlinearity, altering load paths, connections, fire spread, local buckling effects, and realistic failure limit states. The model is validated by comparing the thermal and structural response predictions against the published test data at the member level (steel columns) and system level (steel framed structures).

The validated model is applied to carry out a set of parametric studies on a ten-story braced framed building to quantify the influence of various fire, material, and structural parameters on the onset of fire-induced collapse in steel framed buildings. Results from the parametric studies indicate that the severity of the fire scenario, including the location and extent of burning, fire spread, varying load paths, and temperature-induced local instabilities have a significant influence on the onset of fire-induced progressive collapse. Moreover, accounting for the full effects of high-temperature creep in the fire-induced progressive collapse analysis is needed to obtain realistic failure times under severe to very intense fire exposure. Results from the parametric studies are used to propose guidelines for mitigating fire-induced collapse in critical buildings. Specific recommendations are provided for the treatment of high-temperature creep and local instabilities in the fire resistance analysis of steel structures. The proposed approach for advanced analysis, together with the design recommendations, can be utilized to minimize the onset of fire-induced collapse in critical steel framed buildings.

*To my family.*

## ACKNOWLEDGEMENTS

I would like to extend my sincere gratitude to my Ph.D. advisor, Dr. Venkatesh Kodur for his invaluable guidance and continuous support in undertaking this research work. His constructive suggestions and advice through all stages of my Ph.D. program have made this research experience truly transformative and I thank him deeply for giving me this opportunity. I would like to express my sincere thanks to the members of my committee Dr. Nizar Lajnef, Dr. Roozbeh Dargazany, and Dr. Yiming Deng for their insightful suggestions, support, and guidance.

I would like to thank my peers and friends in the CEE department, particularly Srishti Banerji, Roya Solhmirzaei, Ankit Agarwal, Puneet Kumar, Pratik Bhatt, Saleh Mohammad Alogla, and Augusto Masiero Gil for their support through the course of my research. Special thanks to Dr. Mohannad Naser for his support and encouragement in my initial Ph.D. years. My warmest thanks to all my friends, including Ashwini Tapase, Natasha Elza Simon, Vijayalaxmi Huddar, and Rajendra P. Palanisamy for making my Ph.D. journey memorable.

I am grateful for the support and funding from the CEE department throughout my graduate studies. I also wish to acknowledge the funding from Partnership 2020: U.S.-India Higher Education Cooperation. I would like to thank Laura Post, Bailey Weber, and Shelly Harbenski for their administrative support. In addition, I would like to thank Mr. Siavosh Ravanbakhsh, the former manager of the Civil Infrastructure Laboratory for his support during lab work.

I would like to thank my husband, Srinivasan, for his unwavering support, patience, love, and understanding during my time in the US. In addition, I would like to express my deepest gratitude to my parents for their immense support and motivation. Finally, warm thanks to my sister, Sowmya, for her endless encouragement and support.

## TABLE OF CONTENTS

LIST OF TABLES .....	x
LIST OF FIGURES .....	xii
KEY TO SYMBOLS .....	xviii
CHAPTER 1 .....	1
1 Introduction.....	1
1.1 Background .....	1
1.2 Need for structural fire safety in buildings .....	3
1.3 Fire-induced progressive collapse phenomenon in steel framed buildings .....	7
1.4 Factors influencing fire-induced instability in steel framed structures.....	10
1.4.1 General.....	10
1.4.2 Critical factors influencing fire-induced instability.....	11
1.4.2.1 Fire severity .....	11
1.4.2.2 Fire spread.....	12
1.4.2.3 Load paths (and restraints).....	12
1.4.2.4 High-temperature creep .....	13
1.4.2.5 Local instabilities.....	13
1.4.2.6 Loss of fire insulation .....	14
1.4.3 Approach to fire resistance assessment of steel framed structures.....	14
1.5 Research approach .....	15
1.5.1 Hypothesis .....	15
1.5.2 Key objectives.....	16
1.5.3 Methodology.....	17
1.6 Layout of thesis.....	18
CHAPTER 2 .....	20
2 State-of-the-art Review .....	20
2.1 General.....	20
2.2 Recent fire-induced collapses in steel framed buildings.....	21
2.3 Evacuation models for high-rise buildings .....	27
2.4 Experimental studies on steel framed structures exposed to fire .....	29
2.5 Numerical studies on steel framed structures exposed to fire.....	34
2.6 High-temperature properties of steel.....	40
2.6.1 Thermal and mechanical properties at elevated temperature.....	41
2.6.2 High-temperature creep effects on steel structures.....	42
2.6.2.1 Creep at the material level .....	43
2.6.2.2 Creep at the structural level .....	46
2.7 Properties of fire insulation.....	49
2.8 Local instability effects on fire performance of steel structures.....	50
2.9 Fire resistance provisions in standards and codes.....	55
2.10 Knowledge gaps.....	57



5.3	Parametric studies on the effect of fire scenarios on fire-induced instability .....	138
5.3.1	Selection of steel framed building for analysis.....	138
5.3.2	Varied parameters and range .....	139
5.3.3	Analysis details.....	142
5.3.4	Results and discussion .....	143
5.3.4.1	Effect of fire intensity .....	143
5.3.4.2	Effect of varying extents of burning on a single floor.....	146
5.3.4.3	Effect of varying extents of burning on multiple floors .....	148
5.3.4.4	Effect of fire spread .....	150
5.4	Parametric studies on the effect of high-temperature creep on fire-induced instability ..	154
5.4.1	Effect of high-temperature creep on member instability .....	154
5.4.1.1	Selection of steel columns for analysis.....	154
5.4.1.2	Varied parameters and range .....	155
5.4.1.3	Analysis details.....	156
5.4.1.4	Results and discussion .....	157
5.4.1.4.1	Effect of creep under varying load (stress) levels .....	157
5.4.1.4.2	Effect of creep under varying thermal gradients .....	158
5.4.1.4.3	Effect of creep under varying slenderness.....	159
5.4.1.4.4	Effect of creep under varying fire severity .....	160
5.4.2	Effect of high-temperature creep on structural instability .....	162
5.4.2.1	Selection of steel frame for analysis.....	162
5.4.2.2	Varied parameters and range .....	163
5.4.2.3	Analysis details.....	164
5.4.2.4	Results and discussion .....	165
5.4.2.4.1	Effect of creep under varying fire locations within a story .....	166
5.4.2.4.2	Effect of creep under varying locations of the fire floor .....	174
5.4.2.4.3	Effect of creep under varying extents of burning on a single floor .....	176
5.4.2.4.4	Effect of creep under varying extents of burning on multiple floors.....	179
5.4.2.4.5	Effect of creep under varying fire severity .....	180
5.5	Parametric studies on the effect of structural parameters on fire-induced instability.....	183
5.5.1	Varied parameters and range .....	184
5.5.2	Analysis details.....	185
5.5.3	Results and discussion .....	186
5.5.3.1	Effect of altering load paths due to variation in structural configuration.....	186
5.5.3.2	Effect of altering load paths due to variation in fire (burning) location ..	188
5.5.3.3	Effect of local instability.....	192
5.5.3.4	Effect of analysis regime .....	195
5.6	Summary .....	198
CHAPTER 6 .....		200
6 Design Guidelines.....		200
6.1 General.....		200
6.2 Critical factors for tracing fire-induced progressive collapse in steel framed buildings .		201

6.2.1	Fire scenarios .....	201
6.2.2	Material models .....	202
6.2.3	High-temperature creep effects.....	203
6.2.4	Altering load paths and load redistribution.....	204
6.2.5	Connections .....	205
6.2.6	Local buckling effects.....	206
6.3	Current provisions for evaluating progressive collapse in buildings.....	207
6.3.1	Emerging trends – Fire resistance and resiliency of steel framed structures under fire.....	207
6.3.2	Fire design provisions for steel framed structures.....	208
6.4	Recommendations for evaluating the fire-induced progressive collapse in buildings.....	209
6.4.1	Guidance for the treatment of creep in fire resistance analysis .....	210
6.4.1.1	Scenarios where high-temperature creep effects are not critical .....	211
6.4.1.2	Scenarios where implicit creep is sufficient .....	212
6.4.1.3	Scenarios where high-temperature creep is to be considered explicitly..	213
6.4.2	Guidance for identifying critical scenarios for fire-induced collapse.....	220
6.4.3	Strategies to minimize the onset of fire-induced collapse .....	223
6.4.4	Guidance for undertaking advanced analysis for tracing fire-induced progressive collapse.....	225
6.5	Limitations .....	228
6.6	Summary .....	229
CHAPTER 7 .....		231
7	Conclusions.....	231
7.1	General.....	231
7.2	Key findings.....	233
7.3	Research impact.....	235
7.4	Recommendations for future research .....	236
APPENDICES .....		238
APPENDIX A Computation of Evacuation Time using the Hydraulic Model .....		239
APPENDIX B Material Properties at Elevated Temperatures.....		242
APPENDIX C Illustration of Fire-Induced Progressive Collapse in a Steel Framed Building using Advanced Analysis – Numerical Example.....		247
REFERENCES .....		252

## LIST OF TABLES

Table 2-1: Reported numerical studies on 2D steel frames .....	36
Table 2-2: Reported numerical studies on 3D steel framed buildings.....	40
Table 2-3: Reported high-temperature creep tests on different grades of steel .....	45
Table 2-4: Reported numerical studies that explicitly incorporate creep in fire resistance analysis.....	47
Table 2-5: Reported numerical studies that incorporate local buckling effects in fire resistance analysis.....	52
Table 3-1: Evacuation time for different cases considered in the parametric study.....	71
Table 4-1: Parameters for creep model.....	102
Table 5-1: Critical parameters investigated to study the effect of fire scenarios on fire-induced instability.....	141
Table 5-2: Summary of varied parameters and results from the parametric study on the effect of fire scenarios.....	153
Table 5-3: Critical parameters investigated to study the effect of transient creep in steel columns.....	156
Table 5-4: Summary of varied parameters and results from the parametric study on transient creep effects in steel columns .....	161
Table 5-5: Critical parameters considered to investigate the transient creep effects at a system level.....	164
Table 5-6: Summary of transient creep effects in the braced frame building for different scenarios considered .....	182
Table 5-7: Critical parameters investigated to study the effect of structural parameters on fire-induced instability .....	185
Table 5-8: Summary of varied parameters and results from the parametric study on the effect of structural parameters.....	197
Table 6-1: Extent of creep in steel members based on temperature and stress level.....	214

Table 6-2: Time at which creep deformations become dominant in steel columns exposed to different fire exposure scenarios .....	215
Table 6-3: Creep critical temperatures for A992 steel at different stress levels .....	216
Table 6-4: Extent of creep in steel framed buildings based on fire severity and extent of burning on a single floor .....	217
Table 6-5: Extent of creep in steel framed buildings based on fire severity and extent of burning on multiple floors .....	217
Table 6-6: Treatment of high-temperature creep in fire resistance analysis of steel structures .	219
Table B-1: Values of main parameters used in the stress-strain relations of concrete .....	243
Table B-2: Values of main parameters used in the stress-strain relations of steel .....	246

## LIST OF FIGURES

Figure 1.1. Fire development process in a typical compartment. ....	4
Figure 1.2. Progression of fire in a high-rise building. ....	5
Figure 1.3. Schematic representation of fire response mechanism of a typical steel framed building. (a) Thermal expansion and material degradation. (b) Load redistribution following column loss. ....	8
Figure 1.4. Steel frame exposed to fire. ....	9
Figure 1.5. Deformed shape of (a) steel frame at 205 min and (b) column AB at 180 min. (c) Axial deformation of column AB. ....	10
Figure 2.1. Fire test locations for the Cardington test program [63]. ....	31
Figure 2.2. Degradation of strength and stiffness properties of steel at elevated temperatures. ..	52
Figure 3.1. Typical floor layout with the distribution of occupants. ....	66
Figure 3.2. Side view of the 32-story high-rise building. ....	66
Figure 3.3. Floor layout with dimensions of different egress components. ....	68
Figure 3.4. Comparison of evacuation time predicted using Pathfinder and hydraulic model. ....	70
Figure 3.5. Evacuation time with different story heights. ....	74
Figure 3.6. Evacuation time for different locations of stairways. ....	76
Figure 3.7. Evacuation time with a varying number of stairways. ....	78
Figure 3.8. Evacuation time for different widths of stairways. ....	80
Figure 3.9. Evacuation time with different fire locations. ....	81
Figure 3.10. Evacuation simulation with a uniform number of stairways and situational awareness (SA). ....	82
Figure 3.11. Evacuation simulation with a non-uniform number of stairways and situational awareness (SA). ....	84
Figure 4.1. Various levels of analysis of a steel framed structure. ....	90

Figure 4.2. Flowchart illustrating the steps in the fire-induced progressive collapse analysis using the nonlinear quasi-static analysis approach. ....	94
Figure 4.3. Flowchart illustrating steps in the fire-induced progressive collapse analysis using the nonlinear dynamic explicit analysis approach. ....	96
Figure 4.4. Standard and design fire exposure scenarios in a building.....	97
Figure 4.5. (a) Fire spread in a single story and (b) variation of fire temperatures in the compartments with time.....	98
Figure 4.6. Specific node points for temperature output for (a) W section and (b) HSS section [123].....	103
Figure 4.7. Linking of beam and shell elements in ABAQUS. ....	106
Figure 4.8. Dimensions (in mm) and fire exposure region of tested steel column [52]. ....	111
Figure 4.9. Comparison of measured and predicted sectional temperatures in the steel column.....	113
Figure 4.10. Comparison of measured and predicted (a) axial deformation and (b) axial force in the steel column. ....	114
Figure 4.11. Elevation details, loading, and fire exposure regions of test frame (dimensions in mm) [71]. ....	116
Figure 4.12. Measured and predicted sectional temperatures in (a) beam 1 and (b) column 2 on floor 1.....	117
Figure 4.13. Deflected profile of the frame at (a) 30 min and (b) 60 min of fire exposure time. ....	119
Figure 4.14. Variation of measured and predicted lateral displacement of the frame with fire exposure time. ....	120
Figure 4.15. Variation of measured and predicted deflection of beams with fire exposed time. ....	120
Figure 4.16. (a) Axial deformation and (b) axial force in fire-exposed columns in the floor. ...	122
Figure 4.17. Evolution of total strain and creep strain in column 2.....	124
Figure 4.18. Details of the floor plan at level 2 and compartment used for the fire test. ....	125
Figure 4.19. Gas temperature as measured in the corner fire test compartment.....	126

Figure 4.20. Discretization of the FE model and boundary conditions. ....	127
Figure 4.21. (a) Thermal gradients in the cross-section at 90 min. (b) Comparison of measured and predicted sectional temperatures for slab S1. ....	128
Figure 4.22. (a) Thermal gradients in the cross-section at 90 min. (b) Comparison of measured and predicted sectional temperatures for beam B1 (UB 356x171x51). ....	128
Figure 4.23. (a) Thermal gradients in the cross-section at 90 min. (b) Comparison of measured and predicted sectional temperatures for beam B2 (UB 305x165x40). ....	129
Figure 4.24. Deformed configuration of level 2 of the test building at a fire exposure time of 150 min. ....	131
Figure 4.25. Comparison of measured and predicted deflections for (a) slab S1, (b) beam B3, (c) beam B2, and (d) column C1.....	132
Figure 5.1. Details of steel framed building. (a) Elevation (b) Plan. ....	139
Figure 5.2. Standard and design fire exposure scenarios.....	141
Figure 5.3. (a) Horizontal fire spread in a single story and (b) variation of fire temperatures in the compartments with time.....	142
Figure 5.4. Temperature at mid-depth of web under different fire exposure scenarios for (a) interior column W14x145 (E5) and (b) interior beam W21x50 (E-5-6) on floor 1.....	144
Figure 5.5. (a) Lateral displacement at the top story of the building with fire exposure time under varying fire exposure scenarios. (b) Deformed shape of the steel structure under ASTM E119 fire exposure. ....	145
Figure 5.6. Lateral displacement at the top story of the building with fire exposure time under varying extents of burning in one story. ....	147
Figure 5.7. Axial forces in columns in the fire-affected and adjacent compartments for the scenario with single compartment burning. ....	147
Figure 5.8. Deformed shape of the steel framed building with burning in (a) one compartment and (b) ten compartments in one story.....	148
Figure 5.9. (a) Lateral displacement at the top story of the building with fire exposure time under varying extents of burning on multiple floors. (b) Deformed shape of the steel framed building under fire scenario with burning in three stories (two compartments per floor). ....	149

Figure 5.10. Lateral displacement at the top story of the building with fire exposure time under varying fire spread scenarios. ....	150
Figure 5.11. Axial forces in columns in the fire-affected and adjacent compartments for the scenario with horizontal fire spread with DF-120 fire exposure. ....	151
Figure 5.12. Deformed configuration of building at the onset of collapse under (a) horizontal fire spread with DF-120 fire exposure and (b) vertical fire spread with DF-120 fire exposure. ....	152
Figure 5.13. Axial forces in columns in the fire-affected and adjacent compartments for the scenario with horizontal fire spread with DF-60 fire exposure. ....	152
Figure 5.14. (a) Axial deformation response of steel columns under varying load levels. (b) Deflected profile of steel column under 40% LL at a fire exposure time of 155 min. ....	158
Figure 5.15. Axial deformation response of steel columns under varying thermal gradients. ...	159
Figure 5.16. Axial deformation response of steel columns with varying slenderness ratios.....	160
Figure 5.17. Axial deformation response of steel columns under varying fire severity. ....	161
Figure 5.18. Different fire exposure scenarios considered in the study.....	164
Figure 5.19. Sectional temperatures in (a) beam W21x50 (A-4-5) and (b) column W14x193 (A4) on floor 2. ....	167
Figure 5.20. (a) Axial deformation, (b) axial force, and (c) evolution of total strain and creep strain in column A4 on floor 2.....	168
Figure 5.21. Axial force profile of frame indicating the utilization ratio (%) of beams and columns at (a) room temperature following the application of initial loads and (b) 155 min of fire exposure using analysis “with creep”. ....	169
Figure 5.22. (a) Axial deformation and (b) axial force in columns A3 and A5 on floor 2.....	170
Figure 5.23. Lateral displacement at different floor levels for the scenario with fire in <i>Floor 2 – A &amp; 3-5</i> .....	171
Figure 5.24. Mid-span deflection of beams in the fire affected compartments for the scenario with fire in <i>Floor 2 – A &amp; 3-5</i> .....	172
Figure 5.25. (a) Axial deformation and (b) axial force in fire-exposed columns for the scenario with fire in <i>Floor 2 – A &amp; 4-6</i> . ....	173

Figure 5.26. Lateral displacement at different floor levels for the scenario with fire in <i>Floor 2 – A &amp; 4-6</i> .....	174
Figure 5.27. Deflected profile of the frame at a fire exposure time of (a) 190 min for the scenario with fire in <i>Floor 2 – A &amp; 3-5</i> and (b) 180 min scenario with fire in <i>Floor 2 – A &amp; 4-6</i> .....	174
Figure 5.28. Lateral displacement at the top left corner of the frame for scenarios with varying locations of the fire floor. ....	175
Figure 5.29. Deflected profile of the frame at a fire exposure time of (a) 190 min for the scenario with fire in <i>Floor 5 – A &amp; 3-5</i> and (b) 195 min scenario with fire in <i>Floor 9 – A &amp; 3-5</i> .....	176
Figure 5.30. Lateral displacement at the top left corner of the frame for scenarios with varying (a) number of fire-exposed compartments and (b) number of fire-exposed floors. ....	178
Figure 5.31. Deflected profile of the frame at a fire exposure time of (a) 240 min for the scenario with fire in <i>Floor 2 – A &amp; 4-5</i> and (b) 155 min scenario with fire in <i>Floor 2 – A &amp; 2-5</i> .....	178
Figure 5.32. Deflected profile of the frame at a fire exposure time of (a) 170 min for the scenario with fire in Floors 2 & 3 – A & 3-5 and (b) 155 min scenario with fire in Floors 2, 3 & 4 – A & 3-5. ....	180
Figure 5.33. Lateral displacement at the top left corner of the frame for different fire exposure scenarios. ....	182
Figure 5.34. Lateral displacement at the top story of the building with fire exposure time for varying structural configurations. ....	187
Figure 5.35. Deformed shape of (a) 2D building frame and (b) 3D building with a fire on floor 2.....	188
Figure 5.36. Axial forces in columns in the fire-affected and adjacent compartments for scenarios with burning in corner and interior compartments on floor 1.....	189
Figure 5.37. Axial forces in columns in the fire affected and adjacent compartments for scenarios with burning on floors 6 and 9.....	190
Figure 5.38. Lateral displacement at different floor levels for scenarios with burning in different stories. ....	191
Figure 5.39. Deformed configuration of steel structure for scenarios with burning in different stories at the onset of failure (global). ....	192

Figure 5.40. Flange and web slenderness limits for columns. ....	193
Figure 5.41. (a) Lateral displacement at the top floor level of the frame and (b) axial deformation of column A4 with fire exposure time.....	195
Figure 5.42. Deformed shape of the steel frame with (a) W14x53 lateral columns and (b) W14x74 lateral columns in the ninth story. ....	195
Figure 5.43. Lateral displacement at the top floor level of the frame under different analysis regimes.....	196
Figure 6.1. Definition for yield limit and proportionality limit in EC3 and ASCE.....	203
Figure 6.2. Average sectional temperatures in a steel column (W14x53) under different fire exposure scenarios. ....	214
Figure 6.3. Fire exposure scenarios for different fire load densities. ....	222
Figure C.1. (a) Fire spread pattern and (b) design fire exposure scenario.....	247
Figure C.2. Time-temperature curves for the design fire exposure scenario with horizontal spread used in the analysis.....	248
Figure C.3. Fire exposure conditions for (a) an interior column (E5) and (b) an interior beam (E-5-6).....	249
Figure C.4. Sectional temperatures in the interior column E5 as a function of fire exposure time. ....	249
Figure C.5. Sectional temperatures in the interior beam E-5-6 as a function of fire exposure time. ....	249
Figure C.6. Deformed shape of the building at different fire exposure times. ....	251
Figure C.7. Lateral displacement at the top story of the building as a function of fire exposure time.....	251

## KEY TO SYMBOLS

- D = Population density per unit area
- $W_{e(x)}$  = Effective width of egress component 'x' (x: corridor, door, or stairs)
- k = Constant for computing speed of occupants
- a = Constant for computing speed of occupants
- S = Speed of occupants
- $F_{s(x)}$  = Specific flow of occupants for an egress component 'x' (x: corridor, door, or stairs)
- $F_{sm(x)}$  = Maximum specific flow for an egress component 'x' (x: corridor, door, or stairs)
- $F_{c(x)}$  = Calculated flow of occupants for an egress component 'x' (x: corridor, door, or stairs)
- $t_p$  = Time required by occupants to pass a point in an egress route
- $P_o$  = Population in a building
- $L_s$  = Length of stairways on each floor
- $\Delta\bar{\epsilon}$  = Total strain increment in steel
- $\Delta\bar{\epsilon}^{el}$  = Elastic strain increment in steel
- $\Delta\bar{\epsilon}^{pl}$  = Plastic strain increment in steel
- $\Delta\bar{\epsilon}^{th}$  = Thermal strain increment in steel
- $\Delta\bar{\epsilon}^{cr}$  = Creep strain increment in steel
- $\dot{\bar{\epsilon}}^{cr}$  = Creep strain rate in steel
- $\tilde{q}$  = Stress in steel
- $\bar{\epsilon}^{cr}$  = Creep strain in steel
- A = Temperature-dependent material parameter for computing the creep strain in steel
- n = Temperature-dependent material parameter for computing the creep strain in steel
- m = Temperature-dependent material parameter for computing the creep strain in steel

$t$  = Time

$T$  = Temperature

$h$  = Height of the steel column

$d_w$  = Depth of web in a W-section

$b_f$  = Width of flange in a W-section

$L$  = Length of beam (or slab)

$d$  = Effective depth of beam (or slab)

$H$  = Height of the building

$k_s$  = Stiffness of axial spring

$k_\theta$  = Stiffness of rotational spring

$P$  = Load applied on a member

$q$  = Load applied on a member

$U_x$  = Translation in x-direction

$U_y$  = Translation in y-direction

$U_z$  = Translation in z-direction

$UR_x$  = Rotation x-direction

$UR_y$  = Rotation y-direction

$UR_z$  = Rotation z-direction

$T_{\text{peak}}$  = Peak fire temperature

$f_{sy}$  = Yield strength of steel at room temperature

$E_s$  = Young's modulus of steel at room temperature

$\theta$  = Temperature in concrete

$c_p$  = Specific heat of concrete

$\lambda_c$  = Thermal conductivity of concrete  
 $\varepsilon_{c,th}$  = Thermal strain in concrete  
 $\sigma_c$  = Stress in concrete  
 $\varepsilon_c$  = Strain in concrete  
 $f_{c,\theta}$  = Compressive strength of concrete at temperature ' $\theta$ '  
 $\varepsilon_{c1,\theta}$  = Strain in concrete corresponding to  $f_{c,\theta}$   
 $\varepsilon_{cu1,\theta}$  = Ultimate strain in concrete at temperature ' $\theta$ '  
 $f_{ck}$  = Characteristic compressive strength of concrete at room temperature  
 $\theta_a$  = Temperature in steel  
 $c_a$  = Specific heat  
 $c_a$  = Specific heat of steel  
 $\lambda_a$  = Thermal conductivity of steel  
 $\Delta l/l$  = Relative thermal elongation  
 $\sigma_s$  = Stress in steel  
 $\varepsilon_s$  = Strain in steel  
 $E_{s,\theta_a}$  = Young's modulus of steel at temperature ' $\theta_a$ '  
 $f_{sp,\theta_a}$  = Proportional limit of steel at temperature ' $\theta_a$ '  
 $f_{sy,\theta_a}$  = Yield strength of steel at temperature ' $\theta_a$ '  
 $f_{su,\theta_a}$  = Ultimate strength of steel at temperature ' $\theta_a$ '  
 $\varepsilon_{sp,\theta_a}$  = Strain in steel corresponding to  $f_{sp,\theta_a}$   
 $\varepsilon_{sy,\theta_a}$  = Yield strain of steel  
 $\varepsilon_{st,\theta_a}$  = Strain in steel at the end of the plastic zone

$\varepsilon_{su,\theta_a}$  = Ultimate strain in steel

$a$  = Variable used in the stress-strain relations of steel

$b$  = Variable used in the stress-strain relations of steel

$c$  = Variable used in the stress-strain relations of steel

## 1 Introduction

### 1.1 Background

Recent trends in the construction sector are focused on designing resilient infrastructure that is safer, robust, durable, and demonstrates acceptable levels of performance during a disaster, including fire exposure. Progressive collapse is one of the key scenarios to be avoided for achieving resiliency in critical high-rise buildings. Undertaking progressive collapse analysis is highly complex and this phenomenon is characterized by the nonlinear dynamic response of the structure, including inelastic behavior, large deformations, and local (and global) instabilities. Significant advances have been made in modeling techniques over the past few decades to evaluate progressive collapse in high-rise buildings under extreme loading events such as blasts, earthquakes, and impact. However, currently, progressive collapse is not specifically evaluated under fire hazards in most scenarios. This is mainly due to the limited availability of validated numerical models and guidelines in the literature for tracing the fire-induced progressive collapse phenomenon in buildings [1].

Fire-induced progressive collapse in steel framed buildings can be particularly critical since severe fires can lead to an early onset of instability in the building. Steel framing is widely adopted in multi-story buildings owing to the enhanced strength and ductility properties of steel as well as the ease of fabrication and construction of such structures. However, steel framed buildings are more vulnerable to damage under fire exposure as steel possesses high thermal conductivity and undergoes rapid degradation of its strength and stiffness properties with the temperature rise. To overcome this problem steel structures always need some level of fireproofing (insulation) applied to them. Moreover, steel sections are susceptible to instabilities owing to specific design

considerations (such as the use of non-compact sections in compression members) and develop significant temperature-induced creep effects beyond 400°C that can lead to large inelastic deformations in the structure [2]. Further, any detachment of fire insulation from the steel members can lead to an early onset of instability in steel members leading to sudden or abrupt failure of the structure. Such a failure can jeopardize the safety of the occupants and first responders, provide insufficient time to tackle the spread of fire, and affect the integrity of the entire building itself.

Several fire incidents have occurred in the recent past that have caused severe damage or collapse in steel framed buildings around the world [3–7]. Some notable examples of fire-induced collapse include WTC Towers 1, 2, and 7 [7], Windsor Tower, Spain [4], and Plasco Building, Tehran [3], and in all cases fire resistance issues were the critical factors that led to the collapse of the structure. The above-listed collapse in buildings and associated damages incurred to life and property have motivated studies to explore different mechanisms and factors contributing to the onset of fire-induced progressive collapse in steel framed buildings. However, the majority of the fire resistance studies in the literature on steel structures have been carried out using member or assembly level approaches and do not capture the realistic fire, loading, and restraint conditions present in a steel framed building [8–11].

Specifically, limited numerical studies have been reported in the literature that traces the fire-induced progressive collapse in steel framed buildings [12–17]. In these studies, advanced numerical analysis approaches at a system level (primarily 2D frames) have been applied to investigate the influence of critical factors including, the geometry (framing), load level, connection failures, type of fire scenarios, and level fire insulation on the overall stability of steel framed buildings. Very few studies have evaluated fire-induced progressive collapse using 3D building models [13,15,17]. However, even the above-cited studies [12–17] included several

simplifications in the analysis and did not consider all the critical factors, including instability effects in steel sections and different collapse mechanisms due to fire spread (extent of burning and progression of fire) and varying load paths, that influence the fire-induced progressive collapse in steel framed structures. Moreover, previous studies incorporated high-temperature creep effects in the finite element (FE) model using an implicit approach that only accounted for partial creep strains that are built into temperature-dependent stress-strain relations, as in Eurocode 3 (EC3) [18]. Hence, a rational approach that accounts for realistic fire scenarios, high-temperature properties including transient creep effects of steel, load paths and restraints, and temperature-induced instabilities is needed for the reliable prediction of fire-induced progressive collapse in steel framed buildings. The complexities involved in tracing the fire-induced progressive collapse, including various factors that influence the onset of instabilities in steel framed buildings are discussed below to present a better understanding of the problem.

## **1.2 Need for structural fire safety in buildings**

Fire in a building can get initiated as a primary (ex. electric short circuit) or as a secondary event (following an earthquake, impact, blast, or explosion) in one or more compartments (rooms). Figure 1.1 shows the different phases in the development of a typical compartment fire in a building. The duration of each phase depends on factors such as geometry and physical dimensions of the compartment, fuel load, fuel type, and ventilation availability [19]. Most of the evacuation should occur during the initial ignition phase when the temperatures in the compartment are low and there are very little or no toxic gases. According to National Institute of Standards and Technology (NIST) [20], when the human skin temperature reaches 72°C, either from direct contact with fire/smoke or through convection and radiation, the skin is completely burnt (destroyed). Beyond this stage, evacuation becomes difficult. In many cases, depending on the

level of active fire protection (such as sprinklers, extinguishers, etc.) and compartmentation, the fire is prevented from reaching the flashover stage which indicates a transition to the burning phase of the fire. However, in some cases, due to a lack (or malfunction) of active or passive fire protection measures, the fire may reach the flashover stage and is associated with high temperatures of over 600°C [1].

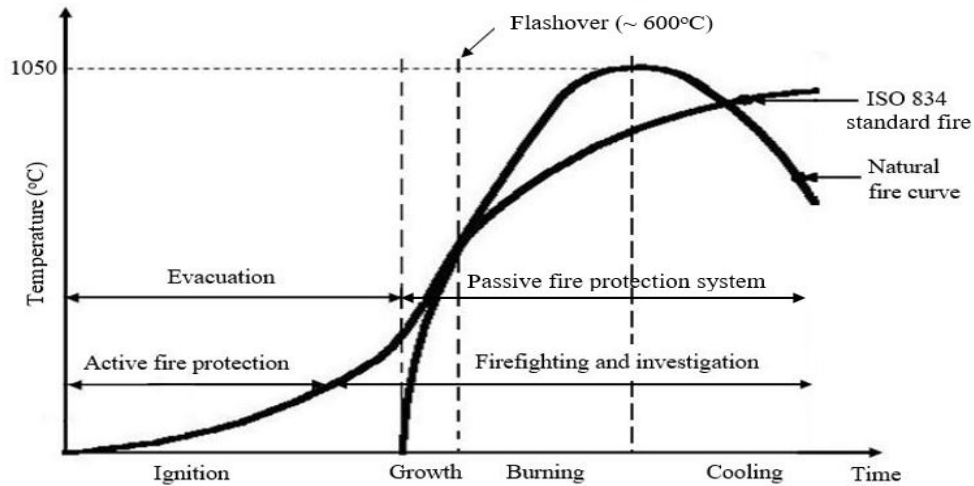


Figure 1.1. Fire development process in a typical compartment.

In the post-flashover stage, the structural members and compartment boundaries are exposed to high temperatures in the range of 600 to 1100°C. The fire may also spread within the building horizontally and vertically (as shown in Figure 1.2) when there is a breach in compartmentation severely affecting the evacuation process as well as the stability of the structural system. In the survey conducted by the National Fire Protection Association (NFPA) [21], office buildings have the highest probability of fire spread beyond the room and floor of origin. Most of the firefighting operations continue through this phase. In this stage, survival is very unlikely due to extreme conditions of temperature, heat, and toxic gases. Depending on the availability of fuel and oxygen, the fire may continue to burn until the fuel burns out or the oxygen supply depletes resulting in a drop in temperature levels in the cooling (decay) phase.

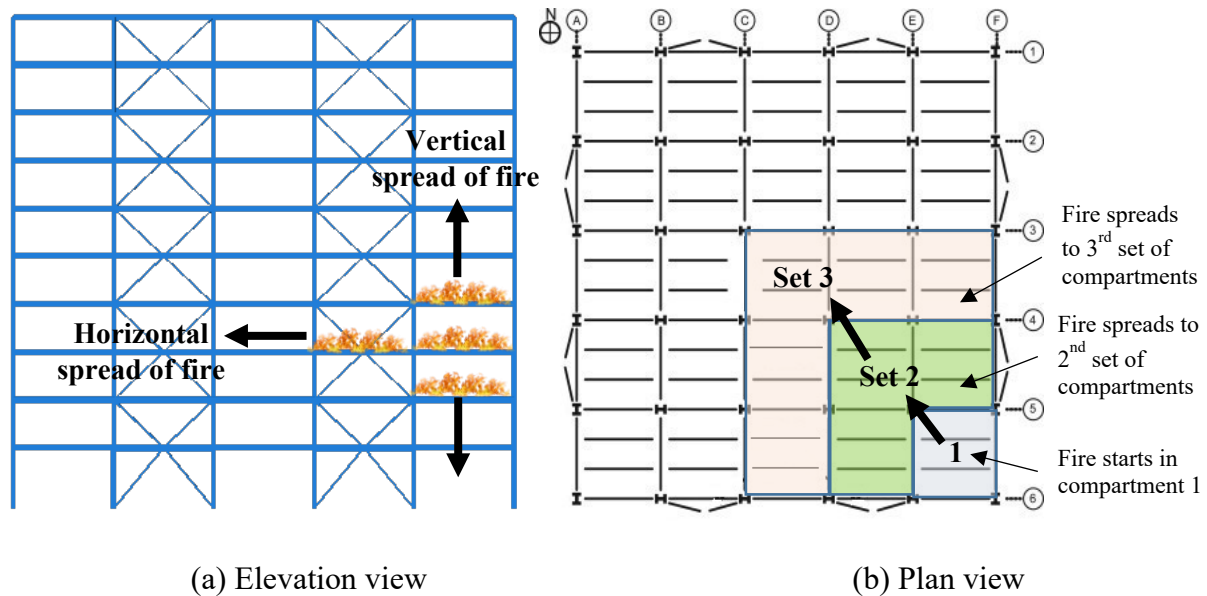


Figure 1.2. Progression of fire in a high-rise building.

The structure is required to meet different performance objectives during and after a fire event such as life safety, functionality, property protection, and environmental protection to minimize death, injury, property loss, and damage to the environment [22]. Building codes specify provisions for life safety and property protection, often with a higher emphasis on life safety measures. Depending on the performance objectives to be met, the design of buildings may require that the structure withstand the fire exposure for a particular duration without undergoing failure to allow for occupant evacuation and firefighting operations to take place. In such scenarios, the design for fire safety primarily involves controlling fire and smoke spread and providing minimum fire resistance ratings for structural members. In some buildings where the evacuation of occupants is difficult (or time-consuming) or the belongings of the building and the building itself have a significant value (e.g., heritage structures), preventing structural collapse is critical to the safety of the occupants and first responders as well the contents and fabric of the structure.

Over the past few decades, there has been a great impetus towards performance-based guidelines for fire resistance design of structures. Current performance-based design approaches focus on the

fire response of individual structural components (members) such as beams, columns, floor slabs, etc. The interaction with the surrounding structure or members is mostly neglected or is accounted for using simplistic idealizations [1]. Although member level approaches provide a comprehensive understanding of the local behavior of different structural components under fire exposure, these approaches fail to capture the system level response of the entire structure under fire conditions, specifically the continuously varying load paths in a structural system and collapse mechanisms. There is a need for performance-based design approaches that focus on system level response of structures during fire exposure.

More recently, few studies have shown that incorporating cognitive abilities into a structure through a framework of integrating sensors with structural members to provide situational awareness can enhance the monitoring of the structure during and after the fire event [23,24]. Situational awareness refers to the ability to assess in real-time the continuously changing response of occupants, structure, and as well as of the environment in a building. In the initial phases of fire development (refer to Figure 1.1), situational awareness provides the occupants with information such as the location of burning, levels of temperature and smoke within the building, etc. that can assist in identifying accessible exit routes for faster and safer evacuation. Additionally, in later stages of fire, situational awareness can also help evaluate the overall state (response) of the structure in terms of damage, available load carrying capacity, and probable imminent collapse at any point during the disaster. This information can aid first responders in responding to the disaster and developing effective firefighting operations. Implementing such novel techniques for disaster response in buildings heavily relies on the availability of advanced numerical models capable of accurately tracing system level behavior of buildings during and after a fire event, including different (failure) collapse modes.

### **1.3 Fire-induced progressive collapse phenomenon in steel framed buildings**

The progressive collapse in buildings gets initiated with the failure of a primary structural element (e.g., columns, floor slabs, primary beams, etc.) due to extreme loading events such as earthquake, blast, and impact. This can initiate instability in adjoining structural members, which in turn may cause the global collapse of the structure. The progressive collapse has a pancaking effect and once initiated, it becomes impossible to prevent the collapse of the building. The process is highly dynamic and is characterized by inelastic behavior and large deformations. Progressive collapse under fire conditions can be more severe since intense fires can lead to an early onset of instability in a building. The rapid spread of fire can result in multi-story burning, which in turn can lead to continuously changing load paths and abrupt failure of the structure. Moreover, fire induces large inelastic deformations and restraint forces that result in the early failure of structural members. Figure 1.3 illustrates the fire response mechanism leading to the progressive collapse in a typical steel framed building.

Steel framed buildings provide superior performance under gravity and lateral loads at ambient (temperature) conditions due to the high strength and ductility properties of steel. However, exposure to fire is a major vulnerability that undermines the stability and integrity of these structures. During a fire incident, steel members in the fire-exposed compartment experience a rise in sectional temperatures due to the transfer of heat from the fire source to the exposed faces of the members. The steel members are provided with some level of fire protection (such as fire insulation) to delay the rise in temperature within the cross-section. In the initial stage of fire exposure, the fire-exposed members undergo thermal expansion. However, depending on the extent of restraint offered by the surrounding structure, the expansion of members is partially restrained. During this stage, the degradation of strength and stiffness properties of steel is

minimum, and the load-induced deformations are low. With a further rise in fire temperature, the strength and stiffness properties of the member degrade rapidly leading to increasing deformations in members in the fire compartment(s). High-temperature creep that develops beyond 400°C also contributes to much of the deformation experienced by the steel members in the later stages of fire exposure and can lead to the failure of one or more structural members [2].

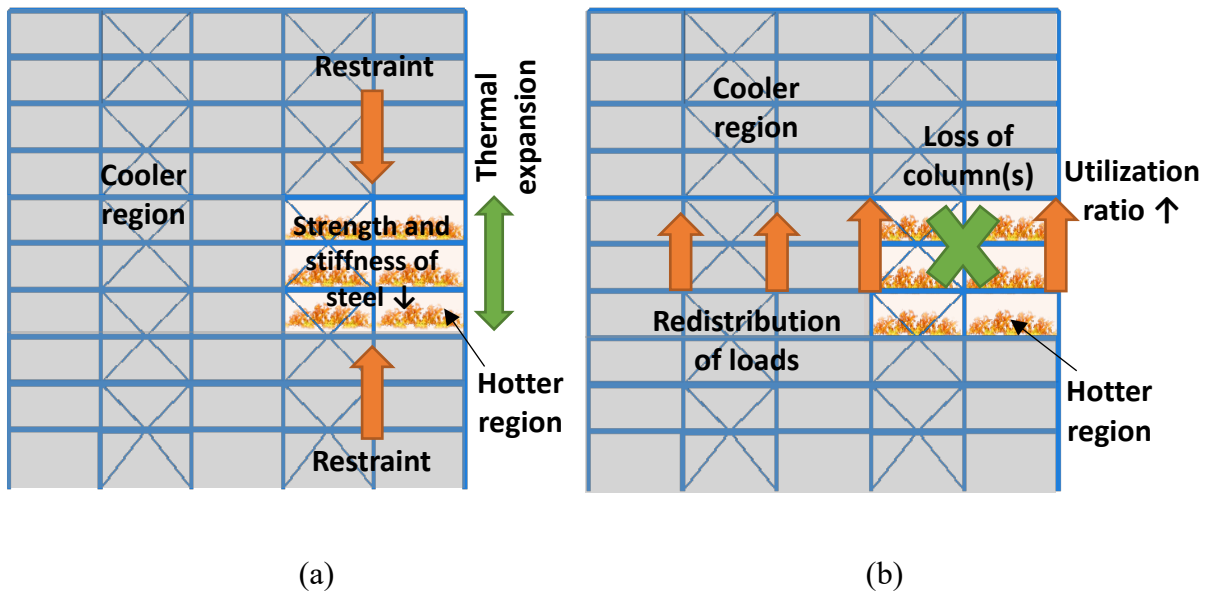


Figure 1.3. Schematic representation of fire response mechanism of a typical steel framed building. (a) Thermal expansion and material degradation. (b) Load redistribution following column loss.

Failure of a structural member can induce an initial instability (or local failure) in the overall structural system. However, the inherent redundancy present in the framing system allows for the redistribution of forces from the failed (or failing) member to adjoining members, as shown in Figure 1.3(b). In cases where the adjoining structural members are unable to withstand the redistributed loads, instability propagates through the system resulting in the successive failure of multiple members, and it can lead to progressive collapse (or global failure) of the structure. Significant advancement in modeling is required to capture this highly complex phenomenon with due consideration to the dynamic process, nonlinear material behavior at high temperatures, large

deformations, and rotations, temperature-induced restraint forces, the onset of local and global instabilities, etc.

In current fire design practice, the fire resistance of steel framed structures is obtained through member level analysis, where the structural member subjected to fire is modeled considering idealistic restraints such as pinned or fixed supports. Such idealizations do not account for restraint effects offered by the adjoining structure and load distributions. To compare the system level response over the member level failure, the steel frame shown in Figure 1.4 is exposed to standard ASTM E119 [25] fire. Failure of column AB is traced through member and system level analysis approaches. The deformed shapes of the steel frame and column AB are shown in Figure 1.5. The deformations in the member and the structure are obtained through finite element analysis.

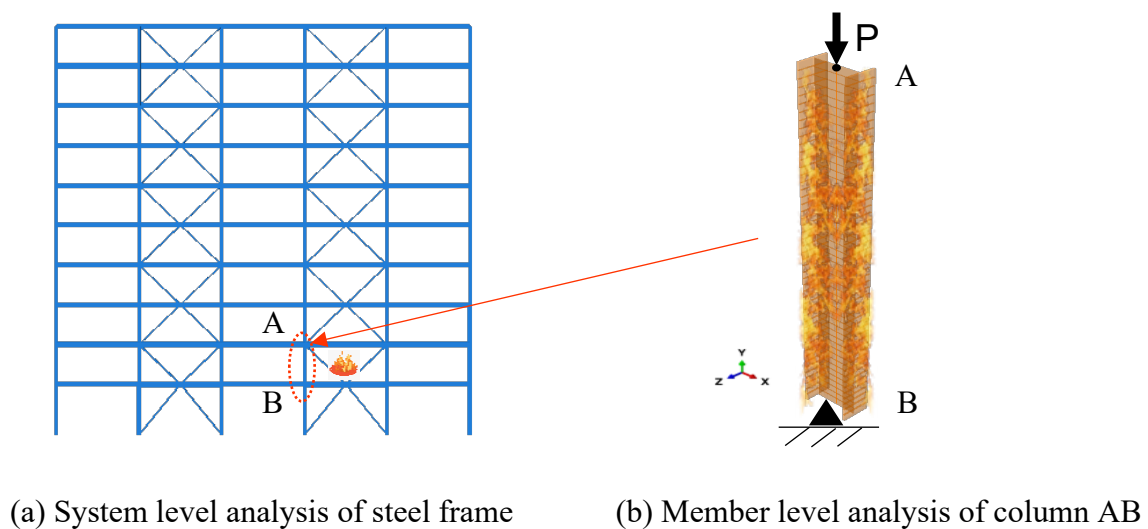


Figure 1.4. Steel frame exposed to fire.

Figure 1.5 © shows the axial deformation response of the column obtained using member and system level analysis approaches. The column experiences higher expansion in the member level approach and a lower failure time of 180 minutes. Due to the restraint offered by the surrounding structure, the expansion in the column is lower in the system level approach and the column can carry the load for a longer duration until it fails at 205 minutes. The significant difference in the

fire response predictions between the two analysis approaches shows that the member level analysis is unable to capture the realistic onset of instability in steel framed structures. Not accounting for the contribution of the structural system including the restraint effects and load distribution influences the predicted fire response and results in the unrealistic estimation of failure times. Moreover, the onset of instability under fire conditions leading to the progressive collapse in a steel framed building is influenced by several factors such as the fire exposure scenario, high-temperature properties of constituent materials, local instabilities, available load paths, and the extent of fire protection. These factors are to be properly considered while tracing the fire-induced progressive collapse in a steel framed structure.

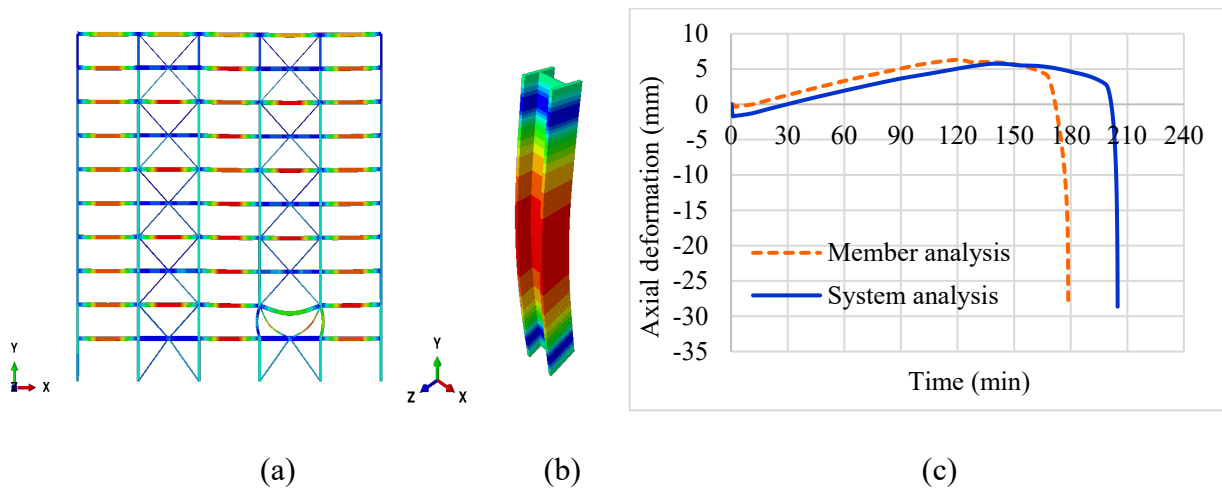


Figure 1.5. Deformed shape of (a) steel frame at 205 min and (b) column AB at 180 min. (c) Axial deformation of column AB.

## 1.4 Factors influencing fire-induced instability in steel framed structures

### 1.4.1 General

The response of steel framed buildings and their robustness against progressive collapse under ambient temperature conditions have been studied in detail in the past. In these studies, it is widely accepted to treat the loss of column(s) as the initiation of local instability in the structural system that may lead to the partial or entire collapse of a building [12,26]. This scenario is more applicable

to extreme events such as sudden impact loading where all structural members are at room temperature. However, during a fire event, more than one structural member often experiences a loss of capacity (or experiences instability) due to fire exposure. Further, the onset of instability in a steel framed building under fire conditions is governed by several factors including the configuration of structural framing (including connections), fire severity, loading, material properties of steel at elevated temperatures, level of fire protection, etc. The effect of different types of framing, level of gravity loading, connection behavior, and level of fire protection on the system level response of steel-framed buildings have been reported in the literature [12–17]. However, critical factors such as the type of fire scenarios including fire spread from one compartment (or floor) to another, varying load paths, stability issues, high-temperature creep, and loss of fire insulation on the onset of instability in steel-framed buildings are not fully explored. These factors are discussed in the following section in more detail.

#### ***1.4.2 Critical factors influencing fire-induced instability***

##### *1.4.2.1 Fire severity*

Fire severity is typically evaluated in terms of heating rate, peak temperature (intensity), and duration of fire exposure. For evaluating the fire-induced progressive collapse in steel framed buildings, fires with low to moderate severity may not be critical. However, severe to very intense fire exposure scenarios are more likely to cause excessive damage and need to be considered for evaluating the onset of the fire-induced collapse. In addition, the extent of fire spread (number of compartments or floors burning) and location of burning can also influence the onset of instability in a steel framed building and need to be considered for tracing the fire-induced collapse of steel framed structures.

#### *1.4.2.2 Fire spread*

A fire that originates in one compartment (or floor) may spread to another through the breaching of floor/ceiling assemblies, concealed spaces, service ducts, shafts, or stairways [22]. Such fire spread scenarios, which are dynamic throughout the fire exposure, can alter the load paths and failure sequences in the structural system and hence, are critical for tracing the progressive collapse in steel framed buildings. Much of the current knowledge focuses on standard fire exposure such as ASTM E119 [27], ISO 834 [28], etc. in a single compartment. Although these scenarios are effective in predicting localized failure (e.g., failure at a member level), they do not trigger a collapse of the entire building. The onset of progressive collapse in steel framed buildings under realistic fire scenarios, especially accounting for the spread of fire from one region of the building to another, has not been fully studied in the literature [16].

#### *1.4.2.3 Load paths (and restraints)*

Member or section level analysis, which is commonly utilized for evaluating fire resistance of steel framed structures, is suitable for simulating localized behavior or failure of a structural member. However, for evaluating the onset of fire-induced collapse, the altering load paths following the failure of one or more structural members, as well as the redistribution of loads to adjacent members need to be traced. Such effects can only be accounted for through a system level analysis approach (rather than member level treatment) to predict the onset of fire-induced progressive collapse in steel framed buildings. Further, the transverse framing and floor slabs, including the composite action between the slab and the beams, can influence the extent of redistribution of loads and thus, needs to be included in the fire-induced progressive collapse analysis.

#### *1.4.2.4 High-temperature creep*

Creep is the time-dependent inelastic deformation that occurs in steel under applied stress and temperature. Previous high-temperature studies on steel members [8,29–32] have shown that creep effects, when not fully accounted for, can lead to unrealistic predictions of fire resistance. Creep deformations, however, can be more critical to the stability of a fire-exposed steel structure leading to a progressive collapse in severe cases. The failure of a structural member results in a redistribution of loads to the adjoining members leading to higher stress levels in the adjacent members. The increased stress levels, combined with high-temperature levels, produce large creep strains, which can lead to an early onset of instability in the structural members, and this may lead to the collapse of the structure. At present, however, the full effects of transient creep are not included in the fire-induced progressive collapse analysis of steel framed structures.

#### *1.4.2.5 Local instabilities*

Steel members cannot develop their ultimate load carrying capacity if the elements of the cross-section (flanges or web) are so slender that local buckling occurs. Local instabilities can become dominant when a fire-exposed member is sufficiently slender, when the member is subjected to eccentric loading, or when concentrated loads are placed near the end supports [1]. For tracing the fire-induced progressive collapse in steel framed buildings, the structure is subjected to continuously changing fire spread scenarios and load paths that can expose steel members to nonuniform fire exposure and eccentric loading. Such scenarios increase the susceptibility of steel sections to undergo local buckling, which in turn can lead to an early onset of instability at member and system levels. Very limited research has been carried out in the past, primarily at a member level, to study the effect of local instabilities [9,11,33–35]. At a structural level, the effect of local instability is usually ignored in most FE models.

#### *1.4.2.6 Loss of fire insulation*

Delamination (or loss) of fire insulation leads to the partial or full exposure of steel members to fire which results in a faster rise in sectional temperatures. This leads to faster degradation of strength and stiffness in the members which results in larger strains or deformations, and in turn more delamination. The catastrophic collapse of the World Trade Center buildings showed that the delamination of fire insulation from steel members can significantly weaken the stability of the structure [7]. Under severe fire exposure, fire insulation can be damaged due to excessive deformation or failure of some steel members, which can precipitate the onset of fire-induced collapse in steel framed buildings. Hence, the delamination of fire insulation is a critical factor that needs to be considered in the fire-induced progressive collapse analysis.

#### *1.4.3 Approach to fire resistance assessment of steel framed structures*

Fire resistance of steel structures is currently evaluated through prescriptive approaches such as listings and correlation methods recommended in ASCE [36], Eurocode 3 [18], or other codes. These prescriptive methods are developed based on standard fire tests on steel members and do not consider many critical factors, including the effect of high-temperature creep strain [1]. To a limited extent, simplified approaches such as the Lumped Heat Capacity approach specified in AISC 360-16 [37] are used to determine the fire resistance of protected and unprotected steel members. In these approaches, the onset of instability is determined using “critical temperature” or strength-based criteria [1]. The material model only includes degradation of strength and stiffness and does not capture the entire stress-strain response at elevated temperatures. These methods do not specifically account for the temperature-induced transient creep of steel.

Advanced analysis approaches for the evaluation of fire resistance of steel structures are mainly used in research applications and very rarely for design purposes. The advanced analyses typically

involve a sequential thermal and mechanical analysis and are implemented using finite element software such as ABAQUS or ANSYS. The majority of the advanced analyses are carried out at a sectional or member level and do not account for the realistic loading and restraint scenarios present in the structure. Very limited studies include the system level behavior of steel framed structures under fire exposure [13]. Even in these studies, the influence of different fire exposure scenarios including fire spread, load paths, and local buckling effects on the onset of fire-induced instability are not evaluated. In addition, temperature-induced creep strain is accounted for implicitly through temperature-dependent stress-strain relations of steel. Recent studies highlight the need for an explicit treatment of high-temperature creep in the fire resistance analysis of steel framed structures [8,29–32]. Further, progressive collapse is not specifically evaluated under fire conditions for steel framed structures.

## **1.5 Research approach**

### ***1.5.1 Hypothesis***

To address the existing knowledge gaps and develop a better understanding of the fire-induced progressive collapse phenomenon in steel framed buildings, this research is developed with a hypothesis, which is stated as follows:

*“The onset of instability leading to the fire-induced progressive collapse of steel framed structures is significantly influenced by continuously varying critical factors such as fire spread, load paths, restraint forces, and degrading mechanical properties including transient creep effects. Therefore, evaluating fire-induced progressive collapse in a steel framed structure requires due consideration to all critical factors, and this can be achieved only through an advanced analysis carried out at the system level.”*

### ***1.5.2 Key objectives***

This study aims to develop a fundamental understanding of the fire-induced progressive collapse of steel framed buildings and quantify the effect of critical parameters influencing the onset of collapse through comprehensive numerical analyses. As part of this thesis, the following are the specific research objectives that will be addressed:

- Carry out a state-of-the-art review on the behavior of steel framed structures under fire conditions. The comprehensive review includes evaluating the collapse mechanisms in steel framed buildings that experienced a fire in recent years, experimental and numerical studies carried out on fire exposed steel framed structures, and studies on high-temperature creep and local buckling in steel structures.
- Undertake a set of evacuation simulations in high-rise buildings to illustrate the importance of structural stability in facilitating emergency evacuation during a real fire event. The simulations will be used to evaluate the occupant evacuation time in high-rise buildings during a fire drill and under realistic fire conditions.
- Develop a high-fidelity finite element-based numerical model to trace the overall response of a steel framed structure under fire exposure, specifically incorporating the evolution of temperature-induced instability at member and system levels. The model will account for temperature-dependent strength and stiffness degradation of constituent materials, connection configurations, load paths, geometric nonlinearity, and realistic failure limit states.
- Develop an approach to specifically account for the high-temperature creep effects in the fire-induced progressive collapse analysis. The transient creep strain that develops in steel members under fire conditions will be explicitly incorporated in the developed numerical

model through a built-in creep sub-model to evaluate the effect of high-temperature creep on the onset of instability in steel structures.

- Validate the developed numerical model by comparing the thermal and structural predictions with the test data available in the literature from fire experiments carried out on isolated steel structural members and steel-composite structures under fire conditions.
- Carry out parametric studies to evaluate the effect of various critical factors including the extent of fire spread, fire severity, high-temperature creep, and structural parameters that govern the stability of steel framed structures under fire conditions.
- Develop guidelines for improving the fire performance and minimizing the onset of fire-induced instabilities, including progressive collapse, in steel framed buildings.

### ***1.5.3 Methodology***

The above-stated objectives will be realized by conducting extensive numerical studies on steel framed structures under fire conditions. A comprehensive finite element-based model will be developed in ABAQUS to trace the overall response of a steel framed building under fire conditions in the entire range of loading, from pre-fire exposure to full collapse scenario. The developed model can be applied to undertake fire resistance analysis at different levels, including member and system levels, using an appropriate discretization of the structure, material properties, and boundary conditions. The numerical model will account for high-temperature stress-strain curves (including strain hardening and softening) of steel and concrete, temperature-dependent thermal properties, realistic fire exposure scenarios, altering load paths, and temperature-induced instabilities. In addition, the temperature-induced transient creep strain of steel will be explicitly included in the analysis through a creep sub-model in ABAQUS. The model will have the capability to trace the evolution of instability in the structural system and structural response

beyond stages of a local member failure can be evaluated. Data from previous fire tests on steel members and steel framed structures will be used to validate the developed numerical model for thermal and structural response. The validated model will be applied to quantify the effect of critical parameters such as fire scenarios, high-temperature creep, and structural parameters on the onset of instability leading to the progressive collapse in steel framed structures. Results from the parametric studies will be utilized to develop guidelines for mitigating the onset of fire-induced instabilities, including the progressive collapse in steel framed structures.

## **1.6 Layout of thesis**

The research undertaken as part of this dissertation is presented in seven chapters. Chapter 1 provides general background on the need for structural fire safety in buildings and critical factors influencing the onset of instabilities leading to the progressive collapse in steel framed structures. Chapter 1 also lays out the key objectives and methodology adopted for this study. Chapter 2 provides a detailed state-of-the-art review of the behavior of steel framed buildings under fire exposure. The review includes a summary of recent collapses in steel framed buildings due to fire, experimental and numerical studies carried out on steel framed structures, and current fire design provisions in codes and standards. This chapter also reviews the tests carried out at material and member levels to evaluate the high-temperature creep effects of steel and numerical studies undertaken to evaluate the effect of local instabilities on the fire performance of steel structures. Chapter 3 presents evacuation simulations carried out on high-rise buildings under normal and fire exposure conditions. The role of structural stability on emergency evacuation strategies in buildings is also discussed in this chapter. Chapter 4 provides details of the numerical model developed for tracing the fire-induced progressive collapse in steel framed buildings. Validation of the developed model with available experimental data at member and system levels is also

presented in this chapter. Chapter 5 presents the results from the parametric studies undertaken to evaluate the effect of critical parameters on the onset of instabilities leading to the progressive collapse in fire-exposed steel framed structures. The range of the varied parameters and a detailed discussion of results obtained from the numerical analyses are provided in this chapter. Chapter 6 presents design guidelines for mitigating the onset of fire-induced instabilities in steel framed structures. Recommendations for the treatment of high-temperature creep in the fire resistance analysis and strategies for identifying and minimizing scenarios critical for fire-induced collapse are provided in this chapter. Finally, conclusions and recommendations for future research are summarized in Chapter 7.

### 2 State-of-the-art Review

#### 2.1 General

Fire in buildings poses a significant threat to occupants, first responders, and as well as the structure. The rapid spread of fire and smoke in buildings can hinder the process of evacuation and firefighting operations resulting in injuries and loss of human life. Such situations call for a reliable egress system for the safe evacuation of occupants in minimal time. Currently, there are limited evacuation studies in the literature that account for varying fire scenarios, human behavior, and building characteristics. Besides, severe fires can induce excessive damage to the structural members, leading to the partial or complete collapse of the building. Unlike concrete structures, steel framed structures are more vulnerable to damage under fire exposure as steel undergoes rapid degradation of its strength and modulus properties with the temperature rise. Issues specific to steel structures such as high-temperature creep effects of steel and local instability issues can lead to an early onset of instability in the building. At present, there is very limited data on the system level behavior, specifically on the fire-induced progressive collapse of steel framed buildings.

Evaluation of fire-induced progressive collapse in steel framed buildings requires a detailed analysis of the thermal and structural response of the entire structural system, which in turn requires proper consideration of several critical factors that influence the onset of instabilities at member and global levels. However, only limited studies have been reported that trace the progressive collapse of a steel framed building under realistic fire exposure conditions. Preliminary studies have shown that high-temperature creep in steel significantly influences the onset of instability in steel members. Very few studies have been reported that include the creep effects explicitly in the fire resistance analysis of steel structures. Moreover, only limited studies have

included the effect of local buckling in the fire resistance evaluation, and that too at the member level only. At present, there is a lack of information on the effect of high-temperature creep and local buckling on the onset of fire-induced collapse in steel framed buildings.

This chapter presents a state-of-the-art review of the currently available studies on the behavior and collapse mechanisms of steel framed structures during severe fire incidents. First, some of the recent collapses in steel framed buildings are reviewed to highlight the magnitude of the problem. Second, existing studies that evaluate evacuation in high-rise buildings are reviewed. Next, previously reported experimental and numerical studies on the system level response of steel framed structures under fire exposure are reviewed. Then, existing experimental data on temperature-induced transient creep strain of different grades of steel and the current approaches for incorporating the high-temperature creep in the fire resistance analysis of steel structures are discussed. In addition, studies carried out to evaluate the effect of local instabilities on the fire performance of steel structures are reviewed. Finally, a review of design guidelines in current codes and standards for the fire-resistant design of steel framed structures is presented. Based on the review, knowledge gaps relating to the evaluation of fire-induced progressive collapse of steel framed buildings are identified.

## **2.2 Recent fire-induced collapses in steel framed buildings**

Over the past two decades, fires in several high-rise buildings were reported around the world. In many of these incidents, the fire was suppressed through active and passive fire protection measures, thereby minimizing the damage, and preventing the collapse of the structure. However, in severe fire incidents, the buildings experienced partial or complete collapse despite being equipped with some level of fire protection. Some of the notable fire incidents that occurred in

steel framed buildings in the recent past are discussed below to illustrate the main issues that contributed to the onset of fire-induced instability in these structures.

*Plasco building, Tehran, Iran (Jan 19, 2017)* [3,38–40]- The Plasco building was considered an iconic high-rise building in Tehran, Iran, during its construction in the 1960s. The building was made up of a steel framed tube-like structure comprising closely spaced steel columns along the perimeter tube and four interior columns in the core. The perimeter frames were braced using diagonal bracing members which formed the primary lateral load resisting system, while the interior frames were provided with semi-rigid connections which partly resisted gravity and lateral loads. The composite floor system is comprised of primary and secondary trusses supporting a lightweight concrete slab.

At the time of the fire and collapse, the 16-story building was primarily occupied by several garment businesses such as shopping malls, textile businesses, etc. Being a 1960s structure, there was a lack of fire protection systems in the building. The steel structural members were not provided with any fire insulation [38]. There was an ongoing attempt to improve the fire safety of the building, but it was postponed due to financial constraints and restraint from the tenants [39]. Moreover, the tenants (businesses) stored large amounts of fabric (textile) were stored in the building. The fire initiated in the tenth story, due to electrical issues, which later spread both horizontally to the entire floor and vertically to stories above. The building was able to withstand the fire for about 3 hours following which the northwest panels on floors 10 and 11 collapsed triggering the complete progressive collapse of the structure. The lack of fire protection systems, both active and passive, the high concentration of inflammable material in the building, and the unobstructed growth of fire to multiple stories were found to be some of the contributing factors to the collapse of the building [3,38,39].

Investigations carried out by Behnam [3] for the Tehran Fire Safety Department (TFSD) indicated that no failure occurred when the burning remained to the tenth story. The vertical spread of fire to multiple stories resulted in the failure of one of the main trusses in the ceiling of the 11<sup>th</sup> floor, which in turn increased the unbraced length of columns resulting in the buckling of multiple columns in the upper stories and subsequent collapse of the building. The studies also indicated that very high fire load density (resulting from textile shops, etc.) has a dominant role in the severity of fire exposure which in turn produced the collapse of the building. The change in building occupancy type over the years resulted in an increase in fire load from 510 MJ/m<sup>2</sup> (as per the original occupancy) to 1900 MJ/m<sup>2</sup> at the time of the fire incident. The studies showed that collapse could have been avoided if the fire load had remained at 510 MJ/m<sup>2</sup> [3].

*Windsor Tower, Madrid, Spain (Feb 12, 2005)* [4]– The Windsor tower was a 32-story office building in the financial center of Madrid. This building partially collapsed in a severe fire incident that occurred in 2005 and it has since been demolished. This composite building comprised of a concrete core at the center and reinforced concrete columns in the interior framing while steel columns were used in the perimeter framing. The building was also provided with two heavily reinforced transfer structures (girders) on floor 3 and floor 17, which supported the perimeter steel columns. Major refurbishment works, including the application of fire insulation on the perimeter steel columns and internal steel beams, were ongoing when the fire broke out. The fire protection for the steel framework was completed only up to floor 17 and the gaps between the floor slabs and vertical cladding were not sealed with fireproofing material at the time of the fire incident [4]. The fire started on the 21<sup>st</sup> floor due to electrical short-circuiting and within an hour spread to all stories above. Then, the fire gradually spread to the lower stories as well and the total burning duration was estimated to be about 18-20 hours. The unprotected steel columns above floor 17

buckled resulting in the partial collapse of the floor slabs in the upper stories. However, the columns below floor 17, which were protected, did not buckle. On the other hand, no major damage was reported in the concrete core, reinforced concrete columns, waffle slabs, and transfer structures even under such a severe fire scenario. The structural integrity and redundancy of the remaining parts of the building contributed to the overall stability of the building preventing total collapse [4].

*World Trade Center (WTC) Buildings 1 and 2, New York City (Sep 11, 2001)* [5,7] – The collapse of the WTC twin towers, in the 9-11 terrorist incidents, is one of the worst building disasters that occurred in the United States which resulted in 2830 deaths and billions of dollars of property losses. The damage and collapse mechanisms of these buildings were widely studied [41,42] to develop improved recommendations for building design and performance evaluation under extreme loading events. WTC 1 and WTC 2 were the two primary towers in the seven-building complex that were hit by hijacked aircraft. Each tower is comprised of 110 stories above the floor level and 7 stories below the grade. Both the towers were tubular steel framed structures with floor systems comprising of concrete deck slabs. Although similar, the two towers had slight differences in the configuration of building core; while the core was oriented in the E-W direction in WTC 1, the core in WTC 2 was oriented in the N-S direction. Additionally, WTC 1 also supported a 360 ft tall transmission tower. The orientation of the two buildings resulted in somewhat different wind pressures on the two towers, and in turn, slightly different lateral load resisting structural system. The towers were equipped with active fire protection systems including detection systems, sprinkler systems, smoke management systems, and passive systems such as fire protection on structural elements and compartmentation. The north tower (WTC 1) was hit by the aircraft between floors 94 and 98, whereas the south tower (WTC 2) was hit between floors 78 and 84.

Two-thirds of the columns on the impacted faces were fractured resulting in the partial collapse of the affected floors. Investigations carried out by FEMA [7] indicated that the intense fire, with a severity higher than typical office fires, that ensued on multiple floors after the initial impact was crucial to the collapse of the towers. The loss of fire protection from the structural elements following the impact severely undermined the behavior of steel members during the fire. Further, the sudden failure of primary structural elements (columns, main trusses, etc.) due to impact resulted in increased demand for the remaining structural members. The reduced strength and stiffness of steel at elevated temperature combined with significant creep due to the increased stress levels from the redistributed loads resulted in the failure of these members.

The NIST carried out a detailed analysis program to investigate the collapse mechanisms of the towers [5]. The global structural behavior of the towers including the aircraft impact and fire conditions that followed were modeled using the finite element software ANSYS. The model accounted for large deformations (geometric nonlinearity), temperature-dependent material properties, creep effects, and failure of connections. Fire temperatures in various regions of the structure were obtained using computational fluid dynamics. A series of static analyses at incremental time steps were carried out, where the results from the previous analysis step were used as the initial conditions of the next analysis step. The study concluded that inelastic flexural buckling of steel columns in multiple stories, failure of floor trusses, and high-temperature creep effects significantly influenced the onset of collapse in the towers [5]. The study also found that without the damage (or delamination) of fire insulation, the temperatures in the steel columns would have been much lower, resulting in reduced plasticity, creep, and buckling, the sag in floor trusses would have been smaller, the damage to core columns and exterior wall would have been

much lesser, and hence, the likelihood of collapse of the twin towers would have been much lower [5].

*World Trade Center (WTC) Building 7, New York City (Sep 11, 2001)* [6,43,44] – WTC 7 was a traditional 47-story steel framed office building in the seven-building WTC complex. The performance of the building during a fire and subsequent progressive collapse raised several questions from the point of fire safety of typical steel framed buildings. The structural configuration of the building is primarily comprised of four perimeter moment frames and two-story belt-trusses between floors 5 and 7 and floors 22 and 24. Additionally, an interior braced core extended from the foundation to floor 7 [6]. Numerous column transfers were provided between floors 5 and 7 using transfer trusses and girders to allow for load transfer from the non-concentric columns above floor 7 to the existing girders and columns below on floor 5. The transfer systems were needed to accommodate for the discrepancy in the column locations that developed due to the proposed expansion with a larger floor area and height than the originally intended layout of the building. The building was equipped with sprinkler system, smoke detectors, and aids for emergency evacuation and passive fire protection was provided on all steel members with a 2-hour fire rating.

The fire in WTC 7 is believed to have started from the flying debris coming from WTC 1. The southwest corner of the building was damaged to some extent. Fires that started on non-contiguous floors continued to burn for about 7 hours until the structure collapsed. Insufficient water in the sprinkler system due to the collapse of WTC towers 1 and 2 resulted in the unobstructed growth of fire to multiple stories in the building. Sections of floor slabs on floors 5 to 15 were partially damaged due to the debris and further weakened due to fire rendering the columns in the affected area unsupported between these floors. The collapse was initiated due to the bucking of an interior

column between floors 5 and 14 closely followed by the buckling of adjacent columns and the downward progression of the floor slabs.

NIST carried out a three-step analysis approach to model the collapse of the WTC 7 building [6]. Fire temperatures in different parts of the building were obtained using Fire Dynamics Simulation (FDS) and visual data. The fire-induced damage on different floor levels was simulated using a sub-assembly model of the fire-affected stories in ANSYS until the initiation of collapse. Finally, the collapse of the building was simulated using the finite element software LS-DYNA using an explicit dynamic analysis. The temperature data and fire-induced damage from ANSYS were provided as input to the LS-DYNA model. The studies showed that the fire was the primary contributing factor to the collapse of the building and not the damage inflicted due to debris impact from the collapsing WTC towers.

### **2.3 Evacuation models for high-rise buildings**

From the fire-induced collapses discussed in the previous section, it is evident that efficient evacuation strategies are critical in ensuring the safety of occupants in high-rise buildings, especially in the event of an emergency such as a fire. The spread of fire, toxic products of combustion, and smoke may result in inaccessible exit routes, reduced visibility, and congestion which in turn impede the process of evacuation [45]. Different analytical and computer models have been used in the literature to model evacuation in high-rise buildings. However, the majority of these studies do not account for the effects of fire, varying human behavior, and building characteristics that influence the emergency evacuation in a building. A review of studies that evaluate evacuation scenarios in high-rise buildings is given below.

The SFPE Handbook [45] provides an analytical hydraulic model to estimate the evacuation time in buildings. It is an engineering method that uses a series of equations to represent the flow of

occupants from one egress component to another. The change in the flow of people at critical regions of transitions (such as door entrance or staircase entrance) is captured. The results obtained from the model are quantitative but only work for symmetric and simple building layouts. It is not efficient for calculating evacuation time for complex structures under real fire conditions. In addition, the model does not account for varying human behavior during evacuation.

Computer models allow for a more detailed evaluation of the evacuation process. The most recent review by Kuligowski et al. [46] provides a detailed characterization of 28 egress models. The models were compared based on the approach adopted to model evacuation, movement, behavioral capabilities, and other features specific to each model. The review provides information for choosing suitable models for specific studies. Ronchi et al. [47] presented a list of tests for validation of building evacuation models. These tests were designed to evaluate different capabilities of the evacuation models such as pre-evacuation time, movement and navigation of occupants, exit usage, route availability, and flow constraints. Ronchi and Nilsson [48] compared seven evacuation strategies in high-rise buildings using a combination of different egress components, such as stairs, elevators, transfer floors, and sky-bridges. Strategies involving sole use of elevators and employing combined vertical (stairs and elevators) and horizontal (transfer floors and sky bridges) egress components were found to be most efficient. The study did not include the effect of varying fire scenarios and geometric characteristics of egress components on the evacuation process. Soltanzadeh et al. [49] evaluated the use of refuge floors in combination with other egress components (such as stairs and elevators) for evacuation. The study concluded that increasing the number the refuge floors in a building increased the evacuation time due to congestion. Providing a single refuge floor at mid-height was found to be optimum based on the

study of a 40-story high building. The evacuation study, however, did not consider varying building heights and fire exposure scenarios.

In the event of an emergency, it is crucial to provide enough time for occupants and first responders to tackle with adverse effects of the disaster and safely evacuate the building. Prior research has shown that resilient structural systems that maintain acceptable levels of functionality during and after a disaster improves the efficiency of evacuation and response operations under emergencies [23,50,51]. In a recent study, Naser and Kodur [23] showed that incorporating cognitive abilities into a structure to enhance resilience can aid in the process of evacuation. A framework of integrating sensors with structural members to provide situational awareness during the emergency evacuation was presented in this work. Situational awareness allows occupants and first responders to comprehend the severity of the disaster, such as the location of people within the building and the nature of fire growth. It also provides a future projection of the status of the building and occupants that can assist in the process of evacuation.

Even though evacuation strategies are critical to the safety of occupants and first responders, the structure needs to withstand the fire exposure without undergoing collapse to allow for the complete evacuation and firefighting operations to take place. For this reason, a comprehensive understanding of the response of the building under fire exposure, including different collapse mechanisms, and proper design measures to ensure adequate fire resistance of the structure is needed. The subsequent sections review the experimental and numerical studies reported in the literature that evaluate the fire performance of steel framed structures.

#### **2.4 Experimental studies on steel framed structures exposed to fire**

To study the fire resistance of steel structures, extensive experimental studies have been carried out in the past at a member level and to a lesser extent at a system level. The majority of the fire

tests have been carried out on isolated steel members (beams, columns, girders, etc.) under different loading, restraint, and fire conditions. A few other fire tests have also been carried out to study the behavior of different connection assemblies and the composite action between beams and the slab on floor systems. While a considerable amount of literature is available on fire resistance experiments on individual steel members and floor assemblies [52–58], very limited experiments have been carried out to evaluate the system level response of steel framed structures under fire conditions owing to the high cost and difficulty of carrying out such experiments. These limited experimental studies carried out at a system level are discussed herein.

The Cardington fire tests were sponsored by British Steel (BS), European Coal and Steel Community (ECSC), Building Research Establishment (BRE), and a few other organizations. These large-scale fire tests were conducted in the Large Building Test Facility (LBTF) at Cardington, U.K. to evaluate the inherent fire resistance of multi-story steel framed buildings and generate quality data on the overall behavior of steel framed structures under localized fire scenarios [59–63]. The test building was eight stories high (with a story height of about 4.2 m) and was five bays long by three bays wide, with a floor area of about 945 m<sup>2</sup>. Necessary lateral resistance (in the form of cross-bracing) was provided around the lift shaft and staircases to render the building a no-sway structure. The beams were designed as simply supported acting compositely (through shear studs) with the floor slab. The floor system consisted of a steel deck topped with a lightweight concrete slab. The imposed loads on the test building were achieved by placing sandbags uniformly on the floor slabs.

A total of six fire tests were carried out under the test program as shown in Figure 2.1. In the first test, an unprotected restrained steel beam (along with the floor slab) was subjected to fire inside a custom-built 8 m x 3 m gas furnace. The beam was heated at a rate of 3 to 10°C/min until a peak

temperature of about 900°C was reached. The surrounding structure including the columns and connections was not heated. A maximum deflection of 232 mm was recorded during the test. Runaway deflections, which are typical in simply supported steel beams during a standard fire test, were not observed in the test beam even at 900°C indicating that the member level test may not be a reliable indicator of the fire performance of the structure. The test beam failed due to local buckling of the web and lower flanges near the supports. The second fire test was carried out on a plane frame consisting of four columns and three primary beams. The primary and secondary beams and floor slabs were unprotected. The columns were protected, except for about 800 mm near the top end portion that included the connections. When the exposed portion of the columns reached 670°C, the columns were squashed by about 180 mm, resulting in a vertical displacement of the structure above. The fin-plate connections that were provided between the primary and secondary beams were also sheared during the fire test.

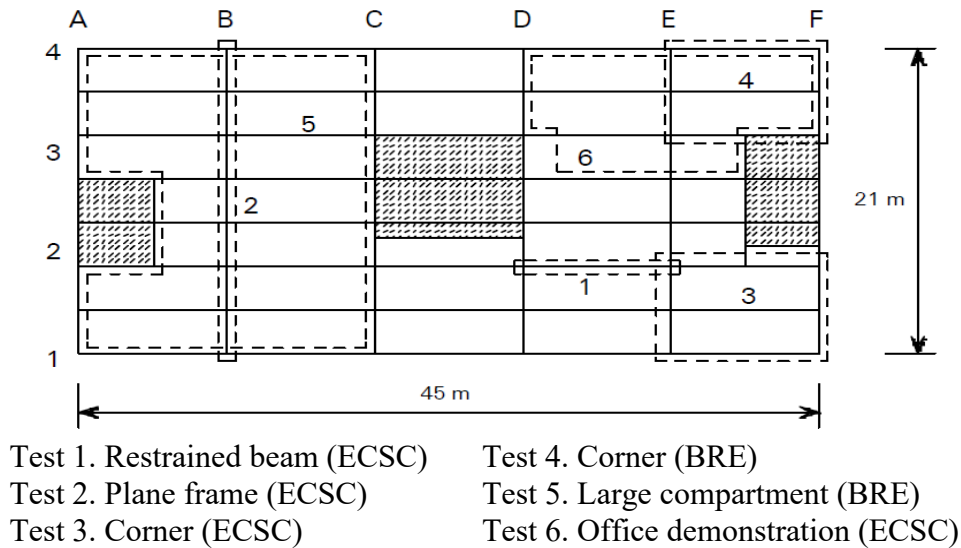


Figure 2.1. Fire test locations for the Cardington test program [63].

The third fire test was conducted in a corner compartment on the first floor of the building. All columns, beam-to-column connections, and edge beams were protected using a ceramic fiber

blanket. The fire load was equivalent to an office fire scenario. The secondary beams experienced large deflections, however, the structure performed well with no signs of collapse. Local buckling was reported near some of the beam-column connections. The fourth test was also performed on a corner compartment on the second floor of the building. All the structural members were left unprotected except the columns which were protected up to the underside of the floor slab. Gas temperatures reached a peak of about 1051°C with the maximum steel temperature of 903°C recorded in the secondary beam. The deflection at the center of the floor slabs was observed to be 270 mm and about 160 mm of this deflection was recovered after the fire. Local buckling in one of the beams was reported.

In test 5, a large compartment on floor 3 spanning the entire width of the building on one side and 18 m long on the other was subjected to fire (with a fire load of 40 kg/m<sup>2</sup>). All structural members except the columns and beam-to-column connections were left unprotected. A peak gas temperature of 746°C was recorded in the center of the compartment. Although the temperatures in the compartment were relatively low, the deformations in the slab were large with a maximum of 557 mm which only recovered to 481 mm in the cooling phase. Local buckling was observed near beam-to-column connections and end-plate connections fractured during the cooling phase. However, the complete collapse was not triggered. The final (sixth) fire test was an office demonstration test in which the structural performance was evaluated under a realistic fire scenario. Again, a large corner compartment (18 m x 9 m) with an open plan office was subjected to a fire load of about 46 kg/m<sup>2</sup>. Similar to the previous test, only the columns and beam-to-column connections were fire protected. The maximum temperature in the unprotected steel members reached 1150°C while the maximum deflection in the slabs was observed to be 640 mm which recovered to 540 mm in the cooling phase. The composite floor slab showed significant cracking

around one of the columns in the fire compartment. However, overall structural stability was maintained throughout the fire test.

From the Cardington tests, it is evident that the performance of the entire structure (at the system level) is significantly different from the behavior of isolated structural members in a standard fire test. This can be attributed to the difference in the structural interactions and associated load redistributions that tend to govern the overall structural stability of the building during fire exposure. Very few fire tests have been carried out at the system level on steel frames or sub-assemblies mainly because of the complexity and the high costs accompanied by these tests [64–68]. To overcome these limitations, in these tests, reduced scale frames or assemblies have been used. However, the structural response of a reduced scale assembly can be significantly different from that of a real building fire. An even fewer number of full-scale tests have been carried out on steel frames under fire conditions.

Dong and Prasad [69] carried out full-scale fire tests on two composite steel portal frames at a furnace located at Qingdao Technological University, China. The test frames were 2.8 m high and 3.6 m wide and comprised of two steel columns and a composite beam. In one of the test frames, only the beam-to-column connections were fire protected, while in the other, both the columns and connections were protected. The frames were subjected to vertical loads of 150 kN at the top of each column and four load blocks of 4.5 kN each, placed equidistantly on the beam. The test frames were exposed to heating (as per the standard ISO 834 fire curve [28]) and cooling phases of a fire. The test frames were sufficiently instrumented with thermocouples and LVDTs to measure the temperature and displacement of the frame during the fire test. Results from the tests indicated that the fire performance of the composite beams was significantly better than that of the steel columns.

The test frames performed much better, even when the structural elements were unprotected, than individual members under fire conditions.

In addition to the previous work, Dong et al. [70,71] carried out a series of fire tests on full-scale two-story two-bay composite steel frames. The frames were tested under combined gravity and thermal loads. Each test varied from the other in terms of the location and number of compartments exposed to fire. Fire exposure on the test frames comprised of a heating phase followed by a cooling phase. In the first four tests, the beam-to-column connections and columns were fire protected. In the second four tests, only the connections were protected. In some of the tests, local buckling in steel beams and failure of beam-to-column connections during the cooling phase of fire were reported. However, no local buckling was observed in the columns. The study highlighted that full-scale tests that include the structural interaction between different structural members can be critical in evaluating the fire resistance of steel members. Results from the study also showed that the behavior under the cooling phase of fire can be significant to the stability of the steel frame.

## **2.5 Numerical studies on steel framed structures exposed to fire**

Numerical studies on simulating the behavior of steel framed structures under fire conditions can be carried out at a section, member, and system level through finite-element-based methods. A sectional analysis is carried out at a critical cross-section (or several sections along the span of the member) to evaluate the behavior of a structural steel member exposed to fire. In a member level analysis, the structural member is discretized using a commercially available finite element package such as ABAQUS or ANSYS and then, a sequentially coupled or uncoupled thermal and mechanical analysis is carried out by applying suitable boundary conditions. Analysis at a system level includes a 2-D or 3-D model of the complete structure which is then analyzed under combined thermal and mechanical loading. Primarily, a sectional or member level analysis is widely adopted

for the fire resistance evaluation of steel framed structures [1]. Although such analyses are useful to understand the local behavior and mechanisms of different structural steel members under fire conditions, these analyses do not capture the structural interactions, redistribution of loads between members, and as well as the onset of instability in a steel framed structure. Therefore, analysis carried out at the sectional or member level will not be able to capture the overall response (as well as potential collapse) of the structure under fire scenarios.

At a system level, several numerical studies have been carried out in the past to evaluate the response of steel framed buildings and their robustness against progressive collapse at ambient temperature conditions. In these studies, it is widely accepted to treat the loss of column(s) as the initiation of local instability in the structural system that may lead to the partial or entire collapse of a building [12,26]. This scenario is more applicable to extreme events such as sudden impact loading where all structural members are at room temperature. However, during a fire event, more than one structural member often experiences a loss of capacity (or experiences instability) due to fire exposure. A relatively smaller number of numerical studies have been carried out to investigate the response of steel framed structures subjected to fire exposure. Most of the previous fire resistance studies at the system level are limited to the numerical analysis of 2-D steel frames (or sub-frames) exposed to standard fire (time-temperature) exposure conditions [12,14,16,72–74]. Some of the major studies on 2-D steel frames exposed to fire conditions are summarized in Table 2-1.

Table 2-1: Reported numerical studies on 2D steel frames

Reference	Building details	Fire scenario	Main Findings
Sun et al. [12,72]	4-story moment and braced frames	Parametric fire curve	<ul style="list-style-type: none"> <li>• In an un-braced frame, a lower loading ratio and larger beam section result in a higher failure temperature and global collapse. However, a higher loading ratio and smaller beam section result in a localized failure.</li> <li>• Vertical bracing systems in steel framed structures are effective in increasing the lateral restraint of the frame and preventing the collapse from progressing from local to global failure compared to that of horizontal hat bracing systems.</li> </ul>
Lange et al. [73]	The substructure of a 12-story steel moment-resisting perimeter frame with an interior rigid core	Generalized exponential curve	<ul style="list-style-type: none"> <li>• Two tall building collapse mechanisms, namely weak floor mechanism, and strong floor mechanism were simulated.</li> <li>• A simple assessment approach for identifying the upper bound collapse mechanisms for tall buildings under multiple floor fires was proposed.</li> </ul>
Jiang et al. [14]	8-story braced frame	Standard ISO-834 fire curve	<ul style="list-style-type: none"> <li>• Four collapse mechanisms for steel frames were proposed based on varying load ratios, beam sizes, and fire location.</li> <li>• The common collapse mechanism of steel frames is through the lateral drift of frames above the heated story combined with the downward collapse of the frame along the heated bay.</li> </ul>
Rackauskaite et al. [16]	10-story moment-resisting frame	Standard, design, and traveling fire scenarios	<ul style="list-style-type: none"> <li>• The structural response of the steel frame under traveling fire and uniform fire scenarios varied significantly.</li> <li>• The member utilization ratios showed irregular oscillations between 2-38% for the smallest traveling fire sizes, which were not observed in any of the uniform fire scenarios.</li> </ul>
Gernay and Gamba [74]	20-story moment-resisting frame	Localized design fire with heating and cooling phase	<ul style="list-style-type: none"> <li>• The redistribution of loads in a steel framed structure due to the thermal effects during the cooling phase of a fire can affect the stability of the structure and lead to progressive collapse.</li> <li>• Large tensile forces are induced in the fire-exposed column during the cooling phase of the fire. The adjacent un-exposed columns are subjected to higher compressive forces during the cooling phase than in the heating phase of the fire.</li> </ul>

Sun et al. [12,72] developed a static-dynamic approach to trace the progressive collapse of steel frames under fire conditions. The model was implemented in the finite element program Vulcan and was used to conduct a series of numerical simulations on steel frames to examine the effect of

loading ratio, beam sections, and bracing systems. The frames were subjected to standard ISO-834 fire exposure [28] with varying fire locations. The failure of the steel frames was reported as a critical fire temperature. The study concluded that in an un-braced frame, a lower loading ratio and larger beam section result in a higher failure temperature and global collapse. However, a higher loading ratio and smaller beam section result in a localized failure. Vertical bracing systems in steel framed structures are effective in increasing the lateral restraint of the frame and preventing the collapse from progressing from local to global failure. On the other hand, horizontal hat bracing systems have a limited capacity to resist the pull-in of columns on the heated floor, thereby, being ineffective in preventing global collapse.

Lange et al. [73] simulated the behavior of a substructure of a 12-story composite steel moment-resisting frame with an interior rigid core subjected to a three-story fire scenario using ABAQUS. The structural interactions leading to the two tall building collapse mechanisms, namely weak floor mechanism and strong floor mechanism identified by Usmani et al. [75] were illustrated. Results from the study showed that in both the mechanisms the fire-exposed columns were pushed out due to the thermal expansion of the fire floors before being pulled back to the original position. In the strong floor mechanism, it was observed that the pivot floors (floors adjacent to the fire floors) were able to support the horizontal force developed in these floors due to the contraction of the fire floors, and hence, a three-hinge collapse mechanism was developed. On the other hand, the weak floor collapse mechanism was observed when the pivot floors were not sufficiently able to resist the increasing horizontal force leading to the buckling of columns in the unexposed stories and ultimately resulting in progressive failure of the structure.

Jiang et al. [14] studied the collapse mechanisms of 8-story braced frames under varying scenarios of load ratios, beam sizes, and fire locations. An implicit dynamic analysis in OpenSees software

was used to trace the response of the steel frames under fire exposure. The fire scenario was restricted to a single compartment fire, either in the center or the edge compartment and the fire temperatures were assumed to follow the standard ISO-834 fire curve [28]. Four collapse mechanisms were proposed based on the numerical studies. The study concluded that the most common collapse mechanism of steel frames is through the lateral drift of frames above the heated story combined with the downward collapse of the frame along the heated bay. This study also reported the failure of the steel frames in terms of critical fire temperature.

Rackauskaite et al. [16] studied the behavior of a 2-D ten-story steel moment frame under different fire scenarios including traveling fires [76], Eurocode parametric fires [77], standard ISO-834 fire [28], and constant compartment temperature curve as per SFPE standard [78]. An explicit dynamic analysis was carried out in the finite element software LS-DYNA to simulate the response of the steel frame under fire exposure. Results from the study indicated that the response of the steel structure under uniform and traveling fire scenarios differed substantially. The member utilization ratios showed irregular oscillations between 2-38% for the smallest traveling fire sizes, which were not observed in any of the uniform fire scenarios.

Gernay and Gamba [74] investigated the effect of the cooling phase of localized fire exposure on the stability and collapse mechanisms in moment resisting steel frames. The numerical simulations were carried out in the finite element program SAFIR. The fire scenarios considered in the study were restricted to a single column burning. The study concluded that the fire-exposed column experiences a significant amount of tensile force during the cooling phase of fire while the adjacent un-exposed columns develop higher compressive forces than in the heating phase of the fire. Peak fire temperature and relative stiffness of the fire-exposed column were found to critically affect the tensile forces developed in the column during the cooling phase of the fire.

The above studies provide insight into the effect of different critical parameters and failure mechanisms in steel framed structures exposed to fire conditions at a system level. However, the stiffness and redundancy offered by the 3-D framing and floor system are not considered in these studies. Therefore, the behavior predicted in these studies may not completely characterize the response of steel framed buildings under realistic fire exposure conditions. Very few studies have been reported in the literature, as tabulated in Table 2-2, that have included the behavior of the complete structure, including the transverse framing and floor slabs in the numerical analysis of steel framed buildings exposed to fire.

Agarwal and Varma [13] carried out an analysis of two ten-story steel framed buildings under fire conditions; one with a moment frame and the other with a rigid core. The numerical model developed in ABAQUS accounted for the 3D framing, floor slabs, and failure in shear-tab connections. Based on the analysis, they reported that gravity columns play a significant role in the overall stability of the structural frame under fire conditions. Also, this study concluded that the level of reinforcement in the floor system could contribute to better load redistribution and resistance to fire-induced progressive collapse. The fire scenarios considered in this study were restricted to a single compartment fire. However, in a real fire event, the fire exposure conditions may vary based on the duration of the fire, the location of the fire in the building, and the area affected by the fire, which needs to be accounted for in the analysis.

Nguyen et al. [15,79] also conducted progressive collapse analysis on two ten-story buildings, one with a moment frame and the other with a rigid core. The buildings were subjected to standard ASTM E119 [27] fire exposure. Design improvements in terms of reduced thickness of fire insulation for different structural members and alternate sections for the secondary beams were proposed. The study, however, did not consider realistic fire exposure scenarios with varying

duration, cooling phases, etc. Qin and Mahmoud [17] carried out a progressive collapse analysis of a six-story steel framed building subjected to two fire scenarios: corner compartment and complete first-floor fire. Component-based models were used to simulate the behavior of moment and shear connections at elevated temperatures. Results from the study indicated that system level failure occurred at temperatures higher than 650°C – 700°C. Two collapse modes, including lateral sway in the case of corner compartment fire and vertical collapse in the case of complete first-floor fire, were reported. All the above numerical studies on steel framed structures accounted only for the partial creep strains through an implicit treatment of creep. Such an implicit treatment does not capture the full extent of creep deformations that develop under severe fire exposure scenarios.

Table 2-2: Reported numerical studies on 3D steel framed buildings

Reference	Building details	Fire scenario	Main Findings
Agarwal and Varma [13]	Two 10-story steel buildings with moment frame and rigid core	Parametric fire curves [77]	<ul style="list-style-type: none"> <li>• Gravity columns are critical components for the overall stability of a steel framed structure exposed to fire conditions.</li> <li>• The presence of steel reinforcement (greater than the minimum shrinkage reinforcement) in the composite floor system contributes to better load redistribution from the failed column to adjacent columns.</li> </ul>
Nguyen et al. [15,79]	Two 10-story steel buildings with moment frame and rigid core	Standard ASTM E119 fire curve [27]	<ul style="list-style-type: none"> <li>• The addition of fire protection to columns and increasing the capacity of the columns were found to increase the robustness of a steel framed building.</li> <li>• The addition of fire protection to beams and increasing the capacity of the beams or the floor slab had a minor effect on the performance of the steel framed building under fire exposure.</li> </ul>
Qin and Mahmoud [17]	Six-story steel framed building	Standard ASTM E119 [27] and parametric fire curves [77]	<ul style="list-style-type: none"> <li>• System level failure occurred at temperatures higher than 650°C – 700°C</li> <li>• Large deformations were reported in shear-tab connections leading to failure. Large rotations were observed in moment connections under severe fire exposures.</li> </ul>

## 2.6 High-temperature properties of steel

Knowledge of the high-temperature properties of steel, together with that of fire insulation, is necessary for evaluating the fire resistance of steel structures using numerical models. For the

numerical analyses, two sets of properties, namely, thermal properties and mechanical properties of steel are needed. In the previous studies, the material models specified in codes and standards, such as the Eurocode 3 [18] and ASCE standard [36] are commonly used. Other material models developed by past researchers, such as those developed by Poh [80], Anderberg [81], and Williams-Leir [82] have also been used to a limited extent. In this section, a review of the thermal and mechanical properties of steel is presented. Further, studies that evaluate the effect of high-temperature creep of steel at material and member levels are reviewed.

### ***2.6.1 Thermal and mechanical properties at elevated temperature***

Thermal properties include thermal expansion, specific heat, and thermal expansion of steel. These properties determine the temperature distribution within the steel sections and the expansion of the member during fire exposure. Relationships established for thermal properties of steel are available in codes and standards (Eurocode 3 [18] and ASCE [36]), as well as in published literature [83–87]. Overall, only minor variations exist between the different models proposed for high-temperature thermal properties of steel.

Mechanical properties of steel include modulus of elasticity, yield strength, stress-strain relations, and creep. The strength and modulus properties of steel, including the constitutive relationship, at elevated temperatures, have been studied extensively in the past [80–82]. Different test regimes (such as loading, heating rate, etc.) are used to measure the strength and stiffness of steel. Mainly, two types of testing regimes are reported in previous studies, namely, transient and steady-state tests. In the transient testing method, the steel specimens are subjected to constant stress and then exposed to uniformly increasing temperatures. Stress-strain values are measured at a constant stress level. On the other hand, in the steady-state testing method, the steel specimen is heated to

a specific temperature and then a tensile test is carried out to record the stress-strain values at a constant temperature.

Depending on the test parameters, the test measurements varied across the tests, leading to the differences in the constitutive relationship of steel specified in codes and standards [88]. The Eurocode 3 [18] material model is widely used in the numerical analysis of steel structures. The main difference between Eurocode 3 and other material models (like ASCE [36] or Poh [80]) is that it distinguishes the proportionality limit (point until which the stress-strain curve is linear) from the yield limit (the point at which the nonlinear elastic response ends) [88]. The reason for introducing the proportionality limit in the EC3 stress-strain curves is to capture the viscoelastic behavior that is partly due to the creep effect of steel at elevated temperatures [88]. Beyond the proportionality limit, the response is nonlinear, and the stress causes more strain than in the linear elastic range. This simplification enables the stress-strain curves of EC3 [18] to partially account for creep strains at elevated temperatures.

### ***2.6.2 High-temperature creep effects on steel structures***

Creep is defined as the permanent time-dependent deformation that develops in steel when subjected to constant stress and temperature. Creep in steel is primarily attributed to the movement of dislocations in the crystal lattice of steel [89]. The creep strain in steel comprises three phases, namely, primary, secondary, and tertiary creep phases [2]. During the primary phase, the creep strain rate is high but decreases with time. In the secondary phase, the creep strain rate is almost constant, and this phase is termed steady-state creep. In the final phase (tertiary phase), the creep strain rate increases exponentially with time until steel undergoes a necking failure [2]. At room temperature and severe load levels, creep deformations occur in steel at a very slow rate (typically spread over years) before they induce considerable influence on the deformation response of a

structural member. However, at elevated temperatures, the rate of creep strain significantly increases with an increase in stress levels (which occurs due to temperature-induced loss in mechanical properties) resulting in high deformations in steel members.

The creep deformations become apparent in metals at temperatures corresponding to 35% of the melting point at a constant stress state which in the case of steel corresponds to 400°C [89]. When exposed to transient heating conditions, as encountered during fires, steel develops transient creep strain, in addition to thermal and mechanical strain. The extent of transient creep strain in a steel member depends on several factors, including, the magnitude, duration, and rate of development of stress and temperature level in steel attained during the fire exposure. These creep strains are extremely hard to measure, especially at elevated temperatures when the creep strain is very high. Also, the transitions from primary to secondary to tertiary creep becomes hard to distinguish with increasing stress and temperature levels. A detailed review of the experiments and numerical studies that have been carried out in the past at material and member levels to study the effect of temperature-induced creep in steel structures is provided in the following sections.

#### *2.6.2.1 Creep at the material level*

The creep behavior of steel at elevated temperatures has been studied in the past for different grades of steel. Creep tests can be carried out by two methods, namely, steady-state and transient tests [30]. In the steady-state test, the applied stress and temperature are kept constant, and the variation of strain with time is measured during the test. In the transient creep test, the test specimen is subjected to constant stress and then is exposed to uniformly increasing temperature. Variation in temperature and strain at constant stress is recorded during the test. The thermal strain that develops in the specimen (separately evaluated from a different test) is subtracted from the total strain measured in both the test methods to obtain the creep strain. Although the transient test

method is more realistic for simulating the behavior under fire exposure conditions, the steady-state method is widely adopted in the literature owing to the ease of conducting the steady-state test as compared to the former method. Previous creep experiments that have been reported in the literature for different grades of steel are tabulated in Table 2-3 and discussed herein.

One of the earliest creep tests was carried out on SS41 (A36) grade steel by Fujimoto et al. [90]. The steel coupons were subjected to a temperature range of 350°C to 600°C and stress levels varying between 20% to 88% of yield strength. Only primary and secondary creep strains were reported from these tests. The study concluded that the temperature-induced creep strain tends to be significant in the evaluation of deformation behavior beyond a temperature of 450°C. Brnic et al. [91] carried out steady-state creep tests on A618 steel under varying stress levels from 35% to 77% of yield strength and at three different temperatures (400°C, 500°C, and 600°C). No significant creep was observed at a temperature of 400°C and stress levels below 50% and a temperature of 500°C and stress levels below 40%. Creep at 600°C and stress levels higher than 40% were found to be dominated by tertiary creep.

Morovat et al. [92,93] carried out comprehensive high-temperature creep experiments on ASTM A992 steel. The test coupons were cut out from flange and web plates of W4x13 and W30x99 steel sections. The coupons were tested in the temperature range of 400°C to 1000°C and stress levels of 30% to 77% of room temperature yield strength. Results from the experiments indicated that creep at temperatures beyond 600°C and stress levels greater than 50% were dominated by tertiary creep. Further, the creep of the flange material was found to be higher than that of the web material in a steel W-section. The test results were compared with that of Harmathy [94] and Field and Fields [95] creep models that were developed for A36 steel and a good agreement was not observed

with either of these models. The study recommends the need for more reliable creep models for structural steel at elevated temperatures.

Kodur and Aziz [30] conducted tests to characterize the high-temperature creep behavior of ASTM A572 steel. A572 steel is high-strength low-alloy steel that is widely used in bridge and building applications owing to its better strength, corrosion/weather resistance, and weldability. The steel coupons were tested at temperatures ranging from 400°C to 800°C and stress levels varying from 11% to 55% of yield strength. Results indicated that creep deformations dominate the structural response beyond a temperature of 500°C. Creep at stress levels of 50% and temperatures above 550°C was predominantly tertiary creep.

Wang et al. [96,97] carried out creep tests on high-strength steels of grade Q450 (A575) and Q690 under varying temperature and stress levels. Results from the tests showed that creep strains become significant at temperatures beyond 400°C in Q460 steel. In the low-temperature range of 300°C to 450°C, primary creep and secondary creep were observed. In moderate and high-temperature ranges of 450°C to 550°C and 600°C to 900°C, the creep response is mainly comprised of secondary and tertiary creep. In Q690 steel, creep strains were found to be significant at temperatures beyond 450°C. Overall, the creep strain in Q690 was found to be higher than the Q460 and Q345 grades of steel.

Table 2-3: Reported high-temperature creep tests on different grades of steel

Reference	Steel Grade	Strength	Creep test parameters	Main findings
Fujimoto et al. (1980) [90]	SS41 (A36)	Fy = 250 Mpa Fu = 400 Mpa	Temperature – 350°C to 600°C Stress level – 20% to 88%	<ul style="list-style-type: none"> <li>High-temperature creep tends to be significant in the evaluation of deformation beyond 450°C</li> </ul>

Table 2-3 (cont'd)

Brnic et al. (2009) [91]	A618	Fy = 335 Mpa Fu = 500 Mpa	Temperature – 400°C to 600°C Stress level – 35% to 77%	<ul style="list-style-type: none"> <li>• No significant creep occurs up to 400°C and stress levels below 50% and up to 500°C and stress levels below 40%.</li> <li>• Creep at 600°C and stress levels higher than 40% are dominated by tertiary creep.</li> </ul>
Morovat et al. (2012) [92,93]	A992	Fy = 345 Mpa Fu = 448 Mpa	Temperature – 400°C to 1000°C Stress level – 30% to 77%	<ul style="list-style-type: none"> <li>• Creep beyond 600°C and stress levels greater than 50% are dominated by tertiary creep.</li> <li>• The creep of the flange material is higher than that of the web material in a steel W-section.</li> </ul>
Kodur and Aziz (2015) [30]	A572	Fy = 345 Mpa Fu = 448 Mpa	Temperature – 400°C to 800°C Stress level – 11% to 55%	<ul style="list-style-type: none"> <li>• Creep deformations dominate the structural response beyond 500°C. Creep at stress levels of 50% and temperatures above 550°C is predominantly tertiary creep.</li> </ul>
Wang et al. (2013) [96]	Q460 (A575)	Fy = 492 Mpa Fu = 621 Mpa	Temperature – 300°C to 900°C Stress level – 15% to 90%	<ul style="list-style-type: none"> <li>• Between 300°C and 450°C, primary and secondary creep are observed.</li> <li>• In moderate and high-temperature ranges of 450°C to 550°C and 600°C to 900°C, the creep response mainly comprises secondary and tertiary creep.</li> </ul>
Wang et al. (2018) [97]	Q690	Fy = 760 Mpa Fu = 860 Mpa	Temperature – 450°C to 900°C Stress level – 38% to 90%	<ul style="list-style-type: none"> <li>• Creep strains are found to be significant at temperatures beyond 450°C.</li> <li>• Creep strain in Q690 is higher than that of Q460 and Q345 grades of steel.</li> </ul>

### 2.6.2.2 Creep at the structural level

High-temperature creep can be incorporated into the fire resistance analysis of steel structures through implicit or explicit creep models. In the implicit creep model, only partial creep strains that are built into temperature-dependent stress-strain relations, as in EC3 [18] are included in the analysis. On the other hand, high-temperature creep can be explicitly included in the fire resistance

analysis through a separate built-in or user-defined creep model that captures the full effects of creep at elevated temperatures. The majority of the numerical studies reported in the literature accounted for only the partial creep strains through temperature-dependent stress-strain relations of steel. Such an implicit treatment of transient creep does not capture the full extent of creep deformations that develop under severe fire exposure scenarios and explicit treatment of creep strains is needed to accurately capture the fire response of steel structures [8,29,30]. Limited studies [8,29,31,32] have been undertaken, primarily at a member level, in which the temperature-induced creep effects are explicitly incorporated in the fire resistance analysis. These studies are listed in Table 2-4 and discussed herein.

Table 2-4: Reported numerical studies that explicitly incorporate creep in fire resistance analysis

Reference	Structural member	Main Findings
Kodur and Dwaikat [8]	Beam-column	<ul style="list-style-type: none"> <li>• Load level, heating rate, fire scenario, and fire-induced axial restraint significantly affect the extent of creep deformations.</li> <li>• Implicit treatment of creep underestimates the deflections and overestimated the fire resistance of the member.</li> </ul>
Li and Zhang [31]	Axially restrained column	<ul style="list-style-type: none"> <li>• Neglecting high temperature creep effects leads to unrealistic critical buckling temperatures in steel columns under varying levels of axial restraint and heating rates.</li> </ul>
Morovat et al. [29]	Pinned column	<ul style="list-style-type: none"> <li>• Critical buckling load depends not only on the slenderness and temperature level but also on the duration of the applied load.</li> <li>• Implicit treatment of creep underestimates the buckling strength of columns compared to the test values, especially at steel temperatures above 600°C.</li> </ul>
Hantouche et al. [32]	A shear tab connection assembly	<ul style="list-style-type: none"> <li>• Transient heating scenarios with a slower heating rate and longer cooling durations can lead to high creep deformations.</li> </ul>

Kodur and Dwaikat [8] developed a numerical model to evaluate the effect of high-temperature creep on the fire response of restrained beams in which the transient creep strain was accounted for explicitly using the ANSYS finite element software. This study showed that the load level, heating rate, fire scenario, and fire-induced axial restraint significantly affect the extent of creep deformations that develop at elevated temperatures. Accounting for creep implicitly through

stress-strain relations was shown to underestimate the deflections and fire-induced axial tensile forces and overestimate the fire-induced axial compressive forces in the beams during fire exposure. Li and Zhang [31] studied the high-temperature creep effects in axially restrained steel columns by using the ANSYS creep model developed by Kodur and Dwaikat [8] to include the creep strains explicitly. The study showed that neglecting creep effects can lead to unrealistic critical buckling temperatures in steel columns subjected to varying levels of axial restraint and heating rates.

Morovat et al. [29] carried out experimental and numerical investigations on steel columns subjected to varying stress and temperature levels. The study indicated that transient creep has a significant influence on the strength (capacity) of steel columns and that the critical buckling load depends not only on the slenderness and temperature level but also on the duration of the applied load. Results showed that the AISC [37] and Eurocode 3 [18] predictions underestimate the buckling strength of columns when compared to the test values, especially at steel temperatures above 600°C. The study showed that an explicit creep model is needed to realistically capture the failure times of steel columns subjected to fire conditions.

Hantouche et al. [32] developed a numerical model in the finite element program ABAQUS incorporating the creep effects explicitly to study the behavior of a shear tab connection assembly under steady-state and transient heating conditions. The results showed that transient heating scenarios with a slower heating rate and longer cooling durations can lead to high creep deformations. Further, the study showed that at temperatures above 600°C, the load resisting mechanism in beams shifts from flexural to catenary action due to high creep strains developed in the steel assembly.

## 2.7 Properties of fire insulation

Steel structural members are typically provided with external fire protection to achieve the required fire resistance and maintain integrity during fire exposure. Often, spray-applied resistive materials (SFRM) are used as fire insulation. Since the strength and stiffness properties of the insulation are low, only the thermal properties of the insulation are of interest in the fire resistance analysis. Similar to the properties of steel and concrete, the properties of the fire insulation also vary with temperature. The fire insulation properties used in the fire resistance analysis are usually obtained from the manufacturers' listings for room temperature conditions [1]. However, prior studies [98,99] have shown that neglecting the variation of insulation properties with temperature can result in unconservative fire resistance values.

Very limited information is available in the literature on the high-temperature properties of insulation materials. Kodur and Shakya [98] carried out tests to evaluate the thermal properties of SFRM-based insulation such as CAFCO-300, Carbolite Type-5MD, and Tyfo WR-AFP in the temperature range of 20-1000°C. Thermal properties including thermal conductivity, specific heat, thermal strain, and mass loss were measured in this test program. The study inferred that the thermal properties of the SFRM insulation materials varied significantly with temperature. Further, property relations were proposed in this study, which can be used for defining the material properties of insulation in numerical models for evaluating the fire resistance of steel structures.

The fire insulation is susceptible to undergoing delamination or fracture under blast or impact, which can occur before or during a fire incident in a building. The development of high dynamic interfacial stresses at the SFRM-steel interface in highly stressed regions of the structure and the poor bond between steel and SFRM insulation are the main causes of delamination [99]. Delamination of fire insulation can result in increased exposure of steel members to fire

temperatures, which leads to a faster degradation in the mechanical properties of steel, and in turn more delamination and an early onset of failure in the member. Most of the studies assume that the fire insulation remains intact while evaluating the fire resistance of steel structures. There are very limited studies that include the effect of delamination in the analysis of steel framed structures and most of these studies evaluate the effect of delamination under seismic or impact loading [99–102].

Arablouei and Kodur [99] applied a fracture mechanics-based approach to evaluate the delamination of SFRM insulation from a steel beam-column subjected to blast loading. Results indicated that the extent of delamination can be directly related to the blast overpressure and insulation thickness, and inversely related to the elastic modulus and fracture energy of the insulation. Based on these results, a delamination characteristic parameter was proposed that defines the extent of delamination that occurs in the member following blast loading. Using the extent and location of delamination from the above study, Arablouei and Kodur [102] further explored the effect of loss of insulation during fire exposure following an explosion or seismic event. Results showed that the consequences of delamination of fire insulation over the plastic hinge regions in a beam and from the column flanges can be adverse to the fire resistance of the structure. However, the studies used a pre-defined delaminated member for the fire resistance analysis and the delamination that can occur during fire exposure was not modeled.

## **2.8 Local instability effects on fire performance of steel structures**

The stability limit state is a key consideration in the ambient temperature design philosophy of steel members. However, the current fire design provisions neglect the effect of sectional instabilities in evaluating the failure of steel structural members. The susceptibility of a steel section to undergo local buckling depends on the width-to-thickness ratio (slenderness) of each of

the cross-sectional elements. This effect is accounted for in evaluating the capacity of the member under room temperature conditions. For instance, the AISC manual [103] classifies the steel sections based on the slenderness ratio of flanges and web into a compact, non-compact, and slender section and recommends a reduced capacity based on the section classification. Limiting values of the width-to-thickness ratio of steel sections are a function of stiffness and strength properties ( $\sqrt{E/f_y}$ ) of steel.

When steel structures are exposed to fire, the strength and stiffness properties of steel begin to degrade at about 400°C and 150°C respectively, and these properties degrade at different rates as shown in Figure 2.2. Since no specific recommendations are specified in the current standards for the limiting slenderness ratios at elevated temperatures, the room temperature criteria for section classification are often applied to fire conditions in advanced analysis and this can be unrealistic [33]. Moreover, since the stiffness (modulus) starts to degrade at 150°C itself and at a faster pace, the susceptibility of local buckling at lower temperatures (in the 150°C to 400°C range) increases and may lead to a reduction in capacity [33]. This loss in capacity in addition to the temperature-induced strength degradation of steel needs to be properly accounted for in the fire resistance analysis of steel structures. Very few studies have incorporated the effect of local buckling in steel sections while tracing the fire response of steel structures, primarily at a member level. These studies are summarized in Table 2-5 and discussed herein.

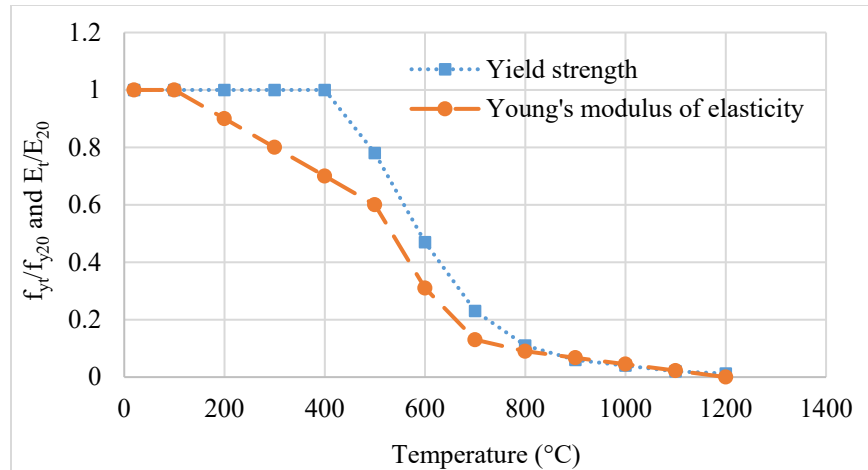


Figure 2.2. Degradation of strength and stiffness properties of steel at elevated temperatures.

Table 2-5: Reported numerical studies that incorporate local buckling effects in fire resistance analysis

Reference	Structural member	Main Findings
Uy and Bradford [104]	Cold-formed steel plates	<ul style="list-style-type: none"> <li>• Except for slenderness values less than 30, elastic local buckling was found to occur in all plates at elevated temperatures.</li> <li>• Recommendations for the assignment of slenderness limits at elevated temperatures are provided.</li> </ul>
Heidarpour and Bradford [105]	Steel beam	<ul style="list-style-type: none"> <li>• The combined loading effects have a significant influence on the local buckling response, and on the limiting depth to thickness ratio that delineates a non-compact section at elevated temperatures.</li> <li>• When <math>T &lt; 300^{\circ}\text{C}</math>, the beam web that is classified as non-compact at ambient temperature can become slender at elevated temperature. When <math>T &gt; 300^{\circ}\text{C}</math>, a web that is non-compact at ambient temperature will also be non-compact at elevated temperature and one that is slender at ambient temperature may become non-compact at elevated temperature.</li> </ul>
Seif and McAllister [35]	Wide flange steel columns	<ul style="list-style-type: none"> <li>• Local buckling was observed in members with slender flange and/or web elements with <math>b/t_f &gt; 10</math> and <math>h/t_w &gt; 35</math>.</li> <li>• Localized flange buckling was only reported in members with slender web elements with <math>h/t_w &gt; 35</math>. In these members, the flanges acted as two independent columns, and each flange buckled about its minor axis near the support section of the member.</li> </ul>

Table 2-5 (cont'd)

Kodur and Naser [33]	Steel beams	<ul style="list-style-type: none"> <li>• Room temperature classification of steel beams based on local stability can change with fire exposure time.</li> <li>• A compact section under ambient conditions can change to non-compact/slender at elevated temperatures and this change can result in the early onset of failure before flexural yield and/or shear limit states.</li> </ul>
Agarwal et al. [11]	Steel columns	<ul style="list-style-type: none"> <li>• Column strength and failure behavior depended on the slenderness, axial loading, and heating configuration, and the main failure modes observed included flexural buckling about weak and strong axes and flexural torsional buckling.</li> <li>• No discussion on local buckling trends was provided.</li> </ul>
Chen et al. [34]	3-story moment frame	<ul style="list-style-type: none"> <li>• Results indicated that the explosion resulted in local buckling and permanent deformation in the affected structural members, which in turn may trigger instability in the frame when it is later exposed to fire.</li> <li>• The study did not consider varying column slenderness, thermal gradients due to fire, and realistic failure limit states.</li> </ul>

Uy and Bradford [104] used an inelastic semi-analytical finite strip method to study the local buckling in thin steel plates at elevated temperatures. A parametric study was carried out by varying the support conditions for the plates and strain gradients. Results indicated that except for slenderness values less than 30, elastic local buckling will occur for all other scenarios at elevated temperatures. Based on the parametric study, recommendations are given for the assignment of slenderness limits for plates at elevated temperatures. Heidarpour and Bradford [105] studied the elastic local buckling of the web of an I-section beam subjected to combined axial, bending, and shear forces. A modified spline finite strip method was utilized to analyze the local buckling effects by accounting for the variation in material properties through the web at elevated temperatures. The study showed that the combined loading effects have a significant influence on the local buckling response and the limiting depth to thickness ratio that delineates a non-compact section at elevated temperatures. Results from the study indicated that when the temperature ( $T$ ) is less than  $300^{\circ}\text{C}$ , the beam web that is classified as non-compact at ambient temperature can become slender at elevated temperature. When the temperature is above  $300^{\circ}\text{C}$ , a web that is non-compact

at ambient temperature will also be non-compact at elevated temperature and one that is slender at ambient temperature may become non-compact at elevated temperature.

Seif and McAllister [35] investigated the local and global buckling modes in wide flange steel column sections under varying load and temperature conditions. Nonlinear finite element analysis was carried out using ANSYS in which material nonlinearity, residual stresses, and geometric imperfections were incorporated. Local buckling was observed in members with slender flange and/or web elements with a width ( $b$ ) to thickness ( $t_f$ ) ratio greater than 10 and depth ( $h$ ) to thickness ( $t_w$ ) ratio greater than 35. Localized flange buckling was only reported in members with slender web elements with a depth ( $h$ ) to thickness ( $t_w$ ) ratio greater than 35. In these members, the flanges acted as two independent columns, and each flange buckled about its minor axis near the support section of the member. Kodur and Naser [33] carried out numerical studies using ANSYS finite element software to study the fire behavior of steel beams taking into consideration the temperature-induced sectional instabilities. Results from the numerical studies were used to evaluate the failure of beams under different limit states including flexure, shear, sectional instability, and deflection criteria. The study indicated that the room temperature classification of steel beams based on local stability can change with fire exposure time. Results showed that a compact section under ambient conditions can change to non-compact/slender at elevated temperatures and this change can result in the early onset of failure before flexural yield and/or shear limit states.

Agarwal et al. [11] evaluated the effect of thermal gradients in steel columns subjected to fire loading experimentally and numerically. Effects of geometric imperfections at local and global levels were incorporated into the numerical model. Results showed that the column strength and failure behavior depended on the slenderness, axial loading, and heating configuration, and the

main failure modes observed included flexural buckling about weak and strong axes and flexural torsional buckling. Although local buckling effects were included in the analyses, no discussion was provided regarding the trends observed in the study. Chen et al. [34] studied the behavior of a three-story moment frame subjected to a localized explosion followed by fire loading. The study used a mixed element approach in which the members that were directly subjected to the blast and fire loading were modeled using shell elements, whereas the other members in the frame were modeled using beam elements. The study found that explosion resulted in local buckling and permanent deformation in the affected structural members, which in turn may trigger instability in the frame when it is later exposed to fire. Failure under fire exposure was evaluated based on critical steel temperatures. The study, however, did not give due consideration to varying column slenderness, thermal gradients due to fire, and realistic failure limit states.

## **2.9 Fire resistance provisions in standards and codes**

Most building codes specify the minimum required fire safety requirements and regulations in buildings to ensure life safety, health, building usability, and public welfare, including property protection. In the United States, two building codes are used in practice: International Building Code (IBC) 2021 [106] and NFPA 5000 [107]. These codes specify minimum fire resistance ratings for different structural elements, including framing members, floor assemblies, bearing walls, etc. based on the type of the structure, occupancy, and existing fire suppression systems in the building (e.g., automatic sprinklers). These ratings are highly prescriptive as they are based on standard fire test procedure and acceptance criteria specified in ASTM E119 [27] or UL 263 [108] provisions.

Steel-framed building systems and components in the US are to be designed as per the AISC design manual [103] and ANSI/AISC 360-16 [37] standard. The structural design for fire conditions is

included in the appendix of the ANSI/AISC 360-16 standard [37] which allows for the design of steel members using simplified or advanced calculation methods and by qualification testing per ASTM E119 [27]. Simplified approaches include the use of Lumped Heat Capacity Analysis for computing temperature rise in steel and fire resistance of unprotected and protected steel members. For advanced calculation methods, only general recommendations are given in the standard to account for the deterioration in strength and stiffness with increasing temperature, the effects of thermal expansions, large deformations, time-dependent effects such as creep, and uncertainties resulting from variability in material properties at elevated temperature. However, no specific guidance is given on how to account for creep effects in the fire resistance analysis.

Apart from the AISC standard and design manual, ASCE/SFPE 29 [36] is another standard that is used for the fire resistance design of steel members. This standard provides analytical approaches and empirical relations for evaluating the fire resistance (or ratings) of different structural steel members. The approaches specified in this standard are developed based on results from standard fire tests carried out on steel members. The European codes, namely, Eurocode 3 [18] and Eurocode 4 [109] provide both simplified and advanced calculation methods for evaluating the fire resistance of steel and composite structural members respectively. The simplified approaches are based on evaluating the critical steel temperature through thermal analysis or evaluating the reduced capacity at a critical section by considering the reduction in strength and stiffness of steel with rise in temperature. These methods are at a sectional level and are applicable to steel members subjected to standard fire exposure. The advanced calculation method in Eurocode 3 and 4 involves detailed thermal and mechanical analyses that required the use of sophisticated finite element programs. Even these methods are mostly for a member or an assembly level analysis and no specific guidelines for a system level analysis of steel structures are specified in these codes.

For the design of buildings against progressive collapse, the Unified Facilities Criteria (UFC) [110] and General Service Administration (GSA) guidelines [111] provide detailed guidelines including direct and indirect design approaches for room temperature conditions. The direct design approaches include the use of alternate path methods to determine the robustness of the structure to resist progressive collapse. The design documents recommend the use of any one of the three analysis approaches, namely, linear static analysis, nonlinear static analysis, and nonlinear dynamic analysis to determine the resistance of the structure against progressive collapse. On the other hand, the indirect design approaches include the provision of minimum strength, continuity, and ductility in different structural members. These recommendations are generic and there are no specific guidelines for elevated temperature conditions, especially for evaluating fire-induced instability in steel structures. Currently, there are very limited guidelines on system level analysis and design of buildings against fire-induced progressive collapse, only including general recommendations in ANSI/AISC 360-16 [37], IBC 2021 [106], and NFPA 5000 [107]. No specific guidance in incorporating high-temperature creep effects is given in the current standards.

### **2.10 Knowledge gaps**

The state-of-the-art review presented in this section indicates that fire can be a major threat to the stability of steel framed structures. The onset of instability in steel framed buildings can occur at local, member, or system levels and in severe cases lead to the progressive collapse of the structure. Such a failure would jeopardize the safety of the occupants and first responders, provide insufficient time to tackle the disaster, and affect the integrity of the building itself. Although the fire behavior of steel structures has been well studied at material and member levels, very limited studies have accounted for the system level behavior of steel framed structures under fire scenarios.

Based on the comprehensive literature review, the following are the key knowledge gaps that require further research:

- Limited studies are available in the literature that evaluates occupant evacuation scenarios in high-rise buildings under fire conditions, specifically incorporating situational awareness during an emergency evacuation. These scenarios together with the fire-induced progressive collapse timelines are needed to determine if the building can provide a safe environment during a fire event.
- There is limited data on the system level behavior of steel framed structures exposed to fire conditions, including the onset of mechanisms that lead to the fire-induced progressive collapse of buildings.
- Effect of realistic fire scenarios, including the intensity and duration of fire exposure, the extent of fire spread (number of compartments/floors burning), the spread of fire from one compartment (floor) to another on the onset of instability in steel framed buildings have not been fully evaluated.
- There is no data on the effect of temperature-induced transient creep on the onset of instability in steel-framed structures, including the failure (collapse) mechanisms.
- Limited numerical models are available in the literature that traces the system level response of steel framed structures under realistic load, restraint, and fire scenarios. Most of the current models do not account for the effects of the floor system and transverse framing. Moreover, the full effects of temperature-induced creep and local buckling effects are not accounted for explicitly in the fire-induced progressive collapse analysis.
- There are currently no limiting criteria for evaluating the global failure of steel-framed structures under fire exposure conditions.

- Very limited guidelines are available in current codes and standards for carrying out advanced analysis to evaluate the system level behavior, including the progressive collapse of steel framed structures under fire scenarios. There are no specific guidelines for the treatment of high-temperature creep and local buckling effects in the fire resistance analysis of steel framed structures.

### 3 Emergency Evacuation in High-Rise Buildings

#### 3.1 General

Buildings, as opposed to other structures, are more susceptible to adverse effects during a fire incident since the resulting high temperatures, toxic gases, and structural damage can lead to occupants being trapped in the building, particularly in the case of high-rise buildings. For this reason, buildings are to be equipped with various fire safety features to ensure the safety of occupants. As discussed in Chapter 1, the primary objective of fire safety design in buildings is to minimize the death and injury of occupants, in addition to minimizing property and environmental damage. To achieve this objective, current building code provisions specify several fire safety measures such as the installation of smoke detectors, sprinklers, and as well as suitable egress paths.

The egress system in a high-rise building often comprises one or more egress components such as stairways, refuge floors, sky bridges, etc. The geometric characteristics of the egress system such as width, number, and arrangement of exit paths (stairs) determine the efficiency of the evacuation process. These factors are usually stipulated in the building codes such as the IBC 2021 [106] and are prescriptive. The code provisions establish the minimum requirements for the design of an egress system and often do not account for all critical issues that arise during an emergency evacuation.

Moreover, the behavior of humans during emergencies also plays a critical role in building evacuation. Occupants tend to get involved in different activities, such as, locating the nearest exit path, trying to put off the fire, warning and searching for fellow occupants, etc., which cause delays in the evacuation process [45]. The speed and movement of occupants through the egress routes

are affected by human factors such as age, gender, physical disabilities, behavioral patterns, etc. [45]. In emergencies, such as a fire in a building, way-finding (i.e. how the evacuees find their way to the exits) also affects the flow of occupants due to issues arising from possible blockage of exit routes on account of smoke, counter flow during firefighting operations, etc. [112]. Past studies that consider the geometric analysis of egress components are based on the traditional “hydraulic model” calculations that are simplistic and do not account for human interactions and behavior during an emergency evacuation.

Further, the above-discussed factors influence the efficiency and speed of the evacuation process. For achieving the required safety in a building, the evacuation times should be designed such that they are less than the time to reach possible fire-induced progressive collapse of a building. To address these issues, this chapter examines the adequacy of the existing provisions for egress system design in high-rise buildings in facilitating emergency evacuation during a fire incident. Specific attention is given to incorporating recent changes made in the IBC 2021 [106] in terms of the number and sizing of egress components in high-rise buildings. A parametric study of different evacuation scenarios is conducted to quantify the effect of story height, fire location and size, and number and arrangement of exit paths. The evacuation simulations are carried out using the computer model Pathfinder [113], wherein, complex human behavior during evacuation such as collision avoidance and route choice are considered. Possible improvements and alternatives to the current code provisions are proposed to improve evacuation efficiency during emergencies. In addition, the impact of introducing situational awareness during an emergency evacuation is evaluated.

### **3.2 Egress parameters influencing fire evacuation**

Evacuation during a fire incident is usually complex and depends on several factors that can be grouped under one of the following categories, namely, the geometry of the building, fire characteristics, and human aspects [112]. Building geometry includes architectural layout, dimensions, and shape of the structure, number and arrangement of egress paths, travel distances, the separation between exits, etc. Gwynne et al. [114] inferred that the response of occupants during emergency evacuation directly depends on these factors, for example, preference to use certain exits, familiarity with the egress route, and wayfinding during the process of evacuation. Factors such as passive protection (fire resistance) measure present in the building also come under this category [45]. The construction materials used for the structural system and type of fire protection influence the fire resistance, and thus the time available for occupant evacuation and rescue operations.

Fire characteristics govern the nature of fire development and spread within the building. During the initial stages phase of the fire, the temperatures in the compartment tend to be low and the presence of smoke and toxic gases is also minimal. The majority of the evacuation should occur in this initial phase. Beyond the initial phase of the fire, evacuation becomes difficult due to increasing levels of temperature and smoke (toxic gases). The level of active fire protection (such as sprinklers, extinguishers, etc.) and compartmentation restrict the amount of fire spread that can occur within a building. Fire and resulting smoke spread hinder the movement of occupants through the egress system. Particularly, in evacuation through stairways, the possibility of smoke entering the stairwell due to the opening and closing of doors is very high [115]. A high concentration of smoke can lead to blockage or loss of egress routes which adversely affects the egress capacity of a building.

It should be noted that in emergencies such as fire, situational awareness is an additional factor that influences evacuation. Situational awareness indicates the capacity to evaluate the real-time response of occupants, structure, and environment. Situational awareness can provide the occupants and first responders with information regarding the burning location, temperature and smoke levels, etc. In addition, situational awareness may also be useful in evaluating the state of the building during the disaster, in terms of the extent of damage, available load carrying capacity, and probable imminent collapse (at a local or global level). Overall, situational awareness can aid occupants and firefighters in evacuation and fire-fighting operations.

Situational awareness during a fire event can be achieved by continuously monitoring key response parameters such as air temperatures and concentration of toxic gases in different compartments and cross-sectional temperatures and deformations in structural members through an interconnected network of sensors [23,24]. Typically, data from these sensors need to be analyzed through a processing system (wired or wireless) and subsequently transmitted to occupants and first responders to help in the decision-making process for evacuation and firefighting operations. Daniel and Rein [24] proposed such a model and this model incorporates techniques such as data assimilation, inverse modeling, and genetic algorithm using sensor data to predict the evolution of fire (such as smoke propagation and flame spread) in a building. A similar framework for implementing cognitive abilities to built infrastructure and the associated limitations are also detailed in the paper by Naser and Kodur [23].

Human factors also play a significant role in evacuation during emergencies. Characteristics such as age, gender, physical disabilities, etc. affect the movement, evacuation speed, and response of occupants. A review on human behavior during fire incidents in buildings by Kobes et al. [112] showed that it is essential to take a holistic approach to model building evacuation by incorporating

the characteristics of fire growth, human behavior, and building topology. In addition, Kuligowski et al. has also provided detailed discussions on human behavior in fire [46]. In this chapter, the influence of parameters pertaining to building and fire characteristics on the process of emergency evacuation is evaluated.

### **3.3 Evacuation simulations**

To examine the different geometric parameters of the egress components and quantify the positive impact of situational awareness, evacuation simulations during fire incidents in a building are carried out using Pathfinder. The details of the building used for the simulations, validation, and parametric studies are discussed in the following sections.

#### ***3.3.1 Description of building and evacuation simulation***

The building chosen for emergency evacuation simulations corresponds to a typical office occupancy structure in Denver, Colorado, USA [116] to represent realistic conditions. The building is 32-story high with a story height of about 3.05 m (10 ft). The floor layout is rectangular and has a floor area of about 2675.61 m<sup>2</sup> (36.58 x 73.15 m) (28800 sq. ft (120 x 240 ft)) (refer to Figure 3.1). The building has two staircases in the core of the building (represented as A and B in Figure 3.1). Additionally, the building has six occupant elevators and two service elevators. For this study, the building is assumed to have identical floors throughout its height and each floor is occupied by 250 occupants (refer to Figure 3.2). The assumed number of occupants falls slightly above the number that is required for a typical business (or office) building (as per IBC 2021 [106]) and will represent a worst-case scenario for evacuation studies. The percentage of male and female occupants considered are 57% and 43% respectively [113]. All dimensions and arrangement of the egress components assumed in the building are per IBC 2021 [106].

The evacuation simulation is carried out using Pathfinder 2018.3.0730 [113]. This computer program allows modeling the movement of occupants within the structure while accounting for points of congestion, queuing, and bottlenecks. Two modes, namely SFPE and steering, are offered by the software to model occupant motion. The first mode is based on the hydraulic model presented in the SFPE (Society of Fire Protection Engineers) handbook [45]. In this mode, occupant speed is controlled by density and the flow through the building is determined by the size of the egress components.

The verification and validation for this version of the software comprised of a detailed set of test cases designed to ensure that the simulations capture realistic behavior. The verification tests are synthetic tests that are specifically designed to examine the ability of the software to implement a particular evacuation mode or occupant behavior. Some of these tests include floor rate tests for each of the egress components, behavior tests that verify grouping behavior, merging, collision, etc., and speed tests [117]. Validation tests are based on published experimental data from the literature. These experiments include unidirectional and bidirectional flow in corridors, turning and merging behavior in T-junctions, etc. A more detailed description of these tests and results can be found in the Pathfinder verification and validation document [117].



Figure 3.1. Typical floor layout with the distribution of occupants.

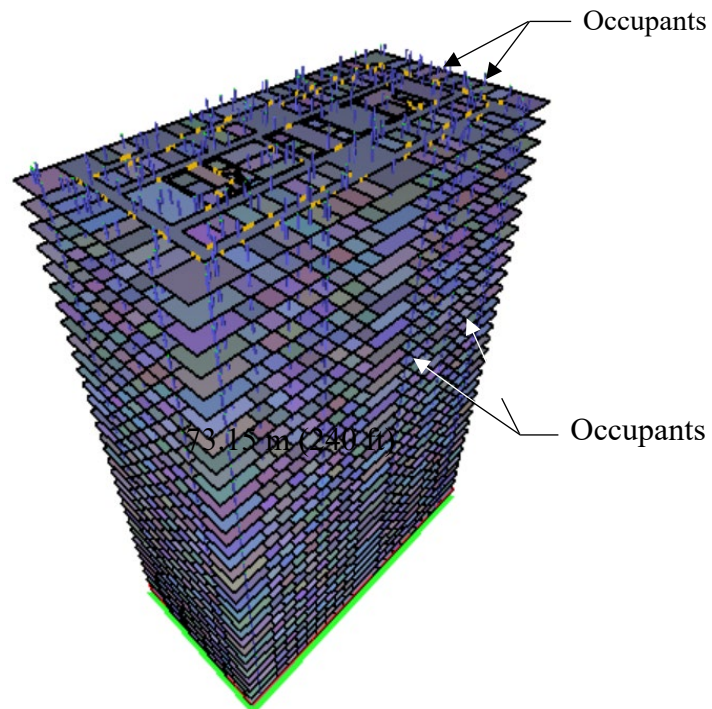


Figure 3.2. Side view of the 32-story high-rise building.

The second mode, steering, is more advanced and realistic in simulating occupant movement [113]. This mode allows for modeling complex occupant behavior and route choice based on the interaction between persons and collision avoidance. Unique characteristics may be assigned to individual occupants to implicitly simulate specific human behavior (response) during evacuation in an emergency. The steering mode in Pathfinder has been used in several evacuation studies [118–120] and also validated against field evacuation data reported in the literature.

Evacuation simulations are carried out to simulate the time required to evacuate a building during a routine fire drill versus an actual fire incident. Simulating the evacuation process during a fire drill aids in evaluating the performance of different egress parameters in a building. However, such simulations do not account for the continuously changing scenarios during a fire event such as inaccessible exit paths, complex occupant behavior, etc. that can cause a significant delay in the evacuation time. For this reason, the evacuation process during a fire incident is simulated to quantify the time required for all occupants to exit the building under such conditions. These simulations can help in the development of egress systems in buildings such that the emergency evacuation times are less than the time for potential structural collapse. Conversely, such simulations allow for a realistic evaluation of fire resistance ratings required in buildings that are based on actual evacuation times during fire emergencies.

### ***3.3.2 Evacuation analysis using the hydraulic model***

As discussed in Chapter 2, the hydraulic model is a simple analytical tool to evaluate evacuation time for a given building (or an egress component). This model gives a quick estimate of the egress performance and also a basis for carrying out a more detailed assessment of different evacuation scenarios (like buildings with complex floor layouts, occupants with different demographics, etc.). In this study, the evacuation time for the building described in the previous section is obtained

using the second-order approximation of the hydraulic model. All occupants are assumed to start egress at the same time and only stairways (not elevators) are used in the evacuation. Figure 3.3 shows the dimensions of the different egress components considered for computing the evacuation time.

To track the egress flow in the building, the flow capacity through the three points of transition, namely, corridors, doors, and stairways are computed based on the following equations.

$$\text{Speed, } S = k - akD \quad (3-1)$$

$$\text{Specific Flow, } F_s = SD \quad (3-2)$$

$$\text{Calculated Flow, } F_c = F_s W_e \quad (3-3)$$

where  $D$  denotes population density in persons per unit area,  $W_e$  are the effective width of the egress component and  $a, k$  are constants defined in SFPE Handbook [45]. The egress component with the least flow capability (measured in terms of  $F_c$ ) will govern the evacuation process.

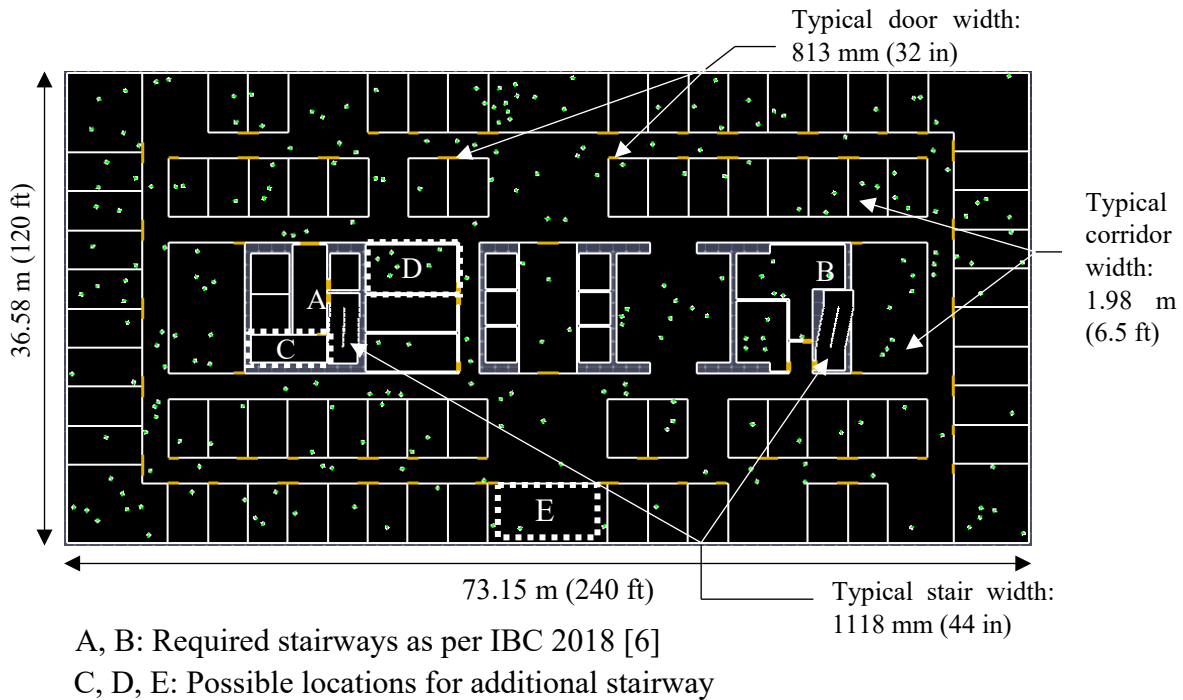


Figure 3.3. Floor layout with dimensions of different egress components.

The time ( $t_p$ ) required by a population ( $P_o$ ) to pass a point in the egress route with the calculated flow ( $F_c$ ) is given by

$$t_p = P_o/F_c \quad (3-4)$$

Using this approach, the evacuation time is found to be 84 min. The detailed calculations for computing the evacuation time using the hydraulic model can be found in Appendix A. Many computer programs, including Pathfinder (SFPE mode) [113], have implemented the hydraulic model approach to evaluate the evacuation time from different types of occupancies in structures. For crowded buildings, as in the case of the building analyzed here, the steering mode in Pathfinder allows capturing realistic occupant motion, including the time-consuming maneuvering that is required to get through the egress components with minimal wall-occupant and occupant-occupant collisions. Evacuation simulation of the building considered here is conducted using the steering mode in Pathfinder. For this purpose, the building is modeled in AutoCAD and imported to the Pathfinder software. The simulation parameters for steering mode, namely, steering update interval and minimum flow rate factor are taken as 0.1s and 0.1 respectively. The steering update interval controls how often (in simulation time) steering calculation gets updated. The higher the value the faster the simulation runs. However, it compromises the accuracy of the simulation as it affects the decision-making skills of the occupant. The minimum flow rate factor is used when occupants are deciding which door to use when there are queues at the doors. A non-zero value will always show the queue near the door to be flowing and hence, prevents the occupants from switching doors when the flow rate is low. This is similar to the actual scenario during an evacuation, as occupants in the building are typically not aware of whether or not the queue at a particular door is moving or not. The initial position of occupants on each floor is randomly assigned at the start of the analysis. All occupants are assumed to have a maximum (unimpeded) walking speed of 1.19

m/s (3.92 ft/s) per SFPE handbook guidelines [45]. The walking speed of occupants is automatically adjusted during the simulation based on population density and geometric characteristics of the egress components. Figure 3.4 shows the number of occupants remaining in the building as a function of time obtained using Pathfinder.

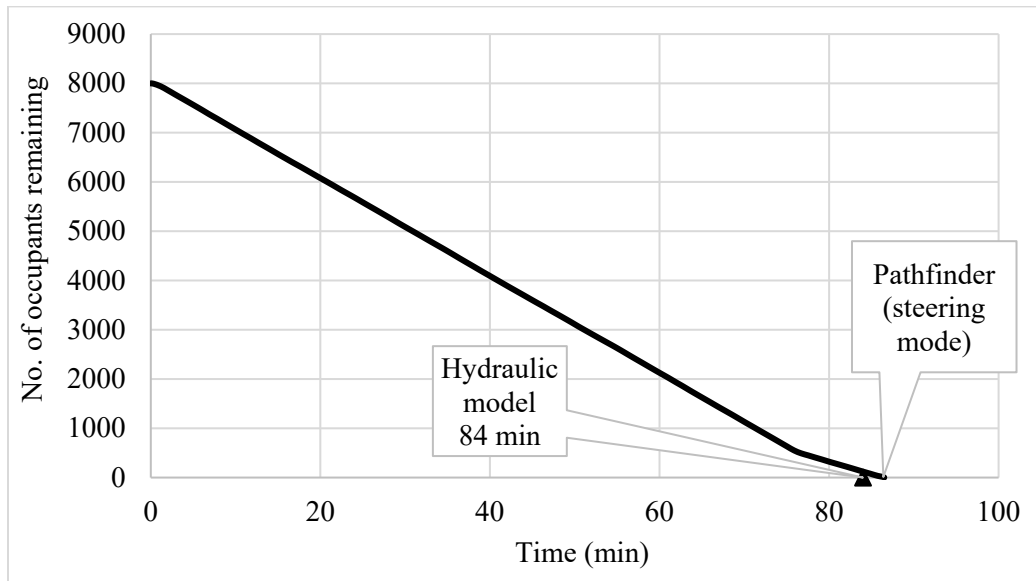


Figure 3.4. Comparison of evacuation time predicted using Pathfinder and hydraulic model.

The time-history plot indicates that the occupants required 87 minutes to evacuate the building. It is seen that the evacuation time predicted by the software (using the steering mode) is close to the one that is obtained using the hydraulic model. All the simulations that are carried out for the parametric study use the steering mode for modeling occupant movement.

### 3.3.3 Parametric study

The parametric studies are broadly grouped into two parts. In the first part, evacuation simulations are carried out under normal conditions (evacuation drill conditions) to understand the effect of geometric parameters on occupant behavior and egress performance. Four broad cases are considered in this part of the study, namely, the number of stories in the building, the location of stairways, the number of stairways, and the stairway width. As part of the first case, evacuation in

four different buildings with the number of stories varying from 20 to 80 is simulated to quantify the effect of varying occupant travel distances on evacuation time. In the second case, three different scenarios are considered for the location of stairways in the building. The first two scenarios follow the traditional layout of buildings, where all stairways are located within the core of the building. In the third scenario, two stairways are placed within the core of the building, while the other is placed outside the core. In the next case, the number of stairways in the building is varied. The first two scenarios consider two stairways and three stairways throughout the building height, whereas in the next two scenarios three stairways are used in the lower half and lower quarter of the building respectively, with two stairways in the upper stories. In the final (fourth) case, three different stairway widths varying from 1118 mm (44 in) to 1676 mm (66 in) are considered.

In the second part, evacuation during fire incidents is simulated. First, the effect of different fire locations is examined by considering fire in the lower portion of the building (stories 3 to 6), the middle portion of the building (stories 12 to 15), and the upper portion of the building (stories 25 to 28). Next, the effect of implementing situational awareness during fire evacuation is examined by considering two broad cases; one, where situational awareness is not accounted for in the evacuation simulation, and the other, where situational awareness is incorporated in the evacuation simulation. Table 3-1 summarizes the different cases considered in the parametric study.

Table 3-1: Evacuation time for different cases considered in the parametric study

Varied parameter	Cases	Stairways used (Refer to Figure 3.3)	Evacuation time (min)
<b>Evacuation drill (during normal conditions)</b>			
Number of stories	20 stories	A-B-C	63
	32 stories	A-B-C	113
	40 stories	A-B-C	150
	80 stories	A-B-C	291

Table 3-1 (cont'd)

Location of stairways	Three stairways within the core	A-B-C	113
	Three stairways within the core	A-B-D	67
	Two stairways within the core and one outside core	A-B-E	74
Number of stairways	Two stairways	A-B	87
	Three stairways	A-B-D	67
	Two in the top 16 and three stairways in the bottom 16 stories	A-B in the top 16 and A-B-D in the bottom 16 stories	72
	Two in the top 24 and three stairways in the bottom 8 stories	A-B in the top 24 and A-B-D in the bottom 8 stories	80
Stairway width	1118 mm (44 in)	A-B-C	113
	1397 mm (55 in)	A-B-C	102
	1676 mm (66 in)	A-B-C	80
<b>Evacuation during fire incidents</b>			
Fire location	Fire occurring in between stories 3 to 6	A-B	182
	Fire occurring in between stories 12 to 15	A-B	152
	Fire occurring in between stories 25 to 28	A-B	117
Without situational awareness (fire occurring in between stories 3 to 6)	Two stairways	A-B	182
	Three stairways	A-B-D	118
	Two in the top 16 and three stairways in the bottom 16 stories	A-B in the top 16 and A-B-D in the bottom 16 stories	122
	Two in the top 24 and three stairways in the bottom 8 stories	A-B in the top 24 and A-B-D in the bottom 8 stories	133
With situational awareness (fire occurring in between stories 3 to 6)	Two stairways	A-B	172
	Three stairways	A-B-D	92
	Two in the top 16 and three stairways in the bottom 16 stories	A-B in the top 16 and A-B-D in the bottom 16 stories	98
	Two in the top 24 and three stairways in the bottom 8 stories	A-B in the top 24 and A-B-D in the bottom 8 stories	101

### 3.3.3.1 Evacuation drill conditions

#### 3.3.3.1.1 Number of stories

The height of a building is a crucial factor that affects evacuation time. As the number of stories increases, occupants need to travel greater distances to exit the structure (building). The number of occupants also increases proportionally with an increase in building height. For instance, with

an occupant load of 250 per floor, a 40-story building will have 10000 occupants as compared to 5000 in a 20-story building. The WTC twin towers that collapsed during the 9/11 attack were 110 stories tall with full occupancy (theoretical) of around 50000 people [7]. The IBC provisions for the number of stairways required were updated following the 9/11 review for high-rise buildings. Except for residential occupancy, all buildings that are more than 128 m (420 ft) in height need one additional stairway more than the minimum required as per the occupancy load per story [106]. The redundant stairway is treated similarly to the other stairways and is permitted to be used under normal conditions. Though there is a significant increase in the total number of occupants with building height, the minimum number of stairways continues to be dependent only on the occupant load per story. It is not known whether one additional stairway will be sufficient for timely evacuation from skyscrapers (buildings exceeding 128 m (420 ft) in height), especially in the event of an emergency. Evacuation simulation of buildings with four different numbers of stories is conducted. The floor plan with three stairways (A-B-C) is adopted for this study.

The results show that the time required to evacuate the building can be significantly longer as the height of the building increases (refer to Figure 3.5). The evacuation time almost doubles when the number of stories increases from 40 to 80. About 291 min (more than 4.5 h) is required for evacuation in the case of the 80-story building with 3 stairways under normal conditions. Further, in the event of a fire, the evacuation time is bound to increase [45]. It is evident from this study that the provision of one additional stairway above the minimum requirements may not be sufficient for evacuating occupants from skyscrapers. Alternate means of egress need to be provided to ensure timely evacuation. According to NFPA 101 [121], for stairs in new buildings serving 2000 or more occupants (from all stories above the level where the stair is considered), the minimum width of the stairway needs to be 1420 mm (56 in). For buildings with 32, 40, and 80

stories, the stairways in the lower levels are likely to fall under this category. The evacuation times simulated are likely to improve if NFPA provisions for stairway width are adopted in these buildings.

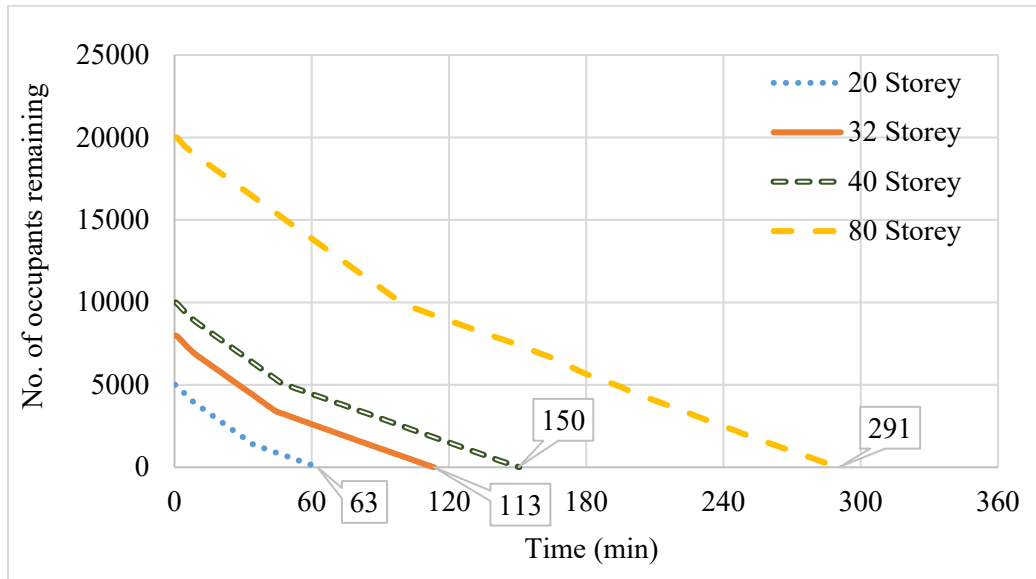


Figure 3.5. Evacuation time with different story heights.

### 3.3.3.1.2 Location of stairways

Stairway location in a high-rise building is one of the primary parameters that is considered in the design of the egress system. The layout of stairways tends to affect occupant behavior during an emergency evacuation. Kobes et. al [112] noted that the choice of a route that the occupants use depends on the location and accessibility of the exit stairways, complexity, and familiarity with the egress layout. As per IBC 2021 [106], the stairway arrangement is decided based on the distance that the occupants need to travel to reach the nearest stairways on a given floor. The maximum travel distance is restricted to 22.9 – 38.1 m (75-125 ft) based on the type of occupancy [106]. However, this distance does not account for the considerable number of floors that occupants need to travel before exiting the building. Further, IBC 2021 also requires two stairways in a building to be spaced from each other at a distance not less than 9.14 m (30 ft) or not less than

one-fourth of the maximum diagonal distance of the building, whichever is lesser. This building code, however, does not stipulate a minimum separation distance for any additional stairways that may be required in high-rise buildings (exceeding 128 m (420 ft) in height). In this study, three different stairway arrangements (which are allowed as per IBC 2021 [106]) are considered (see Figure 3.3). The location of stairways is such that the maximum travel distance from any occupiable point on the floor to the closest exit is 100 ft. This follows the IBC 2021 [106] provisions for business buildings with sprinkler systems. In two of the cases (A and B), all three stairways are placed within the building core (as in the case of collapsed WTC twin towers). In the third case I, evacuation with one of the stairways located outside the core is examined. Though the position of stairway E is shown within the building, it is always possible to locate the stairway outside the building layout to avoid losing the occupiable floor area. It is assumed that the difference in the evacuation time between the two positions will not be significant.

Figure 3.6 shows that the evacuation time is maximum in case A (where two of the stairways are located close to each other, as shown in Figure 3.3). It should also be noted that the time to evacuate in this case is greater than that required when only two stairways are present (see Figure 3.6). The possibility of an increase in congestion (or potential blockage) due to the addition of a stairway needs to be considered while designing the egress system. Additionally, in case A, there is a common wall between the two of the staircases, A and C. From a fire incident point of view, any damage to the wall will affect both the stairways and hence impact the exit capacity of the building. Cases B and C give similar evacuation times of about 67 minutes and 74 minutes respectively. Stairways are often located within the building core (as represented by case B (A-B-D)) due to economic reasons. As the core is centrally positioned, stairways that are present within the core are equally accessible from all sides of the building, and hence reduce the travel distances of the

occupants. During fire incidents or other emergencies, blockage of one of the stairways (and the exit route) can be handled more effectively by using a stairway arrangement with greater separation distance (or remoteness). From this perspective, it is beneficial to consider the possibility of positioning one stairway outside the core (as shown in case C (A-B-E)).

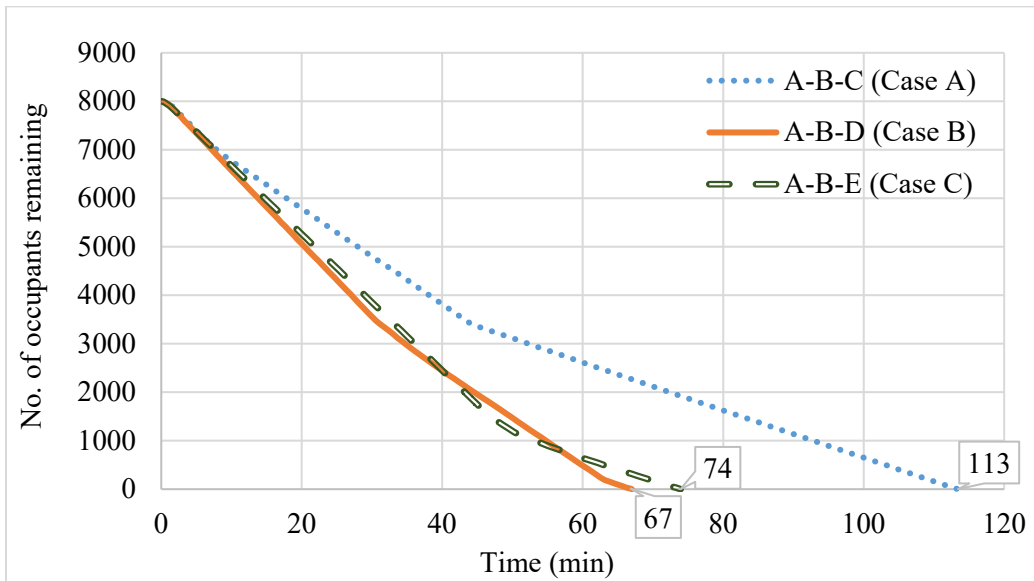


Figure 3.6. Evacuation time for different locations of stairways.

### 3.3.3.1.3 Number of stairways

The number of stairways required in a high-rise building is determined as a function of the occupant load per story. The IBC 2021 provisions require a minimum of two stairways when the occupant load per floor is 500 or less [106]. An increase in the occupant load per story necessitates a higher number of stairways. As the stairways can utilize some amount of occupiable floor area in every story, increasing the number of stairways throughout the building height can be uneconomical. In this study, the number of stairways is increased only in the lower section of the building where the amount of congestion is expected to be high during evacuation. It is assumed that the occupants are familiar with the additional stairway and will relocate when they reach the lower levels of the building. Four cases are examined; two stairways; three stairways (A-B-D);

three stairways in the bottom sixteen stories; and three stairways in the bottom eight stories (refer to Figure 3.3 for the building geometry).

Results from the numerical study (see Figure 3.7) indicate that the evacuation time is minimum for the case with 3 stairways (about 23% reduction in evacuation time as compared to 2 stairways). A greater number of stairways, when carefully located such that no congestion occurs, increases the exit capacity of the building. This can allow more occupants to be evacuated in a given duration of time. In this study, it is noted that the amount of queuing that occurs on the lower floors is much higher as the entire evacuating population from the higher stories needs to pass through the lower-level stairs. From the results for the last two cases, providing an additional exit in the lower part of the building helps reduce the congestion/queuing on the lower floors. The case where 2 stairways are provided in the top 16 stories, whereas 3 stairways in the bottom 16 stories are found to be the optimal case that results in a 17% reduction in evacuation time. The total evacuation time, in this case, is almost similar to that in the case of three staircases provided in all the stories. Such a design will also be an economically more viable option than increasing the number of stairways throughout the building height. However, it is noted that in a real-life situation, people will tend to stay in the same stairway that they started in and may not move to the additional stair when they reach the lower levels of the building. Hence, these scenarios will be more appropriate when situational awareness is considered, and a methodology is developed to have occupants selectively relocate to the additional stairway. Evacuation under these scenarios with situational awareness is discussed in the later part of this paper.

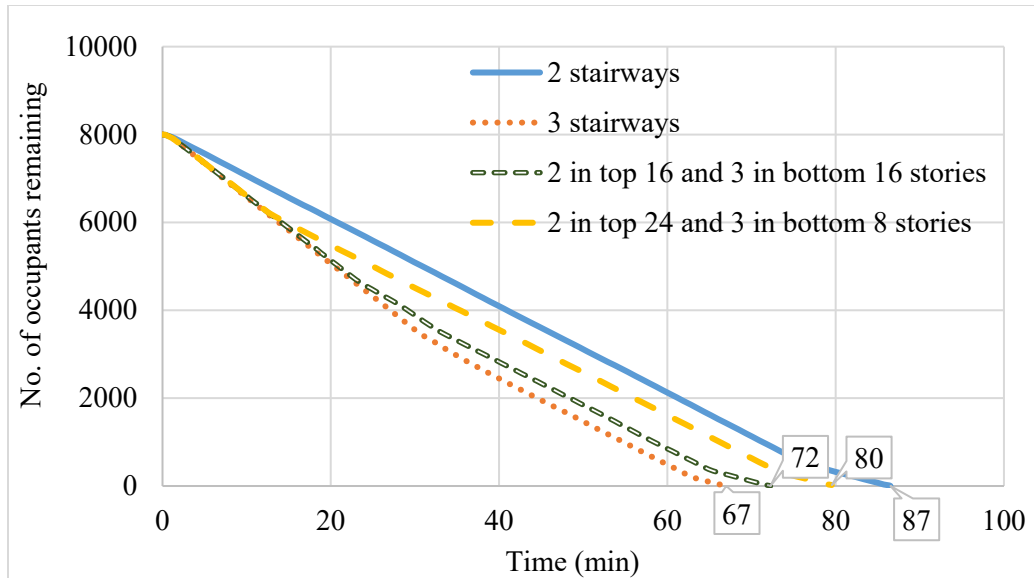


Figure 3.7. Evacuation time with a varying number of stairways.

#### 3.3.3.1.4 Stairway width

The width of the stairway directly determines its capacity and controls the flow of persons passing through the stairway at any given time. Stairway width is a function of occupant load per story. If a higher fraction of the occupants tends to use the stairways, sufficiently increased width of stairs is necessary. The IBC 2021 requires that the minimum clear width of stairways be 1118 mm (44 inches) [106], except, if the occupant load served by the stairway is 49 or less, the code allows the use of 914 mm (36 inches) stairway. While evacuating using stairways, people maintain a boundary layer clearance (between themselves and the wall faces), and only the middle portion of the stairways is effectively used [5]. Often, other projections present within the stairways (such as handrails, etc.) also affect the effective width used during an evacuation. In a fire situation, stairways are prone to be affected by smoke, especially near the floors that are exposed to fire [45]. Increased width of stairs can accommodate increased rows of evacuees and also counterflow that may occur during an emergency evacuation. In this study, the stairway width is varied and the evacuation time in each of the scenarios is studied. Three stairway widths are examined: minimum

required width (1118 mm (44 in)), 25% increased width (1397 mm (55 in)) and 50% increased width (1676 mm (66 in)). 3 stairways with configuration A-B-C are adopted.

Typically, stairways with a width of 1118 mm (44 in) are considered to accommodate two separate files of occupants comfortably, with 559 mm (22 in) for each file. The choice of a 25% increase in stairway width (leading to 1397 mm (55 in) wide stairways) is considered with a view to accommodating an intermediate staggered file of occupants in addition to the existing two files of occupants. A 50% increase in stairway width (resulting in a 1676 mm (66 in) wide stairway) will have 559 mm (22 in) above 1118 mm (44 in) and can comfortably accommodate three files of occupants. The present study adopts the default occupant profiles available in Pathfinder where occupants are modeled as upright cylinders with a maximum width of 460 mm and height of 1.8 m. The dimensions of the occupants support the idea of realistically accommodating the additional person (or a staggered file) when the stairway width is increased by 25% and 50%.

Results plotted in Figure 3.8 indicate that an increase in stairway width by 25% and 50% lead to a 10% and 30% reduction in evacuation time respectively. Although increasing the size of the stairway significantly reduces the evacuation time, providing additional stairways or alternate means of egress is more beneficial under fire events. In this way, the loss of one of the stairways will not greatly reduce the exit capacity of the building. In certain buildings, the stairways on a given floor may not always be of equal width. Stairways of different widths are employed in high-rise buildings to provide access for large items (such as furniture, etc.) or aesthetic purposes. However, in the event of the loss of the bigger stairway due to fire, the available exit capacity of the building may be significantly reduced. It is important to consider this aspect while designing unevenly sized stairways for evacuation.

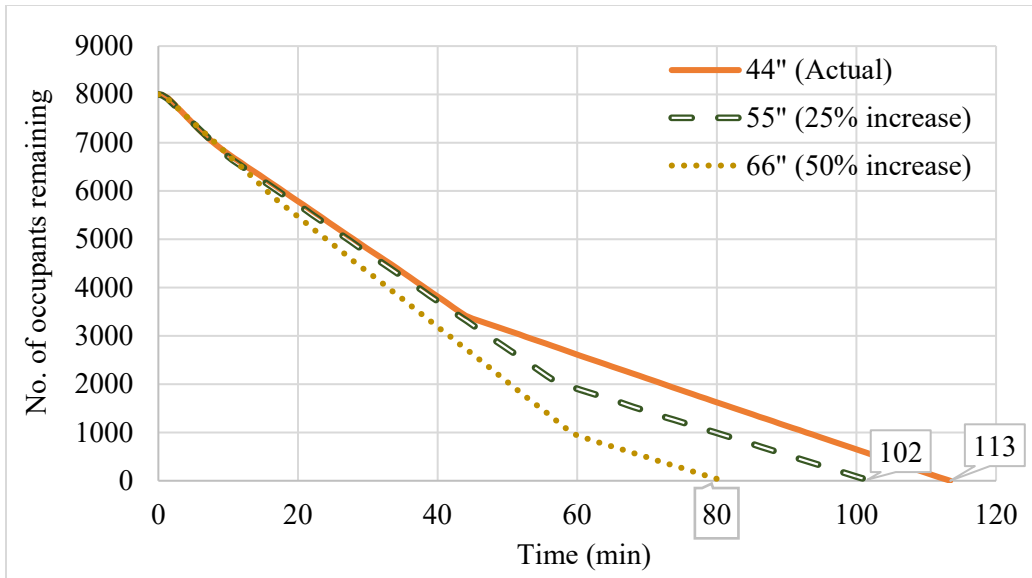


Figure 3.8. Evacuation time for different widths of stairways.

### 3.3.3.2 Fire conditions

#### 3.3.3.2.1 Fire Location

The location of the fire within a building is critical when studying evacuation times and efficiency. Fire location directly affects the portion of the building (or the egress route) that can be safely used by the occupants, as well as first responders during evacuation. Although the actual presence of fire may be contained to one (or more than one) floor, the effect of smoke spread can affect other stories as well [45]. This leads to unsafe egress paths (or blockage) on floors near the fire location that delays the process of evacuation. This study examines 3 fire locations across the building height; lower section (in between floors 3 and 6), mid-section (in between floors 12 and 15), and upper section (in between floors 25 and 28). Staircase A is considered to be blocked (i.e., inoperable for occupants) between the corresponding floors in each case due to a high concentration of smoke after a few minutes of fire.

The time history plot (Figure 3.9) shows that the total evacuation time, when the fire is present in the lower section of the building, is 55% and 20% higher than that when a fire is in the upper and

middle sections respectively. The larger queuing and congestion in the lower stories due to the inaccessible stairway (A) is the cause of longer evacuation time. As per statistics in the NFPA report [21], most fires begin on the lower floors of high-rise buildings, especially in the case of office occupancy. Additionally, prior studies have shown that buildings that experience a fire on the lower floors are prone to higher damage (and potential collapse). As a result, the available time for evacuation (or response operation) is reduced. The location of a potential fire in the lower section of the building should, hence, be treated as a critical case while designing the egress system.

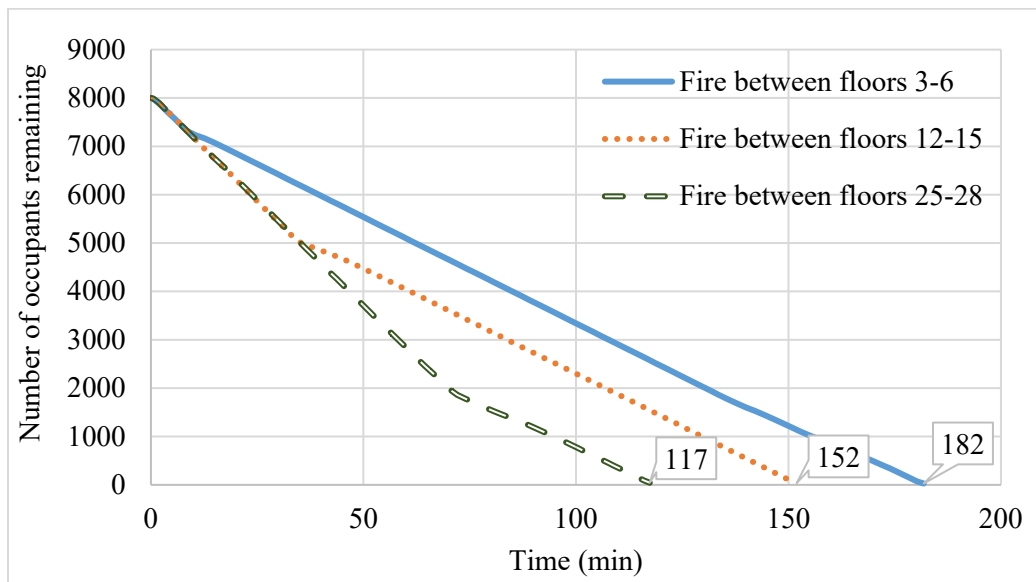


Figure 3.9. Evacuation time with different fire locations.

### 3.3.3.2.2 Situational awareness

To evaluate the influence of situational awareness, two scenarios are compared. In the first scenario, the time for evacuation is estimated in the event of a fire breakout. Fire is assumed to originate between floors 3 and 6 and the resulting smoke spreads vertically blocking stairway A between these floors. The behavior and route choice of individual occupants are suitably modified to account for evacuation under fire conditions with and without situational awareness. In the

simulation model, the occupant behavior is defined such that the occupants continue using the nearest egress path for evacuation. Upon reaching the sixth floor, the occupants trying to continue using stairway A understand (on their own) that stairway A is blocked. Some delay is expected from the time taken by the occupants to evaluate (realize) the situation and proceed to the next nearest exit. In the second scenario, the same fire incident is assumed. However, the occupants are now equipped with situational awareness where the status of fire growth and spread is continuously updated. To simulate this behavior, the occupants are updated with the information regarding the blockage in stairway A between stories 3 and 6. During the simulation, the occupants directly avoid using stairway A between stories 3 and 6 and use other available exits on those levels to evacuate. In all other stories, occupants make use of all three stairways. Figure 3.10 compares the evacuation time simulated with and without accounting for situational awareness when 2 and 3 stairways are provided in the building. The duration of evacuation during a fire drill is also plotted.

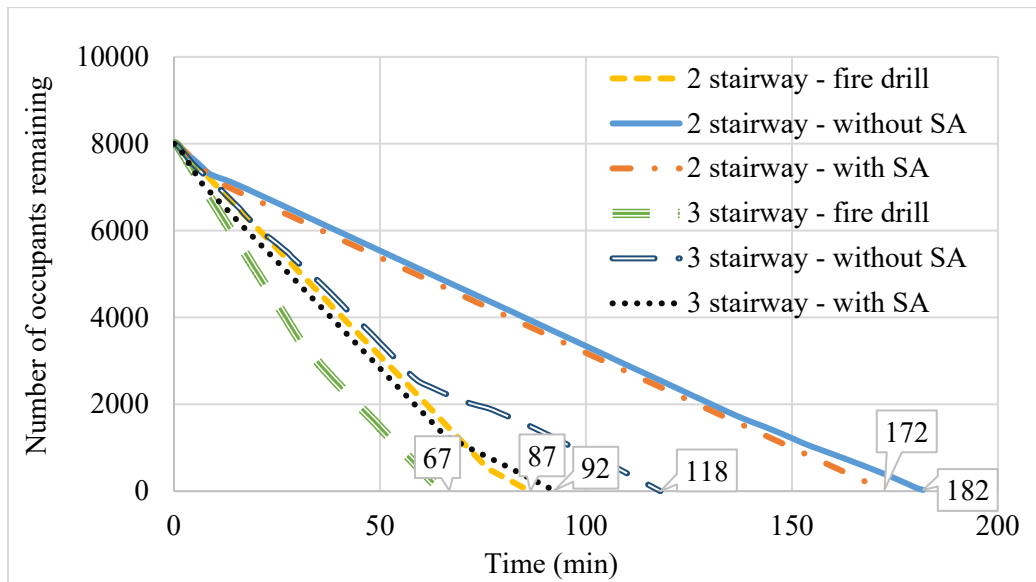


Figure 3.10. Evacuation simulation with a uniform number of stairways and situational awareness (SA).

In the building where only two stairways are used, blockage of one of the stairways in the lower section of the building due to fire breakout results in very long queues. The evacuation time

increases to 182 min during the fire event as compared to 87 min in the fire drill scenario (when there is no blockage of stairs). If the situational awareness provisions are incorporated in the building only results in 5% reduction in evacuation time is obtained. The delay that is caused due to queuing is more significant than that which results from occupants trying to evaluate and locate the available exit in the affected stories. When three stairways are provided throughout the building height, the evacuation time during the fire event is 35% lesser than in the case of two stairways. In addition, accounting for situational awareness is seen to result in a further 22% reduction in evacuation time, during a real fire incident.

The effect of situational awareness, while using an increased number of stairways in the lower portion of the building, is also evaluated. In case A, three stairways are provided in the lower 16 stories of the building, whereas, in case B, three stairways are provided in the lower 8 stories alone. When the evacuation simulation is carried out under fire conditions without accounting for situational awareness, results from Figure 3.11 show that there is a significant reduction in evacuation time (32% and 27%) in cases A and B as compared to the case where two stairways provided throughout the height of the building. When situational awareness is incorporated into the building, evacuation time is further reduced by 20% and 24% respectively in cases A and B. Further, from Figure 3.10 and Figure 3.11, it can be seen that the evacuation time obtained with situational awareness in cases A and B (98 min and 101 min respectively) is very close to that when 3 stairways are used through all stories (92 min). Using a higher number of exits in the lower stories is a better alternative even in the event of fire breakout and blockage of exits when situational awareness is implemented. It should be noted that the practical applicability of situational awareness faces serious challenges including the development of sensors, power, and

data mining requirements that need further research. More details on the current limitations in realizing cognitive structures can be found in the article by Naser and Kodur [23].

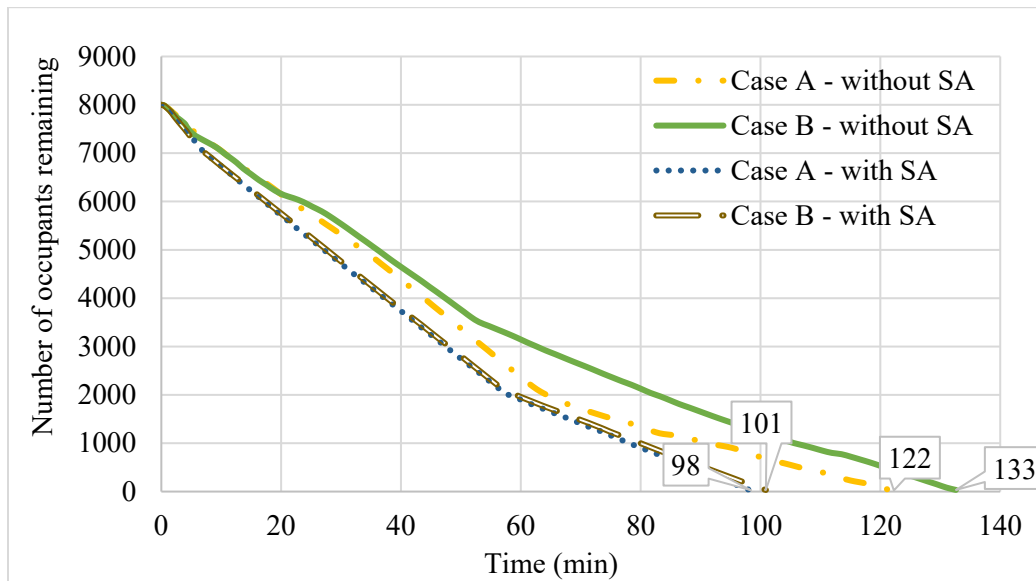


Figure 3.11. Evacuation simulation with a non-uniform number of stairways and situational awareness (SA).

### 3.4 Role of structural stability on emergency evacuation strategies

The focus of this evacuation study is limited to comparing the geometric parameters of the egress system to enhance the efficiency of egress performance. The likely change in evacuation time that can be achieved by adopting different alternatives to the egress design (such as a change in stairway width, number of stairways, etc.) is quantified. In addition, the evacuation times during fire conditions with or without adopting advanced techniques like situational awareness are also evaluated. Results from this study can provide insights to practitioners for the development of architectural layouts of high-rise buildings. Further, the evacuation times obtained under fire conditions can provide a more realistic estimate of the fire resistance ratings required for structural members in buildings. At present, the fire resistance ratings of different structural members are established without due consideration to the factors that influence the evacuation during a fire event (such as delays due to inaccessible routes, complex maneuvering of occupants during the

fire, etc.). On the other hand, the simulations presented in this study offer a more rational approach for evaluating the fire resistance ratings required in buildings. Additionally, the time savings that can be achieved using techniques such as situational awareness in emergency evacuation can be utilized to optimize the fire resistance requirements of different structural elements.

Realizing the evacuation strategies presented in this chapter rely heavily on the adequate structural performance of the building, especially during severe fires. The spread of fire and smoke, as well as structural damage, can result in insufficient time for complete evacuation to take place. Moreover, the reliability of other fire safety features in buildings (such as fire alarms, smoke detectors, and sprinklers) cannot always be guaranteed since the functionality of these fire safety devices may be compromised due to the damage resulting from severe fires. Further, in many instances, firefighting operations may not effectively take place due to constraints such as reaching the disaster location on time (long response times), the rapid growth of the fire, and large extents of fire spread. Hence, it is critical for the building to maintain stability and integrity during fire exposure without undergoing partial or complete collapse to provide sufficient time for safe evacuation and firefighting operations to take place. For these reasons, buildings are to be analyzed for structural stability while giving due consideration to the fire response of the structure at the system level, including fire-induced collapse. Such stability analyses can help in identifying weak regions in the structure and collapse timelines, and in turn in designing egress systems and strategizing the evacuation process and firefighting operations. The approach for tracing the fire-induced progressive collapse in steel framed buildings and the effect of various fire, material, and structural parameters are presented in the subsequent chapters.

### 3.5 Summary

The evacuation studies presented in this chapter, which evaluated the egress times in high-rise buildings under normal and fire conditions, resulted in the following observations:

- Evacuation time in high-rise buildings is highly influenced by the geometric parameters of the egress system including the number of stairways, their location, and width.
- Among the geometric parameters analyzed, the location of stairways influences the evacuation time the most. The reduction in evacuation time is highest (about 40%) when the location of the stairways is changed from A-B-C to A-B-D, owing to the decrease in travel distances and congestion offered by the latter configuration.
- Under fire conditions, the evacuation time is seen to be critically affected when the fire occurs in the lower levels of the building. Fire occurring in between stories 3 and 6 in a 32-story building with two stairways is seen to have a maximum evacuation time of 182 min.
- In the case of skyscrapers, providing one additional stairway in addition to the minimum requirements (as per IBC 2021 [106]) may not be fully effective (or sufficient) in achieving the timely evacuation of occupants. Total evacuation from a 40-story building using three stairways is found to take 2.5 hours, whereas the evacuation from a building with 80 stories takes about 4.5 hours.
- Increasing the number of stairways may not always reduce the evacuation time if the location of the additional stairway increases congestion. While an evacuation time of 87 min is obtained by using two stairways (A-B), the three stairs configuration A-B-C resulted in an evacuation time of 113 min. This location aspect is to be considered in the design of egress systems.

- Providing a higher number of stairways (or exits) in the lower section of the building alone is found to considerably reduce the evacuation time. A reduction in evacuation time of 32% and 27% is obtained by introducing an additional stairway in the lower half and lower quarter of the building (of 32 stories) respectively.
- Updating occupants with situational awareness during emergencies is shown to improve the efficiency of evacuation. Up to a 24% reduction in evacuation time was achieved when situational awareness is implemented in the evacuation of a 32-story building.
- The evacuation strategies presented in this chapter rely on the structure maintaining its stability and integrity during the fire event to allow the complete evacuation to take place, especially under severe fire exposure. Hence, for critical buildings, design for structural stability, including fire-induced progressive collapse is needed.

### 4 Numerical Model for Tracing Fire-Induced Progressive Collapse

#### 4.1 General

The evacuation studies presented in the previous chapter highlighted the need for structural stability in buildings to ensure the safe evacuation of occupants during emergencies. Design for structural stability under fire conditions requires a proper assessment of the fire behavior of the overall structural system, including fire-induced progressive collapse. Evaluating the fire response of structures through fire tests is quite expensive, complicated, and time-consuming. In addition, carrying out a fire test at a system level increases the complexity significantly and such large-scale tests require specialized equipment, sophisticated instrumentation, and skilled personnel. Even in these tests, only certain governing parameters such as temperatures and displacements can be measured at selected locations on the structure. Other parameters such as strains (including creep strains), local buckling effects, delamination of fire insulation, and load redistributions that are critical for evaluating the fire-induced collapse in steel structures cannot be measured. Besides, simulating the fire-induced collapse of a steel framed structure in a furnace setup can pose serious safety issues and hence, cannot be evaluated practically through experiments.

On the other hand, numerical modeling is an effective alternative to evaluate the fire response, including the collapse mechanisms, of steel framed structures. Using the numerical model, the influence of different governing parameters on fire-induced collapse can also be quantified. Further, such advanced numerical models can be utilized for developing disaster response and mitigation strategies by determining possible failure modes and global failure times. For this reason, a three-dimensional nonlinear finite element (FE) model is developed in ABAQUS to evaluate the fire-induced progressive collapse in steel framed buildings. The model accounts for

the variation of material properties with temperature, evolving load paths, creep and local buckling effects, geometric nonlinearity, and realistic failure limit states at member and global levels. The validity of the model in tracing the member and system level response is established by comparing the results obtained from the model with that of test data from experiments reported in the literature. The complete details of the numerical model and validation studies are presented in this chapter.

#### **4.2 Methods of analysis**

Fire resistance of steel framed structures can be evaluated using either prescriptive methods or performance-based approaches. The prescriptive methods include correlation methods, which use the listings in fire resistance directories, and empirical equations specified in codes and standards [1]. These methods can be applied to evaluating the fire resistance of steel members that are subjected to standard fire exposure. The performance-based approaches include rational approaches and advanced calculation models. The rational approaches apply simplified methods to evaluate the fire resistance of steel members but determine failure based on limiting temperature in the steel section or by checking the available sectional capacity at any fire exposure time [1]. In the advanced calculation models, the fire resistance of steel framed structures is evaluated by carrying out detailed finite element analysis using programs such as ABAQUS or ANSYS. This method can be applied at local, member, and system levels through appropriate discretization of the structure and boundary conditions, as shown in Figure 4.1. Temperature-dependent properties of the constituent materials are provided as input to the model. Realistic failure limits based on strength, stability, and deflection are used to evaluate the failure at member and system levels. For tracing the evolution of fire-induced instabilities leading to the progressive collapse in a steel framed structure, an advanced analysis approach is to be applied. A detailed description of the

numerical model developed for tracing the fire-induced collapse, including the analysis procedure, material properties, discretization, incorporation of high-temperature creep and local buckling effects, and relevant failure limit states are discussed in the following sections.

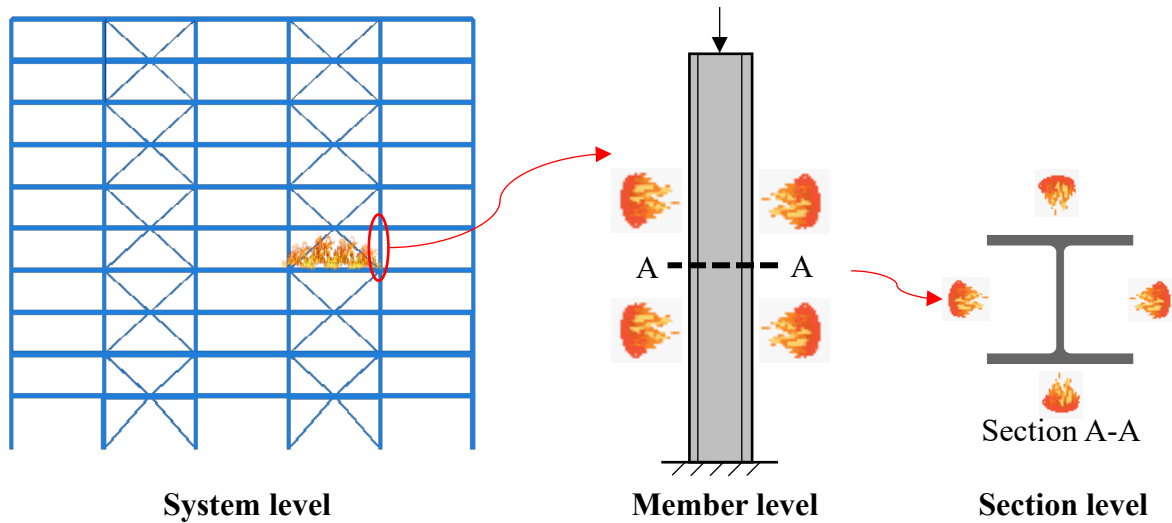


Figure 4.1. Various levels of analysis of a steel framed structure.

### 4.3 Advanced analysis approach for tracing fire-induced collapse

The numerical model for evaluating the fire-induced progressive collapse in steel framed structures is developed using the finite element-based software, ABAQUS. The fire-induced progressive collapse analysis is undertaken at incremental fire exposure time steps and two stages of analysis, namely, the thermal analysis followed by the structural analysis that is carried out at each time step. For the thermal analysis, the heat transfer calculations are performed on a 2-D model of the cross-section of each fire-exposed steel structural member. The steel section (along with any fire insulation present) is exposed to temperatures from 1-, 2-, 3, or 4-sides as encountered in a fire situation. Temperature-dependent thermal properties for steel and insulation are provided as input to the thermal model. A nonlinear transient heat transfer analysis is carried out in ABAQUS to obtain the variation of temperature with fire exposure time (temperature history) in the steel

section. The resulting temperature history at specific nodes is subsequently applied to the corresponding steel members during the structural analysis as thermal load.

The structural analysis of the fire exposed steel framed building consists of two loading sequences. In the first loading sequence, the structural system is subjected to a gravity load of  $1.2 D + 0.5 L$  (where D and L represent the dead load and live load respectively), as per ASCE 7-16 [122] recommendations for low probability loading events such as a fire event. Additionally, a lateral notional load is applied at each story level corresponding to 0.2% of gravity loading on that floor to account for the effects of initial system imperfections [122]. The notional load is applied in the direction that has the maximum destabilizing effect on the structure. In the second loading sequence, sectional temperatures in fire-exposed structural members are applied as predefined temperature fields obtained as output from the thermal model. The temperature variation along the length of the member is assumed constant. Temperature-dependent mechanical property relations for structural steel and concrete are supplied as input to the structural model.

The alternate load path criterion recommended in UFC [110] and GSA guidelines [111] for ambient analysis is extended to elevated temperature conditions and applied to evaluate the stability of the structure under fire exposure conditions. Two different analysis approaches specified in UFC [110] and GSA guidelines [111] can be applied to trace the progression of instability in the steel framed structure at room and elevated temperature, namely, nonlinear quasi-static analysis and nonlinear dynamic analysis. The appropriate analysis (quasi-static or dynamic) regime for carrying out the structural analysis of the fire-exposed steel framed building shall be selected to achieve a computationally efficient and robust solution based on the critical parameters to be included in the model. The steps involved in each of these analysis approaches are detailed below.

#### ***4.3.1 Nonlinear quasi-static analysis***

In this approach, the structural analysis of the steel framed building is carried out using a nonlinear quasi-static (“Visco”) procedure in ABAQUS in multiple steps. In the first step, the gravity and lateral loads are gradually applied to the structural frame at room temperature until the loads are stabilized. In the second step, the structure is subjected to thermal (temperature) loading obtained from the output of the thermal analysis as predefined fields in the model. The analysis continues in incremental time steps until the failure of the first structural member (or members). In the third step, the failed member(s) is (are) removed at a fixed temperature, and the system is allowed to stabilize under the redistributed loads. Removal of a column is accompanied by an increase in gravity loads in floor areas above the failed column by a dynamic load factor of 2 [110] to account for the inertial effects that arise due to the sudden failure of a vertical load-bearing structural member. The inertial forces that develop due to the failure of other members such as braces or beams are assumed minor and hence, are not accounted for in the analysis. The overall frame is then checked for global instability. If the frame stabilizes under the column removal scenario, it is assumed that the inertial effects will be negligible, and the gravity loads are brought back to their initial value while keeping the temperature constant during this process. In the next step, the analysis further continues in incremental time increments with the application of thermal loading until the failure of the subsequent member.

The above procedure is repeated until the end of fire exposure duration or occurrence of global instability (failure), whichever occurs first. The flowchart shown in Figure 4.2 summarizes the various steps utilized in this approach. The nonlinear quasistatic analysis approach is particularly effective to analyze problems with a rate-dependent material response (such as high-temperature creep), temperature-induced local instabilities, and plasticity effects. Since the thermal loading due

to fire is applied for a long time duration and inertial effects can be neglected for much of this duration, the quasistatic analysis provides reasonable results. However, this procedure requires the manual removal of the failed member and the application of a dynamic load factor to account for the inertial forces, which increases the complexity of the model. Moreover, the integration scheme uses a combination of explicit and implicit integration wherein the analysis starts with explicit integration and switches to implicit integration based on either stability or when plasticity is active. Since the number of iterations needed to solve the global set of equilibrium equations in the nonlinear problem can be high, the computational cost of performing each increment is much larger in an implicit analysis than that in an explicit analysis.

#### ***4.3.2 Nonlinear dynamic analysis***

In this approach, a nonlinear dynamic explicit analysis is carried out to obtain the force-deformation response of the structural system at room and elevated temperatures. In the first step of the analysis, the gravity loads are gradually applied to the structural system at room temperature until the loads are stabilized. In the second step, the structural system is subjected to thermal loading obtained from the output of the thermal analysis as predefined fields in the model. The explicit dynamic solver has the capability of numerically overcoming the local instability that occurs due to member level failure and the analysis continues until excessive failure occurs in the structural system. The analysis stops when the structure is no longer able to maintain static equilibrium (or collapse initiation) or till the end of fire exposure duration. Figure 4.3 shows the flowchart outlining the different steps used in this approach.

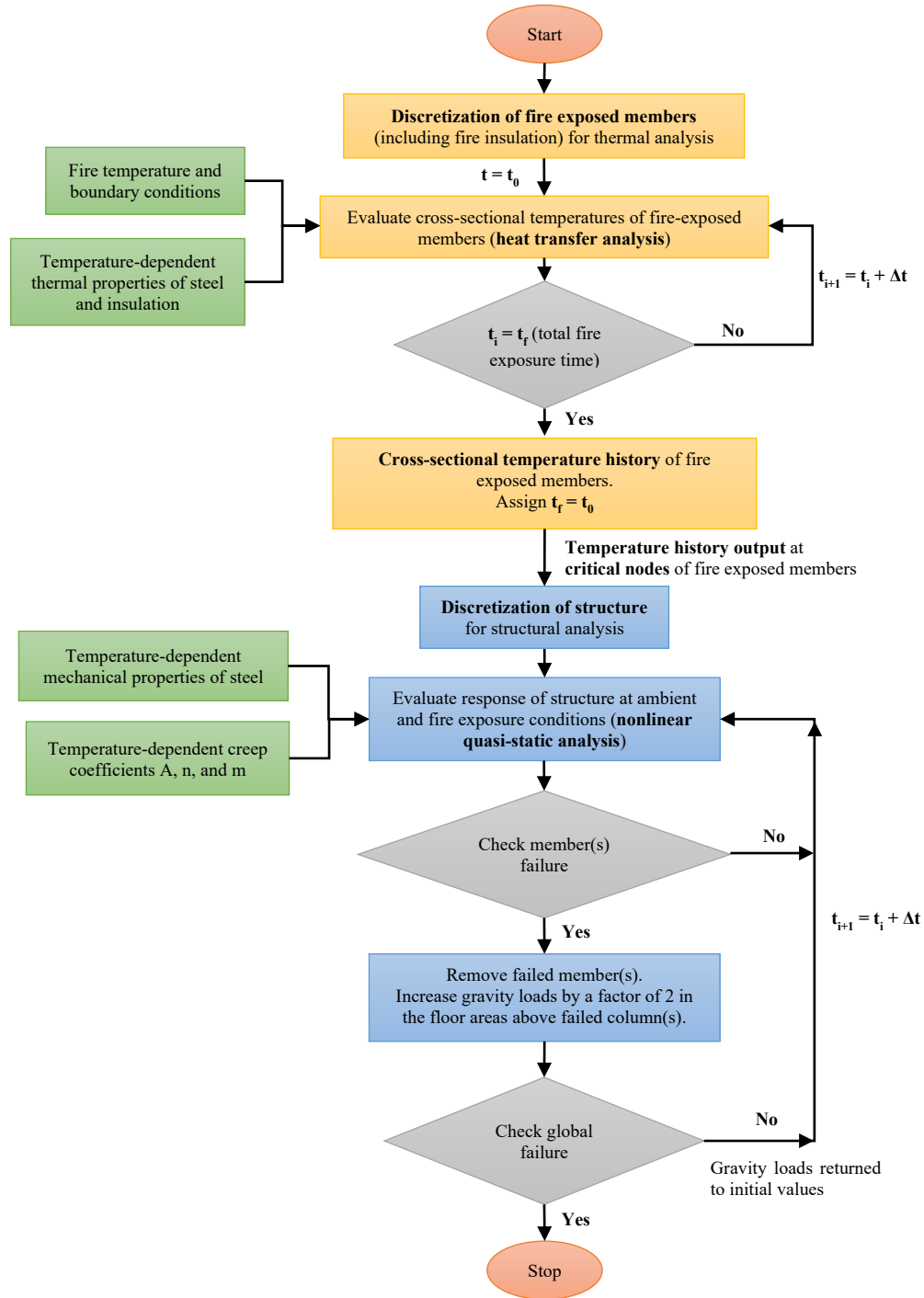


Figure 4.2. Flowchart illustrating the steps in the fire-induced progressive collapse analysis using the nonlinear quasi-static analysis approach.

Unlike the previous quasi-static analysis approach, the explicit method determines the solution to the nonlinear problem without iterating by explicitly advancing the kinetic state of the structure from the previous time increment. Hence, the dynamic explicit analysis is computationally effective to analyze large-scale nonlinear problems such as fire exposure in a 3-D steel framed building (inclusive of transverse framing and slabs). Such problems may require a large number of time increments using the dynamic explicit method; however, the analysis can still be more efficient in an explicit regime as the same analysis in an implicit regime requires many iterations. Another advantage of using the explicit method as opposed to the implicit method is that the explicit method utilizes lesser disk space and memory for each simulation [123]. Further, unlike the previous quasistatic analysis approach where the failed member is to be manually removed, the explicit dynamic analysis allows for the failed member to be automatically removed (or weakened) during the analysis and the loads to be redistributed to the adjacent members. Although this would be more suitable to trace the progression of instability in a steel framed structure during fire exposure, including progressive collapse, it should be noted that the dynamic analysis approach does not allow for the explicit modeling of high-temperature creep strains, since rate-dependent material response requires an implicit solver to obtain a solution.

#### **4.4 Determining fire temperatures**

The temperatures resulting in a compartment and structure are evaluated based on exposure to standard fire such as ASTM E119 [27] or hydrocarbon fire, or any specified design fire scenario using the supplied time-temperature relations. The design fire exposure typically consists of a heating phase followed by a cooling phase and is generated using the parametric time-temperature relations specified in Eurocode 1 [77]. These relations vary in a compartment based on fuel

characteristics in the room, including fuel load density and type, available ventilation (or openings), and the thermal inertia of the lining materials used in the compartment boundaries.

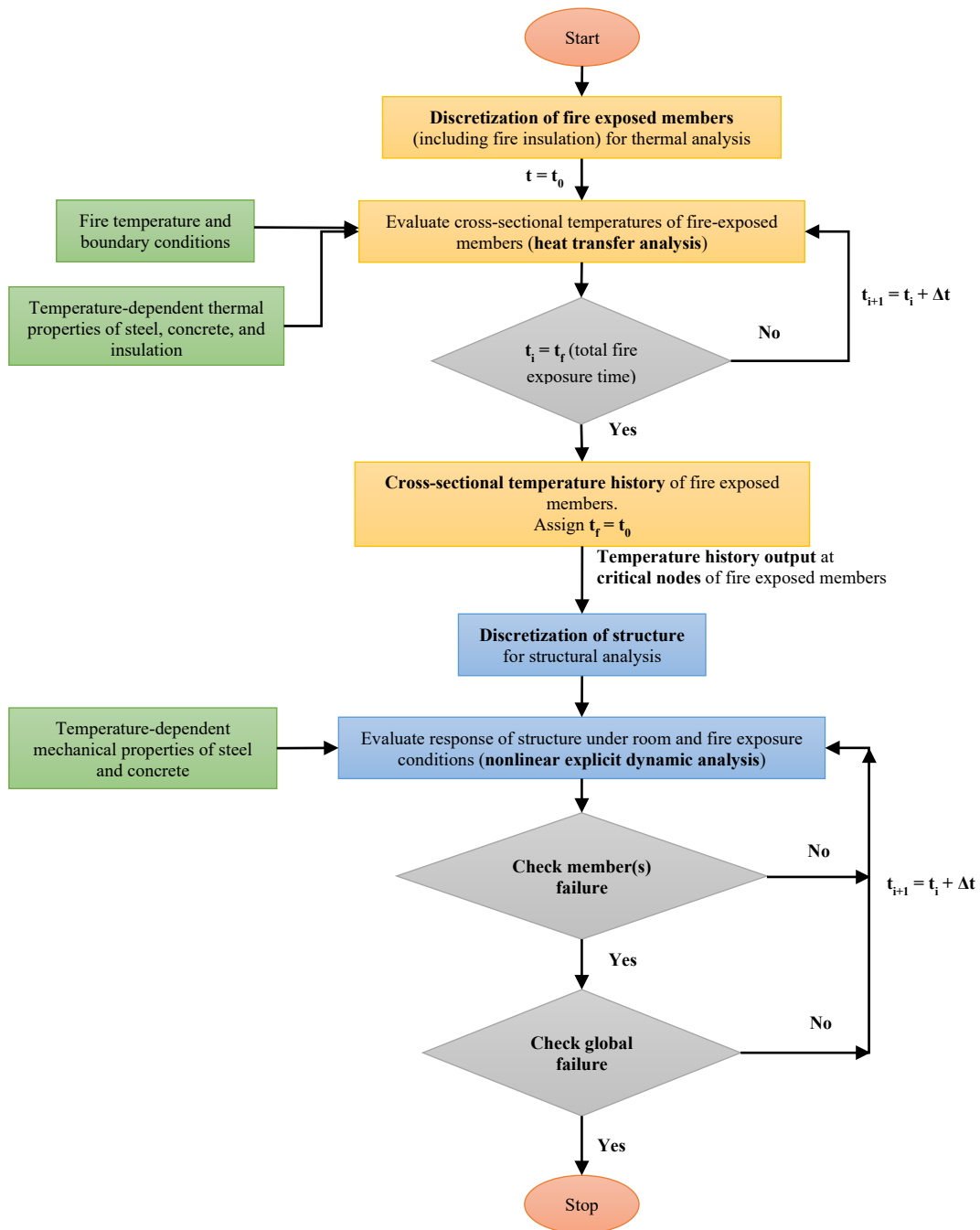


Figure 4.3. Flowchart illustrating steps in the fire-induced progressive collapse analysis using the nonlinear dynamic explicit analysis approach.

For instance, Design Fire 1 and Design Fire 2 (shown in Figure 4.4) are obtained by assuming an office occupancy building (fuel load density = 420 MJ/m<sup>2</sup>) with lightweight concrete walls and slabs (thermal inertia = 840 J/m<sup>2</sup>-s<sup>1/2</sup>-K). The opening factor (O) varies between 0.02 m<sup>1/2</sup> and 0.2 m<sup>1/2</sup> depending on the area of openings in the compartment [77]. Design Fire 1 is generated by assuming a reasonably small opening factor of 0.04 m<sup>1/2</sup> in the compartment while Design Fire 2 is obtained by using a higher opening factor of 0.08 m<sup>1/2</sup>. Design Fire 3, which represents a moderate fire scenario, is obtained by assuming a lower fuel load density of 230 MJ/m<sup>2</sup>, high-density concrete with thermal inertia of 1500 J/m<sup>2</sup>-s<sup>1/2</sup>-K for the lining materials used in the compartment, and a moderate opening factor of 0.06 m<sup>1/2</sup>.

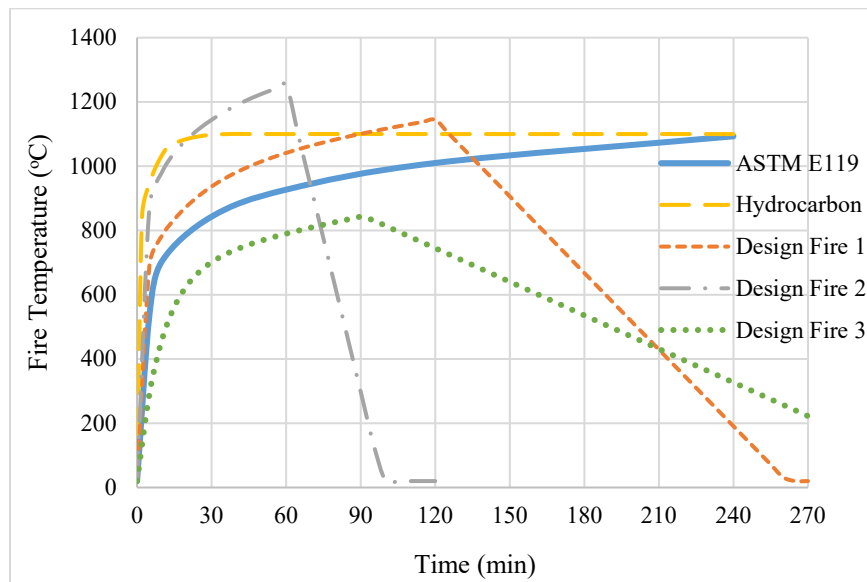


Figure 4.4. Standard and design fire exposure scenarios in a building.

To model the horizontal spread of fire from one compartment(s) to another compartment within a floor, the fire temperatures in the first set of compartments are evaluated based on the time-temperature relations of “Fire in Comp. 1”, as shown in Figure 4.5. As the fire spreads to the next set of compartments, the fire temperatures in this second set of compartments are computed based on “Fire in Set 2”. This procedure is repeated as the fire spreads to the subsequent set of

compartments. A similar procedure is used to model the vertical spread of fire from one story to another. The fire temperatures are applied to the boundaries of the fire-exposed structural members through convection and radiation. Convective heat transfer coefficients ( $\alpha_c$ ) of  $25 \text{ W/m}^2\text{-}^\circ\text{C}$  and  $35 \text{ W/m}^2\text{-}^\circ\text{C}$  are used for the surface film condition on the fire exposed faces of the structural member for standard and design fires respectively, as specified in Eurocode 1 recommendations [77], to simulate the transfer of heat from the fire source to the structural member through convection. A radiant emissivity factor of 0.8 and Stefan-Boltzmann radiation constant of  $5.67 \times 10^{-8} \text{ W/m}^2\text{-K}^4$  are assumed for evaluating the radiative heat transfer coefficient on the fire exposed faces. The unexposed structural members in the building are subjected to ambient (room) temperature conditions throughout the analysis time. The convective heat transfer coefficient and emissivity factor are taken as  $9 \text{ W/m}^2\text{-}^\circ\text{C}$  and 0.2 respectively on the unexposed faces of the structural members [77].

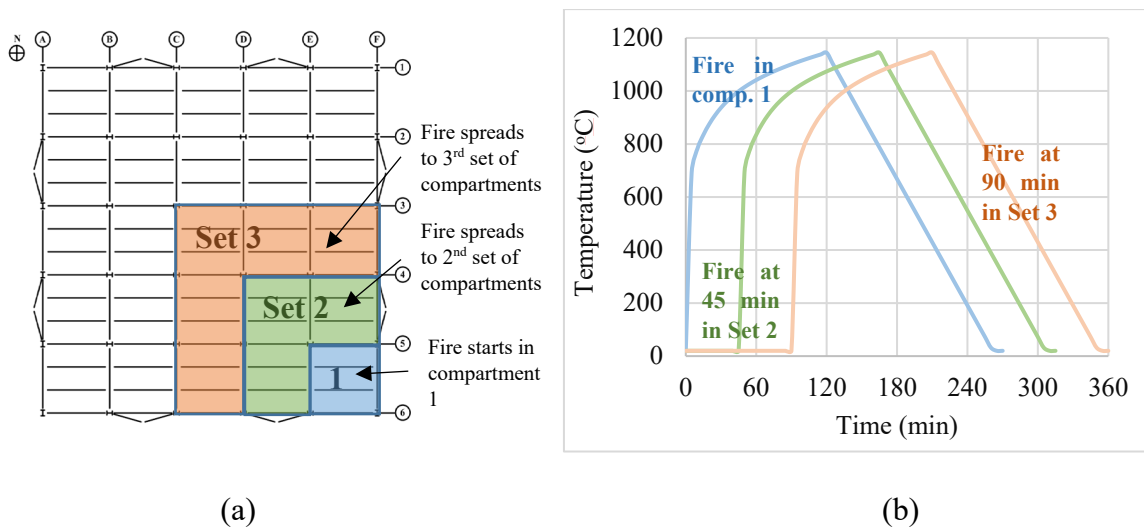


Figure 4.5. (a) Fire spread in a single story and (b) variation of fire temperatures in the compartments with time.

#### **4.5 Material models**

To model the behavior of a steel framed structure under fire exposure conditions, temperature-dependent property relations specified in Eurocode 3 [18] are used to simulate the thermal and mechanical behavior of steel at elevated temperatures. The temperature-dependent properties of structural steel specified as input to the thermal model include density, isotropic thermal conductivity, and specific heat. Spray-applied fire-resistive material (SFRM) type fire protection material is assumed for all structural framing members. The properties of the SFRM type insulation, namely, density, thermal conductivity, and specific heat are assumed to be 240 kg/m<sup>3</sup>, 0.0815 W/m-K, and 1047 J/kg-K respectively [124] which are specified for a temperature of 25°C. The variation of thermal properties of the fire insulation with temperature is neglected in the present study.

For modeling the structural response, the temperature-dependent stress-strain behavior of concrete and steel is considered as per the Eurocode 2 (EC2) [125] and Eurocode 3 [18] relations. The classical metal plasticity model in ABAQUS that uses the Mises yield surface with the associated plastic flow and isotropic strain hardening is utilized to define the constitutive relationship for steel at room and elevated temperatures. On the other hand, the concrete damaged plasticity (CDP) model in ABAQUS is used to define the constitutive relations for concrete. Thermal expansion of steel and concrete is specified as isotropic temperature-dependent coefficients. The high-temperature material property relations for concrete and steel are provided in Appendix B.

#### **4.6 Incorporating high-temperature creep in fire-induced instability**

Creep strains at elevated temperatures can be quite substantial and thus play a critical role in the onset of fire-induced instability and progressive collapse of the building. High-temperature creep in steel can be accounted for in the numerical analysis through one of the two following options.

The first option is to account for transient creep effects implicitly wherein only the temperature-induced transient creep strains built into the stress-strain relations of steel (such as the EC3 [18] relations) are automatically incorporated into the analysis. The EC3 [18] stress-strain relations were derived based on transient tests under slow heating rates [81]. In these relations, part of the transient creep strain is included in the resulting temperature-dependent stress-strain curves by underestimating the stress causing the plastic strain in the steel specimen [81]. However, this implicit creep strain includes only primary creep and part of the secondary creep that develops in the early stages of fire exposure. Much of the creep strain that develops beyond steel temperatures of 400°C under prolonged fire exposure, which tends to be governed by secondary and tertiary creep effects, is not accounted for in the Eurocode stress-strain relations [8,29,31,126]. Moreover, creep strains vary significantly with time, and stress and temperature also vary with time, i.e., duration of fire exposure [8]. Since no explicit calculation of creep strain for a given duration (both absolute time and rates), stress, and the temperature level is involved, the implicit creep model (as in the case of EC3 stress-strain relations) does not account for much of the temperature-induced creep strain, particularly close to the failure of a member when stress and temperature levels are high [127]. It should be noted that accounting for secondary and tertiary creep strains is critical for tracing the onset of global instability and thus the progressive collapse of structures.

The second option to account for high-temperature creep effects involves an explicit definition of the full extent of transient creep strain that develops at elevated temperatures through a separate creep model. The built-in creep power law in ABAQUS is used to evaluate the transient creep strain at each time increment for specified stress and temperature level. At each time step, the total strain in steel at any given stress and temperature levels is calculated as a linear summation of mechanical, thermal, and creep strain in ABAQUS, as shown in Eq. 4-1. The mechanical strain

(which includes the elastic and plastic strains) and thermal strain are computed using the constitutive relations and the expansion coefficient respectively at various temperatures, whereas the transient creep strain is evaluated using the creep power law relations for a given stress and temperature level.

$$\Delta\bar{\epsilon} = \Delta\bar{\epsilon}^{el} + \Delta\bar{\epsilon}^{pl} + \Delta\bar{\epsilon}^{th} + \Delta\bar{\epsilon}^{cr} \quad (4-1)$$

in which  $\Delta\bar{\epsilon}$  is the total strain increment and  $\Delta\bar{\epsilon}^{el}$ ,  $\Delta\bar{\epsilon}^{pl}$ ,  $\Delta\bar{\epsilon}^{th}$ , and  $\Delta\bar{\epsilon}^{cr}$  are the strain components, namely, elastic, plastic, thermal, and creep strain increments respectively.

The creep power law can be applied in two forms, namely, the time hardening form and strain hardening form. The strain hardening form of power law (shown in Eq. 4-2) is adopted, as it is relevant for fire resistance analysis, where the stress state of the material varies with time and time is of smaller durations (i.e., in hours).

$$\dot{\bar{\epsilon}}^{cr} = (A\tilde{q}^n[(m+1)\bar{\epsilon}^{cr}]^m)^{\frac{1}{m+1}} \quad (4-2)$$

in which,  $\dot{\bar{\epsilon}}^{cr}$  is the creep strain rate,  $\tilde{q}$  is the stress,  $\bar{\epsilon}^{cr}$  are the creep strain and A, n, and m are temperature-dependent creep material parameters and these parameters are to be determined using test data [92]. The creep increment ( $\Delta\bar{\epsilon}^{cr}$ ) at each time step is calculated by integrating the creep strain rate ( $\dot{\bar{\epsilon}}^{cr}$ ) with respect to time (step) as:

$$\Delta\bar{\epsilon}^{cr} = \int_0^t \dot{\bar{\epsilon}}^{cr}(\bar{\epsilon}^{cr}, \tilde{q}) dt \quad (4-3)$$

The nonlinear quasi-static analysis approach is adopted to explicitly incorporate the creep strain into the analysis. An integration scheme that uses a combination of explicit and implicit integration is used in the creep analysis with an error tolerance of  $5 \times 10^{-5}$ . The high-temperature creep data from tests carried out by Morovat et al. [92] for A992 steel is used to calibrate the creep material model in ABAQUS using the nonlinear regression fitting technique. The model is capable of

accounting for primary and secondary creep strains that occur at elevated temperatures. The values of parameters A, n, and m at different temperatures are tabulated in Table 4-1.

Table 4-1: Parameters for creep model

Temperature	Parameters		
T (°C)	A (Mpa) <sup>-n</sup> (min) <sup>-m-1</sup>	n (1)	m (1)
400	1.30E-08	1.770	-0.810
500	6.62E-10	2.294	-0.711
600	1.21E-10	2.921	-0.744
700	5.60E-11	3.788	-0.288
800	5.97E-09	3.525	-0.137

It should be noted that explicit modeling of transient creep together with the application of the EC3 [18] stress-strain relations for steel may lead to double counting some of the creep effects since the stress-strain relations include partial creep effects that develop in the initial stages of fire exposure. However, the creep strain that develops in this duration is minor and does not lead to a large overestimation of strains, as will be shown in the following sections. Close to the failure of the member, creep effects tend to be significant due to high stress/temperature levels. Creep strains that develop at this stage are not accounted for in the EC3 [18] stress-strain relations and are captured only using the explicit creep model.

Concrete that is used in floor slabs of steel framed buildings can also develop transient creep strains under exposure to elevated temperatures. Due to the low thermal conductivity and high specific heat of concrete, temperatures in much of the slab cross-section do not exceed 400°C for most of the fire scenarios studied [128], as will be shown in the later sections. In such cases, concrete is expected to develop only primary (low to moderate levels) creep that can be captured reasonably through an implicit approach, such as using the EC2 [125] stress-strain relations [128].

## 4.7 Discretization

For conducting the thermal analysis, the cross-section of the fire-exposed steel members and surrounding fire insulation are discretized using the DC2D4 element (4-noded linear quadrilateral element), having only one active degree of freedom, i.e., the temperature at each node. The discretization of the steel section is such that the nodes of the fire insulation are coincident with the corresponding nodes of steel at the steel-insulation boundary. The transfer of heat from the external fire source directly to the steel member (or insulation, when present) occurs through convection and radiation and this is simulated using surface film condition and radiation interaction modules. A tie constraint is used to apply the nodal temperatures from the insulation to the steel section at their interface. The fire insulation is assumed intact during the entire duration of fire exposure. Although this assumption is realistic under most of the fire exposure scenarios, some extent of delamination may occur under severe fire exposure due to excessive deformations (or failure), especially close to the onset of instability in the structure which can, in turn, precipitate the collapse of the building. The temperature variation with fire exposure time is obtained at specific nodes in the member cross-section, which subsequently is integrated during the structural analysis for beam elements. As per ABAQUS documentation [123], five specific nodes are selected for W sections and four for HSS sections, as shown in Figure 4.6.

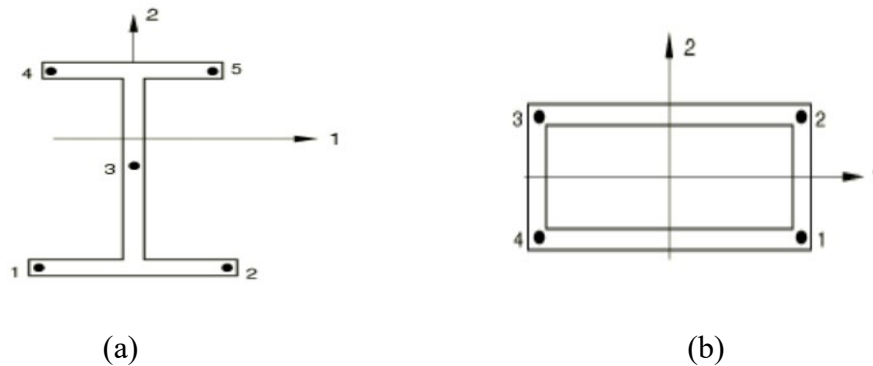


Figure 4.6. Specific node points for temperature output for (a) W section and (b) HSS section [123].

For carrying out the structural analysis, two different discretization are used to represent the steel framed building in ABAQUS. In the first model, the steel framing members (i.e., beams, braces, and columns) are discretized using the 3-D B31 element (2-noded linear beam element), having six degrees of freedom at each node, namely, three translations and three rotations. This Timoshenko beam element can capture large strains, specifically which occur due to transient creep effects under fire conditions, and also shear deformations. The slabs are modeled as 4-noded composite shell (S4R) elements of uniform effective thickness. The effective thickness of the slab is taken as the thickness of the concrete slab above the deck plus the half-height of the rib. The rebars in the slab are assigned to the composite shell as area per unit length. The composite action between the beams and the slab is achieved by rigidly connecting the beam elements to the shell elements. Partition walls are not considered in the structural model.

In the second model for structural analysis, the framing members are modeled using a mixed element approach in ABAQUS. In this approach, the framing members that are directly exposed to fire temperatures are modeled using 4-noded homogenous shell elements (S4R), while the framing members that are not exposed to fire are modeled using beam elements (B31). Based on the location and extent of fire spread in the building, compartments that are subjected to fire exposure are determined, and the framing members, including beams, columns, and braces present in these compartments are discretized as shell elements, while the rest of the members in the building are discretized as beam elements. The use of shell elements for fire-exposed members is to capture the effects of local buckling, inelastic lateral-torsional buckling, residual stresses, or any other distortions in shape (such as warping) that may occur under elevated temperatures. The beam elements, although computationally efficient, cannot capture the above-mentioned locally induced instability effects in framing members. In this model, the beneficial effect of the composite floor

slab and transverse framing are ignored since the inclusion of these features would significantly increase the computational complexity of the model. The second model (with shell elements) will primarily be applied to evaluate the effect of local instabilities on the onset of fire-induced progressive collapse in steel framed buildings.

Proper linking of members discretized as shell elements with members discretized as beam elements is critical to achieving the required load transfer between these members. Figure 4.7 shows the linking mechanism between beam and shell elements used at member intersection points. For instance, member I, which is not directly exposed to fire, is modeled using beam elements. Members II and III, which are located in the burning compartment, are modeled using shell elements. A small offset is provided between the end sections of members II and III from the end of member I to account for the different temperatures and corresponding material properties in these members. The translational and rotational degrees of freedom of the nodes on the end section of member II and member III is controlled by centroidal nodes ii and iii respectively. This is achieved by using a rigid body tie constraint in ABAQUS. Further, the translational and rotational degrees of freedom of the centroid nodes ii and iii are kinematically controlled by end i to achieve either rigid moment connections or pinned shear connections depending on the connection configuration present in the building. This is achieved by using the kinematic coupling option in ABAQUS.

In both the structural models, all other connections including beam-to-column, brace-to-beam, and brace-to-column connections are modeled using the connector assignments in ABAQUS. The moment connections are modeled as completely rigid by restricting the translations and rotations in all three directions, whereas the shear connections are modeled as pinned joints in which the translations in all three directions and rotation about the longitudinal axis are restricted. The

connections are assumed to be completely protected against fire exposure and the failure of connections is not explicitly modeled in the analysis.

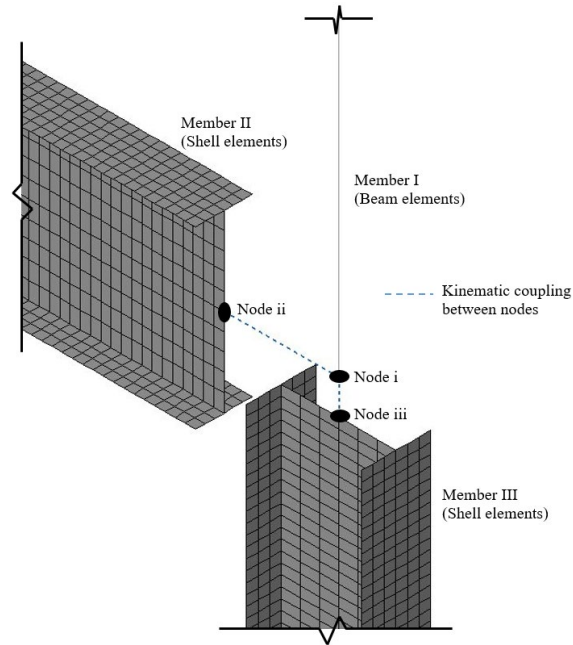


Figure 4.7. Linking of beam and shell elements in ABAQUS.

#### 4.8 Incorporating geometric imperfections and local buckling effects

Geometric imperfections due to the initial out-of-straightness of columns that can affect the stability of the column (and the structure) are included in the analysis. The initial member imperfections are applied by superposing a scaled Eigen mode shape obtained from carrying out an eigenvalue buckling analysis on a column subjected to a concentric axial load in ABAQUS. The Eigen modes corresponding to the global buckling modes, i.e., flexural buckling about the weak and strong axes, are scaled to achieve an imperfection amplitude of  $h/1000$ , where  $h$  is the height of the column, as per AISC-360 specifications [37]. Initial system imperfections that arise typically due to out-of-plumbness of columns are included in the analysis by the application of notional lateral loads at each floor level corresponding to 0.2% of gravity loads on that floor [37].

When the fire-exposed framing members are modeled using shell elements, the initial local imperfections in these members are also included in the analysis by superposing additional scaled Eigen mode shapes corresponding to local buckling of flange and web plates. These Eigen mode shapes are obtained from the buckling analysis carried out on steel members in ABAQUS. The scaling factor is chosen such that the maximum imperfection amplitude in the web is  $d_w/150$ , or the maximum rotation in the flange from its normal orientation is  $b_f/150$  at the flange tip, where  $d_w$  is the depth of the web and  $b_f$  is the width of the flange in a W-section. These are commonly used imperfection amplitudes for local buckling and have been adopted in previous studies as well [35].

#### **4.9 Failure limit states**

While undertaking a system level analysis of a steel framed structure, different failure criteria are to be applied to predict the onset of instability at member and global levels. At a member level, failure can be evaluated by applying strength (force-controlled) or displacement-controlled failure limit states. At any given fire exposure time, failure is said to have occurred due to force-controlled actions when the demand to capacity ratio (DCR) for a structural member exceeds 1. DCR for a steel member is computed as the ratio of internal force (i.e., axial, shear, or moment) due to the applied loading and the expected capacity at the critical section of the member at a given temperature. Since deformations can play a significant role in the onset of instability in a member, the failure during fire exposure can be determined through deformation-controlled actions as follows. The below limits are as per BS-476 [129], which have been established based on standard fire tests on different steel members.

- At any fire exposure time, the deflection of the beam (or slab) exceeds  $L/20$  (mm) or the rate of deflection exceeds  $L^2/(9000d)$  (mm/min), where  $L$  is the length of the beam (or span of the slab) (mm), and  $d$  is the effective depth of the beam (or slab) (mm) [129].
- At any fire exposure time, the vertical displacement of the column exceeds  $0.01h$  mm or the rate of deflection exceeds  $0.003h$  (mm/min), where  $h$  is the height of the column (mm) [129].

At a system level, there are no such established failure criteria since the response of a structural system under fire exposure is complex and the initiation of global failure is more difficult to predict. The global failure (or collapse initiation) occurs when multiple members in the structure fail, leading to run-away deformations, and the structure is no longer able to maintain static equilibrium. In this study, the system level failure is evaluated by limiting the displacement of the structure at the top story level. Global failure is said to have occurred if the lateral displacement or the rate of lateral displacement at the top story of the structure exceeds  $H/25$  (mm) or the  $0.001H$  (mm/min) respectively, where  $H$  is the building height (mm). The above limiting criteria prescribed for member and system failure are not necessarily representative of any “true failure” in the structure. However, establishing different failure limits can help monitor the response of a fire-exposed building during a disaster and planning fire response operations.

#### **4.10 Complexities in modeling and simulation**

Numerical simulations for tracing fire-induced collapse are technically complex and computationally expensive due to various factors. The primary challenge in applying system level analysis approach is a large number of structural members (elements and nodes) with varying boundary conditions that are present in the structural model, which significantly increases the computation time. The properties of the constituent materials such as steel and concrete vary

continuously with temperature changes. The temperature dependency and nonlinear material behavior introduce material nonlinearity to the problem. The explicit treatment of creep further adds to the complexity. Moreover, during fire exposure, the structural members undergo large displacements and rotations, especially close to failure, which adds to the issue of geometric nonlinearity. The combined effect of the above factors increases the complexity of the problem and typically, a large number of time steps are needed to simulate the response of a steel framed structure at a system level for the entire duration of fire exposure until collapse. Further, the continuously changing “states” of structural members in a building during the progression of fire (for instance, some members are at room temperature while others are in the heating, and a few others entering the cooling phase of fire) with changing fire spread with time can be extremely complex to capture in the model. Multiple failures of members at different locations in the structure can result in numerical instabilities during the simulation and small timesteps (and mesh refinement) are often required to obtain convergence. All these factors lead to the non-convergence of solutions frequently.

In order to overcome these modeling complexities, different mesh sizes, time, and mass scaling factors were considered to achieve convergence and reduce computational time. For the nonlinear quasi-static analyses, the plasticity and creep mechanisms of steel controlled the mesh sizes and time increments. The “automatic incrementation” option was used, which allowed the time increments to be reduced close to the failure of a member to avoid numerical instabilities. For the nonlinear dynamic analyses, time and mass scaling were used to decrease the computational time of the simulation. The appropriate scaling factors were chosen such that the effect on the overall dynamic behavior of the model is negligible [123]. Since these simulations at a system level require a large memory space, computer systems with sufficient memory and multiple parallel processors

were used to reduce computational time. In addition, significant effort and expertise are needed to identify and analyze the large amount of analysis (output) parameters generated from each simulation.

#### **4.11 Model validation**

To establish the efficacy of the model in predicting the fire response at various levels, the above-described numerical model is validated both at the member level and system level. The details of the validation studies are presented in the subsequent sub-sections.

##### ***4.11.1 Approach for validation***

First, the numerical model is validated at a member level. For this, one of the column tests carried out at Michigan State University is used [52]. In this study, the thermal and mechanical response predicted by the model is compared against the data reported in the fire test. Second, the validity of the numerical model in tracing the system level response of steel framed structures is established. Owing to the high cost of conducting fire tests and the practical difficulties involved in testing at a large scale, previously reported fire tests on steel framed structures are utilized for system level validation. To determine the validity of the two different analysis approaches presented in this chapter, namely nonlinear quasi-static and nonlinear dynamic explicit, validation studies are conducted on two different steel framed structures. The nonlinear quasi-static analysis procedure is validated with published experimental data on a fire test carried out by Dong et al. [70] on a two-story, two-bay moment frame. On the other hand, the nonlinear explicit dynamic analysis procedure is validated by comparing the results of the numerical model against one of the Cardington fire test data [59–62], namely the “BS corner test”. The validation process at a system level involved comparing the thermal and structural response parameters, including the sectional temperatures in different steel members, displacements at different points on the structure, and as

well as member and global failure modes and times. Also, the validation studies compared the response obtained using material models with and without explicit creep with that of experimental data.

#### 4.11.2 Model validation at the member level

The data from the fire resistance test on a steel beam-column under ASTM E119 standard fire reported by Dwaikat et al. [52] is utilized for member level validation. This beam-column is made of a W8x48 section of A992 steel and is 3.3 m in length. The details of the tested member are shown in Figure 4.8. The beam-column is subjected to an axial load of 650 kN, corresponding to 25% of its yield capacity at room temperature. SFRM insulation with an average thickness of 45 mm is applied on all four sides of the steel section along the heated length. Some insulation, near the top, is removed to achieve thermal gradients in the cross-section that are representative of perimeter columns or floor beams with three-sided heating.

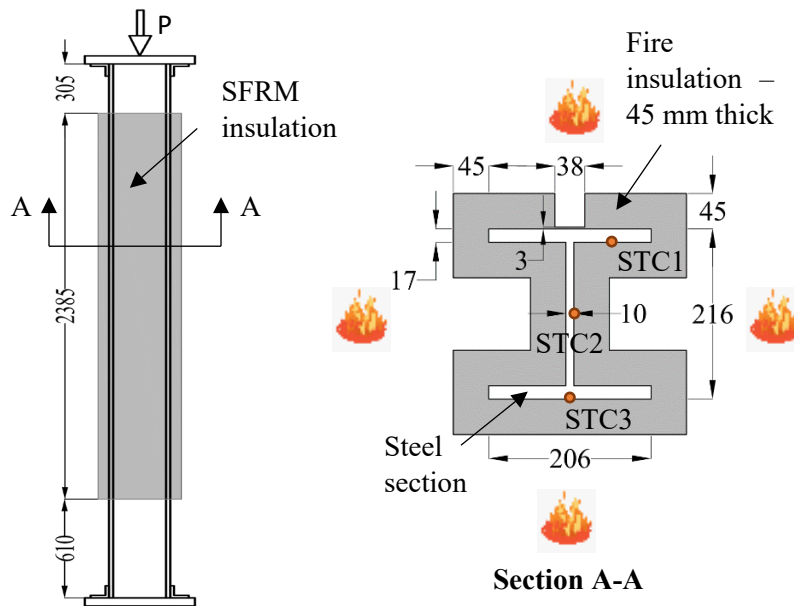


Figure 4.8. Dimensions (in mm) and fire exposure region of tested steel column [52].

The cross-section of this beam-column member along with the fire insulation is modeled in ABAQUS as described in Section 4.7. The fire temperatures are applied to the insulation boundary on all four sides of the section, as shown in Figure 4.8, to obtain the thermal gradients as a function of fire exposure time. These nodal temperatures are then applied to the structural model as thermal loading, resulting from the fire exposure. For the structural analysis, the beam-column member is discretized using beam elements as described in Section 4.7. The bottom end of the beam-column is considered completely fixed, whereas the support conditions for the top end are achieved using an axial spring,  $k_s$  ( $= 25000$  kN/m), and rotational spring,  $k_\theta$  ( $= 2500$  kN-m/rad). No lateral translation is allowed at the top end. The nonlinear quasi-static analysis approach is applied to obtain the axial displacement and top-end rotation of the beam-column as functions of fire exposure time.

Figure 4.9 shows the comparison of measured and predicted sectional temperatures in the steel column. The temperatures within the cross-section gradually increase at a rate of  $5^\circ\text{C}/\text{min}$  in the initial period of fire exposure. Then, the rate of temperature rise slows down to  $2^\circ\text{C}/\text{min}$  as the increase in fire temperature reduces with time. The FE model predicts slightly higher temperatures than the measured test results at thermocouple location STC1 and slightly lesser at locations STC2 and STC3. The variation can be attributed to the difference in insulation thickness and properties present in the actual test and those adopted in the numerical model. It should be noted that it is common to have some variation in the thickness of the insulation due to practical issues in applying the insulation.

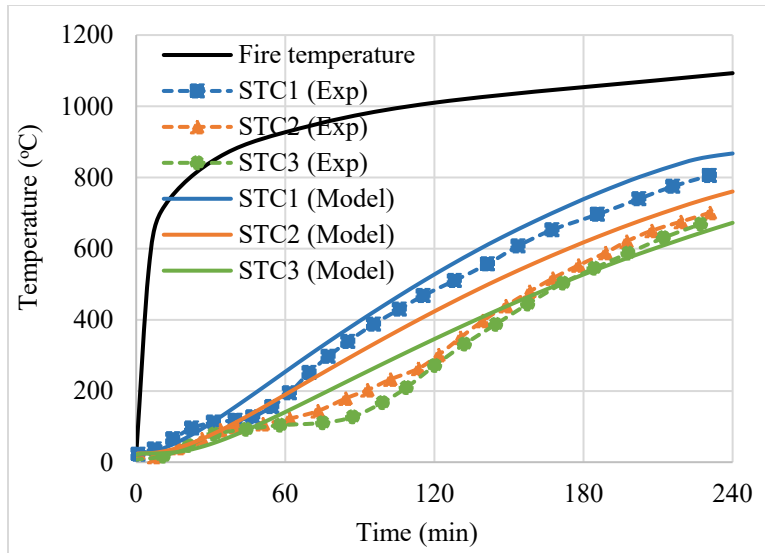


Figure 4.9. Comparison of measured and predicted sectional temperatures in the steel column.

Comparisons of measured and predicted axial deformation and axial force in the steel column are presented in Figure 4.10. The finite element analysis results are shown for two cases: one is *with creep*, where the high-temperature creep is explicitly incorporated in the analysis together with implicit creep strains, and the other is *without creep*, where only partial creep effects are included implicitly through EC3 stress-strain relations. The stress-strain relations at different temperatures are obtained using the appropriate reduction factors for the yield stress, proportionality limit, and the modulus of steel defined In Eurocode 3 [18] for a particular temperature. The initial stage of axial deformation response is governed by the thermal strains and much less mechanical and transient creep strain and the column expands. During this stage, the temperatures in much of the column cross-section are lower than 400°C and hence, there is not much degradation of mechanical properties of steel, and stress levels in the column are below 30%. In this stage, the trends predicted by the models *with creep* and *without creep* are similar. The creep effects at this stage are negligible.

As the temperatures in the cross-section rise beyond 400°C, there is larger degradation in the strength and stiffness properties of steel, and stress levels rise to 40%. This results in an increase in mechanical strain and also the onset of transient creep strain which offsets some of the thermal strain. In this stage, the column continues to expand as this column is lightly loaded; however, the rate of expansion reduces. In the final stage, the temperatures increase beyond 600°C, and stress levels reach 50%. Mechanical and transient creep strain dominates the response as the axial deformation of the column shifts from expansion to contraction. Instability begins to set in when the axial force in the column starts to drop to zero and the column fails at about 240 min closer to the test failure time of 220 min. During this stage, the difference in the deformation and force response predicted using the models *with creep* and *without creep* becomes evident. The failure time when creep effects are not fully included is 265 min, which is higher than the one measured in the fire test (220 min). The model without explicit creep is seen to underestimate the axial deformation and overestimate the axial force in the steel column and hence, overestimates the onset of instability (or time to failure).

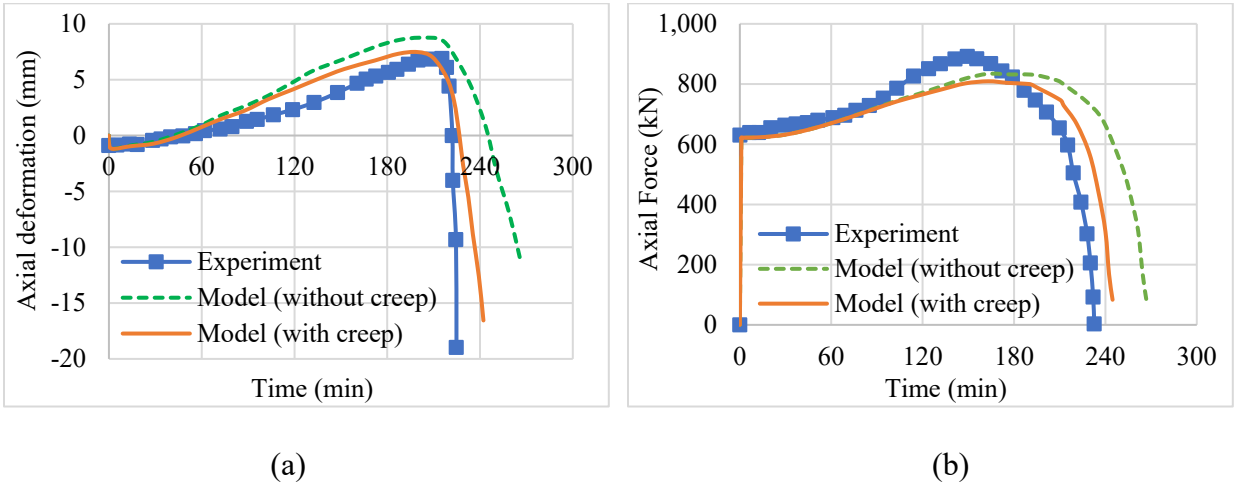


Figure 4.10. Comparison of measured and predicted (a) axial deformation and (b) axial force in the steel column.

### ***4.11.3 Model validation at the system level***

#### ***4.11.3.1 Nonlinear quasi-static analysis – NIST steel framed building***

To establish the validity of the developed numerical model at the system level (nonlinear quasi-static analysis), one of the fire tests carried out by Dong et al. [71] on a full-scale two-story, two-bay steel sway portal frame is simulated in this study. The test frame consisted of three steel columns and four composite beams as shown in Figure 4.11. The columns had an H-section (H200×200×8×12) and were made of Q235 steel (yield strength = 235 MPa). The composite beams comprised of a 100 mm thick and 1 m wide reinforced concrete slab made of C30 concrete (cubic compressive strength = 30 MPa) and a Q235 steel H-section (H250×125×6×9). The floor slab was provided with anti-crack rebars of  $\phi 6$ mm in the longitudinal and  $\phi 10$ mm in the transverse directions at a spacing of 150mm. The composite action between the slab and the steel section was achieved using shear studs. The beam-to-column connections were designed to resist both moment and shear while the column bases were welded to 16 mm thick steel plates which in turn were fixed to the test bed using  $\phi 10$ mm Grade 10.9 bolts. Additionally, the frame was laterally braced in the out-of-plane direction using steel pipes which only provided out-of-plane restraint to the frame and negligible restraint in-plane to the frame.

The frame was subjected to three vertical loads (P) of 100 kN, applied to the top of each column. Additionally, four weight blocks (q), each weighing 4.5 kN, were placed equidistantly on each of the composite beams as shown in Figure 4.11. The fire test simulated in the numerical study corresponds to Test 5 in the experimental program carried out by Dong et al. [71] in which both the compartments on floor 1 were subjected to fire. The fire temperatures in the heated compartments were allowed to follow the standard ISO 834 [28] fire curve. The test was carried out until the hydraulic jacks were unable to maintain a constant vertical load on the columns. At

this point, the furnace was shut off and allowed to cool down to the ambient temperature. For the entire duration of the fire test, the beam-column connections were protected using an aluminosilicate refractory fiber blanket while the columns and beams were left unprotected.

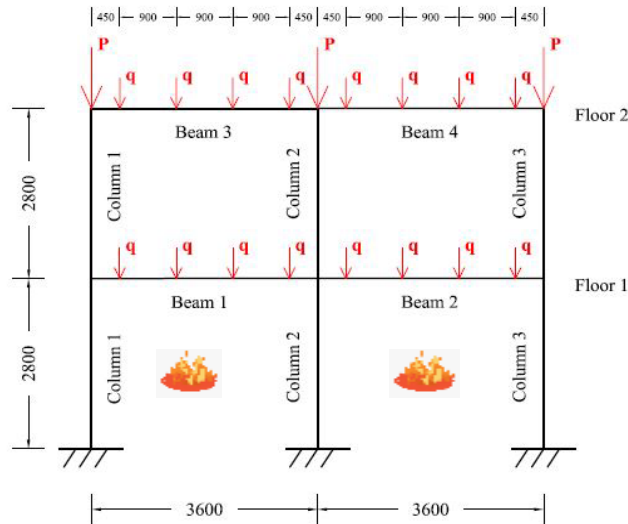
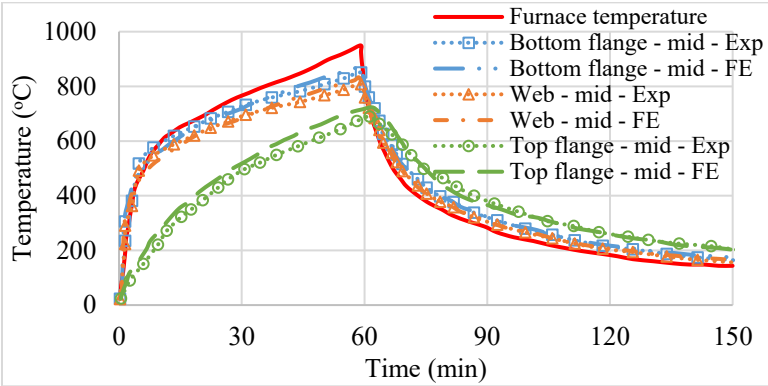


Figure 4.11. Elevation details, loading, and fire exposure regions of test frame (dimensions in mm) [71].

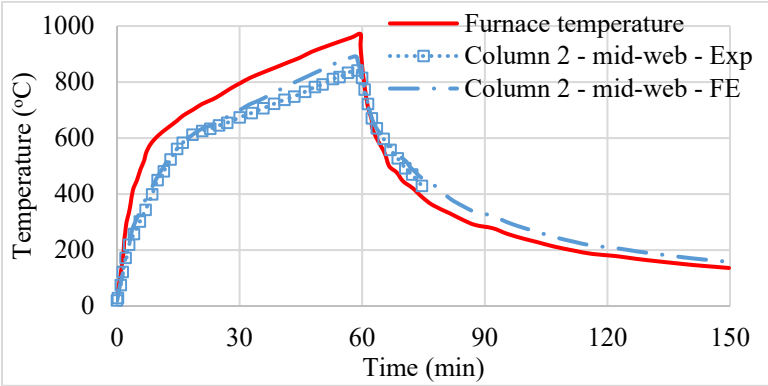
The cross-section of the steel columns and composite beam (comprising of both the concrete slab and steel section) in floor 1 is modeled in ABAQUS with appropriate elements as described in Section 4.7. The fire temperatures are applied to all four sides of the middle column and the bottom three sides of the beams. In the case of perimeter columns, since the burners are positioned towards the flanges facing the interior of the fire compartments, the exterior faces of the column are partially shielded from direct fire exposure and hence, these columns are assumed to be exposed to 3-sided fire exposure.

Figure 4.12 shows the comparison of the predicted sectional temperatures from the numerical analysis with that of the experimental data for the composite beam and column 2 on floor 1 as a function of fire exposure time. The temperature variation in the cross-section of the composite beam is plotted at three different locations, namely, at the center of the bottom flange, web, and

top flange of the steel section. As the steel section is unprotected, the temperatures in the bottom flange and web are seen to increase rapidly, close to the furnace temperature, while the top flange heats up more gradually due to the presence of the concrete slab which acts as a protection to the top flange from the fire exposure. In the case of column 2, the temperatures increase uniformly across the cross-section due to the lack of fire protection, and the temperature trend closely follows that of the furnace temperature. The variation of temperature in columns 1 and 3 also follow similar trends as that of column 2, however, reaching slightly lower peak temperatures due to the 3-sided heating. Overall, the predicted temperature variations follow the measured values at all the locations in the beam and column sections.



(a)



(b)

Figure 4.12. Measured and predicted sectional temperatures in (a) beam 1 and (b) column 2 on floor 1.

For the structural analysis, the beams and columns in the frame are discretized using beam elements as described in Section 4.7. The beam-column connections are modeled as completely rigid, and the base of the columns is assigned with fixed support conditions. The contribution of the concrete slab and rebar mesh is neglected in this study. The effect of local buckling is also neglected in this study as the steel sections used for beams and columns in the frame are compact and hence are not expected to experience sectional instability during fire exposure. The nonlinear quasi-static analysis procedure described in Section 4.3.1 is applied to derive the stresses and deflections of various structural members in the frame as a function of fire exposure time. To illustrate the effect of temperature-induced transient creep, the frame is analyzed under two scenarios: one explicitly incorporating transient creep (“*with creep*”) and the other incorporating implicit creep only (“*without creep*”).

The deformed configuration of the steel frame at 30 min and 60 min of fire exposure time resulting from the analysis with and without creep is presented in Figure 4.13. At 30 min, the frame is in the expansion phase, where all the members in the fire compartments are undergoing thermal expansion. This can be seen from the outward movement of the perimeter columns 1 and 3 due to the thermal expansion of the beams and columns on floor 1. At this stage, the creep effects are minimal and hence, the difference between the deformed shapes obtained using models with and without creep is also minor. At 60 min, the difference between the responses obtained using the two models, with and without creep, becomes more significant. In the deformed shape obtained using the model with creep, it can be seen that the middle column on floor 1 has already buckled while the deformations obtained using the model without creep in the fire-exposed members are still lower.

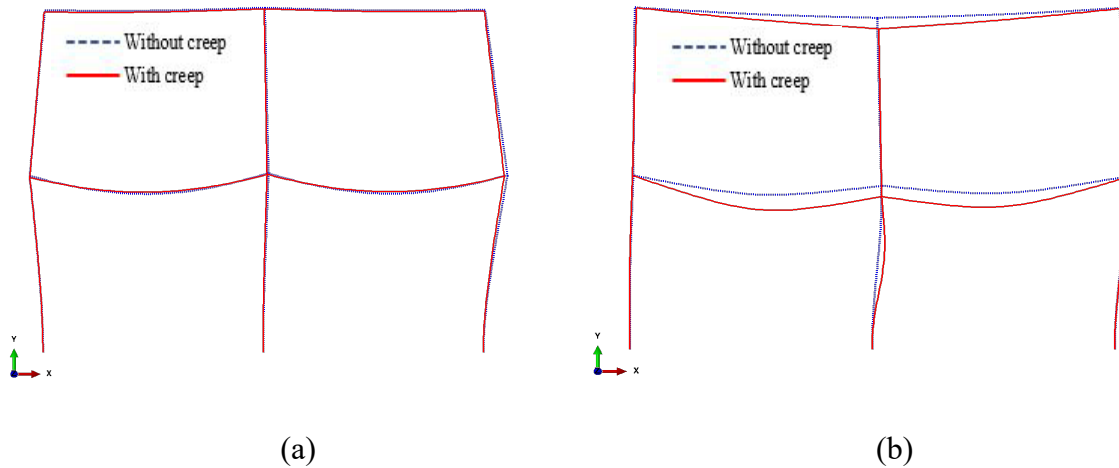


Figure 4.13. Deflected profile of the frame at (a) 30 min and (b) 60 min of fire exposure time.

Comparisons of the measured and predicted lateral displacement of the frame and mid-span deflection of the beams are shown in Figure 4.14 and Figure 4.15. In the initial stage of fire exposure, as the expansion of the beams and columns in floor 1 pushes columns 1 and 3 away from each other, these columns show lateral displacement in opposite directions at floor 1 level. During this stage, the lateral displacement of the frame at floor 2 level is very minimal and the models “*with creep*” and “*without creep*” predict similar trends. With an increase in temperature, the lateral displacement at floor 1 continues to increase until the middle column, which is subjected to higher temperatures than the perimeter columns, buckles first, causing a sudden increase in the lateral displacement at the mid-height of column 2. The lateral displacement of the frame at other points also increases rapidly towards the right indicating the impending collapse of the frame. During this stage, the difference in the displacement response predicted using the models with and without creep becomes evident. The model “*with creep*” predicts a failure time of 57 min, which is close to that in the fire test (59 min), while the model “*without creep*” predicts a slightly higher failure time of 65 min.

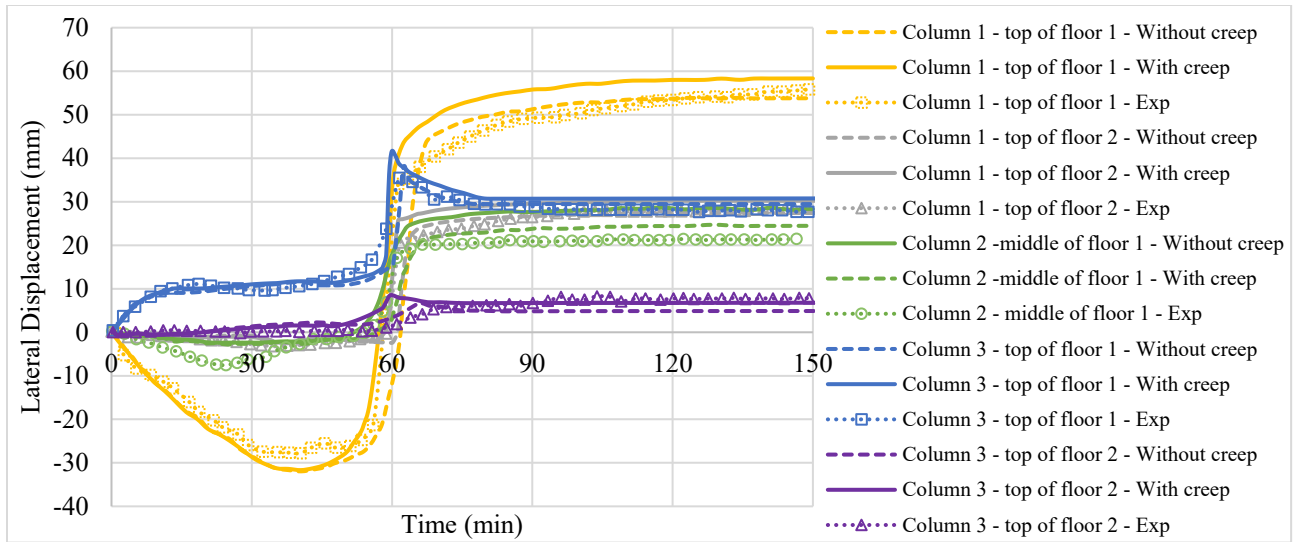


Figure 4.14. Variation of measured and predicted lateral displacement of the frame with fire exposure time.

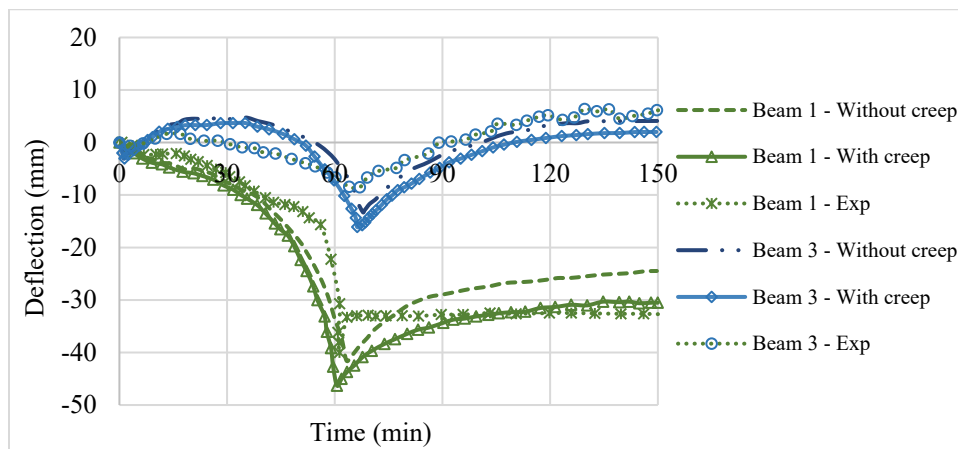
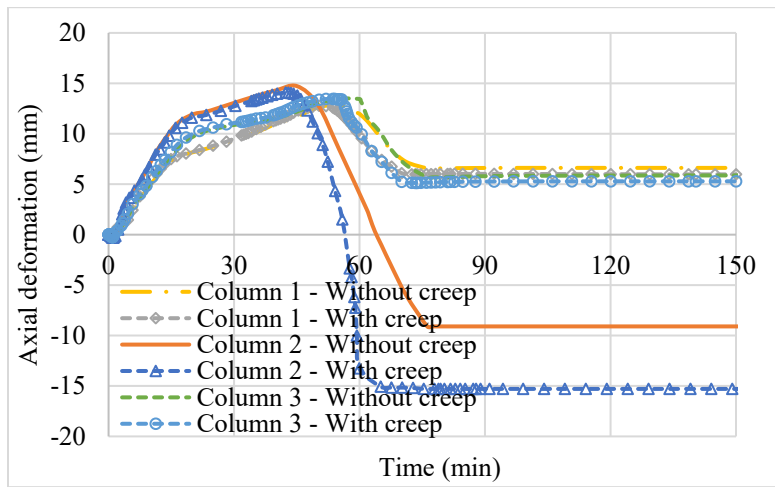


Figure 4.15. Variation of measured and predicted deflection of beams with fire exposed time.

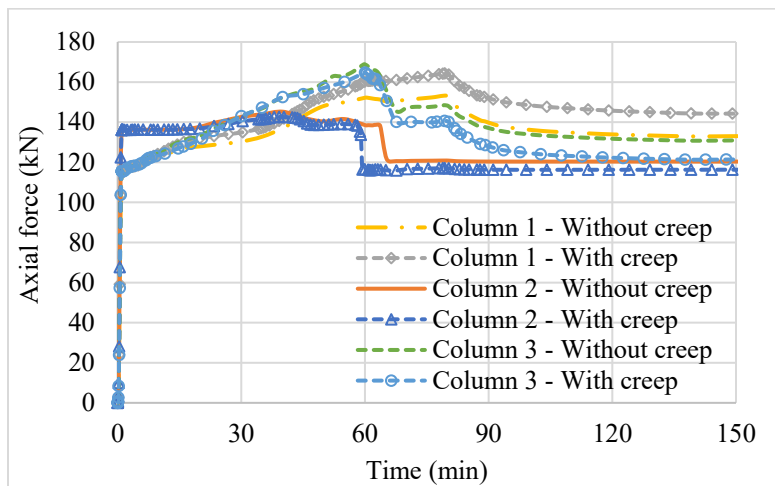
Following the failure of column 2, the furnace was turned-off and some deformation gets recovered in the cooling phase of the fire exposure. The residual lateral displacements predicted in columns 1 and 3 are 58 mm and 30 mm using the model “with creep” and 53 mm and 29 mm using the model “without creep”. In the test, residual displacements of 56 mm and 28 mm are reported for columns 1 and 3 respectively. The model predictions are slightly higher than the test results owing to neglecting the contribution of the slab (heat sink effect) in the structural response. The model “without creep” underestimates the residual displacement of the frame when compared to that

obtained using the model “with creep”. The beam on floor 1 undergoes a maximum deflection of 40 mm which recovers to 32 mm upon cooling. The model with and without creep predicts a maximum deflection of 46 mm and 42 mm and a residual deflection of 31 mm and 24 mm respectively. The model “without creep” predicts a slightly higher recovery of 18 mm compared to 15 mm using the model “with creep”, mainly because in the implicit creep model, much of the inelastic creep deformation that occurs in the heating phase is included in the elastic recoverable deformation. The beams on floor 2, which are not exposed to fire, show very minimal deflections. To demonstrate the evolution of creep effects in the frame during the fire exposure, the predicted axial deformation response and axial load in columns are plotted in Figure 4.16. Burning of compartments on floor 1 results in the thermal expansion of the fire-exposed columns in the initial stage of fire exposure, increasing the axial deformation response of the columns. The temperature in the cross-section of column 2 is lower than 400°C, hence, there is not much degradation of the mechanical properties of steel, and the stress level in the column is below 30% of its strength at that temperature. During this expansion stage, the deformation response of the frame is primarily governed by the thermal strain and much less mechanical and transient creep strain. As the columns are unprotected, the temperatures in the cross-section of columns quickly rise beyond 400°C, there is a larger degradation in the strength and stiffness properties of steel at this stage. Moreover, the restraint to expansion caused by the cooler members in the frame results in additional temperature-induced stresses in the fire exposed members. The stress levels in the columns on floor 1 rise above 40%, with the middle column (column 2) experiencing slightly higher stress levels than the perimeter columns due to the faster rise in temperature in column 2. This results in an increase in mechanical strain and also the onset of transient creep strain which offsets some of the thermal

strain. In this stage, the columns on floor 1 continue to expand as the columns are lightly loaded; however, the rate of expansion reduces.



(a)



(b)

Figure 4.16. (a) Axial deformation and (b) axial force in fire-exposed columns in the floor.

In the final stage, the temperatures in the columns increase beyond 600°C, and stress levels reach above 50%. Mechanical and transient creep strain dominates the response as can be seen in the case of analysis “with creep” and the axial deformation response shifts from expansion to contraction. Instability begins to set in when the axial force in column 2 starts to drop and column

2, which experiences higher temperatures than the perimeter columns, fails first at about 59 min. The model without explicit creep is seen to underestimate the axial deformation and overestimates the axial force developed in the steel column and hence, overestimates the onset of instability (or time to failure) as 65 min. Although the structural members are unprotected and the temperatures in the columns reach up to 800°C, no instability occurs in the column until 60 minutes of fire exposure. This is unlike that in the case of an individual steel column which when left unprotected fails in about 20 minutes of standard fire exposure [1]. This shows that the onset of instability in a steel frame is significantly different (delayed) from that of individual members as the realistic load redistributions and load paths are not captured in the member level analysis. Since the furnace was turned-off following the failure of the column, no progressive collapse was observed in the frame. Figure 4.17 shows the evolution of total strain and creep strain in column 2. It is seen that the creep strain predicted using the explicit creep model forms a considerable portion of the total strain experienced by column 2 close to failure. On the other hand, the model with implicit creep underestimates the total strain before the failure of the column. It is evident that the creep effects are significant near the failure of the column and affect the time of onset of instability in the member as well as in the frame. Overall, the numerical model is able to predict the system level response of the frame subjected to fire exposure reasonably well, with the model “with creep” showing a better agreement with the test results. Results obtained using the model “with creep” provide a slightly more conservative assessment and the two sets of analyses (with and without creep) provide lower and upper bounds of failure times.

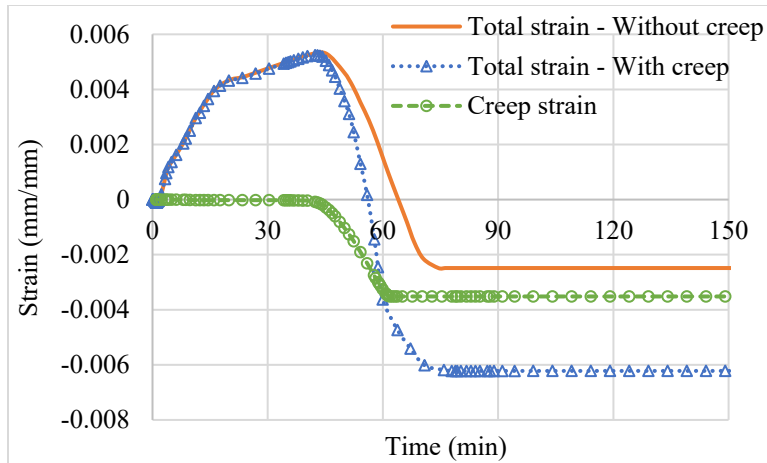


Figure 4.17. Evolution of total strain and creep strain in column 2.

#### 4.11.3.2 Nonlinear dynamic explicit analysis – Cardington steel framed building

To test the validity of the numerical model in predicting the system level response using the nonlinear dynamic explicit analysis approach, one of the Cardington fire tests, namely the “BS corner test”, is simulated in this study. The Cardington fire tests were conducted by British Steel (BS) and Building Research Establishment (BRE) in the Large Building Test Facility (LBTF) at Cardington, U.K. to evaluate the inherent fire resistance of multi-story steel framed composite construction in buildings [59–62]. These large-scale fire tests were used to generate quality data on the overall fire behavior of steel framed structures. The test building was eight stories high (with a story height of about 4.2 m) and was five bays long by three bays wide, with a floor area of about 945 m<sup>2</sup>. Necessary lateral resistance (in the form of cross-bracing) was provided around the lift shaft and staircases to render the building a no-sway structure. The beams were designed as simply supported acting compositely (through shear studs) with the floor slab. The floor system consisted of a 60 mm deep steel deck topped with a 70 mm deep lightweight concrete slab embedded with a steel mesh of 142 mm<sup>2</sup>/m. The loading on the slab included a self-weight of 2.4 kN/m<sup>2</sup> and an imposed load of 2.5 kN/m<sup>2</sup>. The corner fire test was carried out in one corner of the test building in story level 2, enclosing an area of 6m x 9m in plan. Figure 4.18 shows the floor

plan at level 2 of the test building and the compartment used for the fire test. In addition, the detailing of the composite slab and beam at sections A-A and B-B are also shown in the same figure. All columns and edge beams were fire protected using a 25 mm ceramic fiber insulation whereas, the remaining beams and the underside of the steel deck were left unprotected. Figure 4.19 shows the measured gas (fire) temperature within the test compartment. A more detailed description of the Cardington building structural framing and fire test conditions can be found in previously reported studies [59–62].

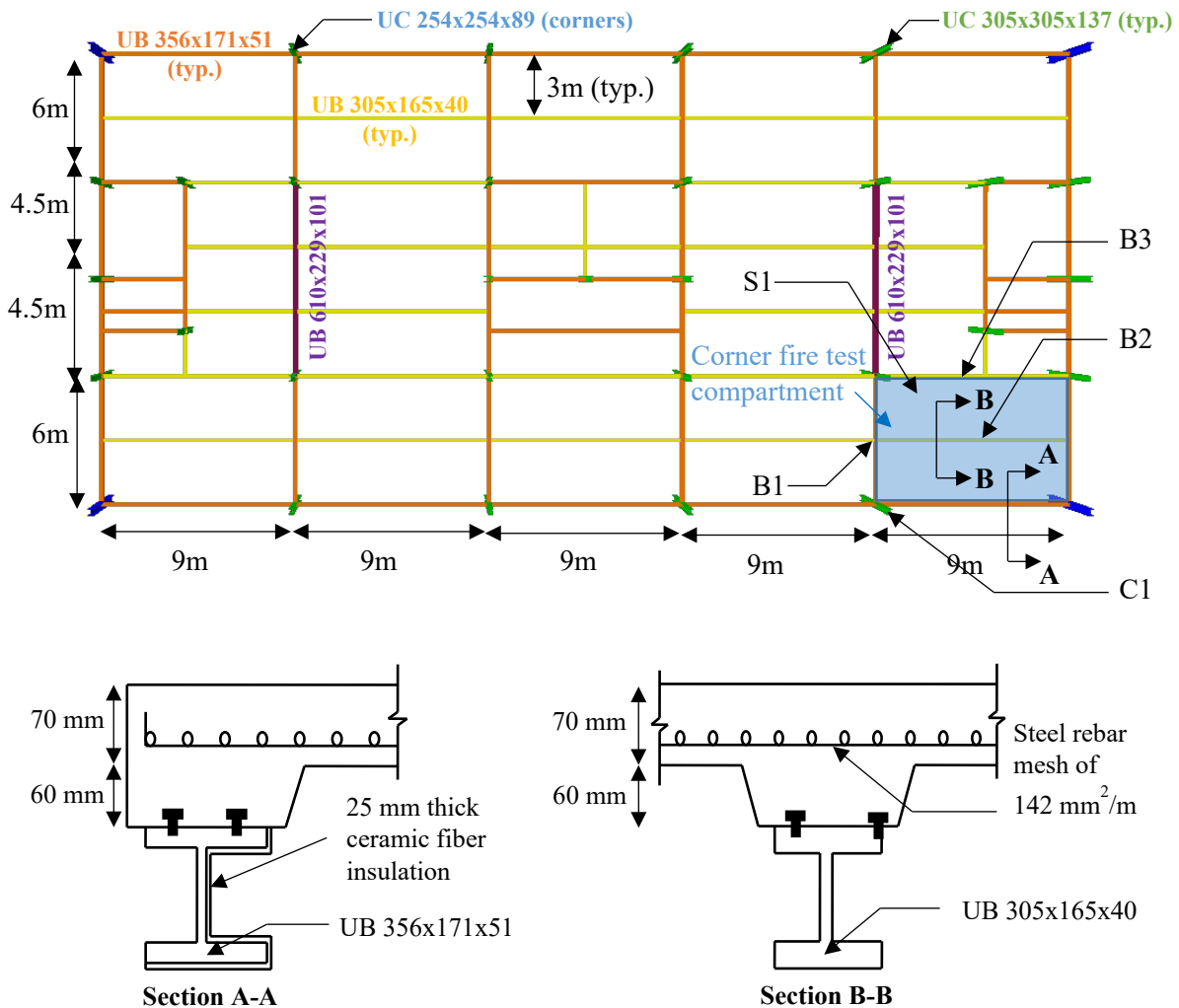


Figure 4.18. Details of the floor plan at level 2 and compartment used for the fire test.

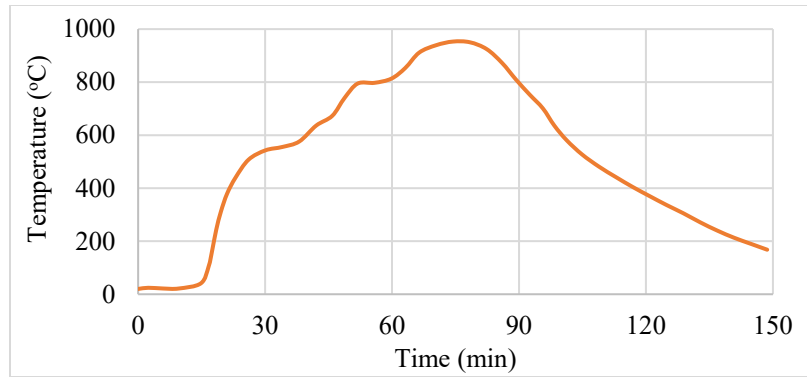


Figure 4.19. Gas temperature as measured in the corner fire test compartment.

For validation, only the part of the building affected by fire (which includes slabs, beams, and columns at level 2 and columns above the affected story) is modeled in ABAQUS. Although a 3-D model of the full building may provide more accurate results, it is not considered due to the high computational resources needed to run the simulations. The boundary conditions applied to the top and bottom columns and the beams connected to the elevator and staircase shafts are shown in Figure 4.20. Self-weight and imposed loads are applied as distributed loads on the slab elements, whereas the loads from higher stories are assigned to the columns in the form of concentrated loads. For a 3-D model, the quasi-static analysis procedure is extremely difficult to apply since it requires the failed elements to be removed manually, which will lead to high numerical instabilities. For this reason, the nonlinear dynamic analysis procedure described in Section 4.3.2 is applied to derive the temperature gradients and deflections of structural members as a function of fire exposure time. For this analysis, the temperature-induced creep strains are implicitly accounted for through the EC3 [18] stress-strain relations for steel.

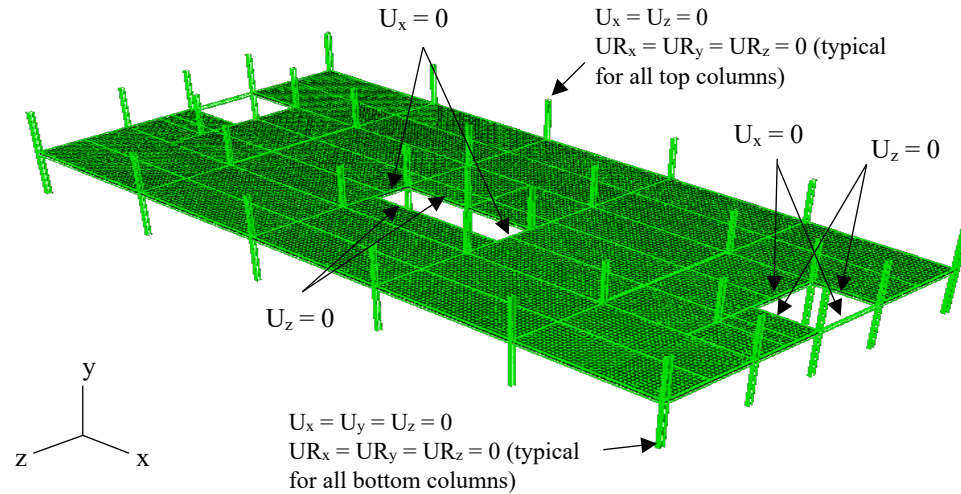
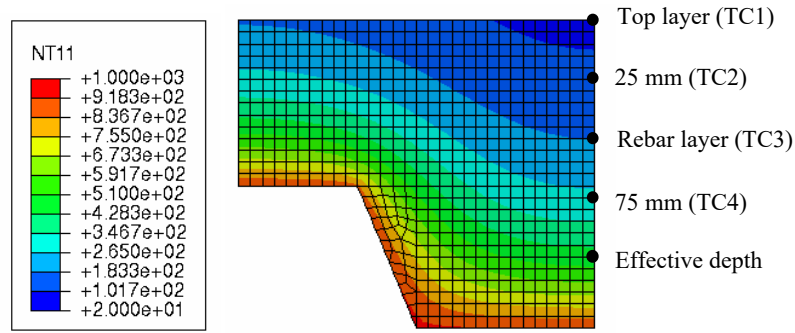
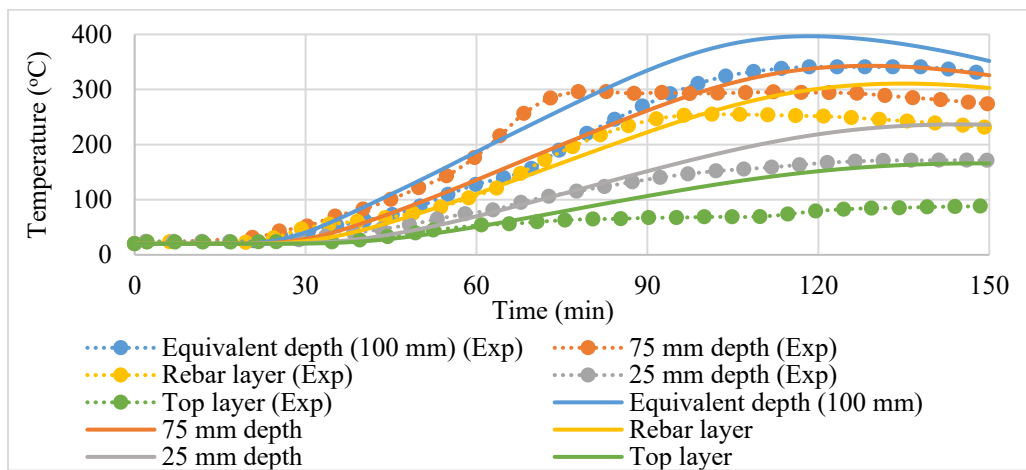


Figure 4.20. Discretization of the FE model and boundary conditions.

Figure 4.21, Figure 4.22, and Figure 4.23 show the comparison of sectional temperatures predicted by the FE model with the test data in the slab, primary and secondary beams. The temperatures developed within the slab cross-section are compared at five different depths of the slab (see Figure 4.21 (a)). Due to the higher thermal inertia of concrete, the temperature at various depths in the cross-section rises slowly despite the lack of fire protection. A peak temperature of 400°C is reached at a depth equal to the effective thickness of the slab, while the temperature on the unexposed surface (top of the slab) tends to be lesser than 200°C. At all depths, the model predicts slightly higher temperatures than those measured in the test. This can be attributed to the difference in the reported fire temperature and boundary conditions present in the actual test and those used in the analysis.

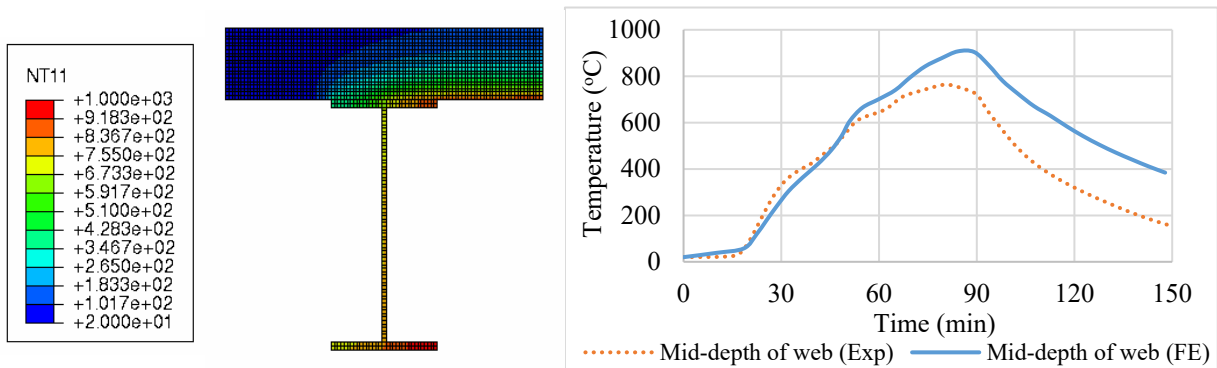


(a)

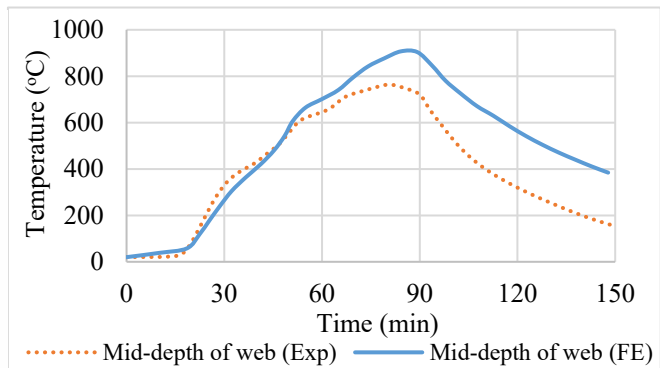


(b)

Figure 4.21. (a) Thermal gradients in the cross-section at 90 min. (b) Comparison of measured and predicted sectional temperatures for slab S1.



(a)



(b)

Figure 4.22. (a) Thermal gradients in the cross-section at 90 min. (b) Comparison of measured and predicted sectional temperatures for beam B1 (UB 356x171x51).

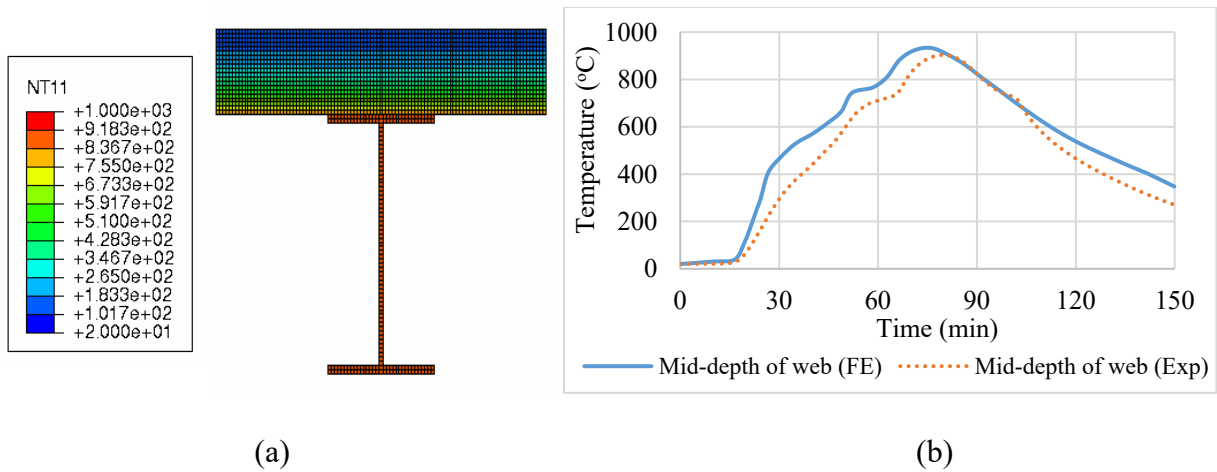


Figure 4.23. (a) Thermal gradients in the cross-section at 90 min. (b) Comparison of measured and predicted sectional temperatures for beam B2 (UB 305x165x40).

In the case of beam B1, located at the edge of the compartment, the temperature increases to about 800°C at 85 min and then drops as the fire starts to cool down. Beam B2, on the other hand, is framed in the middle of the affected compartment and is completely engulfed by fire from the bottom. The temperature gradient in B2 tends to be uniform within the cross-section and the peak temperature reaches above 900°C. The temperatures predicted from ABAQUS in the case of both B1 and B2 compare reasonably well with that measured during the fire test, with model predictions being slightly higher. As both the beams were not provided with any external fire insulation, the temperatures within the cross-section closely follow the gas temperatures.

Figure 4.24 shows the deformed state of the structural model at 150 min of fire exposure time. As seen from the figure, the portion of the slab and beams in the fire-affected compartment undergoes significant deflection. The columns in the fire compartment, on the other hand, experience lesser axial deformations and lateral deflections. The comparison of predicted deflections in the fire affected slab (at 2 m from the left edge of the affected compartment), beams (mid-span), and lateral deflection of column (at floor level) with those measured during the test are shown in Figure 4.25. The slab and beams undergo a rapid rise in deflection (in the downward direction) with a rise in

sectional temperature. The maximum deflection is seen on the secondary beam (B2) of about 420 mm (which reaches a peak temperature of over 900°C). The thermal expansion of the beams results in the lateral displacement of columns in the fire compartment. In perimeter column C1, the lateral displacement (in the major axis direction) increases to 20 mm in about 60 min as the connected beams expand with a temperature rise. The lateral displacement of the column then decreases due to the increasing downward deflection of the connected beams followed by the cooling of the compartment.

Although the interior beams were not provided with any fire insulation, the structure performed well during the fire exposure with no progressive collapse. The unprotected beams reached peak temperatures of 800°C to 1000°C. At these temperatures, structural steel has about 10% of its room temperature strength and modulus left, however, the beams did not fail. This shows that the composite action between the slab and beam and the transverse framing significantly influence maintaining the structural integrity of the floor, thereby preventing collapse. The columns in the burning compartment also did not attain instability during the fire exposure. Since the columns and edge beams with fire protected, the temperatures in these members remained below 450 °C for the entire duration of fire exposure and hence, did not experience any failure. Based on prescriptive approaches in codes, the failure of the beam is calculated when the steel temperatures reach 550°C. The failure predicted using the prescriptive based codes leads to an unrealistic fire resistance of steel structures. The insulation in the columns remained intact for the entire duration of fire exposure which resulted in low sectional temperatures in the column section. Due to this reason, the effect of high-temperature creep on the fire response of the columns and as well as the structure was minimal.

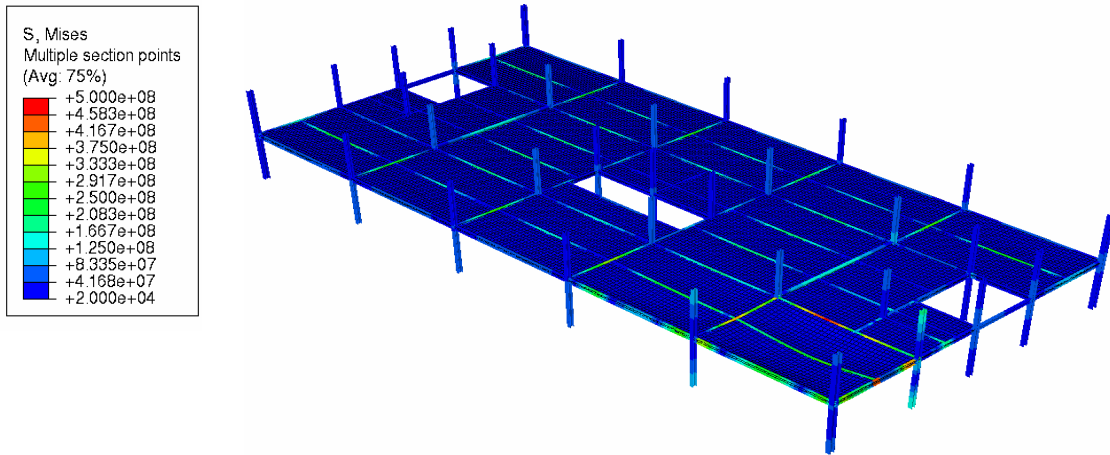


Figure 4.24. Deformed configuration of level 2 of the test building at a fire exposure time of 150 min.

The deflections obtained from the FE model are slightly higher than the measured deflections in the test. This difference may be due to the assumption of uniform heating along the length of the members used for the analysis as opposed to the actual temperature variations in the fire-affected compartment. No failure is observed in the slab, beams, or column for the entire duration of fire exposure (2.5 h) as the deflections remain within the failure limit state. As the fire in the compartment cools down, only a small amount of deflection is recovered which is also predicted by the model. Overall, the numerical model, through nonlinear dynamic explicit analysis, is able to reasonably predict the thermal and structural response at member and system levels.

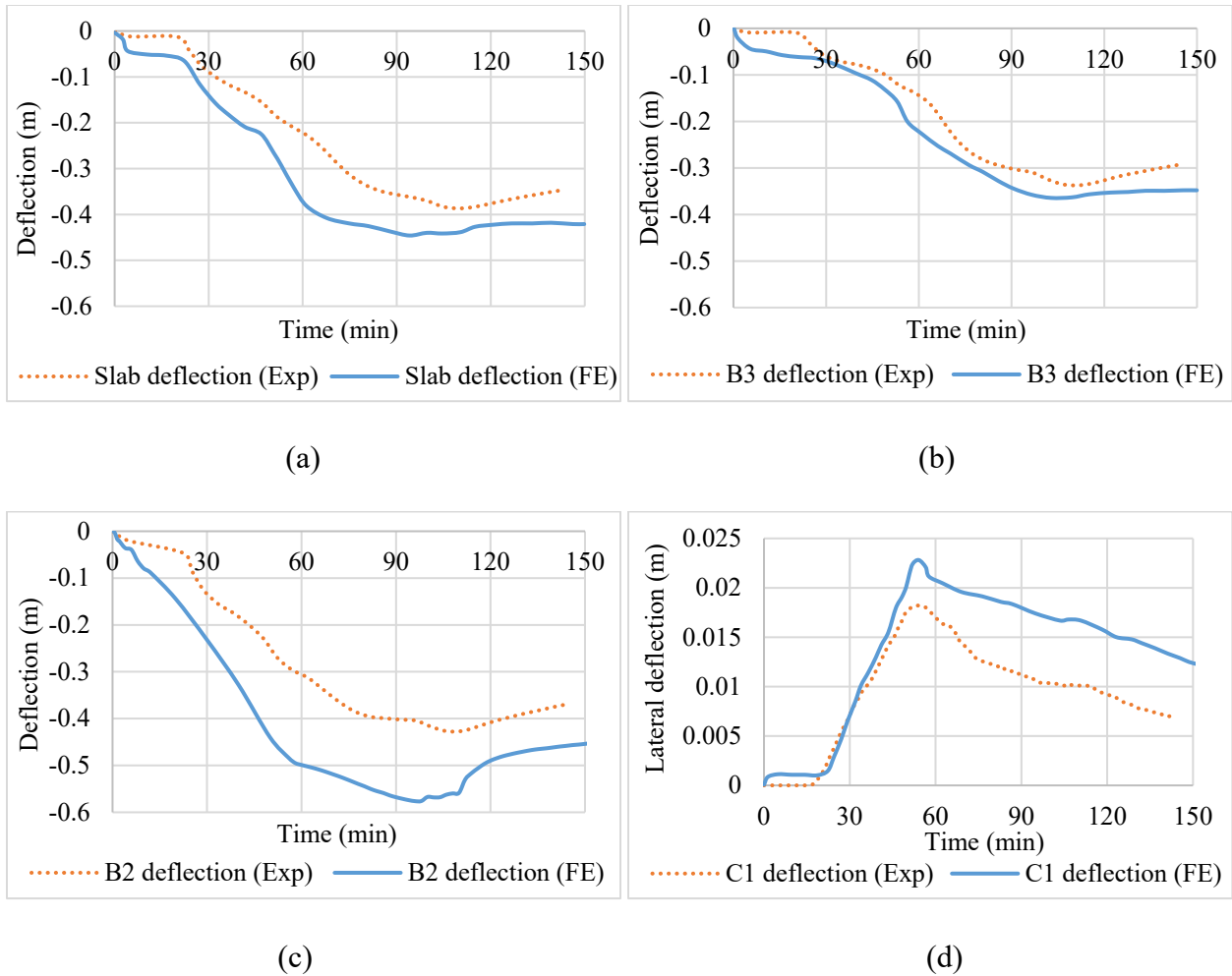


Figure 4.25. Comparison of measured and predicted deflections for (a) slab S1, (b) beam B3, (c) beam B2, and (d) column C1.

#### 4.12 Summary

This chapter presented the development and validation of a numerical model for tracing the fire-induced progressive collapse in steel framed buildings. The numerical model, comprising thermal and structural sub-models, is developed using the finite-element-based software ABAQUS. Two alternate analysis approaches, namely nonlinear quasi-static and nonlinear dynamic explicit, are proposed for tracing the structural response of a fire-exposed steel framed building until collapse. The effects of high-temperature creep and local buckling are explicitly incorporated in the fire-induced progressive collapse analysis in addition to other governing parameters such as material

and geometric nonlinearity, load redistribution, and connection configurations. A realistic failure criterion for evaluating system level failure in steel framed buildings under fire conditions is proposed.

The validity of the numerical model is established by comparing the analysis predictions, namely, sectional temperatures, displacements, and failure times with that of measured values from fire tests carried out on isolated steel members and also on steel framed structures at a system level. The validation studies show that the developed numerical model is able to reasonably predict the response of the steel structure both at member and system levels. The fire performance of the structural system is found to be much better compared to that of an individual steel member due to the ability of the frame to redistribute the forces resulting in higher fire resistance. Further, it is inferred that accounting for the full effects of transient creep strain using an explicit creep model yields a more accurate prediction of the deformations in the structure, as well as failure times. In the next chapter, the validated numerical model will be applied to carry out a set of parametric studies to quantify the influence of critical factors on the onset of fire-induced instability in steel framed structures.

### **5 Parametric Studies**

#### **5.1 General**

The onset of instability in steel framed buildings under fire exposure is influenced by various factors. These instability effects alter the load paths continuously during a fire event. It is critical to identify and quantify the effects of these factors to trace fire-induced progressive collapse in steel framed buildings. Most of these factors are dependent and influence the response of a steel framed building at different levels, namely, material level, sectional level, member level, and/or global level. For instance, the onset of instability at member and system levels is influenced by high-temperature creep effects, which in turn depends on the severity of fire (temperature rise), load (stress) levels, and the extent of burning (fire spread), and so on. Parametric studies can help generate data on various fire, loading, and restraint scenarios that can be utilized to quantify the effect of critical factors that influence fire-induced collapse in steel framed buildings.

The validated numerical model presented in Chapter 4 is applied to investigate critical factors influencing the onset of fire-induced instability in steel framed structures. This is done by carrying out a series of parametric studies, wherein the evolution of failure at member and system levels, including the continuously changing load paths under different fire scenarios are traced. The selection of test parameters and range, analysis details, and results from the parametric studies are presented in this chapter.

#### **5.2 Factors influencing fire-induced structural instability**

Fire-induced instability in a steel member is influenced by various factors including the load (stress) level, geometry (or slenderness) of the member, restraint (support) conditions, fire severity, thermal gradients, and high-temperature properties of steel, including transient creep strains. The

effect of most of these factors on the fire response of individual steel members such as beams and columns has been well studied in the literature [8,11,31,33,130]. On the other hand, limited studies are available in the literature that quantifies the effect of critical factors that govern the fire response of a steel structure at a system level. The factors that influence the onset of structural instability under fire conditions leading to progressive collapse can be broadly grouped under three categories, namely, fire parameters, material parameters, and structural parameters. Fire parameters include the intensity and duration of fire exposure, number of compartments or floors burning (extent of fire spread), location of the fire (burning), etc. The temperature-dependent properties of steel, concrete, and fire insulation, including degradation of strength and stiffness with temperature rise, the onset of high-temperature creep, residual stresses, delamination of fire insulation, etc. are critical material parameters that influence the onset of instability in steel framed buildings. The structural parameters include configuration of structural framing (braced or moment frame, and connection types), development of restraint forces, level (and any loss) of fire protection, continuously altering load paths, the onset of local instabilities, etc.

The influence of different types of framing, level of gravity loading, connection behavior, and level of fire protection on the system level response of steel framed buildings have been studied in the literature [12–17]. However, the effect of critical factors such as the type of fire scenarios including the extent of fire spread from one compartment (or floor) to another, high-temperature creep, altering load paths, and local buckling in steel sections on the onset of instability in steel framed buildings are not well studied. To quantify the effect of these parameters, a series of numerical studies are carried out at member and system levels. Results from parametric studies are presented under three categories: the effect of fire scenarios, the effect of high-temperature creep, and the effect of structural parameters.

The first set of parametric studies presents the effect of varying fire scenarios on the onset of progressive collapse in steel framed buildings. The effect of fire scenarios is a critical factor that has not been fully studied in the literature. Fire severity in steel structures is typically defined in terms of time-temperature curves with varying intensity and duration of fire exposure. While this method is satisfactory at a member level, it does not represent the actual fire scenario in a building. The severity of a building fire depends on the location of the fire, the extent of fire spread (number of compartments or floors burning), intensity and duration of exposure, and as well as the spread of fire from one region of the building to another. The majority of the past numerical studies on steel framed structures have evaluated the effect of standard fire exposure restricted to one compartment [13], as discussed in Chapter 2. To quantify the effect of realistic fire scenarios on the fire response of steel framed buildings, different standard and design fire scenarios including fire spread are considered on a 3D ten-story building. In these analyses, the propagation of failure leading to the collapse of the building is traced under different fire scenarios.

The second set of parametric studies evaluates the effect of high-temperature creep effects on the onset of instability at member and system levels. High-temperature creep effects tend to have a significant influence on the overall fire response, specifically on the onset of instability in a steel structure. The magnitude of temperature-induced transient creep strain in steel is a function of the stress level, temperature level, time duration, and rate of heating and loading [2]. At a component level, the above parameters translate into load ratio, thermal gradients, slenderness, and fire severity which directly affect the rate of development of creep strain at elevated temperatures and hence the fire response of the member. At a structural level, the creep effects are primarily influenced by the location and extent of fire spread (number of floors or compartments burning), severity, and duration of fire exposure. To investigate the extent of transient creep deformations at

member and structural levels under the effect of the different parameters listed above, a series of numerical studies are carried out on steel columns and a ten-story braced steel frame exposed to fire.

In the third set of parametric studies, the effect of structural parameters such as altering load paths, temperature-induced local buckling in steel sections, and the type of structural analysis used to trace fire-induced progressive collapse are studied. Load paths can vary continuously under fire exposure depending on the level of discretization used in the finite element program to model the steel framed building. Most of the prior studies at the system level have been carried out on 2D steel frames under fire conditions without including the floor slabs and transverse framing. To quantify the influence of including the composite slab and transverse framing in the FE analysis for tracing fire-induced collapse, numerical studies are carried out on a ten-story steel framed building with and without the presence of slab and transverse framing. Variation in load paths can also arise due to fire occurring at limited (some) locations within the building. To quantify such effects, different fire locations, including exterior and interior compartments and varying story levels are considered on a 3D steel framed building. Moreover, local buckling in steel members under fire exposure can decrease the load-carrying capacity of the member and hence, affect the overall stability of a building. The effect of local buckling under fire conditions at a structural level has not been reported in the literature. To quantify the effect of local buckling on the onset of fire-induced collapse in steel framed buildings, numerical studies are carried out with steel sections of different slenderness used in the fire-exposed compartments. Modeling approaches that account for local buckling effects are compared with approaches that ignore such effects under fire conditions. Lastly, the type of structural analysis regime (quasi-static or dynamic) adopted can also influence the predictions of the onset of progressive collapse in steel framed buildings. For this

reason, numerical studies are carried out using the nonlinear quasi-static approach and nonlinear dynamic explicit approach to trace the fire response of the steel framed building including collapse.

### **5.3 Parametric studies on the effect of fire scenarios on fire-induced instability**

To quantify the effect of realistic fire scenarios on fire-induced instability in steel framed structures, the numerical model is applied to carry out parametric studies on a 3D steel framed building. In these analyses, the effect of the composite floor system and transverse framing are considered in addition to other critical parameters to trace the various load paths leading to the collapse of the building as in a real fire scenario. The selection of the steel framed building, varied parameters, analysis details, and results from the parametric study are discussed here.

#### ***5.3.1 Selection of steel framed building for analysis***

A ten-story steel framed building, designed for NIST [131] for examining the robustness of the structure to resist disproportionate collapse, is selected for this study. Figure 5.1 shows the plan and elevation of the building along with the detailing of the framing members. The building comprises concentrically braced frames along the perimeter which forms the primary lateral load resisting system. The interior frames are designed to resist only gravity loads. All framing members are made of A992 steel (yield strength,  $f_y = 345$  MPa). The beam-column connections in the building are designed as either single plate or double angle shear connections. Welded gusset plate connections are used for all the bracing to beam (or column) connections. The floor system in the building comprises an 83 mm lightweight concrete (density =  $1760$  kg/m<sup>3</sup>, compressive strength = 21 MPa) slab topping a 76 mm deep ribbed metal deck. The concrete slab is provided with a steel mesh (Grade 60) of 185 mm<sup>2</sup>/m in both directions. The composite action between the slab and beams is achieved through the placement of  $\phi 19$  mm shear studs.



extent of burning, and fire spread. The parametric studies are grouped into four main cases as shown in Table 5-1: fire intensity, the extent of burning on a single floor, the extent of burning on multiple floors, and fire spread. As a part of the first case, the ten-story building is exposed to two standard fire exposure scenarios, namely, ASTM E119 [25] fire and ASTM E1529 [27] hydrocarbon fire, and three design fire scenarios (DF), namely, DF-60, DF-90, and DF-120. The design fire scenarios have a burning period of 60 min, 90 min, and 120 min respectively followed by a cooling phase, as shown in Figure 5.2. In the second case, the extent of burning within a single floor is varied from one compartment, four compartments to ten compartments while in the third case the extent of burning is varied from one story, two stories to three stories with two compartments burning per floor. The vertical and horizontal location and the number of compartments subjected to fire directly affect the structural behavior and the ability of the frame to resist fire-induced collapse. The compartments subjected to fire in each scenario are identified by using the floor level and the gridlines shown in Figure 5.1 which bound these compartments on that floor. For the second and third cases, the structure is exposed to standard fire for 240 min in all scenarios. The fire is assumed to be contained within the affected compartment(s) for the entire duration.

For the fourth case of parametric studies, system level analysis was carried out under four different fire scenarios that include the spread of fire from one compartment (or region) to another. In the first two scenarios, the fire starts in compartment 1 (floor 1), and in 45 min intervals spreads to the compartments in set 2 followed by the compartments in set 3 (refer to Figure 5.3). In the next two scenarios, fire is assumed to spread vertically, starting with the corner of four compartments (between gridlines D-F & 4-6) on floor 1 and in 45 min interval spreads to the same four compartments on floor 2, followed by four compartments in floor 3 after another 45 min. The fire

temperatures in the horizontal and vertical fire spread scenarios are each evaluated under two severities of fire exposure, namely, DF-60 and DF-120, shown in Figure 5.2.

Table 5-1: Critical parameters investigated to study the effect of fire scenarios on fire-induced instability

Varied parameter	Frame Designation	Parameter value	Constant parameters
Fire intensity	3D Frame – F1	ASTM E119	Fire compartments: Floor 1 – D-F & 4-6
	3D Frame – F2	ASTM E1529 (Hydrocarbon)	
	3D Frame – F3	DF-60	
	3D Frame – F4	DF-90	
	3D Frame – F5	DF-120	
Extent of burning in a single floor	3D Frame – F6	Floor 1 – E-F & 5-6 (one compartment)	Fire exposure: ASTM E119
	3D Frame – F7	Floor 1 – D-F & 4-6 (four compartments)	
	3D Frame – F8	Floor 1 – D-F & 1-6 (ten compartments)	
Extent of burning on multiple floors	3D Frame – F9	Floor 1 – E-F & 2-4 (one story)	Fire exposure: ASTM E119
	3D Frame – F10	Floors 2-3 – E-F & 2-4 (two stories)	
	3D Frame – F11	Floors 2-4 – E-F & 2-4 (three stories)	
Fire spread	3D Frame – F12	Horizontal fire spread with DF-120 fire Fire compartments: Floor 1 – C-F & 3-6	Design fire exposure and fire spread
	3D Frame – F13	Vertical fire spread with DF-120 fire Fire compartments: Floors 1-3 – D-F & 4-6	
	3D Frame – F14	Horizontal fire spread with DF-60 fire Fire compartments: Floor 1 – C-F & 3-6	
	3D Frame – F15	Vertical fire spread with DF-60 fire Fire compartments: Floors 1-3 – D-F & 4-6	

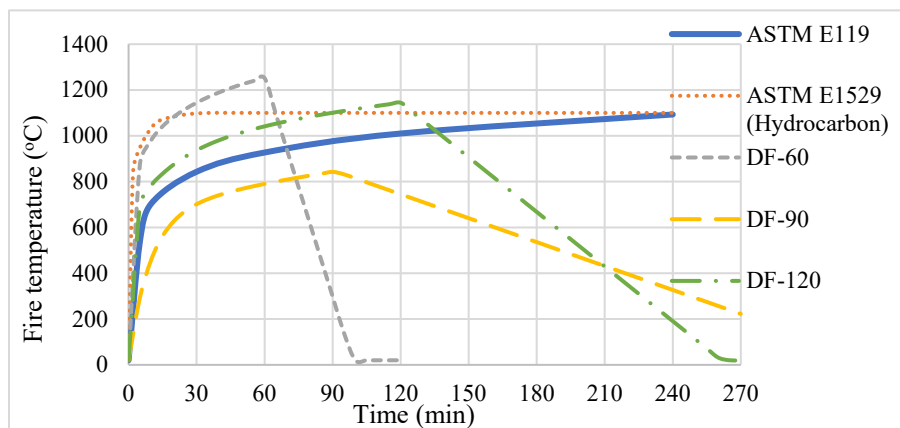


Figure 5.2. Standard and design fire exposure scenarios.

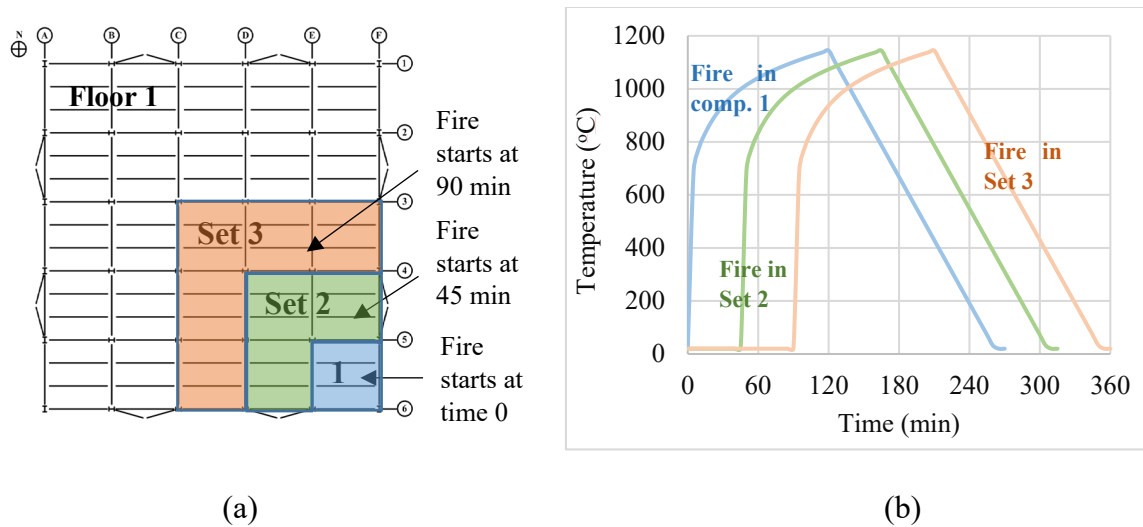


Figure 5.3. (a) Horizontal fire spread in a single story and (b) variation of fire temperatures in the compartments with time.

### 5.3.3 Analysis details

The numerical analysis of the ten-story steel framed building is carried out at a system level considering the effect of the floor system and transverse framing. A 3D model of the building is developed in ABAQUS and discretized using appropriate elements for the framing members and floor system as discussed in Section 4.7. The gravity loading, including the self-weight, imposed loads and live loads, is applied as distributed area loads on the slab elements. The lateral notional loads are applied at each floor level as distributed line loads. The thermal analysis approach described in Section 4.3 is applied to derive the thermal gradients of fire exposed members. The stresses and deflections of the structural system for the duration of fire exposure are evaluated using the nonlinear dynamic analysis approach (Section 4.3.2). Temperature-dependent material property relations for structural steel and concrete are taken from Eurocode 2 and Eurocode 3 provisions [18,125]. High-temperature creep strains are implicitly accounted for in the analyses. Failure of the frame is evaluated by applying realistic strength, deflection, and stability limiting criteria as opposed to the conventional prescriptive limiting state which is based on the critical

temperature in steel. The system level fire resistance analysis on a ten-story building is computationally expensive, owing to a large number of elements used in the 3D FE model, in addition to material and geometric nonlinearity, as well as a large number of time steps. Moreover, significant output values (temperatures, stresses, and displacements) are obtained from each analysis at various points in the structure rather than just in the fire-exposed members. To overcome this, different mesh sizes, time scaling, and mass scaling factors were considered to achieve convergence. A mesh size of 0.5m, a mass scaling factor of 10, and a small time-scaling of about 10 timesteps for 1 min of fire exposure time were found to be adequate and are adopted for the numerical simulations carried out in this study. In addition, the simulations are carried out using computer systems with large memory space and multiple parallel processors to reduce the computational time. Also, an effort is taken to identify critical output parameters from each study, which are presented in the following section.

#### ***5.3.4 Results and discussion***

Results from the parametric studies for quantifying the influence of varying fire scenarios are presented in Table 5-2 and discussed in detail in the sections that follow.

##### *5.3.4.1 Effect of fire intensity*

In this section, results from five different fire exposure scenarios shown in Figure 5.2 are presented. The first two fire scenarios are standard fires, namely, ASTM E119 [25] and ASTM E1529 [27] hydrocarbon fires in which cases the temperatures increase rapidly in the initial few minutes and then continue to increase gradually with time for the remaining duration of fire exposure. The three design fire exposure scenarios considered are representative of typical fire exposure in buildings and in these scenarios the fire temperature reaches a peak value and then cools down to ambient temperature. In all the six scenarios, the corner four compartments between gridlines D-F and 4-6

on floor 1 are subjected to fire exposure. Figure 5.4 shows the thermal response by plotting the temperatures at mid-depth (of the web) of an interior column (E5) and interior beam (E-5-6) under different fire exposure scenarios. The sectional temperatures in the steel members under ASTM E119 fire and hydrocarbon fire show a rapid increase due to the steep rise in fire temperatures in these scenarios. Under the DF-120 fire scenario, the temperature progression in steel members is similar to that of ASTM E119 fire exposure until 160 min (in the heating phase) following which the temperatures begin to drop. Under DF-60 and DF-90 fire scenarios, the steel temperatures do not exceed 550°C due to the shorter burning duration of fire exposure than the other two design fires. The steel beams experience slightly lesser temperatures as compared to that of the columns due to the presence of the concrete slab, which acts as a heat sink, and hence, lowers the temperature rise in the beams.

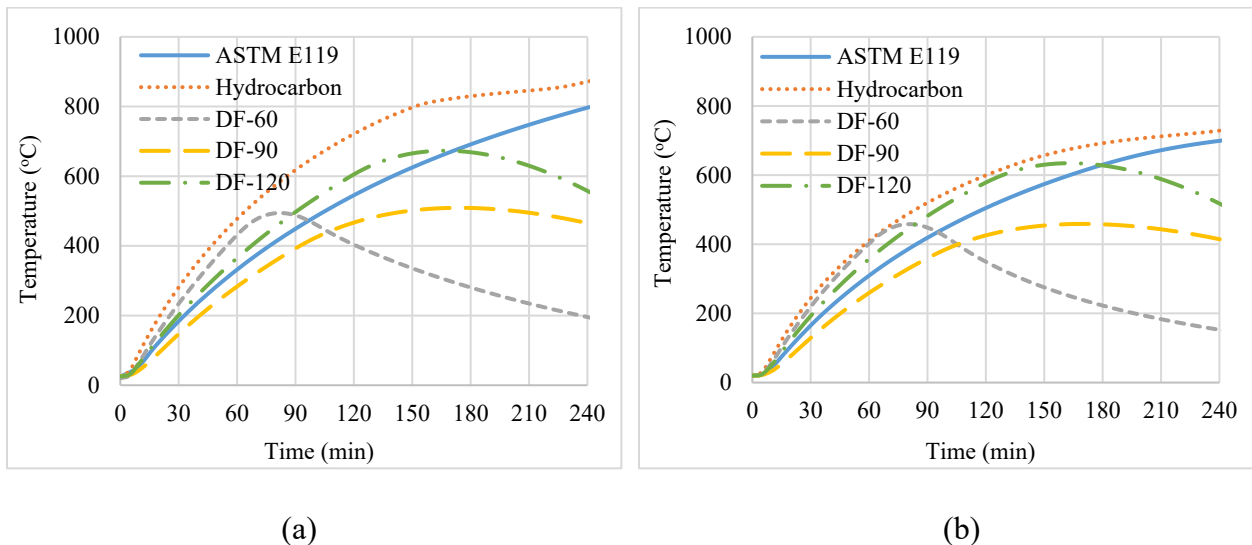


Figure 5.4. Temperature at mid-depth of web under different fire exposure scenarios for (a) interior column W14x145 (E5) and (b) interior beam W21x50 (E-5-6) on floor 1.

Figure 5.5 shows the lateral displacement of the building evaluated at the top floor level with fire exposure time. Under ASTM E119 fire exposure, the lateral displacement shows a very gradual increase with fire exposure time until about 110 min and later increases steeply until the failure of

the building. The rapid increase in the lateral displacement is associated with the progressive failure of multiple columns in the fire compartments and adjacent compartments on floor 1 leading to the progressive collapse of the structure at 132.5 min. The deformed state of the structure at the onset of collapse under ASTM E119 fire exposure is shown in Figure 5.5. The hydrocarbon fire and DF-120 fire scenarios also result in the progressive collapse of the steel framed building at 90 min and 119 min respectively (refer to Table 5-2). This is seen from the rapid increase in the lateral displacement of the top story of the building under these scenarios, as shown in Figure 5.5. The failure times under hydrocarbon fire and DF-120 fire scenarios are about 30% and 10% lower than that obtained under standard ASTM E119 fire exposure in the same set of compartments respectively due to the higher severity of the two former fire scenarios compared to that of ASTM E119 fire exposure. The DF-60 and DF-90 fire scenarios, however, do not result in the collapse of the building. Although peak fire temperatures in these cases exceed 800°C, the steel sections do not experience temperatures over 550°C due to the short burning duration of the fire, and hence, no failure is observed in the members and the overall structure.

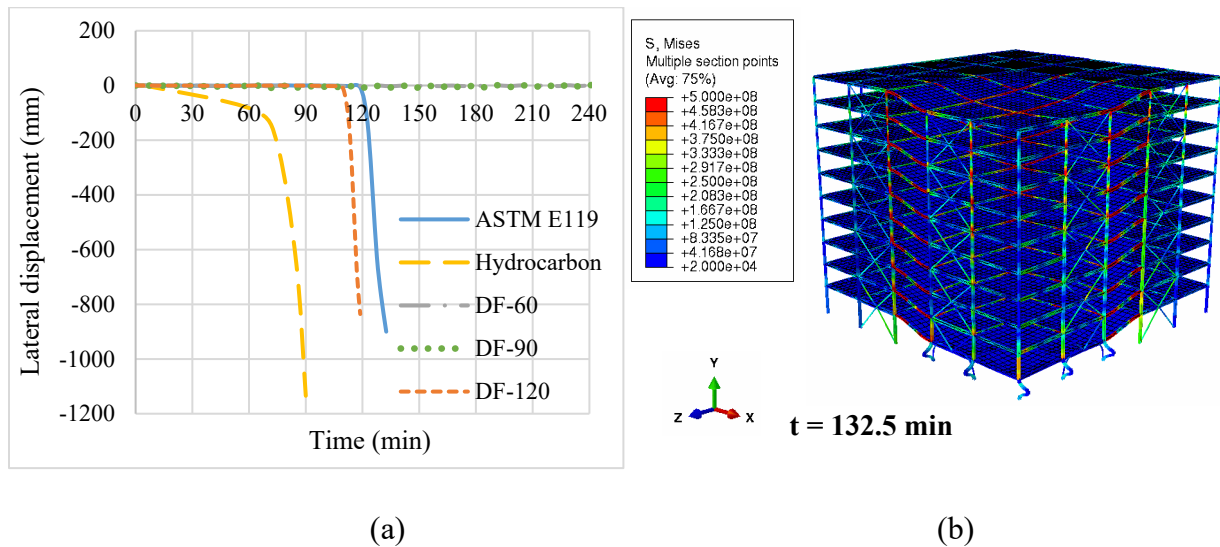


Figure 5.5. (a) Lateral displacement at the top story of the building with fire exposure time under varying fire exposure scenarios. (b) Deformed shape of the steel structure under ASTM E119 fire exposure.

#### *5.3.4.2 Effect of varying extents of burning on a single floor*

To study the influence of the extent of burning within a single story, the number of compartments exposed to fire simultaneously is varied as one, four, and ten, and standard ASTM E119 fire exposure is considered in these cases. Figure 5.6 shows the lateral displacement of the building under varying extents of burning. When only one compartment is subjected to fire exposure, no collapse occurs even though the gravity columns in the fire compartment buckle. The fire-induced axial forces developed in columns in the affected and adjacent compartments are shown in Figure 5.7. The gravity column E5 fails first at about 127.5 min due to its smaller cross-section and a higher level of loading when compared to the other affected columns. This is indicated by a drop in the axial force carried by column E5 to zero. Column F6 which has the same cross-section as E5, but lesser loading, fails next at about 150 min. The lateral columns F5 and E6 do not buckle despite having significant axial and lateral deformations. There is a definite drop in the axial forces carried by these columns, however, the axial force does not reduce to zero. The columns adjacent to the affected columns (D4, E4, and F4) show an increase in axial force as these columns take up the loads previously carried by the failed (or weakened) columns. As the framing members surrounding the fire-affected columns can carry the loads without failure, this fire scenario does not trigger collapse during the analysis (fire exposure) time of 4 h.

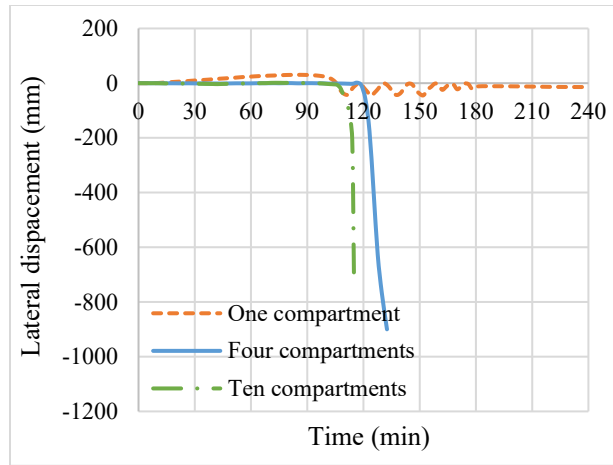


Figure 5.6. Lateral displacement at the top story of the building with fire exposure time under varying extents of burning in one story.

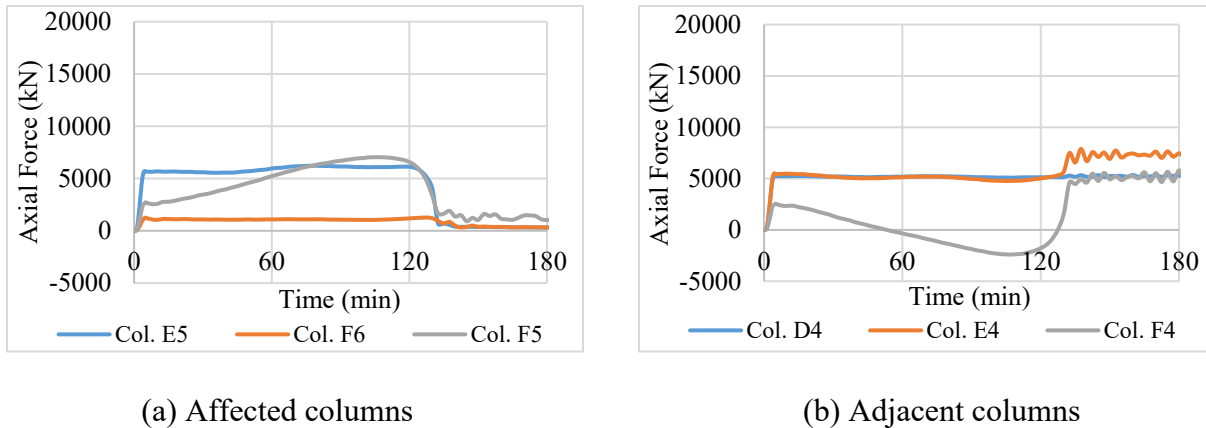


Figure 5.7. Axial forces in columns in the fire-affected and adjacent compartments for the scenario with single compartment burning.

The scenario with burning in a single compartment is similar to the kind of response observed in a real fire incident when the fire is contained within one compartment through active and/or passive fire protection systems, and in such a scenario even if a couple of members experience local failure, overall collapse does not occur due to the inherent redundancy in the structure and redistribution of loads to the adjacent members. When the extent of burning is increased to four compartments (or 15% of the floor area), global collapse initiates at 132.5 min (as shown in Figure 5.6). This is because, as more area (number of compartments) is subjected to fire, the stress levels in the fire

exposed members increase rapidly, due to the degradation in steel properties at elevated temperatures, leading to an early onset of instability at a structural level. Finally, when nearly 40% of the floor area (or ten compartments) is burning, the failure time is the least about 115 min. Figure 5.8 shows the deformed state of the building at the end of fire exposure (240 min) and just prior to collapse when one compartment and ten compartments are exposed to fire respectively. Under one compartment fire scenario, it can be seen from Figure 5.8 that the deformations in the overall building are minimal. However, when ten compartments are burning simultaneously, large deformations are observed in beams and slabs on floor 1 (as seen in Figure 5.8) which resulted in long unsupported columns between floors 1 and 2 and in turn, caused instability in these columns and the overall structure.

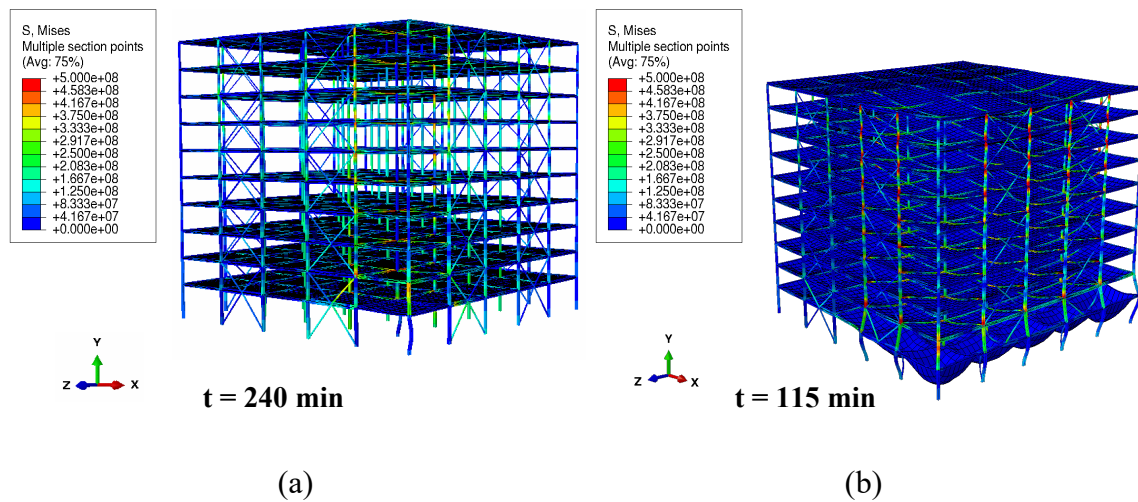


Figure 5.8. Deformed shape of the steel framed building with burning in (a) one compartment and (b) ten compartments in one story.

#### 5.3.4.3 Effect of varying extents of burning on multiple floors

Multiple stories can be impacted by fire due to specific design considerations adopted in steel framed buildings, such as ventilated cladding systems that allow the propagation of fire through the air cavity behind the cladding. To study the effect of simultaneous burning in multiple stories on the onset of progressive collapse, three scenarios are considered: fire exposure in two

compartments on floor 2 (one story), two compartments each on floors 2 and 3 (two stories), and two compartments each in floors 2, 3, and 4 (three stories). Figure 5.9 shows the lateral displacement at the top story of the building under the three fire scenarios. When the extent of burning is within one or two stories, with two compartments burning on each floor, no global collapse is initiated. The gravity and lateral columns in the fire compartments experience flexural buckling, however, the loads are redistributed to the adjacent compartments through the floor system and global failure is prevented. This is evident from the lateral displacement plot (Figure 5.9) which shows that the displacement at the top story of the building stabilizes with time in scenarios with one story and two stories burning simultaneously. However, when the extent of burning is increased to three stories, progressive collapse initiates at 165 min which is indicated by the runaway type of response observed under this scenario in Figure 5.9. The unexposed compartments are unable to withstand the redistributed loads resulting from the failure of columns in three stories, which in turn brings down the entire structure. The deformed shape of the building prior to collapse when three stories are subjected to fire is shown in Figure 5.9.

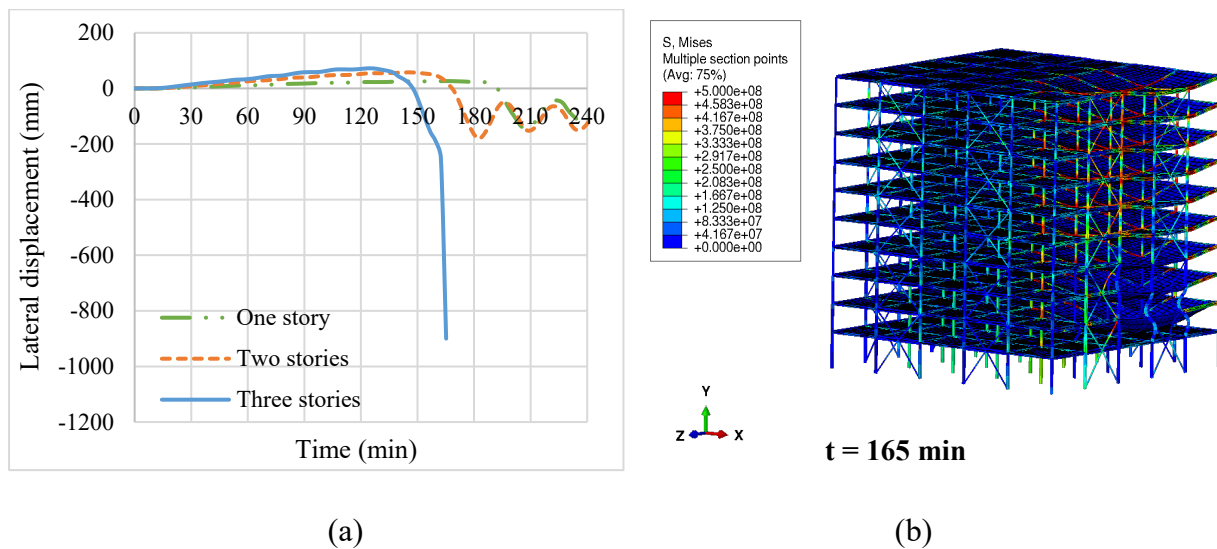


Figure 5.9. (a) Lateral displacement at the top story of the building with fire exposure time under varying extents of burning on multiple floors. (b) Deformed shape of the steel framed building under fire scenario with burning in three stories (two compartments per floor).

#### 5.3.4.4 Effect of fire spread

The fire response of the steel framed building is traced under four design fire exposure scenarios in which the structure is exposed to design fire of varying severity (DF-120 and DF-60) and fire spread (horizontal and vertical). Under the horizontal fire spread scenario with fire temperatures varying according to the DF-120 fire curve, progressive collapse initiates at 154 min (refer to Figure 5.10), after 64 min of burning in the third set of compartments. The failure sequence of affected columns and load distribution to the adjacent columns can be seen in Figure 5.11. Instability initiates in the interior column E5, which fails at 112 min during the heating phase. This shows that the 2 h fire rating for the column is not sufficient under this design fire 1. The column F6 fails next, at around 125 min, although the first compartment starts to cool from 120 min onwards. This shows that structural members may experience failure in the cooling phase as well and needs to be considered in the design. The gravity and lateral columns in set 2 compartments fail subsequently in the time frame of 145 to 150 min. At around 154 min, the deformations in slabs and beams in the affected and higher floors increase rapidly, and collapse initiates in the structure.

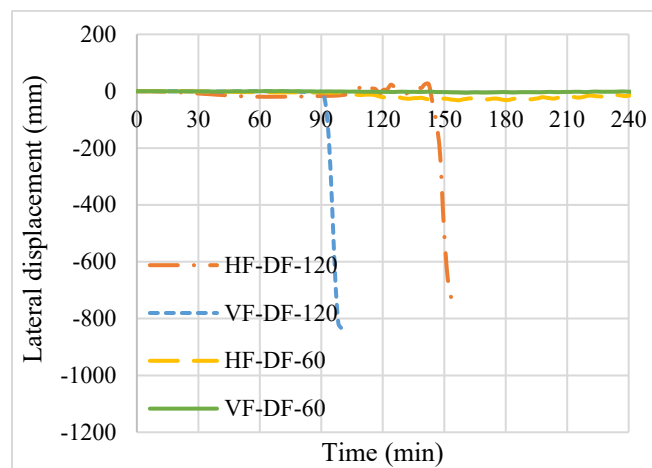
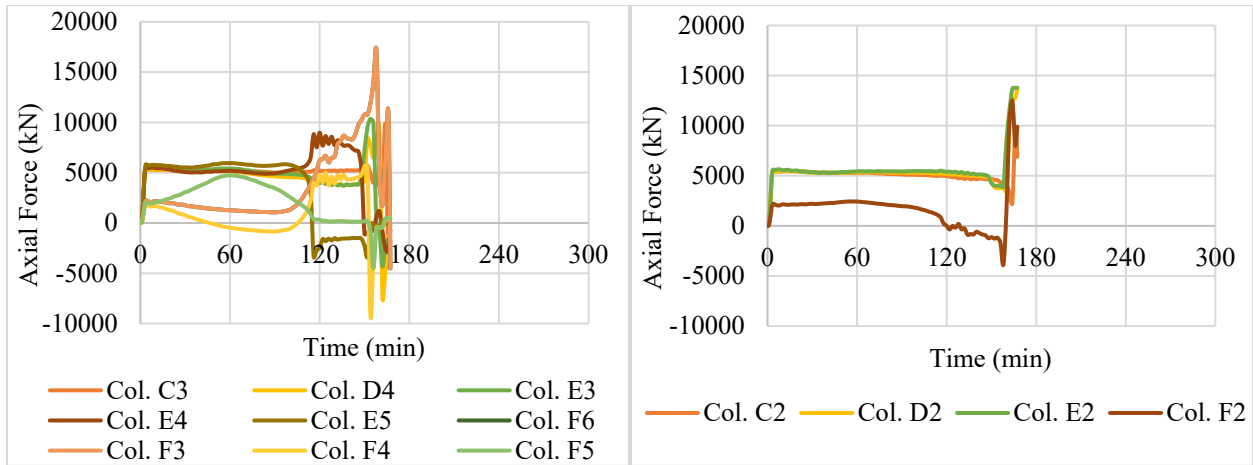


Figure 5.10. Lateral displacement at the top story of the building with fire exposure time under varying fire spread scenarios.



(a) Affected columns

(b) Adjacent columns

Figure 5.11. Axial forces in columns in the fire-affected and adjacent compartments for the scenario with horizontal fire spread with DF-120 fire exposure.

On the other hand, in the fire scenario with vertical fire spread and DF-120 fire exposure, progressive collapse initiates earlier at 100 min (after 10 min of burning in the third story) due to a larger extent of burning and multiple failures in structural members in different floor levels compared to the scenario with horizontal fire spread. From Table 5-2, it is evident that the spread of fire from one region of the building to another induces an earlier onset of instability compared to the scenario where the fire is restricted to one story with four compartments burning simultaneously (failure time of 119 min). The deformed shape of the building prior to collapse under horizontal and vertical fire spread scenarios with DF-120 fire exposure is shown in Figure 5.12.

When the building is exposed to either horizontal or vertical fire spread scenarios with fire temperatures varying according to the DF-60 fire curve, there is no failure observed in the structure, at both local and global levels. Although the fire temperatures rise to a high level of about 1200°C in these scenarios, as the duration of burning (heating) is small (60 mins), the temperatures in steel members do not rise above 500°C. Hence, the members are able to withstand

the applied loading for the entire duration of the fire. The axial forces in columns in the affected and adjacent compartments for the horizontal fire spread scenario with DF-60 fire exposure are shown in Figure 5.13. It can be seen that the axial forces in the column do not drop to zero in any of the columns in the fire affected and adjacent compartments indicating no local failure.

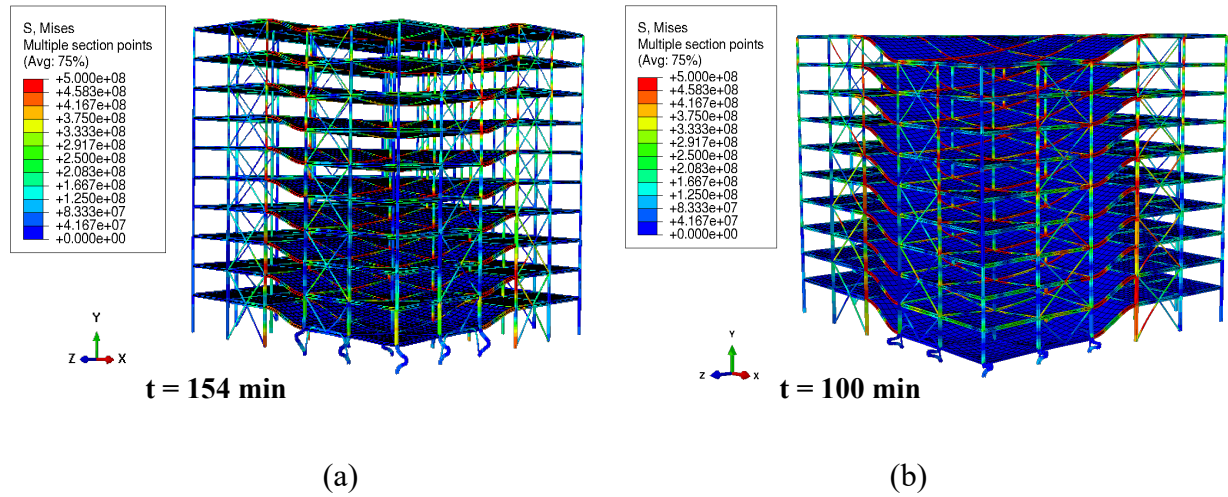


Figure 5.12. Deformed configuration of building at the onset of collapse under (a) horizontal fire spread with DF-120 fire exposure and (b) vertical fire spread with DF-120 fire exposure.

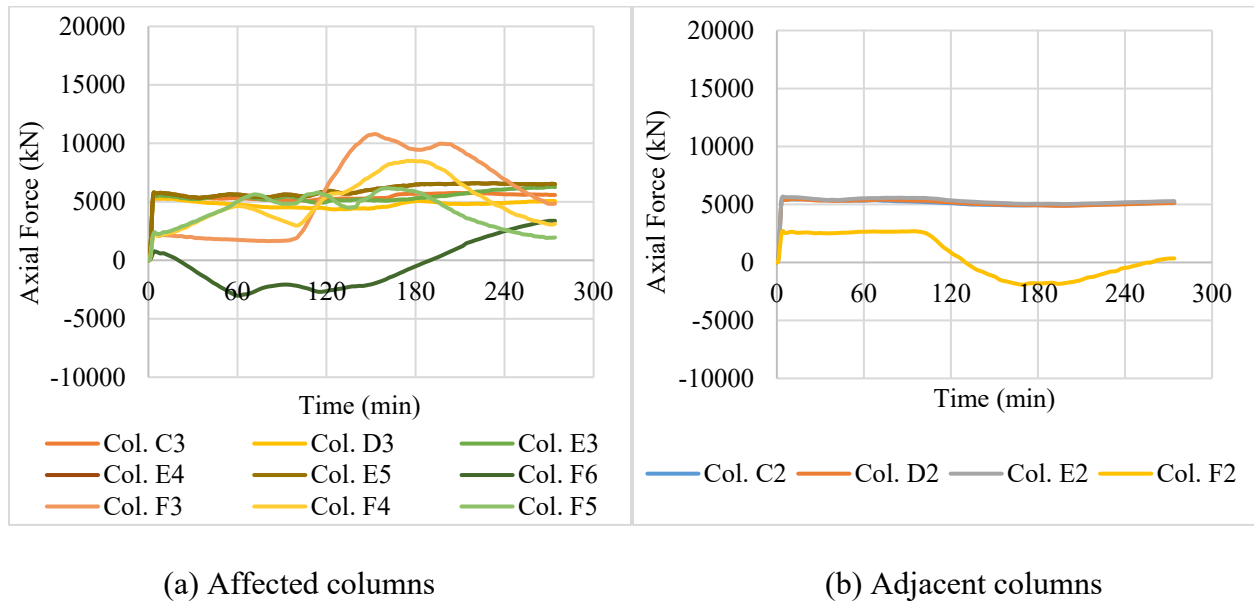


Figure 5.13. Axial forces in columns in the fire-affected and adjacent compartments for the scenario with horizontal fire spread with DF-60 fire exposure.

Table 5-2: Summary of varied parameters and results from the parametric study on the effect of fire scenarios

Varied parameter	Frame Designation	Fire compartment	Fire scenario	Failure time (min)	Occurrence of progressive collapse
Fire intensity	3D Frame – F1	Floor 1 –D-F & 4-6	ASTM E119	132.5	Global collapse occurs.
	3D Frame – F2	Floor 1 – D-F & 4-6	ASTM E1529 (Hydrocarbon)	90	Global collapse occurs.
	3D Frame – F3	Floor 1 – D-F & 4-6	DF-60	NF	No failure at member and system levels.
	3D Frame – F4	Floor 1 – D-F & 4-6	DF-90	NF	No failure at member and system levels.
	3D Frame – F5	Floor 1 – D-F & 4-6	DF-120	119	Global collapse occurs.
Extent of burning on a single floor	3D Frame – F7	Floor 1 – E-F & 5-6 (one compartment)	ASTM E119	NF	Buckling of gravity columns. No global collapse.
	3D Frame – F8	Floor 1 – D-F & 4-6 (four compartments)	ASTM E119	132.5	Global collapse occurs.
	3D Frame – F9	Floor 1 – D-F & 1-6 (ten compartments)	ASTM E119	115	Global collapse occurs.
Extent of burning in multiple floors	3D Frame – F10	Floor 1 – E-F & 2-4 (one story)	ASTM E119	NF	Buckling of columns in fire compartments. No global collapse.
	3D Frame – F11	Floors 2-3 – E-F & 2-4 (two stories)	ASTM E119	NF	Buckling of columns in fire compartments. No global collapse.
	3D Frame – F12	Floors 2-4 – E-F & 2-4 (three stories)	ASTM E119	165	Global collapse occurs.
Fire spread	3D Frame – F13	Horizontal fire spread: Floor 1 – C-F & 3-6	DF-120	154	Global collapse occurs.
	3D Frame – F14	Vertical fire spread: Floors 1-3 - D-F & 4-6	DF-120	100	Global collapse occurs.
	3D Frame – F15	Horizontal fire spread: Floor 1 – C-F & 3-6	DF-60	NF	No failure at member and system levels.
	3D Frame – F1	Vertical fire spread: Floors 1-3 - D-F & 4-6	DF-60	NF	No failure at member and system levels.

NF – No Failure

## **5.4 Parametric studies on the effect of high-temperature creep on fire-induced instability**

A series of numerical studies are carried out using the validated finite element model to evaluate the effect of temperature-induced creep deformations on the fire response of steel framed structures, especially on the onset of instability at component and system levels. For this purpose, the model is first applied to study the effect of temperature-induced creep on the fire response of steel columns. Further, the model is applied to conduct a parametric study on a ten-story braced steel framed building to evaluate the influence of transient creep on the instability of the entire steel frame under varying scenarios of fire exposure.

### ***5.4.1 Effect of high-temperature creep on member instability***

Creep effects tend to be prominent in steel columns exposed to fire conditions because they are the primary load-bearing members and are expected to sustain a long duration of fire exposure. Columns are primarily subjected to a compressive state of loading unlike flexural members, and hence, the entire cross-section of the column is utilized in resisting the loads arising from high stress levels which results in a significant amount of transient creep strain in steel. A parametric study is carried out to quantify the high-temperature creep effects on the time of onset of instability (or fire resistance) of steel columns subjected to fire conditions. The following sections discuss the selection of steel columns, varied parameters, and range, analysis details, and results from the parametric study.

#### ***5.4.1.1 Selection of steel columns for analysis***

The wide flange sections considered in this study are selected from commonly used gravity columns in a typical steel-framed building. The steel sections used in the analysis include W14x53, W14x82, and W14x145. The columns are assumed to be 3.05 m in height, pin supported at both ends, and made of A992 ( $f_{sy} = 345$  MPa) steel. The columns considered in this study are subjected

to only axial loads since creep-induced instabilities tend to be higher in structural members loaded in compression where the entire cross-sectional area is utilized in resisting the load. All columns are protected using SFRM-type insulation to meet a fire rating of 2 hours.

#### *5.4.1.2 Varied parameters and range*

To evaluate the effect of creep on the response of columns, four critical parameters, namely, load level, thermal gradients (arising from varying sides of fire exposure), slenderness (ratio) of the column, and fire severity are considered in the analysis. Load level represents the ratio of the applied axial load to the capacity of the steel column at ambient temperature. The higher the load level higher is the compressive stress on the column. Three different load levels of 30%, 40%, and 60% which range from lightly loaded to heavily loaded columns in a building are selected for this study. Non-uniform fire exposure is another critical factor influencing the onset of instability in steel columns. Based on the location of a column member in a building, whether in the interior, perimeter, or corner of a steel-framed building, the exposure conditions on the member can vary when subjected to fire. Moreover, accidental loss of fire insulation from some or all faces on the column may subject the member to non-uniform fire exposure. To study the creep effects in a column subjected to non-uniform fire exposure, four scenarios with 1, 2, 3, and 4-sided fire exposure are considered.

The slenderness of a column can significantly influence the stability of steel columns under fire exposure. The more slender a column is the lesser is its load-carrying capacity. Columns with varying slenderness are typically used in steel framed buildings. Since the columns in the lower stories experience higher loads than the columns in the upper stories, bulkier columns are used on the lower floors of a building compared to the top floors. To evaluate the effect of creep in columns with different slenderness, the slenderness ratio is varied between 30 and 63 in this study. For the

last study, the effect of creep due to varying fire severities is evaluated. For this purpose, the response of the column under two design scenarios is compared with standard ASTM E119 fire exposure. These design fire curves are obtained using the Eurocode parametric fire curve equation [77]. The selected design fires have a burning period of 90 minutes and 120 minutes respectively, representative of moderate to high fire severities. The range of different parameters considered in this study is presented in Table 5-3.

Table 5-3: Critical parameters investigated to study the effect of transient creep in steel columns

<b>Varied parameter</b>	<b>Frame Designation</b>	<b>Parameter value</b>	<b>Constant parameters</b>
Load level	Column – C1	Load level: 30%	Column: W14x53; Slenderness ratio: 63; Fire scenario: ASTM E119; Exposed sides: 4.
	Column – C2	Load level: 40%	
	Column – C3	Load level: 60%	
Thermal gradients	Column – C4	Exposed sides: 1	Column: W14x53; Load level: 40%; Slenderness ratio: 63; Fire scenario: ASTM E119.
	Column – C5	Exposed sides: 2	
	Column – C6	Exposed sides: 3	
	Column – C7	Exposed sides: 4	
Slenderness	Column – C8	Column: W14x53; Slenderness ratio: 63.	Load level: 40%; Fire scenario: ASTM E119; Exposed sides: 4.
	Column – C9	Column: W14x82; Slenderness ratio: 48.	
	Column – C10	Column: W14x145; Slenderness ratio: 30.	
Fire severity	Column – C11	Fire scenario: ASTM E119	Column: W14x53; Load level: 40%; Slenderness ratio: 63; Exposed sides: 4.
	Column – C12	Fire scenario: DF-90	
	Column – C13	Fire scenario: DF-120	

#### 5.4.1.3 Analysis details

The numerical analyses are carried out using the validated FE model, adopting the nonlinear quasi-static analysis approach for the structural analysis as described in Section 4.3.1. The cross-section of the column is first discretized as per Section 4.7 for thermal analysis. The fire temperatures are applied to the boundaries of the column cross-section through convection and radiation boundary conditions. The variation of temperatures in the cross-section with fire exposure time is provided

as input to the structural model. The column is discretized as per Section 4.7 for structural analysis under fire conditions. The end supports of the column are modeled using kinematic constraints. An initial geometric imperfection of  $H/1500$  mm at mid-height of the column is assumed, where  $H$  is the height of the column (mm). In the first step, the axial load is applied gradually as a vertical downward force at the top end of the column. Then, in the next step, the temperatures obtained from the thermal model at critical nodes in the cross-section are applied to the column as fire load. The stresses and displacement in the column are recorded as a function of fire exposure time. Failure of the steel column is evaluated based on the strength and displacement-based limit states specified in Section 4.9. The results for each case are presented in two scenarios: one *with creep*, where the high-temperature creep is explicitly incorporated, and the other *without creep*, where only partial creep effects are included implicitly in the fire resistance analysis.

#### 5.4.1.4 Results and discussion

Results from the parametric study are used to quantify the influence of critical factors on the creep-induced instability in steel columns subjected to fire exposure. The results are presented in Table 5-4 and discussed in the following sections.

##### 5.4.1.4.1 Effect of creep under varying load (stress) levels

Figure 5.14 shows the time-axial deformation plots of columns subjected to ASTM E119 fire exposure [27] under three different load levels (LL) of 30%, 40%, and 60%, with and without the inclusion of explicit creep. The results indicate that the steel column deteriorates rapidly under increasing load levels, owing to the higher initial stress (load-induced) in the column. The scenario of 60% load level results in the shortest failure time of 99 min. The effect of creep is also higher in columns subjected to higher loads, as transient creep strain increases significantly with an increase in stress levels [1]. Figure 5.14 shows the deformed shape of the column for the case of a

40% load level obtained using models with and without creep at 155 min of fire exposure. It is evident that the model without explicit creep underestimates the deformation of the column at stages close to failure. Although most columns are lightly loaded in typical steel framed buildings, the exposure to fire results in the degradation of strength and stiffness in steel which in turn can induce high stress levels with increasing fire exposure time, resulting in significant creep deformations and an early onset of instability in these columns.

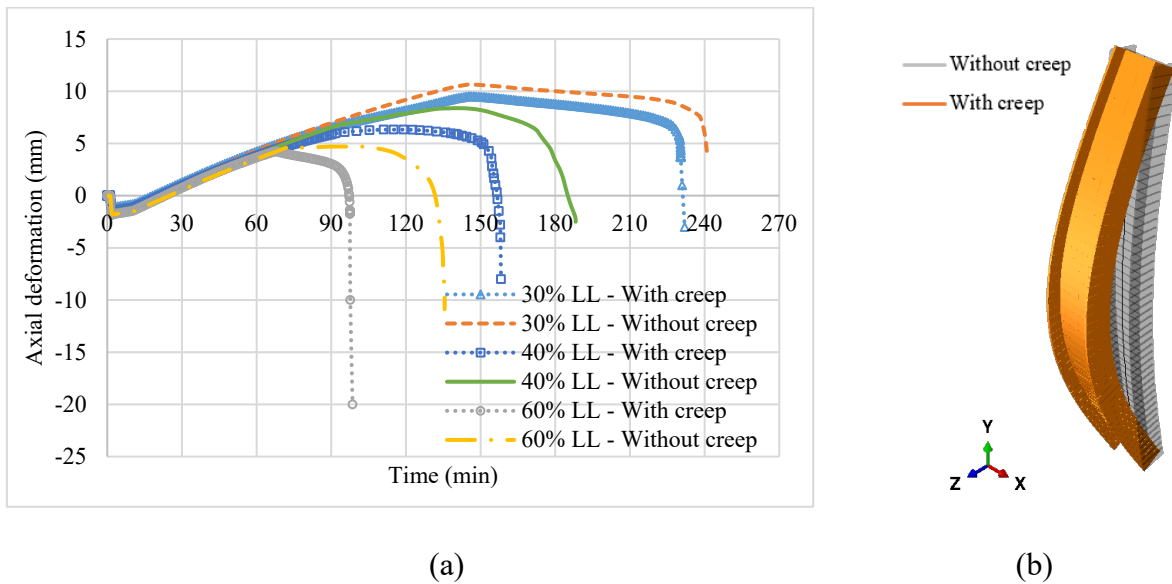


Figure 5.14. (a) Axial deformation response of steel columns under varying load levels. (b) Deflected profile of steel column under 40% LL at a fire exposure time of 155 min.

#### 5.4.1.4.2 Effect of creep under varying thermal gradients

The axial deformation response of columns exposed to fire from 1, 2, 3, and 4 sides, from the analyses *with creep* and *without creep*, is presented in Figure 5.15. Under uniform fire exposure (4-sides), the column member experiences higher temperatures, which in turn leads to faster degradation of strength and stiffness of steel, resulting in an early onset of instability. The influence of high-temperature creep, on the other hand, is the highest in the case of 3-sided fire exposure, with the difference between failure times of 227 min and 273 min respectively predicted using models with and without creep being 46 min. The column experiences uniaxial bending (thermal

bowing), due to the asymmetric thermal gradients that develop under 3-sided fire exposure, which gets further increased due to the differential creep strain that develops in the column section, leading to higher stresses and in turn higher creep deformations and subsequent failure.

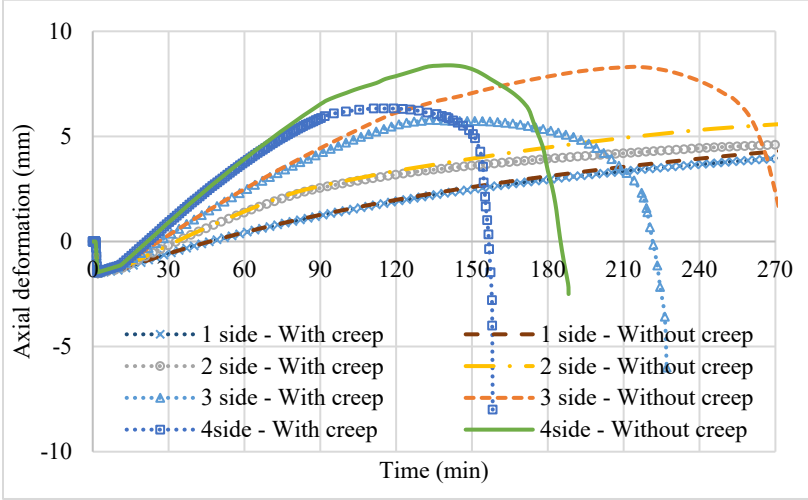


Figure 5.15. Axial deformation response of steel columns under varying thermal gradients.

5.4.1.4.3 Effect of creep under varying slenderness

Three wide flange sections, W14x53, W14x82, and W14x145 with slenderness ratios of 63, 48, and 30 are considered. The slenderness values chosen are representative of those of typical columns used in the upper, middle, and lower stories of a mid-rise steel framed building. Figure 5.16 shows the comparison of the axial deformation response of the three columns considered, with and without incorporating explicit creep. The difference in fire resistance times is the highest (30 min) in the case of the W14x53 column with the largest slenderness ratio. The column with higher slenderness experiences a faster reduction in capacity with rising temperature, which in turn leads to higher stress levels and an early onset of instability.

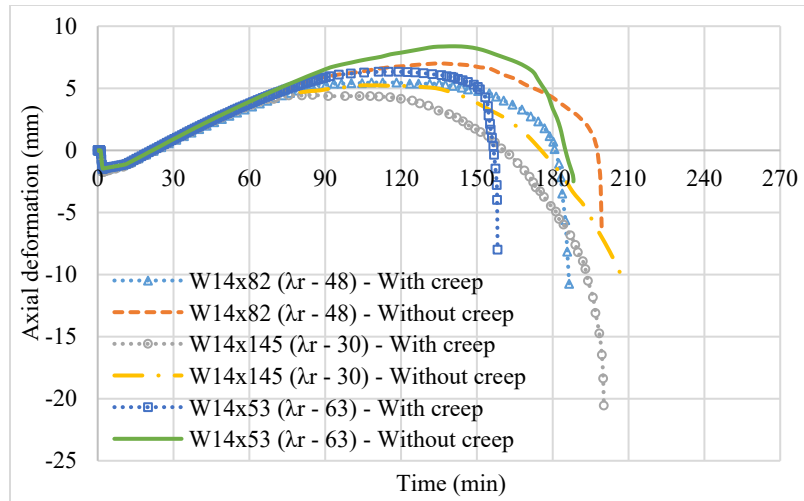


Figure 5.16. Axial deformation response of steel columns with varying slenderness ratios.

#### 5.4.1.4.4 Effect of creep under varying fire severity

To investigate the influence of the severity of fire exposure on the extent of transient creep deformations that develop in steel columns, the response of the steel column was simulated under two design fire scenarios of moderate to high severity, namely, DF-90 and DF-120, as shown in Figure 5.2 is compared with standard ASTM E119 fire exposure. The axial deformation response of the column under exposure to the standard and design fires is presented in Figure 5.17. Under the DF-90 fire scenario, which has a burning period of 90 min, the steel temperatures in the column section are within 400°C for the entire duration of exposure and very less creep deformations develop in the member. On the other hand, exposure to the more severe DF-120 fire scenario results in high temperatures in the column member at quicker times leading to a lower failure time as compared to the standard fire scenario. The effect of creep is high in the case of DF-120 and is evident from the axial deformation response which shows a difference of 30 min in fire resistance times predicted using models with and without creep. Due to the high peak fire temperature (above 1000°C) and a long burning duration (2 hours), significant creep deformations develop in the steel column under the DF-120 scenario. When exposed to severe fires, with peak temperatures above

1000°C and burning for more than 2 hours, and steel temperatures exceeding 450°C, the high level of creep strain that develops in steel can be critical to the stability of the column. In such scenarios, an explicit creep analysis is needed to realistically predict the onset of instability in the steel column.

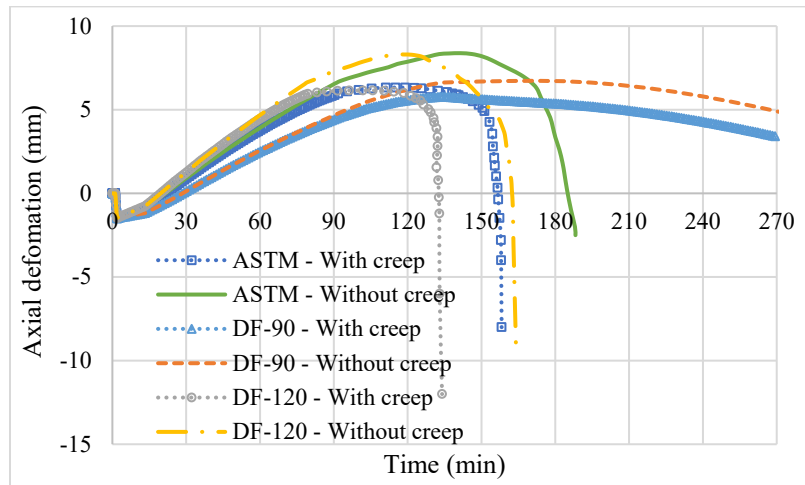


Figure 5.17. Axial deformation response of steel columns under varying fire severity.

Table 5-4: Summary of varied parameters and results from the parametric study on transient creep effects in steel columns

Varied parameter	Column Designation	Column (slenderness ratio, $\lambda_r$ )	Load level (%)	Fire scenario	Exposed sides	Fire resistance (min)		
						With creep	Without creep	Difference
Load level	Column – C1	W14x53 (63)	30	ASTM E119	4	232	241	9
	Column – C2	W14x53 (63)	40	ASTM E119	4	158	188	30
	Column – C3	W14x53 (63)	60	ASTM E119	4	99	136	37
Thermal gradients	Column – C4	W14x53 (63)	40	ASTM E119	1	NF	NF	-
	Column – C5	W14x53 (63)	40	ASTM E119	2	NF	NF	-
	Column – C6	W14x53 (63)	40	ASTM E119	3	227	273	46
	Column – C7	W14x53 (63)	40	ASTM E119	4	158	188	30
Slenderness	Column – C8	W14x53 (63)	40	ASTM E119	4	158	188	30
	Column – C9	W14x82 (48)	40	ASTM E119	4	186	199	13
	Column – C10	W14x145 (30)	40	ASTM E119	4	200	208	8
Fire severity	Column – C11	W14x53 (63)	40	ASTM E119	4	232	241	9
	Column – C12	W14x53 (63)	40	DF-90	4	NF	NF	-
	Column – C13	W14x53 (63)	40	DF-120	4	134	164	30

NF – No failure

#### ***5.4.2 Effect of high-temperature creep on structural instability***

To quantify the effect of high-temperature creep on the fire-induced collapse of steel framed buildings, a system level analysis approach is applied to a ten-story braced steel frame exposed to fire. The effect of creep on the onset of instability at a system level is quantified under varying scenarios of fire exposure. The selection of steel frame, parameters considered, analysis details, and results from the numerical studies are detailed in the following sections.

##### ***5.4.2.1 Selection of steel frame for analysis***

The ten-story braced steel framed building described in Section 5.3.1 is chosen for this study. The structural fire response of the N-S perimeter frame along gridline A is investigated, with due consideration to high-temperature creep effects. This N-S perimeter frame is chosen, in lieu of the E-W frame, because it is likely to be more susceptible to creep-induced instabilities due to the higher distribution of loads (and hence, higher stress levels) in the beams and columns framing in this direction. On account of the 2D representation of the building, the beneficial effect of the composite action between the floor slab and beams is not taken into consideration in the analysis. Further, the redundancy in a 2D building model is lesser compared to that in a 3D structure, and hence the redistribution of forces occurs to a lesser extent in the 2D model. However, prior studies have shown that the 2D model gives conservative failure times and it has been shown that the overall trends in the fire response are in good agreement with the 3D counterparts [14,16]. As the primary objective of this study is to evaluate and compare the influence of high-temperature creep on the stability of steel framed structures under different scenarios, a 2D representation of the building is considered to be adequate for this study.

#### *5.4.2.2 Varied parameters and range*

To investigate the influence of temperature-induced transient creep on the overall stability of the braced steel framed building, different scenarios are considered by varying critical parameters that significantly affect the extent of creep deformations that develop under fire conditions. The parameters varied in this study are tabulated in Table 5-5 and include the location of the fire (burning) in a building, the extent of fire spread (number of compartments or floors burning), and the severity of the fire exposure. For the first four studies, the ASTM E119 standard fire exposure [27] is adopted to calculate the fire temperature in the compartment(s). For the last study, three design fire exposure scenarios are considered, namely, DF-90, DF-120, and DF-180, with burning periods of 90 min, 120 min, and 180 min respectively followed by a cooling phase, as shown by the time-temperature curves in Figure 5.18. These design fire curves are defined as per Eurocode 1 [77] parametric time-temperature relations and represent fires of moderate to high fire severity. The ASTM E119 standard fire scenario is taken as a baseline case. The structure is exposed to fire for 240 min (4 hours) in all the scenarios. The results from the parametric study are also presented for two cases: one explicitly incorporating transient creep (“with creep”) and the other incorporating implicit creep only (“without creep”). The fire compartments are identified by the floor number and gridlines bounding the compartments exposed to fire. The beams and columns are also identified using the gridlines along which the member spans.

Table 5-5: Critical parameters considered to investigate the transient creep effects at a system level

Varied parameter	Frame Designation	Parameter value	Constant parameters
Fire location within a story	2D Frame – H1 2D Frame – H2	Interior compartment: Floor 2 – A & 3-5 Exterior compartment: Floor 2 – A & 4-6	ASTM E119 fire
Fire floor	2D Frame – H3 2D Frame – H4 2D Frame – H5	Floor 2 – A & 3-5 Floor 5 – A & 3-5 Floor 9 – A & 3-5	ASTM E119 fire
Number of compartments burning	2D Frame – H6 2D Frame – H7 2D Frame – H8	One compartment: Floor 2 – A & 4-5 Two compartments: Floor 2 – A & 3-5 Three compartments: Floor 2 – A & 2-5	ASTM E119 fire
Number of floors burning	2D Frame – H9 2D Frame – H10 2D Frame – H11	One story: Floor 2 – A & 3-5 Two stories: Floors 2-3 – A & 3-5 Three stories: Floors 2-4 – A & 3-5	ASTM E119 fire
Fire severity	2D Frame – H12 2D Frame – H13 2D Frame – H14 2D Frame – H15	ASTM E119 DF – 90 DF – 120 DF – 180	Fire compartments: Floor 2 – A & 3-5

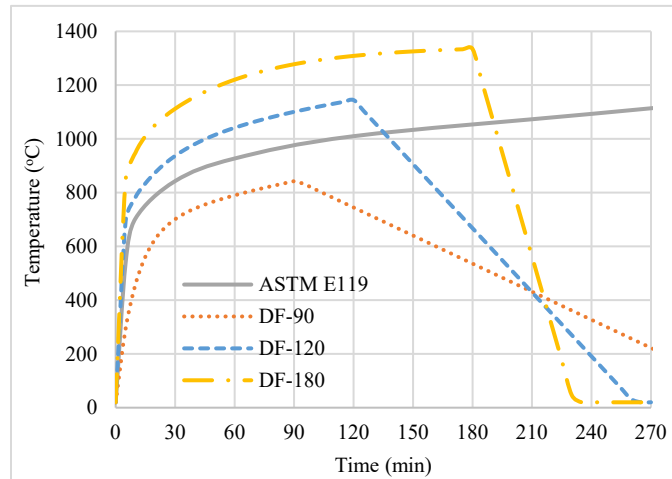


Figure 5.18. Different fire exposure scenarios considered in the study.

#### 5.4.2.3 Analysis details

The system level analysis approach, using the nonlinear quasi-static analysis (as described in Section 4.3.1) for the structural analysis, is adopted for this study. The 2D steel frame is modeled

in ABAQUS and discretized using appropriate elements for the framing members as discussed in Section 4.7. The gravity loading, including the self-weight, imposed loads and live loads, is applied as concentrated loads on the beams at the location of the transverse beams. The lateral notional loads are applied as concentrated loads at each floor level. Additionally, at each floor level, the frame is restrained against out-of-plane displacements. The thermal and structural analysis of the steel frame is carried out as described in Section 4.3 to derive the thermal gradients in fire exposed members from the thermal model and stresses and deflections of the structural system for the duration of fire exposure from the structural model. As the steel framed structure is expected to experience large strains (displacements) during fire exposure, an updated Lagrangian method is adopted in the numerical model wherein the equilibrium of the structure is considered on the deformed shape. Temperature-dependent material property relations for structural steel are taken from Eurocode 3 provisions [18]. High-temperature creep strains are explicitly accounted for in the analyses using a creep sub-model as described in Section 4.6. The structural analysis is carried out in incremental time steps, with an initial, minimum, and maximum increment of 1 second, 1E-5 seconds, and 5 minutes, respectively. The Newton-Raphson method is employed as the solution technique to obtain the nonlinear response at each time step in ABAQUS [123]. Failure of the frame is evaluated by applying realistic strength, deflection, and stability limiting criteria as opposed to the conventional prescriptive limiting state which is based on the critical temperature in steel.

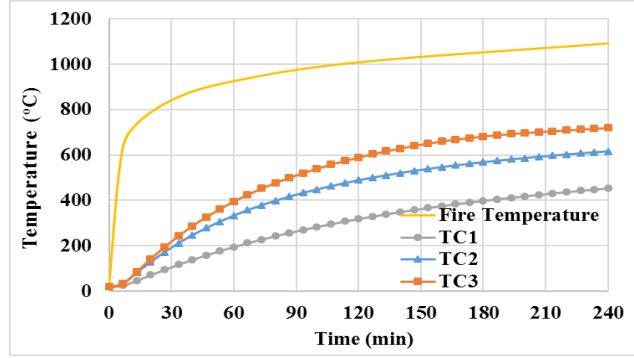
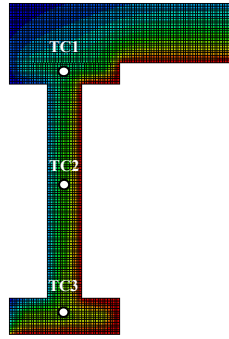
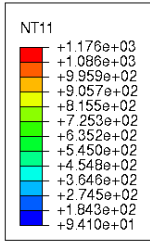
#### *5.4.2.4 Results and discussion*

Results from the parametric study are used to quantify the influence of critical factors on the creep-induced instability in the braced steel frame exposed to fire.

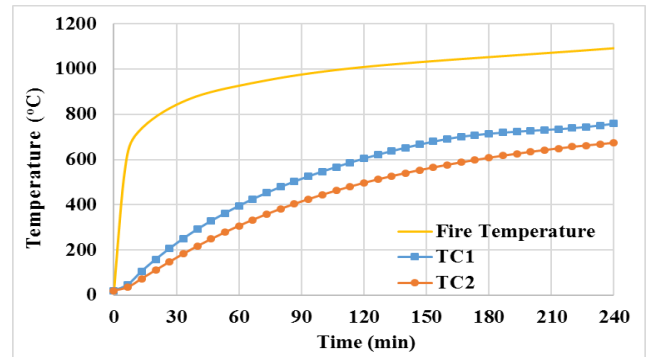
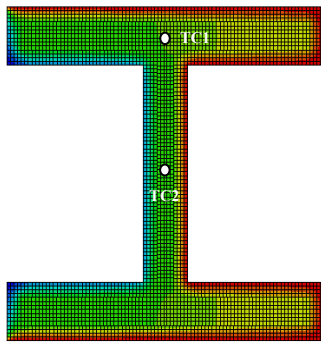
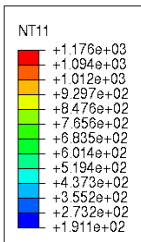
#### 5.4.2.4.1 Effect of creep under varying fire locations within a story

Fire occurring in different locations within the same story (such as in a corner compartment or interior compartment, or a braced or unbraced bay) can result in different levels of creep deformations in the structural members exposed to fire as the level of transient creep strain significantly depends on the stress level and restraint conditions of the member. These creep-induced deformations in the fire-exposed members further affect the deformations in the structural system and thus the stability of the members of the whole frame. System level analysis is conducted on the braced frame structure with fire occurring in two different locations on floor 2: *A & 3-5* (interior bays) and *A & 4-6* (exterior bays).

Figure 5.19 shows the sectional temperatures in beam A-4-5 and column A4 on floor 2 for the scenario with fire (burning) in the interior bays (*Floor 2 – A & 3-5*). As the frame considered in the analysis is an exterior frame, the beam is subjected to a 2-sided fire exposure from the bottom, while the column in the middle of the fire exposure region is exposed to fire from 3 sides. Owing to the fire insulation (protection) present on structural members, the steel temperatures within the cross-section of the beam and column members increase slowly in the initial period of fire exposure. Then, the rate of temperature rise further slows down as the rate of fire temperature rise slows down with time. The presence of the concrete slab further lowers the rise in steel temperature in the beam member, with the top flange of the beam experiencing much lower temperatures than the bottom flange.



(a)



(b)

Figure 5.19. Sectional temperatures in (a) beam W21x50 (A-4-5) and (b) column W14x193 (A4) on floor 2.

In the structural response of the frame under scenario *Floor 2 – A & 3-5*, the column A4 in the middle of the fire region fails first due to the higher temperature that the column experiences as compared to the other fire-exposed columns. Figure 5.20 shows the axial deformation and axial force response of column A4 as a function of fire exposure time. The models with and without creep predict similar trends for much of the fire exposure duration except close to the failure of the column. As the column is lightly loaded (about 20%) prior to fire exposure, the extent of temperature-induced creep strains deformation is low, and the failure times predicted using the models with and without creep are 154 min and 163 min, respectively. The development of total and creep strains plotted in Figure 5.20 shows that the creep strain is minor in the initial stages of

fire exposure. However, close to the failure of the column, creep strain increases significantly and forms a major portion of the total strain. A comparison of total strain predicted using models with and without creep indicates that the model “without creep” underestimates the total strain near the failure since the implicit creep model does not capture the full creep effects at this stage.

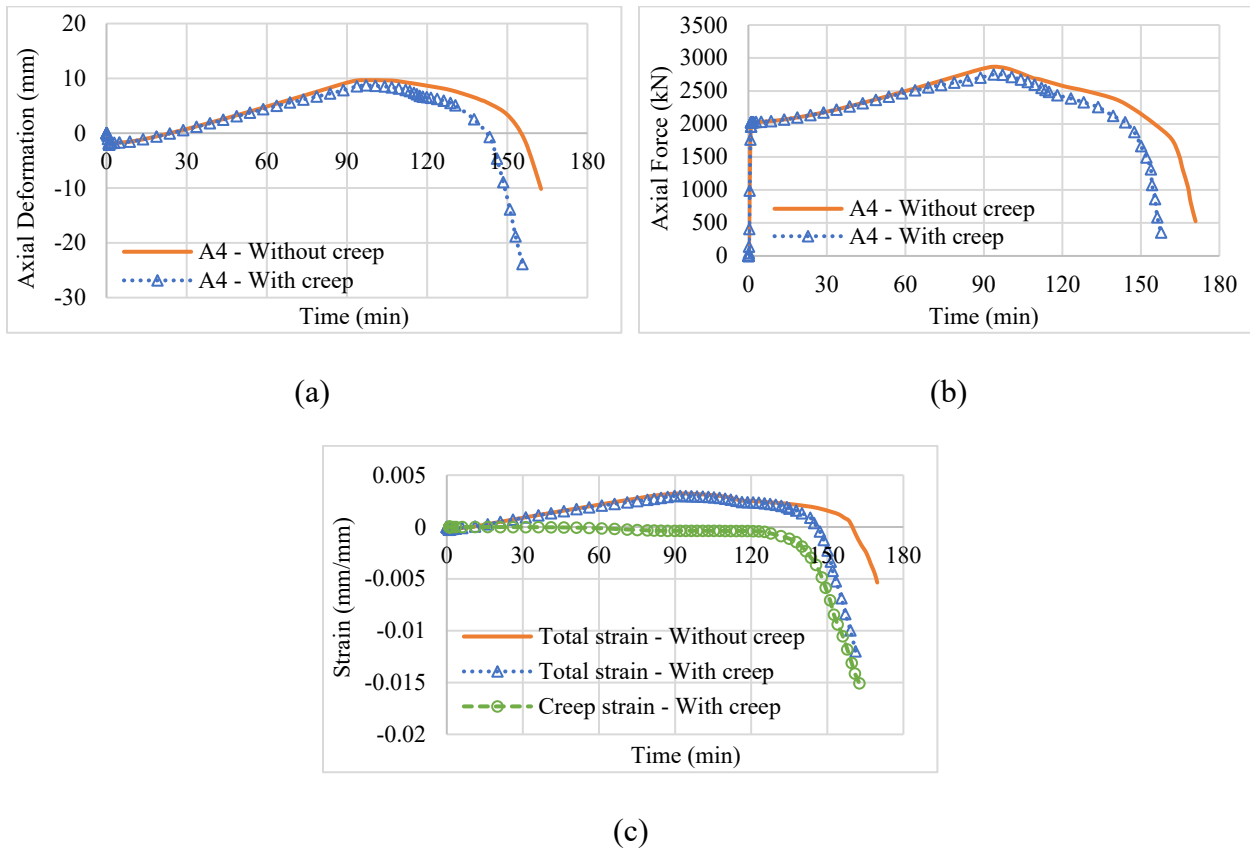


Figure 5.20. (a) Axial deformation, (b) axial force, and (c) evolution of total strain and creep strain in column A4 on floor 2.

Due to redistribution of forces following the failure of column A4, the brace adjoining the failed column immediately fails and hence, is removed from the frame. Figure 5.21 shows the utilization ratio (defined as the ratio of the maximum design force (axial force or bending moment) to the capacity of the member at a given temperature) of beams and columns on floor 2 following the application of gravity and lateral loading at room temperature and the redistributed forces in the frame at 155 min after the removal of column A4 and the adjoining brace. The initial stress levels

in the columns in the fire-affected story are 20% and lesser. Following redistribution of loads, columns A5 and A3 (which are at a temperature of about 500°C) experience a stress level of 60% and 12% respectively. Column A2 (which is still at room temperature) is stressed to 40%. Fig. 36 shows the axial deformation and axial force response of columns A3 and A5. As columns A3 and A5 are exposed to lower temperatures than A4, the axial deformations in these columns are still in the expansion phase until the failure of A4. Following the removal of column A4 and brace, the deformation of column A5 rapidly increases (in the downward direction) due to high stress levels resulting in failure. The models “without creep” and “with creep” predict a failure time of 219 min and 191 min respectively. The difference in failure times using models with and without creep is about 28 min, as compared to a 9 min difference obtained in the case of failure of column A4. The high stress levels in column A5, combined with high steel temperature, result in significantly higher levels of creep strain and in turn, a higher difference in the failure times with and without creep.

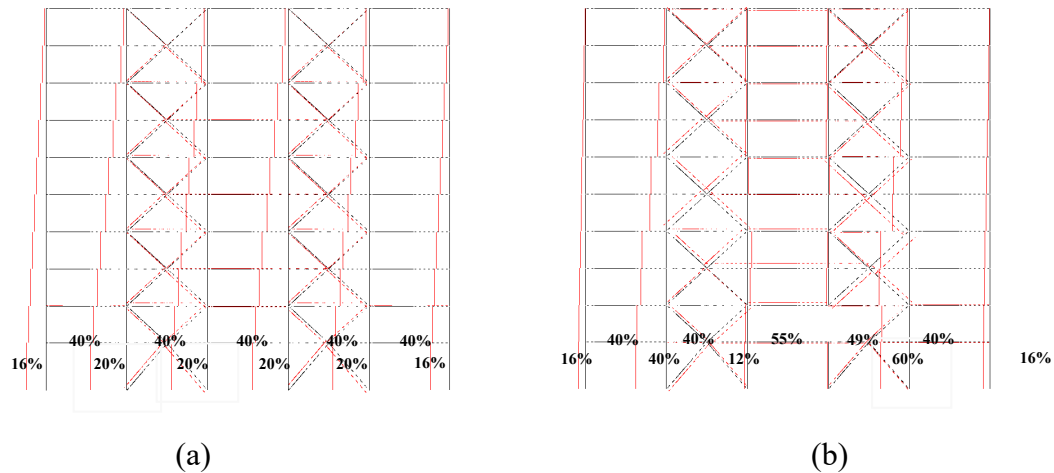


Figure 5.21. Axial force profile of frame indicating the utilization ratio (%) of beams and columns at (a) room temperature following the application of initial loads and (b) 155 min of fire exposure using analysis “with creep”.

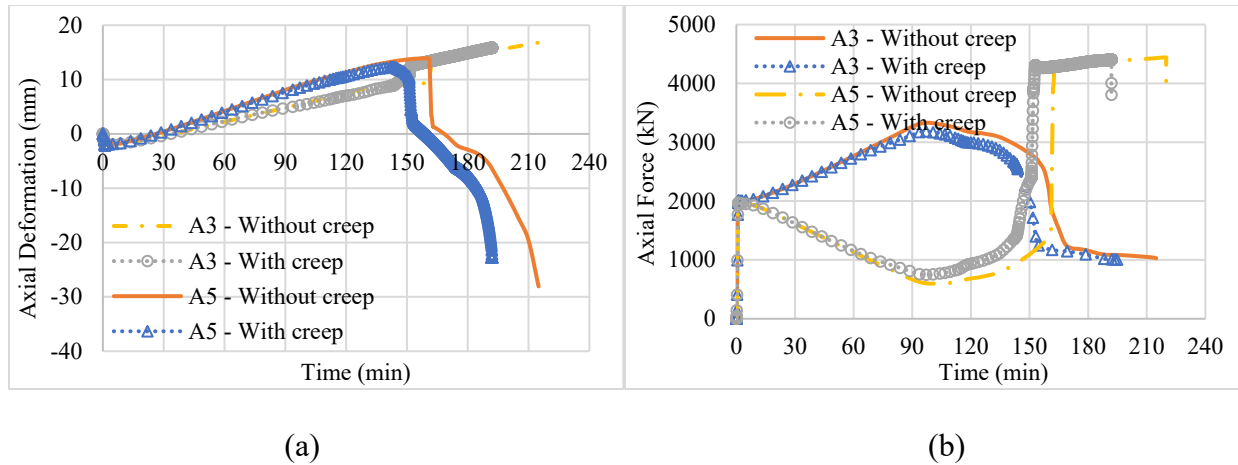


Figure 5.22. (a) Axial deformation and (b) axial force in columns A3 and A5 on floor 2.

Removal of Column A5, in both the analysis “*with creep*” and “*without creep*”, results in the failure of multiple braces on higher floors in Bay 4 due to high levels of redistributed loads. The building begins to rapidly drift to the left indicating the onset of instability and initiation of progressive collapse at this stage. The lateral displacement of the frame evaluated at different story levels is shown in Figure 5.23. Although only two compartments on floor 2 are subjected to fire, it is observed that the deformations that occur in the fire compartments tend to influence the deformations that occur elsewhere in the frame, as the structure tries to maintain equilibrium and compatibility at each time step during the fire exposure. Owing to the thermal expansion of beams A-3-4 and A-4-5, the burning floor (floor 2) expands to the right, while the floors above the fire floor begin to drift leftwards. The lateral displacement predicted using models “*with creep*” and “*without creep*” is almost the same until the failure of column A4, which occurs around 150 min using the model “*with creep*”. The lateral displacement at all floors above floor 2 predicted using the model “*with creep*” shows a sudden increase beyond 150 min, while the model “*without creep*” predicts much lesser displacement. When column A5 fails, the frame begins to rapidly drift to the left hinging at the fire floor until failure, which is seen from the run-away deflections predicted at 191 min and 219 min using models “*with creep*” and “*without creep*” respectively.

The highest lateral displacement occurs at the top story level while the floor below the fire floor shows negligible displacement throughout the fire exposure duration.

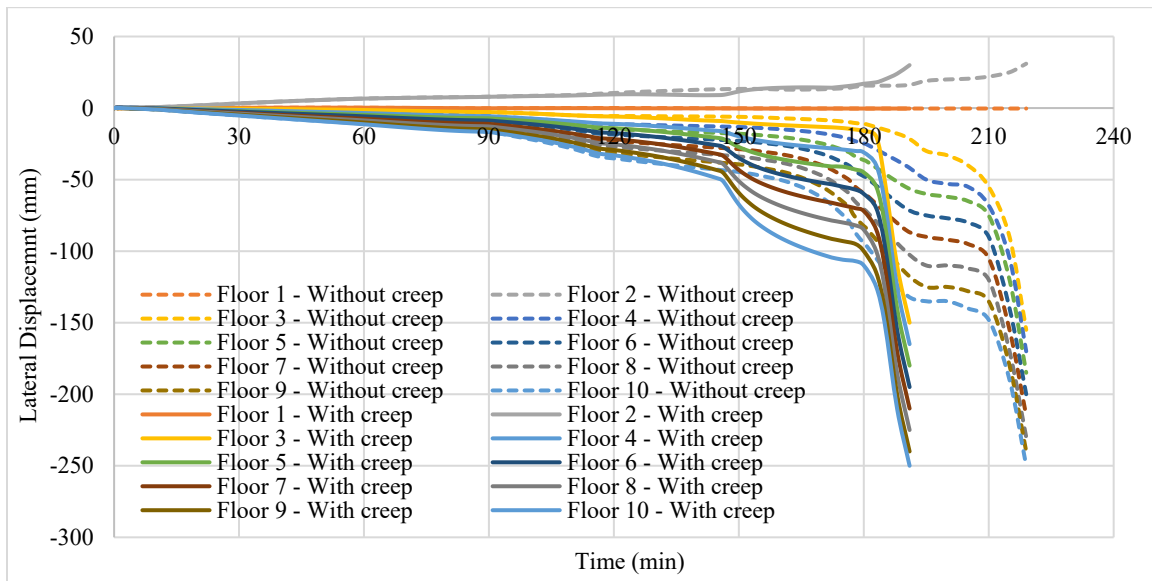


Figure 5.23. Lateral displacement at different floor levels for the scenario with fire in *Floor 2 – A & 3-5*.

Figure 5.24 shows the progression of mid-span deflection in the beams in the fire-affected compartments for the scenario *Floor 2 – A & 3-5*. As beam A-3-4 is in the unbraced bay, it shows much higher deflections as compared to beam A-4-5 which is in the braced bay and hence shows a stiffer response. However, the temperature-induced creep strains developed in beam A-4-5 are much higher as compared to that developed in beam A-3-4. This can be attributed to the larger axial force in beam A-4-5 than in beam A-3-4, although both the beams are subjected to the same level of temperature. In both beams, the model “without creep” underestimates the deflections that occur in the beams. This results in unrealistic predictions of deformations in the adjoining members in the frame.

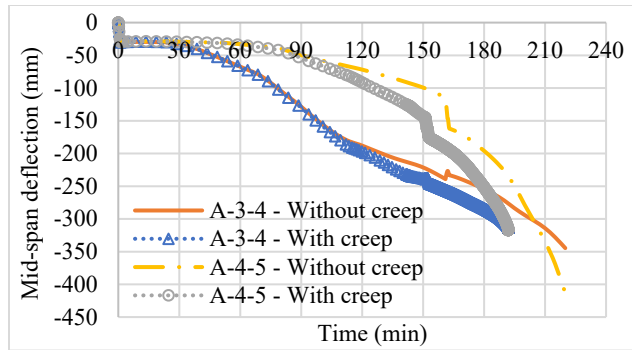


Figure 5.24. Mid-span deflection of beams in the fire affected compartments for the scenario with fire in *Floor 2 – A & 3-5*.

In the scenario with fire in the exterior bays (*Floor 2 – A & 4-6*), columns A4 and A5 in the braced compartment experience more creep deformations than the gravity column A6 due to the higher initial load level in the lateral columns. Additionally, the interior compartment experiences more restraint to thermal expansion from the surrounding cooler regions of the structure as compared to the corner compartment, which further increases the creep strain in columns A4 and A5. This is evident from the axial deformation and axial force response of the fire-exposed columns, shown in Figure 5.25, where the difference between the trends predicted by the models with and without creep is more in the case of the lateral columns A4 and A5 than in A6 with the model “*without creep*” predicting much higher expansion than the model “*with creep*”. With the temperature rise, the lateral column A5 begins to contract first closely followed by A4. The contraction of the lateral columns continues until the sudden buckling of the gravity column A6, simultaneously with the buckling of A5, at 180 min using the model “*with creep*” and 200 min using the model “*without creep*”. Removal of columns A5 and A6 results in the immediate failure of the braces in bay *A & 4-5* and buckling of column A4 and the collapse of bays *A & 4-6* above floor 2.

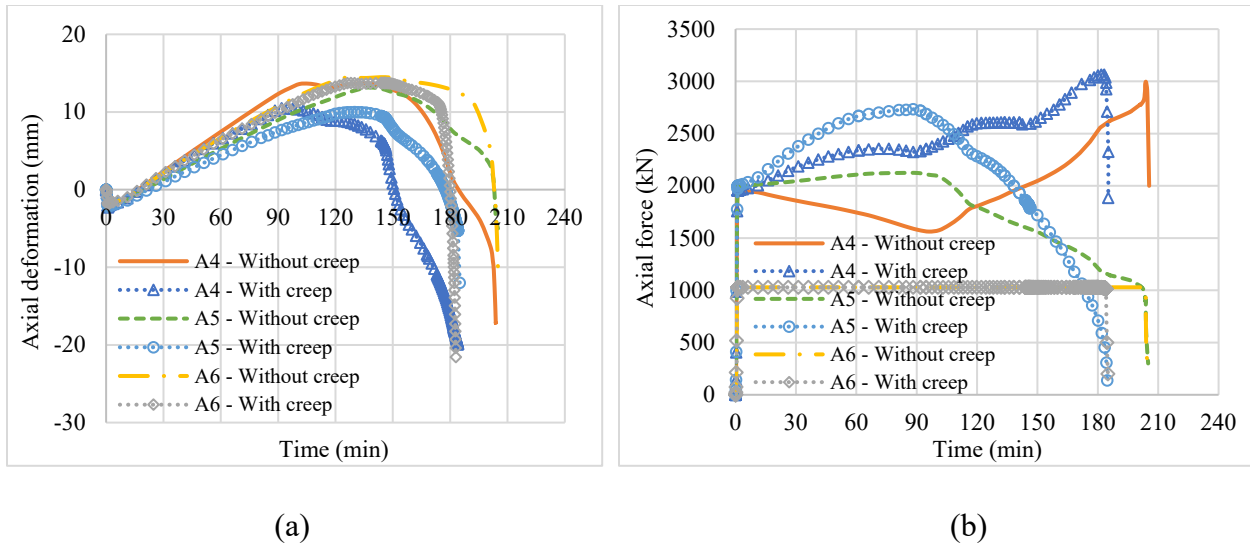


Figure 5.25. (a) Axial deformation and (b) axial force in fire-exposed columns for the scenario with fire in *Floor 2 – A & 4-6*.

The variation of lateral displacement at gridline A6 with fire exposure time at different floor levels using the analysis with and without creep is presented in Figure 5.26. At the fire floor level, the expansion of the corner compartments results in the lateral displacement to the right while the floors above drift to the left to ensure compatibility. As the fire-exposed columns begin to contract, the lateral drift of the floors above the fire floor shifts to the right and continue to increase until failure. It is evident that the analysis “*without creep*” largely overestimates the lateral drift in the expansion phase and underestimates during the contraction phase, thereby overestimating the failure time by 21 min. Figure 5.27 shows the deformed configuration of the building just before the failure time predicted using the analysis “*with creep*” under scenarios of fire in interior and exterior bays. It is seen that the deformations predicted using the model “*with creep*” are much higher in the overall frame for the same fire exposure time.

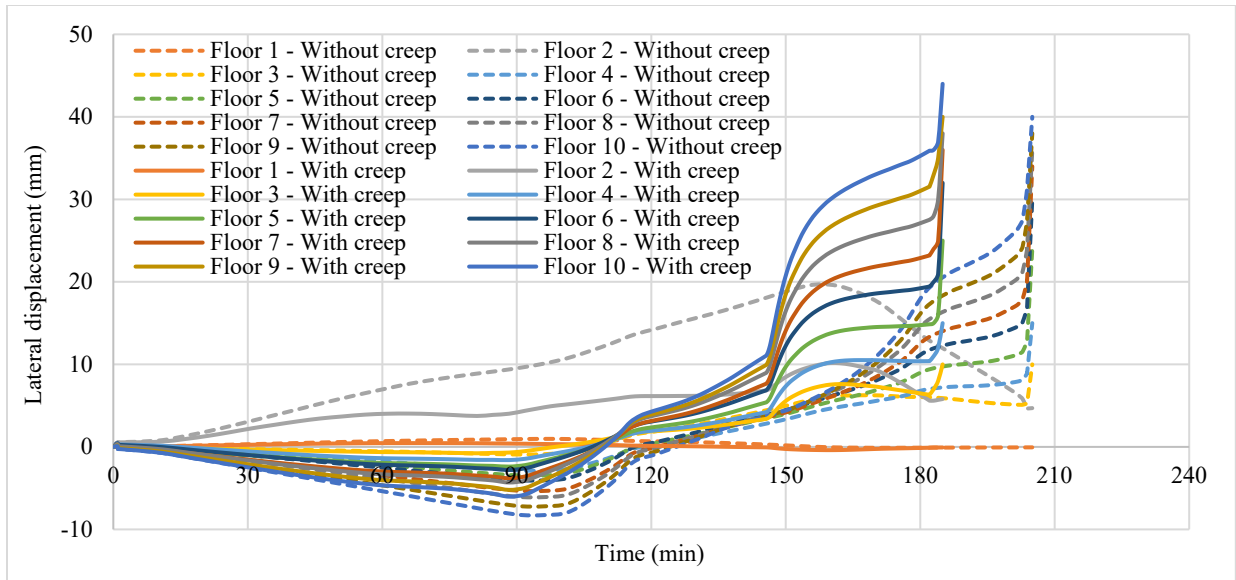


Figure 5.26. Lateral displacement at different floor levels for the scenario with fire in *Floor 2 – A & 4-6*.

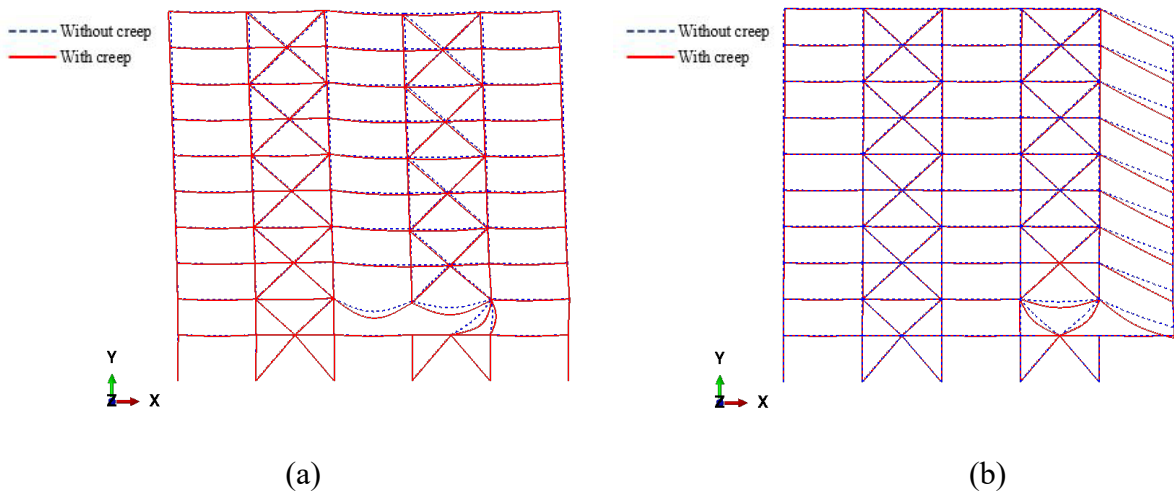


Figure 5.27. Deflected profile of the frame at a fire exposure time of (a) 190 min for the scenario with fire in *Floor 2 – A & 3-5* and (b) 180 min scenario with fire in *Floor 2 – A & 4-6*.

#### 5.4.2.4.2 Effect of creep under varying locations of the fire floor

The location of the burning floor within a steel framed building tends to have a significant impact on the level of creep deformations that occur in the event of a fire. In typical steel framed buildings, relatively smaller steel sections are used in columns as the story level increases for achieving an economical construction. This results in an increase in the relative slenderness of the steel columns

in the higher stories, which can lead to higher creep deformations under fire exposure on upper floor levels. To investigate the response due to a fire occurring on different floors simultaneously, scenarios with fire in bays *A* & 3-5 are considered at three different floor levels: floor 2, floor 5, and floor 9.

The results from the analysis are presented in Figure 5.28 where the maximum lateral displacement of the frame that occurs at the top story level is plotted as a function of fire exposure time for the three scenarios considered. The deflected shapes of the building under scenarios with fire on floors 5 and 9 just before the failure time are shown in Figure 5.29. The progression of instability in the structure under scenarios with fire on floors 5 and 9 is similar to that of fire on floor 2. However, the lateral displacement at the top story level is seen to be lesser as the level of the fire floor becomes higher. This is mainly because the deformations that occur in the fire-exposed compartments in a story tend to affect the deformation in the stories above the fire floor to a greater extent than below. The instability that sets in the fire-exposed columns on floor 2 results in a larger lateral displacement of the frame as compared to the scenarios with fire on floors 5 and 9. Moreover, the initial stress levels in columns in the lower stories are higher than in the upper stories which results in lower failure times when the fire occurs in the lower stories of the building.

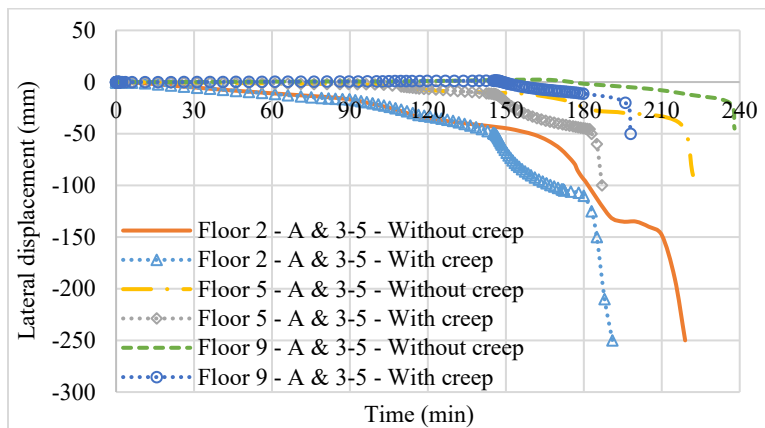


Figure 5.28. Lateral displacement at the top left corner of the frame for scenarios with varying locations of the fire floor.

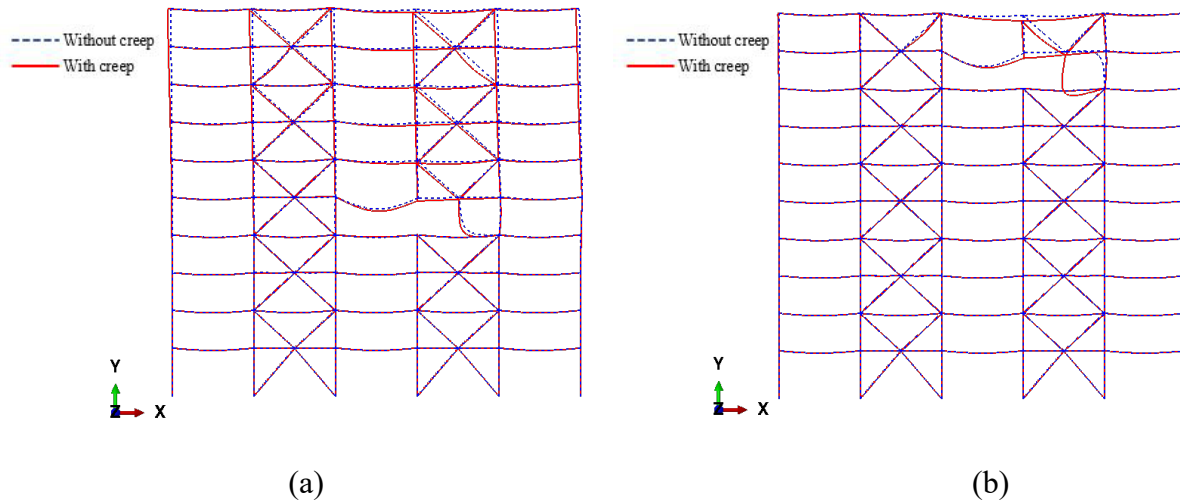


Figure 5.29. Deflected profile of the frame at a fire exposure time of (a) 190 min for the scenario with fire in Floor 5 – A & 3-5 and (b) 195 min scenario with fire in Floor 9 – A & 3-5.

The effect of creep, on the other hand, is greater when the fire occurs in the higher stories. The highest difference between the global failure times predicted using the model “*with creep*” and “*without creep*” of 37 min is observed when the fire occurs on floor 9 as seen in Table 5-5. The fire-exposed column W14x43 which is used on floor 9 is comparatively much smaller in size than W14x132 and W14x193 which are used on floors 5 and 2, thereby having relatively higher slenderness (of about 12%) than the columns in the lower stories. This in turn results in higher stresses under fire exposure leading to higher creep deformations in the fire-exposed columns on floor 9.

#### 5.4.2.4.3 Effect of creep under varying extents of burning on a single floor

The area of fire exposure within a single story directly affects the stability of the steel framed building. As more area (number of compartments) is subjected to fire, the stress levels in the fire exposed members increase rapidly, due to the degradation in steel properties at elevated temperatures, which results in higher creep strain. Moreover, following the failure of any load-bearing member, the stress levels in the adjacent fire exposed columns further increase which can lead to a substantial rise in creep deformations and result in an early onset of instability in the

frame. In this study, the number of compartments exposed to fire in a single story (floor 2) is varied and the overall response of the braced frame building is traced under each of these scenarios. Three scenarios are examined: fire in bay *A* & 4-5 only (one compartment), fire in bays *A* & 3-5 (two compartments), and fire in bays *A* & 2-5 (three compartments).

The lateral displacement response at the top story level for the three scenarios and the deflected profile of the building under scenarios with one and three-compartment fires are shown in Figure 5.30 and Figure 5.31. In the scenario of a one-compartment fire, only 20% of the floor area is burning. The structure is able to withstand the fire exposure until the two lateral columns A4 and A5 buckle simultaneously at around 210 min and 235 min using analysis “*with creep*” and “*without creep*” respectively. Following the removal of these columns, the beams in bays *A* & 2-5 shift from flexural to catenary action and the building can sustain the fire until 240 min and no failure is observed. This is evident from the lateral displacement response which is very minor in the case of one compartment fire as compared to the scenario of fire in two compartments in which 40% of the floor area is subjected to fire exposure. In the third scenario of fire in three compartments, 60% of the floor area is subjected to fire exposure. As more area is burning, the fire-exposed columns lose their strength and stiffness faster. The columns A3 and A4 buckle first which are quickly followed by the buckling of columns A2 and A5, leading to the complete collapse of story 2. The global failure times in the scenario of a three-compartment fire are much lower than in the two-compartment fire scenario. However, owing to the symmetry in the fire loading, the structure undergoes more downward displacement and lesser lateral drift in the three-compartment fire scenario. The effect of creep increases as the area under fire increases, mainly because of the drastic increase in stress levels as more structural members lose their capacity under fire exposure. The three-compartment fire resulted in the maximum difference in failure time of

about 42 min when analyzed using models with and without creep, as compared to 28 min under a two-compartment fire. Therefore, when multiple compartments are burning, full creep effects should be considered through an explicit treatment in the fire resistance analysis of steel framed structures.

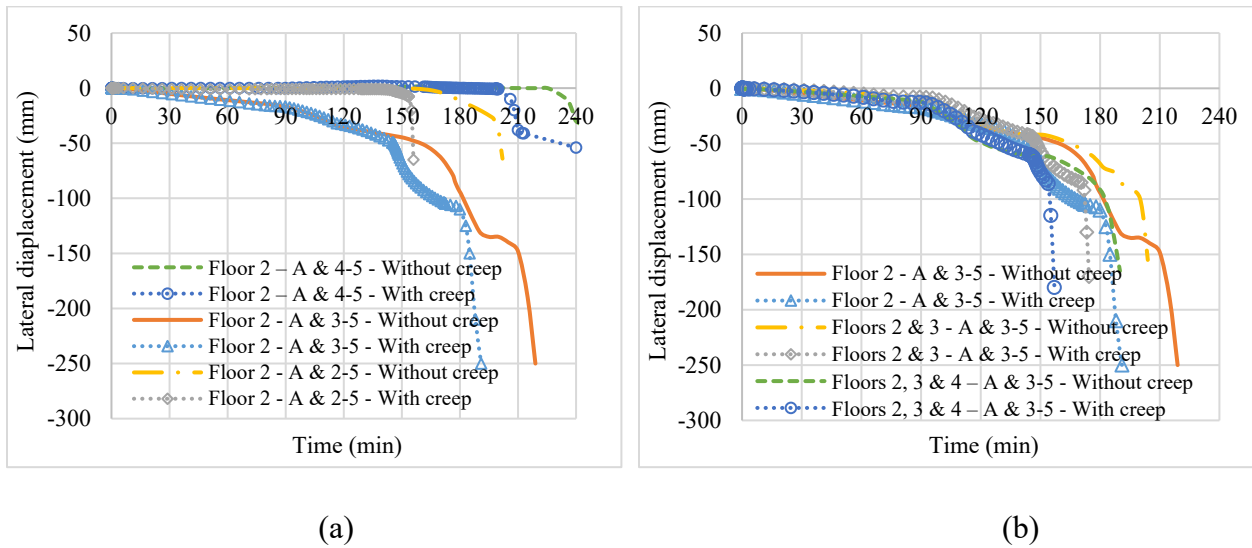


Figure 5.30. Lateral displacement at the top left corner of the frame for scenarios with varying (a) number of fire-exposed compartments and (b) number of fire-exposed floors.

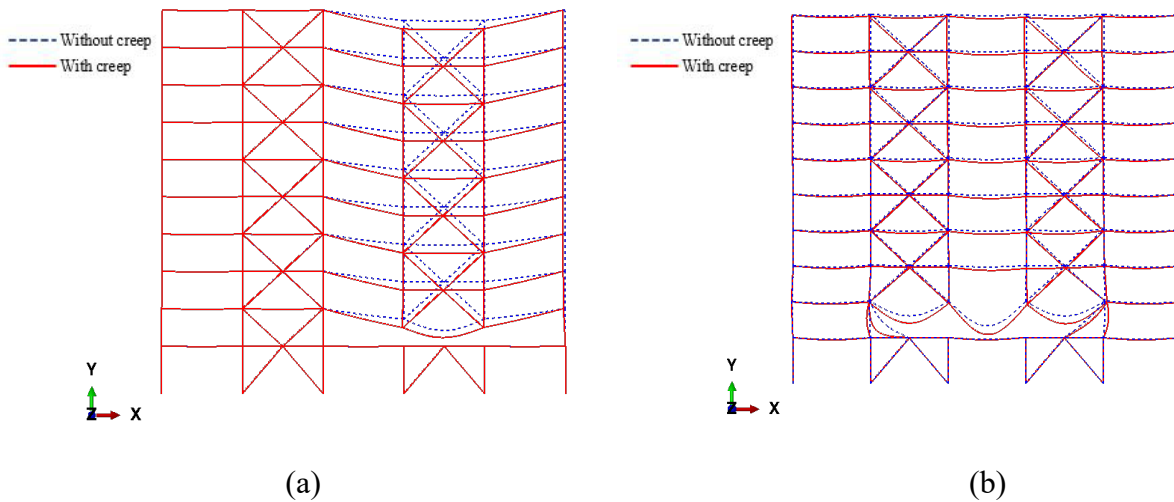


Figure 5.31. Deflected profile of the frame at a fire exposure time of (a) 240 min for the scenario with fire in *Floor 2 – A & 4-5* and (b) 155 min scenario with fire in *Floor 2 – A & 2-5*.

#### 5.4.2.4.4 Effect of creep under varying extents of burning on multiple floors

Similar to the scenario where multiple compartments in a single story are exposed to fire (horizontal spread of fire), as discussed above, the number of floors burning simultaneously (vertical spread of fire) can also have a significant impact on the creep-induced instability of a steel framed structure. When a single story is burning, the cooler stories above and below the burning floor provide more restraint to the thermal expansion of the story under fire. However, when multiple stories are burning simultaneously, the level of restraint from the adjacent floors reduces, especially on fire floors away from the cooler stories. The varying restraint conditions between single and multiple stories burning can lead to varying levels of creep strains in the fire exposed steel members and can alter the load paths in the overall structural system. To evaluate the effect of transient creep strain under scenarios where multiple floors are burning, 3 cases are considered with fire exposure in bays A & 3-5: fire on floor 2 only (one story), fire on floors 2 and 3 (two stories), and fire in floors 2, 3, and 4 (three stories).

A comparison of the lateral displacement evaluated at the top floor level for the three scenarios (presented in Figure 5.30) shows that the displacement is similar for the initial fire duration in all three cases. This is because the loss in capacity of the fire-exposed members in each story is primarily redistributed to the adjacent members within the same story and the response in all three scenarios is somewhat similar. However, in scenarios of burning in more than one story, multiple steel members fail at the same time resulting in a rapid increase in the lateral drift of the structure as seen from the deflected profiles in Figure 5.32. Table 5-5 shows that the global failure times decrease as the number of stories subjected to fire increases. It is also evident that the difference between the failure times predicted between the models “*with creep*” and “*without creep*” increases as the number of fire floors increases. When creep deformations are explicitly

incorporated in the analysis, it is seen that a greater number of structural members fail at quicker times, which significantly increases the stress levels and alters the load path. This can be seen from the deflected configuration just prior to failure using analysis with and without creep in the case of multi-story fires (shown in Figure 5.32), where the same members which have failed in the case of analysis “with creep” are still intact in the case “without creep”.

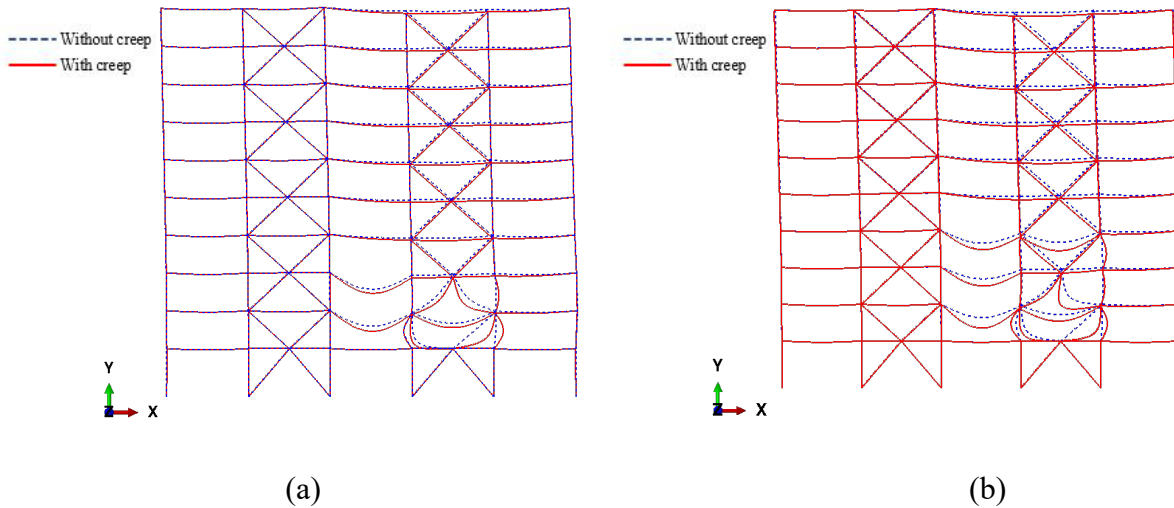


Figure 5.32. Deflected profile of the frame at a fire exposure time of (a) 170 min for the scenario with fire in Floors 2 & 3 – A & 3-5 and (b) 155 min scenario with fire in Floors 2, 3 & 4 – A & 3-5.

#### 5.4.2.4.5 Effect of creep under varying fire severity

To study the effect of fire severity on the transient creep deformations and associated instability in steel frames, the response of the steel frame is traced under three design fire scenarios, as shown in Figure 5.18. The response is compared with that under standard ASTM E119 fire exposure. Fire is assumed to occur in compartments *Floor 2 – A & 3-5* for all the cases. The lateral displacement history at the top story level evaluated at gridline A1 for the different fire scenarios is presented in Figure 5.33. The results clearly show that the fire scenario has a significant influence on the overall response and the extent of creep deformations that occur in the steel frame building. The lateral displacement of the frame increases at a faster rate with an increase in the severity of fire exposure.

This can be attributed to the higher degradation in the strength and stiffness of the fire-exposed members, owing to the higher temperature rise, which results in higher inelastic deformation in the frame. As compared to the standard fire exposure scenario, the displacements under the moderate fire scenario DF-90 are less, while under the two other severe fire scenarios, DF-120 and DF-180, the responses are much worse.

From the perspective of transient creep effects, the peak temperatures attained in the steel members are below 450°C under the DF-90 scenario, and very minimal creep deformations occur during the growth phase of the fire. For the other fire scenarios, the effect of high-temperature creep is the highest in the case of standard fire exposure closely followed by DF-180 and then by DF-120. This is because the standard fire exposure has a lower heating rate than the other severe scenarios and hence, experiences higher temperatures at the same stress level for longer time durations resulting in larger creep deformations. The creep deformations in DF-180 are higher than in DF-120 owing to the longer burning duration of 180 min as compared to 120 min subjecting steel members to higher temperatures for a prolonged period. During the cooling phase, the results indicate that the inclusion of high-temperature creep explicitly results in lower recovery of deflections than in the case of implicit creep as seen from the response under the DF-90 fire scenario. This is because the implicit creep model tends to overestimate the total elastic recoverable strain that develops during the heating phase, which in turn is completely recovered during the cooling phase of the fire.

From the above-shown studies, it is evident that creep deformations are significant both at member and structural levels and the high-temperature creep strain needs to be fully accounted for in tracing the fire-induced instability in steel framed structures leading to progressive collapse.

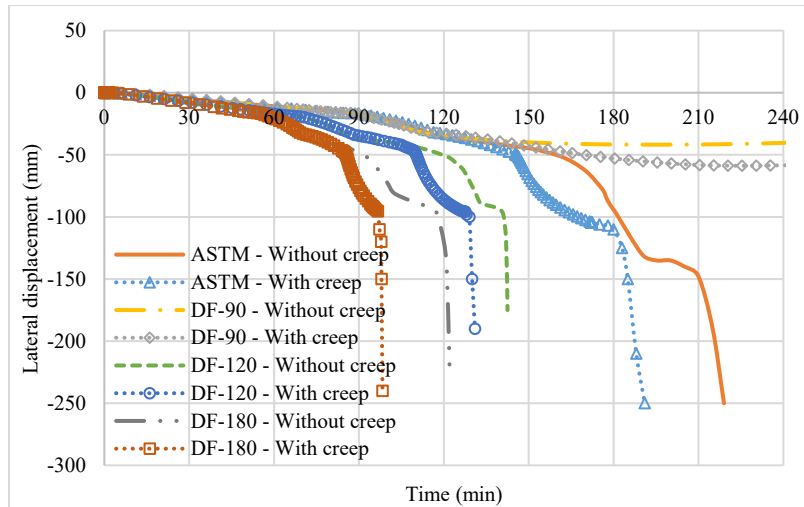


Figure 5.33. Lateral displacement at the top left corner of the frame for different fire exposure scenarios.

Table 5-6: Summary of transient creep effects in the braced frame building for different scenarios considered

Varied parameter	Frame designation	Fire compartments	Fire scenario	Fire resistance (min)			Global failure pattern
				With creep	Without creep	Difference	
Fire location within a story	2D Frame – H1	Floor 2 – A & 3-5 (interior)	ASTM E119	191	219	28	Lateral drift of floors above floor 2.
	2D Frame – H2	Floor 2 – A & 4-6 (corner)	ASTM E119	184	205	21	Partial collapse of bays 4 and 5.
Fire (burning) floor	2D Frame – H3	Floor 2 – A & 3-5	ASTM E119	191	219	28	Lateral drift of floors above floor 2.
	2D Frame – H4	Floor 5 – A & 3-5	ASTM E119	194	226	32	Partial collapse due to lateral drift of floors above floor 5.
	2D Frame – H5	Floor 9 – A & 3-5	ASTM E119	199	236	37	Partial collapse due to lateral drift of floors above floor 9.

Table 5-6 (cont'd)

Number of compartments burning	2D Frame – H6	Floor 2 – A & 4-5 (one compartment)	ASTM E119	NF	NF	-	Significant damage in bays 3, 4 & 5. No global collapse.
	2D Frame – H7	Floor 2 – A & 3-5 (two compartments)	ASTM E119	191	219	28	Lateral drift of floors above floor 2.
	2D Frame – H8	Floor 2 – A & 2-5 (three compartments)	ASTM E119	156	198	42	Downward collapse of floor 2.
Number of stories burning	2D Frame – H9	Floor 2 – A & 3-5 (one story)	ASTM E119	191	219	28	Lateral drift of floors above floor 2.
	2D Frame – H10	Floors 2 & 3 – A & 3-5 (two stories)	ASTM E119	174	209	35	Lateral drift of floors above floor 2.
	2D Frame – H11	Floors 2, 3 & 4 – A & 3-5 (three stories)	ASTM E119	157	196	39	Lateral drift of floors above floor 3.
Fire severity	2D Frame – H12	Floor 2 – A & 3-5	ASTM E119	191	219	28	Lateral drift of floors above floor 2.
	2D Frame – H13		DF – 90	NF	NF	-	No global collapse.
	2D Frame – H14	Floor 2 – A & 3-5	DF – 120	131	143	12	Lateral drift of floors above floor 2.
	2D Frame – H15	Floor 2 – A & 3-5	DF – 180	98	124	26	Lateral drift of floors above floor 2.

NF – No failure

### 5.5 Parametric studies on the effect of structural parameters on fire-induced instability

To quantify the influence of structural parameters such as altering load paths (and restraints), local buckling effects in steel sections, and the type of structural analysis adopted to trace the fire-induced collapse in steel framed buildings, a series of numerical studies are carried out on a ten-story steel framed building. The braced frame building described in Section 5.3.1 is chosen for this study. The varied parameters and range, analysis details, and results from these numerical studies are discussed in this section.

### ***5.5.1 Varied parameters and range***

A total of twelve case studies are carried out to quantify the effect of varying structural parameters to trace the onset of instability leading to the progressive collapse in a fire-exposed steel framed building. These studies are presented under four main cases as shown in Table 5-6: variation in structural configuration, variation in fire location, local instability, and analysis regime. In the first case, the variation in load paths arising from the discretization adopted in the structural model is studied by considering two configurations: 2D steel frame (on gridline F) and 3D steel framed building (including floor slabs and transverse framing). In the second case, the variation in load paths arising from different fire locations is evaluated by considering fire exposure in four different locations in the steel framed building, namely, four interior compartments on floor 1, four exterior compartments on floor 1, four exterior compartments in floor 6, and four exterior compartments in floor 9. In the third set of case studies, the local buckling effects are evaluated by considering two scenarios: first, the original building with W14x53 (lateral) columns in the fire compartments, and second, the lateral columns (A3, A4, and A5) in the ninth story are replaced with W14x74 columns. Standard ASTM E119 fire exposure is applied to two interior compartments in the ninth story of the building. In each scenario, two different structural models are compared; one with only beam elements used for all framing members and the other with shell elements used for fire-exposed steel members and beam elements used for unexposed steel members. Finally, in the fourth case, the analysis regime used to trace fire-induced collapse in steel framed buildings is varied between the nonlinear quasi-static approach and the nonlinear dynamic explicit approach. In each scenario, the compartments subjected to fire are identified by using the floor level and the gridlines that bound these compartments on that floor.

Table 5-7: Critical parameters investigated to study the effect of structural parameters on fire-induced instability

Varied parameter	Frame Designation	Parameter value	Constant parameters
Structural configuration	2D Frame – H16	2D building frame (on gridline F)	Fire compartments: Floor 2 – E-F & 2-4 Fire exposure: ASTM E119 Analysis type: Nonlinear dynamic explicit
	3D Frame – F16	3D building frame (with floor slab)	
Fire location	3D Frame – F17	Floor 1 – C-E & 3-5 (four interior compartments)	3D building frame Fire exposure: ASTM E119 Analysis type: Nonlinear dynamic explicit
	3D Frame – F18	Floor 1 – D-F & 4-6 (four exterior compartments)	
	3D Frame – F19	Floor 6 – D-F & 4-6 (four exterior compartments)	
	3D Frame – F20	Floor 9 – D-F & 4-6 (four exterior compartments)	
Local instability	2D Frame – H17	Column W14x53 – beam elements	2D building frame Fire compartments: Floor 9 – A & 3-5 Fire exposure: ASTM E119 Analysis type: Nonlinear dynamic explicit
	2D Frame – H18	Column W14x53 -shell elements	
	2D Frame – H19	Column W14x74 -beam elements	
	2D Frame – H20	Column W14x74 -shell elements	
Analysis regime	2D Frame – H21	Nonlinear dynamic explicit analysis	Fire compartments: Floor 2 – F & 2-4 Fire exposure: ASTM E119
	2D Frame – H22	Nonlinear quasi-static analysis	

### 5.5.2 Analysis details

The numerical analyses are carried out using the validated FE model presented in Chapter 4. The developed FE model is applied for fire resistance analysis at different levels, including member and system levels (2D or 3D), using an appropriate discretization of the structure, material properties, and boundary conditions, as outlined in Chapter 4. The thermal response including the variation of sectional temperatures in the fire-exposed members is obtained by carrying out a heat transfer analysis. The structural response including the stresses and displacements in different members and varying load paths leading to collapse is evaluated by carrying out either a nonlinear

quasi-static analysis or a nonlinear dynamic explicit analysis approach. The appropriate analysis type is selected based on the parameters considered in a specific numerical study.

### ***5.5.3 Results and discussion***

Results from the parametric studies for evaluating the effect of different structural parameters for tracing fire-induced progressive collapse in steel framed buildings are discussed in this section.

#### ***5.5.3.1 Effect of altering load paths due to variation in structural configuration***

The presence of floor slab and transverse framing can continuously alter the load paths and thus influence the onset of instabilities and initiation of progressive collapse in a steel framed building. To investigate this, two different structural configurations are considered. In the first configuration, only the 2D frame along gridline F is modeled in ABAQUS. In the second configuration, the entire building including the framing members in two directions, and the floor system is modeled. Results from the analyses indicate that the onset of progressive collapse is highly sensitive to the presence, or not, of the floor slab and transverse framing. shows that while the 2D building frame subjected to fire exposure in two compartments experiences collapse at 210 min, the 3D building frame with similar fire exposure does not undergo collapse. From Figure 5.34, it is seen that the 3D building undergoes significant lateral displacement (measured at the top story level) at around 200 min due to the failure of multiple columns in the fire compartments. However, owing to the presence of the composite slab and transverse framing, the loads are redistributed from the failed members to the adjacent members in neighboring compartments in all directions and the building can stabilize without undergoing progressive collapse. The deformed state of the 3D building at the end of 240 min of fire exposure is shown in Figure 5.35.

In the case where only the 2D building frame is considered in the FE model, columns A4 and A5 and braces in the fire compartment fail first. Following the failure of these structural members,

load redistribution occurs only in the direction of the frame through the beams adjoining the failed columns, and the frame is no longer able to maintain equilibrium. Collapse initiates in this scenario at 210 min as seen from the lateral displacement response at the top story in Figure 5.34 and the deformed shape of the frame in Figure 5.35. The consideration of the composite floor slab and transverse framing in the 3D model makes the load redistributions and failure time more realistic than in the 2D model. Moreover, the 2D model only considers fire exposure in steel members present in the perimeter braced frame as opposed to the 3D building model that considers fire exposure in all steel members and slabs in the two compartments. Consequently, the deformations and extent of damage predicted by the 3D model are more realistic and widespread than that predicted by the 2D model.

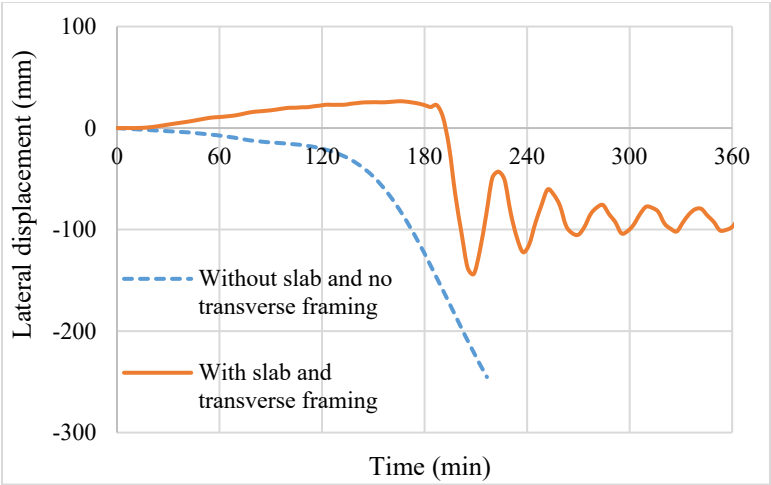


Figure 5.34. Lateral displacement at the top story of the building with fire exposure time for varying structural configurations.

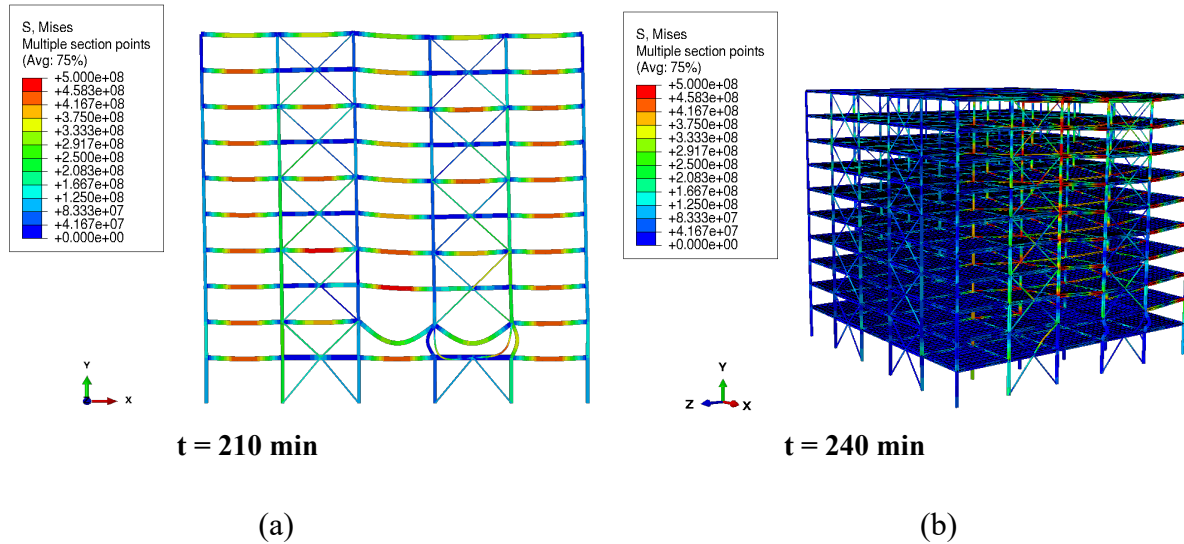
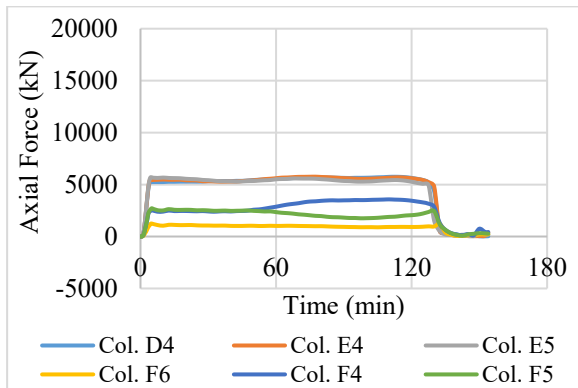


Figure 5.35. Deformed shape of (a) 2D building frame and (b) 3D building with a fire on floor 2.

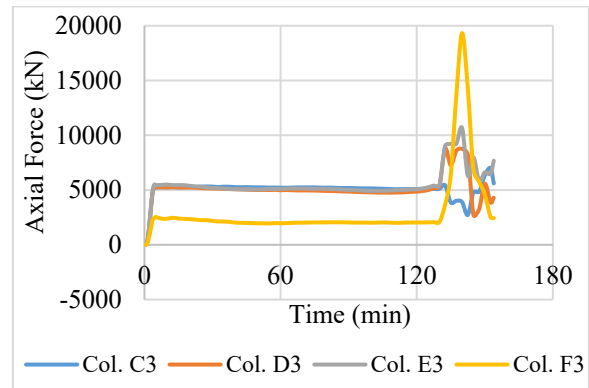
### 5.5.3.2 Effect of altering load paths due to variation in fire (burning) location

To study the effect of altering load paths due to different burning locations in a building, the scenario with fire occurring in exterior compartments is compared with that of the scenario with fire occurring in interior compartments. The failure sequence of affected columns and load distribution to the adjacent columns in these two scenarios can be seen in Figure 5.36. In the case where four exterior compartments (*D-F & 4-6*) are subjected to fire exposure on floor 1, the failure is initiated in an interior gravity column (column E5 at 125 min). This is immediately followed by failure in four additional other gravity columns (D4, D5, E4, and F6), as well as four lateral columns (D6, E6, F4, and F5) and braces that are in the fire-affected compartments. The columns adjacent to the fire-affected compartments carry the additional load which is seen from the rise in the axial force. However, the magnitude of load coming from the failure of columns in four compartments is extremely high which results in the failure of adjacent columns as well. The structure is seen to no longer maintain stability and thus the complete collapse of the frame occurs at 137.5 min. The response of the building frame during fire scenario with burning in four interior compartments (*C-E & 3-5*), all affected gravity columns fail in the time frame of 122.5 to 127.5

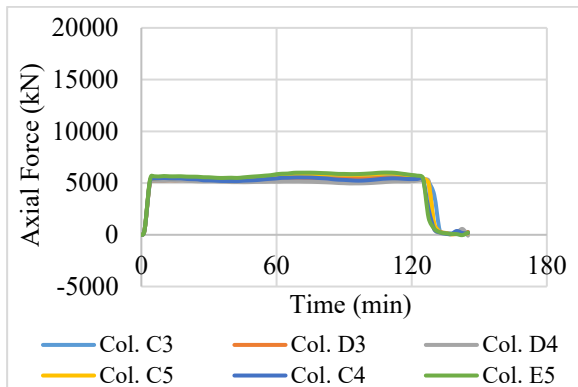
min almost simultaneously due to the similar load level and restraint conditions in these columns. The columns in the adjacent compartments are unable to withstand the redistributed loads and collapse initiates at 135 min. The load paths and the time at which collapse initiates are similar in the scenarios with fire occurring in either exterior or interior compartments on the same floor level.



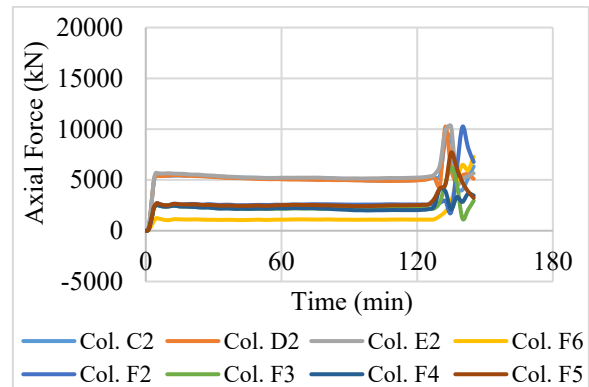
(a) Corner compartment – Affected columns



(b) Corner compartment – Adjacent columns



(c) Interior compartment – Affected columns

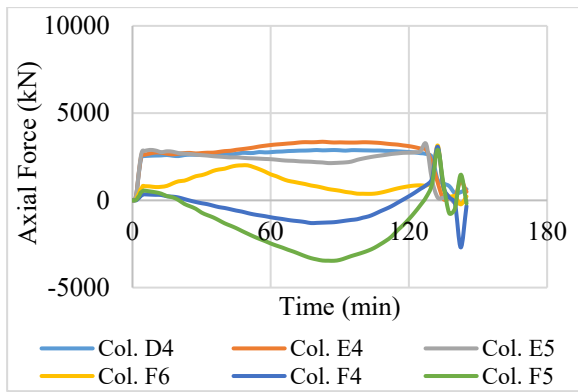


(d) Interior compartment – Adjacent columns

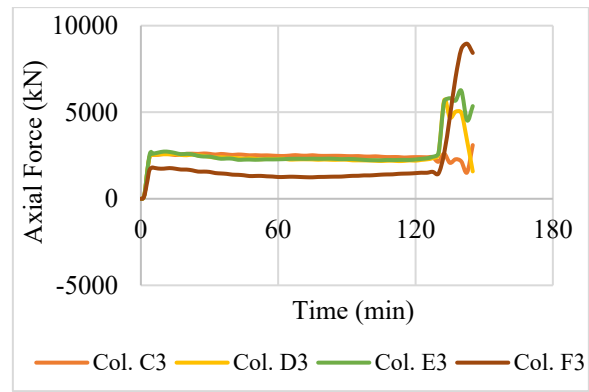
Figure 5.36. Axial forces in columns in the fire-affected and adjacent compartments for scenarios with burning in corner and interior compartments on floor 1.

Further, to evaluate the effect of continuously altering load paths due to fire occurring in different stories, three fire scenarios with burning occurring on floor 1, floor 6, and floor 9 are compared. All three scenarios result in similar failure times (refer to Table 5-8). This is due to the stress levels in the columns being approximately the same since the loads acting on the columns in the higher stories are lesser than those in the lower stories even though smaller steel sections are used in the

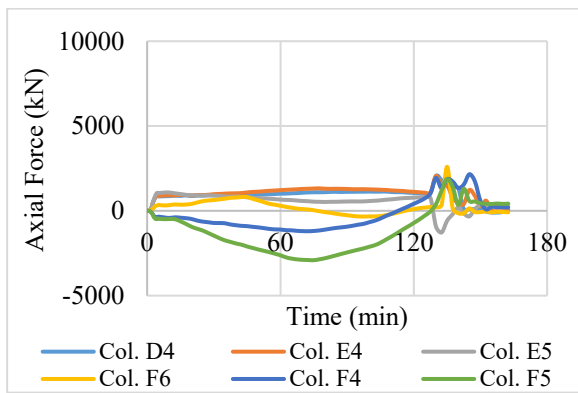
higher stories of the building. Figure 5.37 shows the axial forces in the affected and adjacent compartments for scenarios with fire exposure on floor 6 and floor 9. The load paths in these two scenarios are similar. The gravity columns sustain the loads up to 120 min of fire exposure followed by failure at around 125 min in both scenarios. The lateral columns, however, experience high tension force during fire exposure duration before failure as opposed to that under fire scenario on floor 1 (refer to Figure 5.36). This higher tensile force, resulting from a fire, needs to be accounted for in the design of these columns and their connections.



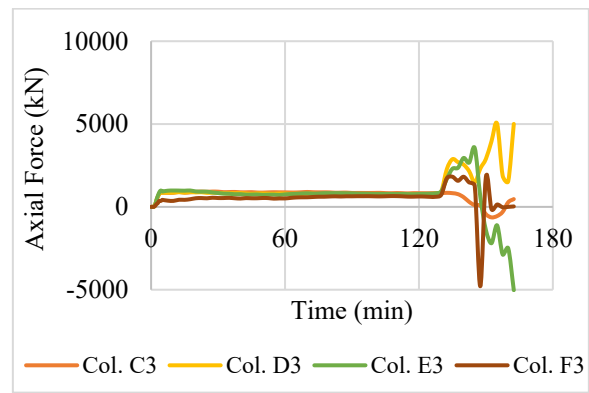
(a) Floor 6 – Affected columns



(b) Floor 6 – Adjacent columns



(c) Floor 9 – Affected columns



(d) Floor 9 – Adjacent columns

Figure 5.37. Axial forces in columns in the fire affected and adjacent compartments for scenarios with burning on floors 6 and 9.

The major difference between the scenario with burning on floor 1 as compared to burning on higher stories is that in scenarios with burning on floor 6 and floor 9, only the fire floor and floors

above experience collapse, and the lower stories remain intact for the entire duration of fire exposure. This can be seen from the lateral displacement evaluated at different story levels under scenarios with burning on floor 1, floor 6, and floor 9 in Figure 5.38. It is evident that the displacement in the floors below the fire floors is negligible compared to that of the floors above indicating that the collapse is only partial. In the case of burning on floor 1, the onset of instability in the columns on floor 1 results in the progressive failure of floor slabs and beams in the stories above leading to the complete collapse of the building. The deformed shape of the building under scenarios with burning on floor 6 and floor 9 is shown in Figure 5.39. It should be noted that although the model accounts for the dynamic (inertial) effects arising from the failure of multiple members, the sudden impact forces due to the upper stories collapsing on the lower stories are not completely captured in the simulation. This could be the reason for not predicting a complete collapse in scenarios with fire in upper stories and, for more accurate predictions, it is preferable to include these additional impact forces to obtain a more realistic prediction of progressive collapse.

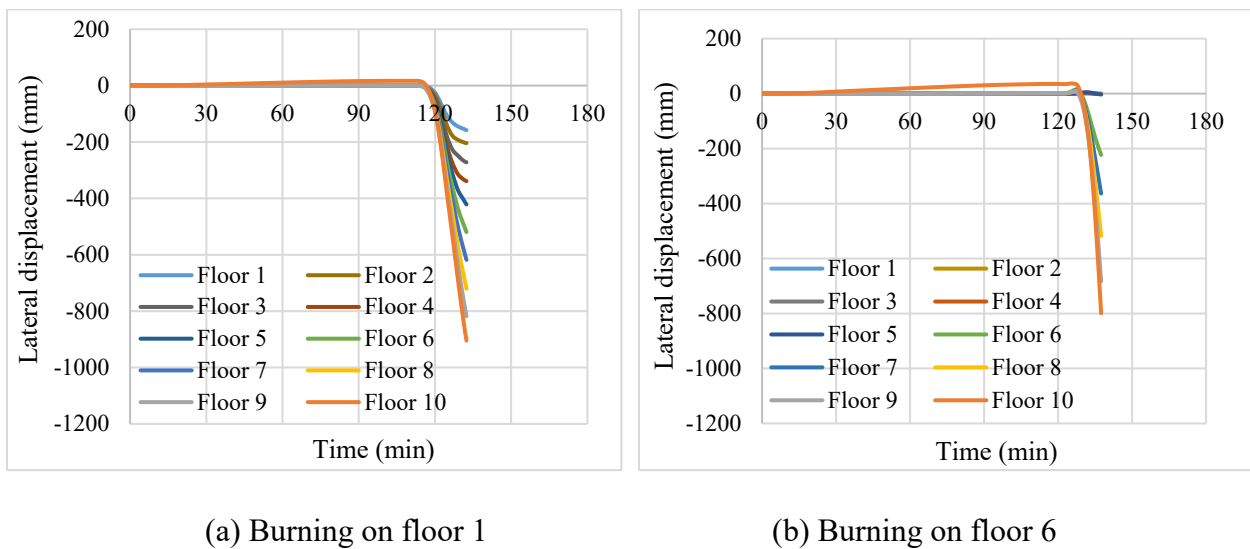
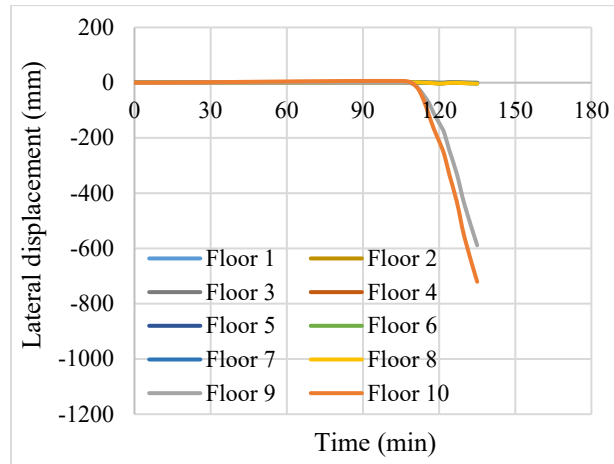


Figure 5.38. Lateral displacement at different floor levels for scenarios with burning in different stories.

Figure 5.38 (cont'd)



(c) Burning on floor 9

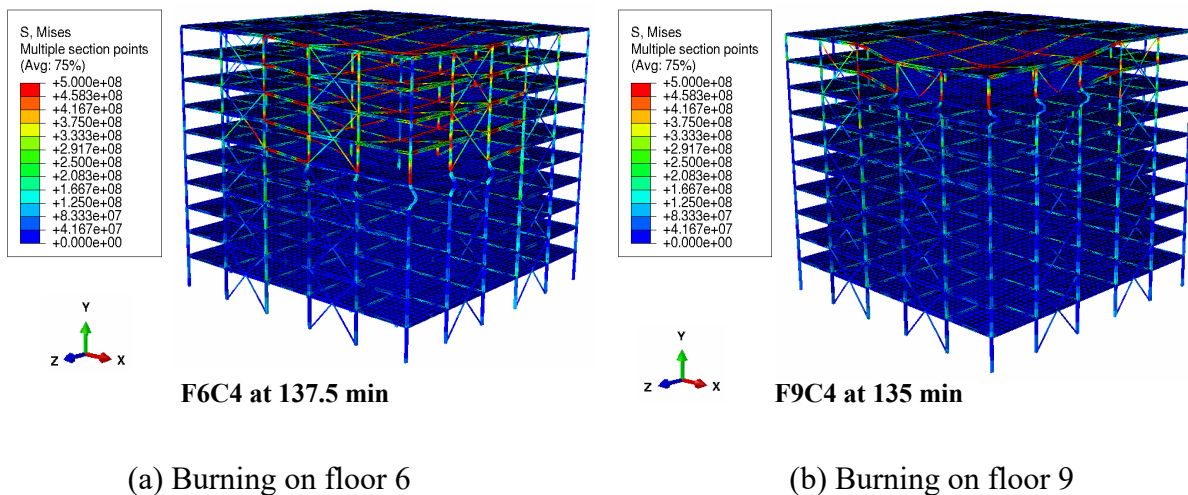


Figure 5.39. Deformed configuration of steel structure for scenarios with burning in different stories at the onset of failure (global).

### 5.5.3.3 Effect of local instability

To evaluate the effect of local instability on the onset of fire-induced progressive collapse in steel framed buildings, the analysis is carried out by assuming fire to occur in two interior compartments in the ninth story of the building. All columns present in the building are non-slender as per AISC [103] classifications, however, columns used in the higher stories are relatively more slender than columns in the lower stories of a building due to economic considerations and hence are more

susceptible to experiencing local buckling under fire conditions. Two scenarios are considered; first, the original building with W14x53 (lateral) columns in the fire compartments, and second, the lateral columns (A3, A4, and A5) in the ninth story are replaced with W14x74 columns. The temperature-dependent variation of web and flange slenderness limits, under the compression limit state, along with the flange and web slenderness ratios of W14x53 and W14x74 sections are shown in Figure 5.40. As can be seen from Figure 5.40, both the columns maintain nonslender flange status for the entire fire duration. However, the web slenderness of the W14x53 section (nonslender at room temperature) becomes slender in the temperature range of 400-800°C and then transforms back to nonslender beyond 800°C. The web slenderness of W14x74, on the other hand, remains nonslender throughout the fire exposure duration. The two different building frames are analyzed using two different structural models, one where all framing members are modeled using beam elements and the other where the framing members in the fire compartments are modeled using shell elements while the rest of the members are modeled using beam elements (as discussed in Section 4.7).

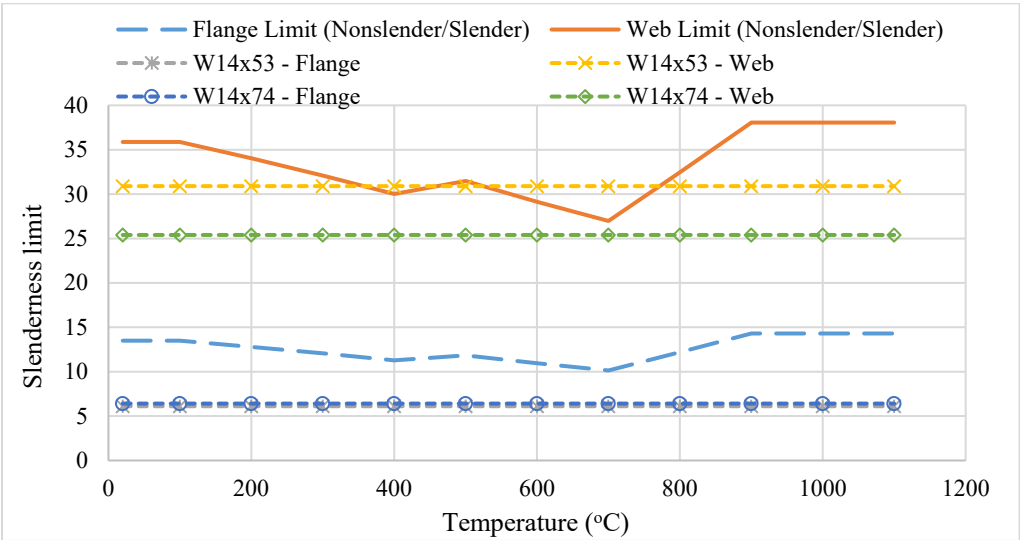


Figure 5.40. Flange and web slenderness limits for columns.

Figure 5.40 shows the lateral displacement at the top story of the building frames for the different cases considered. It can be seen that for the building frame with W14x53 columns, the model using shell elements predicts a failure time of 179 min, 20 min earlier than that predicted using beam elements. This is due to the occurrence of local buckling in the middle column (A4) in the fire compartment (as shown in Figure 5.42) which in turn leads to a reduction in the axial capacity of the column and an early onset of Instability at local and global levels. Also, the beams and columns in the fire compartment undergo significant warping (distortion) due to the nonuniform thermal gradients that develop under fire exposure. These effects are only captured using the model with shell elements. In the scenario with W14x74 columns, it can be seen from Figure 5.41 that the predictions of the model with shell elements and only beam elements are similar. This is because the W14x74 columns being relatively less slender do not experience local buckling for the entire fire exposure duration. Since the capacity of W14x74 is larger than that of W14x53, no failure occurs at member and system levels and hence, progressive collapse is not triggered in this scenario. The axial deformation response (shown in Figure 5.41) shows that the deformation of column W14x74 is much lesser than that of W14x53 for the same fire exposure scenario. Hence, for capturing local instability, and tracing the fire-induced progressive collapse especially when columns of slenderer sections, shell elements are to be used in discretizing the sections. Further, by limiting the slenderness of the column sections to a certain degree, the instability of the columns under fire conditions can be minimized and thus, minimizing the susceptibility of progressive collapse. This limit can be quantified as the lowest slenderness limit that can occur under fire conditions. For instance, for web and flange slenderness, the limits are 25.4 and 10.1 respectively for compression limit state and occur at 700°C for Grade 50 steel.

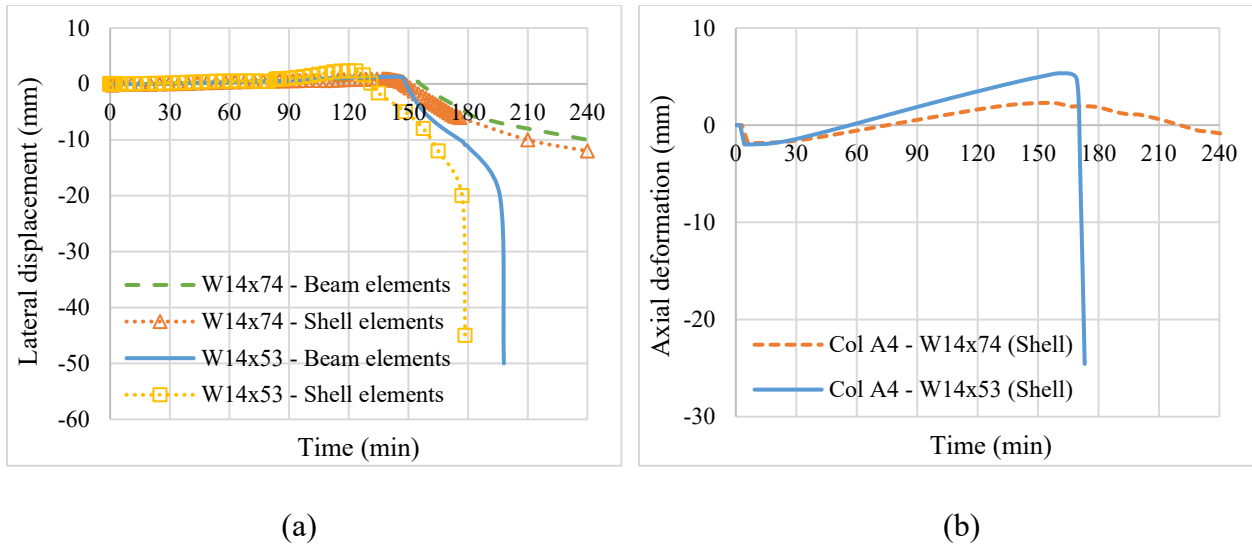


Figure 5.41. (a) Lateral displacement at the top floor level of the frame and (b) axial deformation of column A4 with fire exposure time.

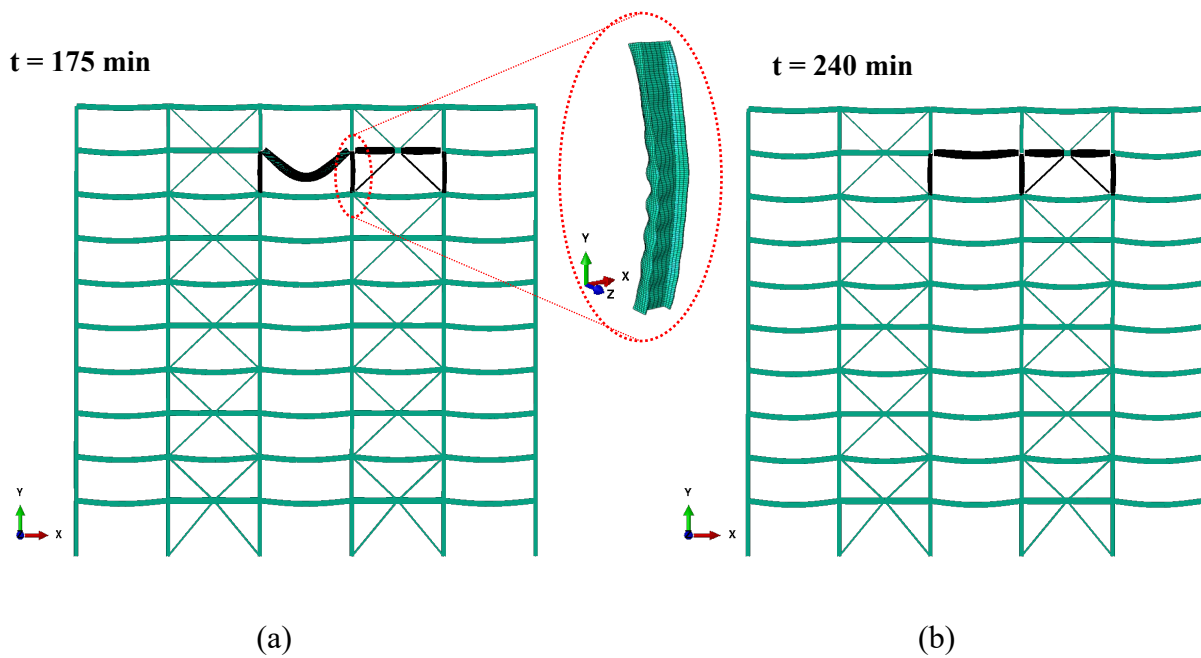


Figure 5.42. Deformed shape of the steel frame with (a) W14x53 lateral columns and (b) W14x74 lateral columns in the ninth story.

#### 5.5.3.4 Effect of analysis regime

Fire-induced progressive collapse analysis is carried out using two different analysis regimes to evaluate the structural response of the steel framed building under fire conditions, namely,

nonlinear quasi-static analysis and nonlinear explicit dynamic analysis. ASTM E119 fire scenario with burning in two compartments on the second floor is considered. Table 5-8 shows that the failure times predicted using the two analysis regimes are similar. The lateral displacement at the top story of the frame predicted using the two models shows a minor difference (refer to Figure 5.43). This is because, in the nonlinear dynamic explicit analysis, the failed members are automatically removed (weakened) during the simulation in contrast to the quasi-static approach in which the failed members are removed manually. For this reason, using the nonlinear dynamic explicit approach can simplify the simulation of fire-induced progressive collapse of steel framed buildings. Moreover, the quasi-static analysis approach is more sensitive to the structural members removed during the simulation and can lead to unrealistic predictions in the event of erroneous removal of members during the analysis.

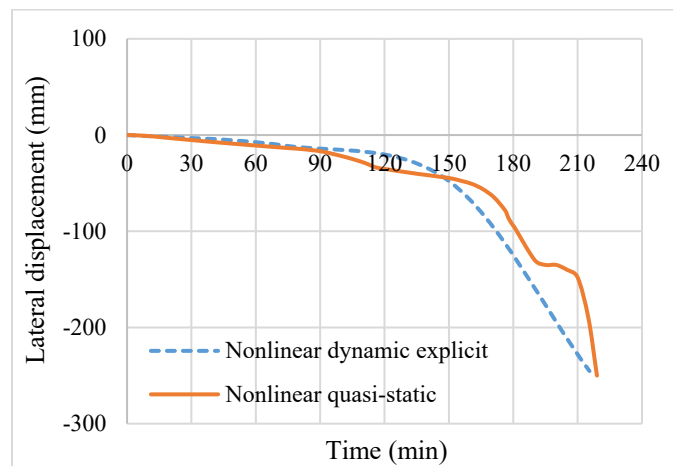


Figure 5.43. Lateral displacement at the top floor level of the frame under different analysis regimes.

Table 5-8: Summary of varied parameters and results from the parametric study on the effect of structural parameters

Varied parameter	Frame Designation	Fire compartment	Fire scenario	Analysis regime	Failure time (min)	Occurrence of progressive collapse
Structural configuration	2D Frame – H16	Floor 2 – F & 2-4	ASTM E119	Dynamic	210	Global collapse occurs.
	3D Frame – F16	Floor 2 – E-F & 2-4	ASTM E119	Dynamic	NF	Buckling of columns in fire compartments. No global collapse.
Fire location	3D Frame – F17	Floor 1 – D-F & 4-6	ASTM E119	Dynamic	132.5	Global collapse occurs.
	3D Frame – F18	Floor 6 – D-F & 4-6	ASTM E119	Dynamic	137.5	Partial collapse of floors above fire floor.
	3D Frame – F19	Floor 9 – D-F & 4-6	ASTM E119	Dynamic	135	Partial collapse of floors above the fire floor.
	3D Frame – F20	Floor 2 – F & 2-4	ASTM E119	Dynamic	210	Global collapse occurs.
Local instability	2D Frame – H17	Floor 9 – A & 3-5	ASTM E119	Quasi-static	199	Partial collapse of floors above fire floor.
	2D Frame – H18	Floor 9 – A & 3-5	ASTM E119	Quasi-static	179	Partial collapse of floors above fire floor.
	2D Frame – H19	Floor 9 – A & 3-5	ASTM E119	Quasi-static	NF	No failure at member and system levels.
	2D Frame – H20	Floor 9 – A & 3-5	ASTM E119	Quasi-static	NF	No failure at member and system levels.
Analysis regime	2D Frame – H21	Floor 2 – F & 2-4	ASTM E119	Dynamic	210	Global collapse occurs.
	2D Frame – H22	Floor 2 – F & 2-4	ASTM E119	Quasi-static	219	Global collapse occurs.

NF – No Failure

## 5.6 Summary

The parametric studies presented in this chapter, which evaluated the influence of several critical parameters on the onset of instabilities leading to the collapse of steel framed buildings, led to the following findings:

- The severity of fire exposure, location and extent of burning, fire spread, high-temperature creep, varying load paths, and temperature-induced local instabilities have a significant influence on the onset of fire-induced progressive collapse in a steel framed building.
- The severity of fire exposure has a significant effect on the fire response of a steel framed building wherein higher severity fires result in an early onset of instability in the structure. Fires with significantly high peak temperatures (exposure of 1000°C) need not necessarily trigger the collapse in a steel framed building if the duration of fire is short enough such that the steel temperatures in the affected steel members do not increase significantly (beyond 500°C).
- Under severe to very intense fire exposure (peak fire temperatures over 1000°C and burning for more than 2 hours), fire-induced progressive collapse is triggered in the following scenarios: one, when the fire spreads to more than 25% of the floor area with burning in a single floor, and the other, when the fire spreads to three stories with 15% floor area burning in a single floor.
- Temperature-induced creep strains influence the onset of instability in steel framed structures. Neglecting transient creep effects in the fire-induced progressive collapse analysis of a steel framed structure can result in underestimation of global failure times.
- The extent of fire spread in a building has a significant influence on the level of creep-induced deformations that occur in steel frames. The failure time in a typical steel frame

with around 60% floor area burning in a single-story decreased to 156 from 198 minutes when creep strains are fully accounted for in the fire resistance analysis. This is owing to the drastic increase in stress levels, as more structural members lose their strength and stiffness upon exposure to fire, resulting in higher creep deformations.

- The stability of the structure is critically affected when the fire occurs in the lower levels of the building. However, the creep effects tend to be higher when the upper stories are subjected to fire, mainly because of the relatively slender members used in the top stories of the building. While the difference in the failure times obtained using models with and without creep is 28 min under the scenario with fire on floor 2, the scenario with fire on floor 9 resulted in a difference of 37 min in failure times.
- The composite slab and transverse framing add significant resistance against fire-induced collapse. Neglecting the slab and traverse framing in the finite element model results in unrealistic load redistributions and failure times.
- Neglecting the effect of local buckling in the finite element model can result in failure times that are 10% higher than models that consider local buckling effects using shell elements for fire-exposed framing members. The difference is sensitive to the slenderness of the steel members present in the fire compartments, where models with slenderer columns have larger sensitivities to local buckling effects.

### 6 Design Guidelines

#### 6.1 General

Steel framed buildings can experience high levels of instability at a local, member, or global level under fire conditions, and in the event of severe fire exposure, these instabilities lead to the partial or complete collapse of the structure. The studies carried out in this thesis indicate that the onset of instability in steel structures is influenced by several critical factors including the severity of fire exposure, location and extent of burning, fire spread, high-temperature creep, varying load paths, and temperature-induced local instabilities. However, the current design provisions [18,36,37,106,107] for evaluating the fire resistance of steel structures are typically based on prescriptive or simplified approaches without proper consideration of the above-mentioned factors. This is mainly due to the high level of complexity in undertaking advanced analysis of steel structures under fire exposure, especially for tracing fire-induced progressive collapse, and limited guidelines available in codes and standards for undertaking such analysis.

At present, designers often refer to recommendations for the design of steel structures against progressive collapse at room temperature conditions provided in guidance documents such as UFC [110] and GSA guidelines [111] for extreme loading events such as blasts, earthquakes, and impact. As a result, progressive collapse of steel framed buildings is evaluated under different “column loss” scenarios, which are treated as the initiation of local instability in the structural system that may lead to the collapse of a building; and neglecting critical influencing factors such as fire severity, fire spread, altering load paths, creep and buckling effects. Further, no specific guidance is provided on how to account for high-temperature creep effects or temperature-induced local buckling in the fire resistance analysis of steel structures.

To overcome these limitations, this chapter provides recommendations on critical parameters to be considered for predicting the onset of instability in steel framed buildings through system level analysis. Specific guidelines are provided for the treatment of creep in the fire resistance analysis of steel structures including recommendations for considering creep effects while tracing fire-induced collapse. Further, guidance is provided for identifying critical scenarios and tracing fire-induced collapse using advanced analysis. These guidelines are aimed at enhancing the fire performance and minimizing the onset of instability in steel framed structures to reduce the probability of fire-induced progressive collapse.

## **6.2 Critical factors for tracing fire-induced progressive collapse in steel framed buildings**

Data from the numerical model and parametric studies presented in this thesis show that the system level behavior of a steel framed building under fire exposure, including the progression of instabilities leading to collapse, is complex and dependent on several factors. The key parameters that are to be considered to predict the onset of temperature-induced instabilities leading to the progressive collapse in a steel framed building are discussed here.

### ***6.2.1 Fire scenarios***

Fire severity is typically evaluated in terms of heating rate, peak temperature (intensity), and duration of the fire, and has a significant influence on the fire resistance of steel members [8,11]. When a steel member is exposed to a severe fire scenario, the member experiences higher peak temperatures resulting in faster degradation of strength and stiffness properties of steel, which in turn leads to an early onset of instability in the member. However, measuring fire severity using only peak temperatures and duration is not sufficient while carrying out a system level analysis for tracing fire-induced collapse. Factors such as the location and extent of fire spread in a building have a significant effect on the onset of instability in a steel framed building. When a larger number

of compartments or floors are exposed to fire, more steel members undergo loss in strength and stiffness and consequently resulting in an early onset of instability in the building. Moreover, the spread of fire from one compartment (or floor) to another imposes different heating and cooling cycles in different compartments (or floors), which can alter the load paths leading to the progressive collapse of the building. Therefore, a realistic prediction of fire-induced collapse in a steel framed building should account for varying fire scenarios including fire spread, as well as material properties, load paths, restraint forces, and local and global instabilities.

### ***6.2.2 Material models***

The material models used in the computational models have a significant influence on the fire resistance predictions of steel structures. Material models for steel, concrete and fire insulation vary at elevated temperatures due to significant degradation in properties with temperature. The variation in these properties needs to be properly accounted for in tracing the fire-induced progressive collapse of steel framed structures. Moreover, current fire design provisions primarily evaluate failure in steel structures based on the critical temperature of steel. Most standards and published data show that steel loses about 50% of its strength at 550°C, which is considered the critical temperature, however, this does not represent a real failure in the structure.

For tracing the fire-induced progressive collapse in steel framed structures, temperature-dependent stress-strain relations, such as the ones presented in EC3 [18] or ASCE manual [36], are to be used to obtain realistic predictions of response (stresses and deformations) and failure time. Based on past studies [8,29–31], the EC3 constitutive model produces slightly more flexible responses compared to that of ASCE or other constitutive models. This is because the EC3 model (at elevated temperatures) introduces a proportionality limit at the end of the linear portion of the stress-strain curve and following this point the response remains elastic but becomes nonlinear as shown in

Figure 6.1. This point is different from the yield limit, which defines the transition from elastic to inelastic material response. This nonlinearity after the proportionality limit results in a larger strain for a given stress level than in the linear-elastic zone. This allows the EC3 model to partly account for the creep effects. The other constitutive models, such as ASCE [36], assume a sharp yield limit to define the transition from linear-elastic to the inelastic response of steel and hence, do not account for the creep effects (refer to Figure 6.1). Hence, it is recommended to use the EC3 constitutive model for tracing the fire-induced progressive collapse of steel framed structures, particularly when high-temperature creep effects are not explicitly considered in the fire resistance analysis.

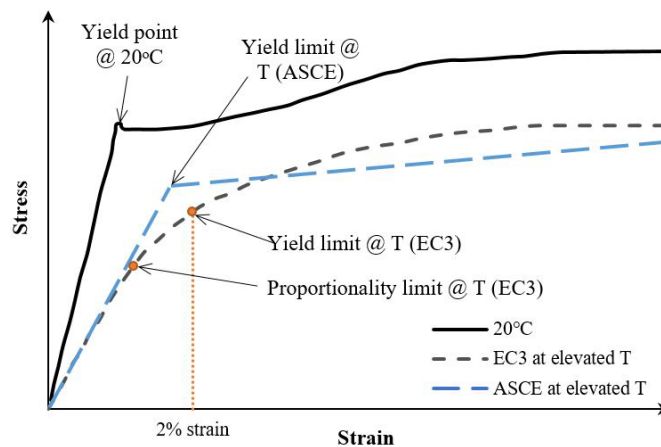


Figure 6.1. Definition for yield limit and proportionality limit in EC3 and ASCE.

### 6.2.3 High-temperature creep effects

High-temperature creep can influence the onset of instability in steel structures especially when steel temperatures exceed 400°C. At a member level, neglecting the full effects of creep can lead to underestimation of deformations and fire-induced forces and hence, lead to unrealistic predictions of fire resistance. At a structural level, the creep deformations can be critical to the stability of a fire-exposed steel framed structure for the two following reasons. Firstly, during a fire incident, the service loads acting on the structure are much lower than the maximum design

loads specified for room temperature conditions, which results in low initial stress levels in the structural members. However, when exposed to fire, the thermal expansion of the fire-exposed members is restrained by the adjoining cooler regions of the building, which results in additional stresses in the fire-exposed steel members. These stresses, when combined with the increase in stresses caused due to the degradation of strength and stiffness of steel at elevated temperatures, can induce high levels of transient creep strain causing an early onset of instability in the structural members.

Secondly, the loss of one or more structural members under fire conditions results in further redistribution of loads to the adjoining members in the structure, which in turn increases the stresses experienced by these members. Exposure to increased stresses, especially at high temperatures, results in increased creep deformations, which can cause imminent instability in the fire-exposed compartment, story, or the whole structure. Further, the level of creep deformations varies depending on the intensity and duration of fire exposure and the extent of fire spread (number of compartments or floors burning) in a steel framed building. Hence, transient creep strain is a critical parameter that needs to be fully accounted for in the finite element model to predict the onset of fire-induced progressive collapse in a steel framed building.

#### ***6.2.4 Altering load paths and load redistribution***

The current prescriptive and simplified approaches for evaluating the fire resistance of steel structures are carried out at a sectional level without due consideration of factors such as redistribution of stresses, fire-induced forces, etc. Even most of the advanced analysis approaches reported in past studies [9,11,33,132–134] are carried out at a member or assembly level and such an analysis is not sufficient for tracing the progression of instabilities in a structure leading to progressive collapse. Moreover, the composite action developed between the floor slab and beams,

temperature-induced restraint forces, and realistic redistribution of loads to different members in the structural system require the full 3D model of the building (including framing members in two directions and floor slab) to be included in the fire resistance analysis. Further, realistic fire scenarios including fire spread from one region to another can only be accounted for in a full 3D building model. Studies presented in this thesis showed that the onset of progressive collapse predicted using a 2D model is inconsistent with that of a 3D model. Hence, it is recommended to consider the effects of transverse framing and floor slab while tracing the fire-induced progressive collapse of steel framed buildings.

### ***6.2.5 Connections***

The connection between different structural members in a building is a critical parameter that needs to be incorporated into the fire-induced progressive collapse analysis. The connections determine the temperature-induced restraint forces in the member, which in turn can affect the onset of instability in the member. At a system level, the connections determine the direction and extent of load redistribution, which can significantly influence the load paths and progressive collapse timelines in a fire-exposed building. Further, during fire exposure, connections can experience high shear, tension (or compression), and rotation demands due to the failing structural members, which can result in the fracture of these connections and abrupt failure in the structure. Most studies that trace the fire-induced progressive collapse of steel framed buildings incorporate simple connection models for shear and moment connections. These models capture the restraint effects and load redistribution during fire exposure and are also computationally effective. However, more complex component-based models that include the degrading behavior of shear and moment connections at elevated temperatures are needed to trace the failure in connections.

Very limited studies are available in the literature that includes the failure of connections in the fire-induced progressive collapse analysis [13,17,79]. The GFA and UFC documents have extensive recommendations for modeling and designing connections for progressive collapse under extreme loading events such as earthquakes and blasts. However, no guidance is available for modeling connection failure at elevated temperatures. Further research is needed for developing reliable high-temperature connection models and design criteria for fire-induced progressive collapse analysis.

#### ***6.2.6 Local buckling effects***

Local buckling of steel sections at elevated temperatures can have a significant influence on the onset of instability in steel structures. The occurrence of local buckling reduces the load-carrying capacity of the steel member and thus initiates early failure at member and global levels. For the design of steel structures under ambient temperature conditions, the stability criterion is given due consideration in the flexure and shear limit states for steel beams and in the buckling criterion for steel columns. However, the local buckling criterion is not specifically considered for fire design. Past studies [33,135,136] on steel members indicated that the degradation in the sectional capacity of members under fire exposure, particularly in sections classified as Class 2, 3, and 4 as per Eurocode 3 [18] specifications, result from the occurrence of temperature-induced local buckling in addition to the degradation of strength and stiffness of steel at elevated temperatures.

In modern steel framed buildings, more and more thin (non-compact) steel sections are being used for aesthetics, cost savings, and specific architectural requirements. Such sections are more susceptible to undergoing local buckling at elevated temperatures due to the low width-to-thickness ratio of the cross-sectional elements (flanges and web). Studies carried out in this thesis showed that the occurrence of local buckling in columns could result in an early onset of fire-

induced collapse in steel framed buildings. Further, limiting the slenderness of the steel sections to a certain degree can reduce the susceptibility of the steel members to undergo local buckling at elevated temperatures and hence delay the onset of progressive collapse.

### **6.3 Current provisions for evaluating progressive collapse in buildings**

#### ***6.3.1 Emerging trends – Fire resistance and resiliency of steel framed structures under fire***

The increasing occurrence of natural disasters and manmade threats have shifted the focus towards the development of resilient infrastructure in the past few decades. Resilient structures are those that maintain acceptable levels of performance during and after the breakout of a disaster [23]. Because of their superior design, resilient structures perform better without undergoing high levels of damage and progressive collapse during a disaster. In critical buildings (or infrastructure), such as high-rise buildings, hospitals, embassy buildings, emergency buildings, etc., where life safety is of utmost importance, resiliency is a key consideration in design. This can facilitate the safe evacuation of occupants and provide first responders with sufficient time to tackle the adverse effects of the disaster.

Resiliency is currently evaluated under extreme loading events, such as earthquakes, blasts, and impacts. However, resiliency is not specifically evaluated under fire hazards. The impact of fire in a building can be critical to the safety of the occupants and first responders, especially if the fire causes significant damage to the structural system leading to a partial or complete collapse of the structure. Fire can induce damage in a building, not just as a primary event (e.g., accidental fires), but much more as a secondary event when a fire breaks out after other extreme events such as earthquakes, blasts, etc. Moreover, many critical structures built over the past decades, such as embassy buildings, institution buildings, etc., are experiencing age-related deterioration and hence, are vulnerable to significant damage under extreme fire conditions. Therefore, evaluating

resiliency and fire-induced collapse under severe fire scenarios can be very important from a design point of view, especially in critical buildings.

### ***6.3.2 Fire design provisions for steel framed structures***

For evaluating the resiliency and fire-induced progressive collapse in steel framed buildings, advanced analysis approaches at a system level are needed. However, the current fire design provisions for steel framed structures in codes and standards such as AISC 360-16 [37], ASCE [36], Eurocode 3 [18], etc. are mainly prescriptive-based, without due consideration to several critical factors that influence the onset of instabilities in steel framed structures. Such design measures can meet the fire resistance requirements and enhance the performance of buildings under low to moderate-sized fire events. However, the prescriptive fire design philosophy may not be sufficient to achieve the required level of resiliency in critical buildings under severe fire hazard and additional measures are needed to limit the onset of instabilities, including fire-induced collapse. Very limited guidance is available in current codes and standards for carrying out advanced analysis on steel framed structures. Eurocode 3 [18] and AISC 360-16 [37] provides some generic guidance for undertaking advanced analysis, however, these guidelines do not have any specifics on the numerical modeling, including the element types to be used, connection models, restraint effects, analysis approach, etc. Further, no specific recommendations are provided in the current standards for incorporating the effects of high-temperature creep and local buckling in the fire resistance analysis of steel framed structures.

For addressing high-temperature creep, Clause 4.3.3 (4) in Eurocode 3 states that “*the effects of transient thermal crepe need not be given explicit consideration*” if the “effective” stress-strain curves specified in Eurocode 3 are used. ASCE manual, on the other hand, specifies that high-temperature creep needs to be included in the fire resistance analysis of steel structures, either

through the use of “effective” stress-strain relations derived from transient tests or through specific transient creep models for steel. Hence, it is left to the designer to adopt one of the two methods for including the creep effects. For accounting for local instabilities under ambient conditions, guidelines are given in AISC 360-16 [37] and Eurocode 3-1 [18] to classify steel sections based on limiting width-to-thickness ratios. For instance, AISC 360-16 classifies steel sections as nonslender and slender for the compression limit state and as compact, noncompact, and slender for the flexural limit state. Likewise, Eurocode 3-1 classifies sections ranging from Class 1 to Class 4. However, no specific recommendations are given for consideration of stability limit state at elevated temperatures. Often, the room temperature classifications are adopted under fire conditions.

Further, no specific guidance is given for tracing fire-induced progressive collapse in steel framed buildings in current codes and standards, including system level modeling approaches, fire scenarios, and load paths to be considered for fire-induced collapse or global failure limit states. Only generic recommendations are specified in AISC 360-16 [37], IBC 2021 [106], and NFPA 5000 [107]. Other guidance documents such as UFC [110] and GSA guidelines [111] provide extensive recommendations for design against the progressive collapse of steel framed structures under extreme events such as blasts and impact. However, even in these documents, no recommendations are provided for evaluating progressive collapse under fire conditions. To overcome some of these drawbacks, a set of recommendations are proposed for mitigating fire-induced progressive collapse in critical buildings based on the extensive numerical studies carried out in this thesis, along with the review of literature conducted in Chapter 2.

#### **6.4 Recommendations for evaluating the fire-induced progressive collapse in buildings**

To achieve the required resiliency in critical buildings, appropriate measures need to be developed to mitigate the occurrence of fire-induced progressive collapse in such buildings. Since high-

temperature creep has a significant influence on the onset of instability at member and system levels, guidelines for the treatment of creep in evaluating the fire resistance of steel structures are presented in the first part of this section. Specific recommendations are provided for including the creep effects for tracing fire-induced progressive collapse. In the second part of this section, preliminary guidelines are provided to identify scenarios that are critical for fire-induced progressive collapse. Although fire poses a threat to steel framed buildings, collapse is a rare occurrence. Hence, it may not be economical or practical to design all steel framed structures for fire-induced progressive collapse. Additionally, strategies to minimize the onset of instabilities in steel framed buildings are proposed. For critical scenarios, guidance is provided for carrying out advanced analysis to trace the progressive collapse phenomenon in steel framed buildings under fire conditions. Such an analysis will greatly help in minimizing the fire-induced progressive collapse in steel framed buildings.

#### ***6.4.1 Guidance for the treatment of creep in fire resistance analysis***

Advanced analysis approaches that explicitly account for high-temperature creep effects, as discussed in Chapter 4, yield realistic fire resistance predictions for steel structures; however, such an analysis is highly complex especially when the effects of high-temperature are to be considered explicitly. Moreover, an explicit treatment of creep effects can further complicate the analysis when carried out at a system level (full structure) for tracing fire-induced collapse. Further, studies presented in Section 5.4 clearly indicate that the transient creep effects influence the onset of instabilities (and collapse) in a steel framed structure only under severe fire exposure and high loading (stress) scenarios. Thus, the question is in determining when high-temperature creep effects are to be considered in the fire resistance analysis. Depending on the extent of high-temperature creep in a given fire, loading, and restraint scenario, design recommendations are

provided for the treatment of creep in member and system level analysis. Recommendations are presented under three scenarios, namely, scenarios where creep effects are minimal and need not be considered, scenarios where implicit treatment of creep through temperature-dependent stress-strain relations is sufficient, and scenarios where explicit consideration of high-temperature creep is required.

#### *6.4.1.1 Scenarios where high-temperature creep effects are not critical*

Under many practical fire exposure scenarios in a steel framed building, high-temperature creep effects are minimal and might not govern the onset of instability in a steel member or the building. In fact, the fire resistance evaluation of steel structures in current codes and standards is based on simplified approaches that do not give any consideration to transient creep strain in steel. The scenarios where creep effects need not be accounted for in the fire resistance analysis of steel structures are given below:

- When the failure of a steel member is likely to be governed by a force-controlled (strength) limit state rather than deformation-controlled actions (e.g., stub columns), neglecting the transient creep effects does not affect the evaluation of the degraded (reduced) capacity and thus, the fire resistance of the member. E.g., stub columns.
- When the sectional temperatures in a steel member do not exceed 400°C under service stress levels (< 50%), the transient creep strains that develop in the steel member are very minimal and hence can be neglected for the evaluation of fire resistance. E.g., protected steel members exposed to low to moderate design fire scenarios (with peak fire temperatures lower than 800°C and lasting only for 1 to 2 h of duration). Examples of this type of fire scenario are office buildings, apartment buildings, low-rise buildings, etc.

#### 6.4.1.2 Scenarios where implicit creep is sufficient

Under certain cases of fire exposure, accounting for transient creep effects implicitly in the fire resistance analysis is sufficient to capture the onset of instability at member and system levels.

These scenarios are summarized as follows:

- In unprotected steel members, the steel temperature increases rapidly and the time to failure is low (around 20 to 30 minutes for typical steel columns). Under such short duration and rapid heating rates, the temperature-induced creep deformations tend to be low even under moderate to severe fire exposure scenarios, and hence an implicit consideration of high-temperature creep is sufficient.
- When the average sectional temperature in a protected steel member does not exceed *creep critical temperature* under service stress levels ( $< 50\%$ ), implicit consideration to creep is sufficient. For a given stress level, the *creep critical temperature* is defined as the temperature that corresponds to the onset of tertiary creep in steel. Examples of this case are composite floor systems, where the steel beam is connected to a concrete slab. In this case, the sectional temperatures in the beam (near the top flange) tend to be low due to the heat sink effect from concrete.
- In steel columns with slenderness lower than 50 and subjected to low stress levels ( $< 40\%$ ), the transient creep strain that develops at elevated temperatures is low even under scenarios of moderate to severe fire exposure, and thus implicit creep is sufficient.
- In steel framed buildings, when the burning is within one or two compartments on a floor (for instance, less than 20% of the floor area is subjected to fire in a ten-story building), the damage is expected to be minimal. In such cases, the creep deformations are not likely

to be critical for the onset of progressive collapse and can be considered implicitly in the FE analysis.

#### *6.4.1.3 Scenarios where high-temperature creep is to be considered explicitly*

Based on the parametric studies carried out on steel framed structures (refer to Section 5.4), the transient creep effects were found to be significant under conditions of severe fire exposure (with peak fire temperatures reaching beyond 1000°C and lasting for more than 2 h), high loading (stress) scenarios (of 50% and above), and large extents of burning (for example, burning in multiple compartments or floors). In such scenarios, creep deformations are critical to the onset of fire-induced collapse in steel framed buildings and thus, need to be explicitly incorporated into the fire resistance analysis.

As discussed earlier, the evolution of transient creep strain in a steel member is a function of stress, temperature, and time (total duration and rate). Hence, certain fire exposure scenarios impose higher temperatures in a steel member than other fire exposures do. In Figure 6.2, the average sectional temperatures in a protected W14x53 column (fire rating of 2 h) are plotted under two standard fire scenarios, namely ASTM E119 [25] and ASTM E1529 [27] hydrocarbon, and one design fire exposure scenario, DF-120, with a burning duration of 120 min. Since steel develops only marginal creep strains below 400°C, temperatures below this value are to be considered creep-safe temperatures. When the sectional temperatures rise above 400°C, the creep strain rate increases rapidly and moderate to large creep deformations can occur in the steel column depending on the applied load level. Also, it is evident from Figure 6.2 that fires with different severity require different times to reach such high temperatures and thus induce creep strains at a rapid pace. In general, the extent of creep strain that develops in a steel member can be classified under three categories, namely, ‘minor’, ‘moderate’, and ‘severe’ based on the level of temperature

and stress experienced by the steel member. Table 6-1 presents the categories of creep strain under different temperature ranges and applied stress levels on the member. It can be seen that even at a moderate temperature range of 400 – 550°C, the severity of creep increases as the applied stress level increases. Similarly, even for low to service load levels, moderate to severe creep strains can develop if the temperatures exceed 550°C as shown in Table 6-1.

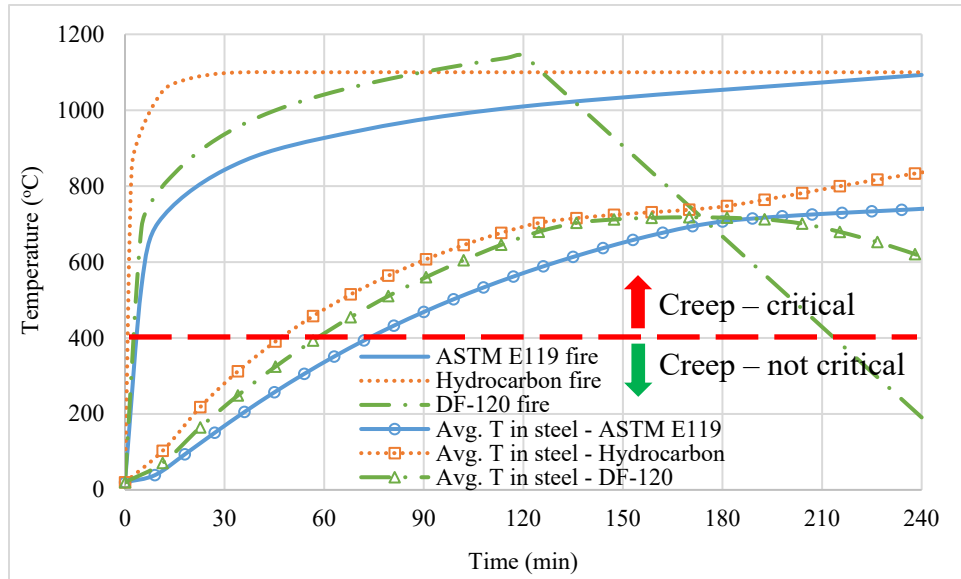


Figure 6.2. Average sectional temperatures in a steel column (W14x53) under different fire exposure scenarios.

Table 6-1: Extent of creep in steel members based on temperature and stress level

Stress level %	Temperature		
	20°C to 400°C	400°C to 550°C	> 550°C
30	Minor	Minor	Moderate
40	Minor	Moderate	Moderate
50	Minor	Moderate	Severe
60	Minor	Severe	Severe
70	Moderate	Severe	Severe

Steel columns in buildings are always provided with some form of fire insulation with a fire resistance rating of 1 to 4 h. Depending on the fire rating of the column, the time taken for temperatures in the column to attain critical values beyond which creep effects tend to dominate

the response varies. To simplify the identification of scenarios where creep can be critical in steel columns, recommendations based on temperature and stress levels are provided in Table 6-2 as the time at which creep deformations begin to significantly influence the onset of instability in columns with different fire ratings (1-3 h) under two standard fire exposure, ASTM E119 fire, and ASTM E1529 hydrocarbon fire. Under both fire scenarios, it can be seen from Table 6-2 that an increase in the stress level reduces the time at which creep deformations become critical. Moreover, due to the higher severity of hydrocarbon fire than the ASTM E119 fire exposure, the critical times are lower in the case of hydrocarbon fire scenario for all the columns.

Table 6-2: Time at which creep deformations become dominant in steel columns exposed to different fire exposure scenarios

Stress level (%)	Time (min)					
	ASTM E119 fire exposure			ASTM E1529 Hydrocarbon fire exposure		
	W14x53 (1 h)	W14x53 (2 h)	W14x53 (3 h)	W14x53 (1 h)	W14x53 (2 h)	W14x53 (3 h)
30	55	100	170	40	75	140
40	50	90	150	35	65	120
50	45	80	140	30	60	100
60	40	70	130	25	55	75
70	30	55	100	15	45	55

For other column sections with different fire resistance ratings, the time at which high-temperature creep effects become dominant can be determined based on the time taken for the average temperatures in the steel section to reach the *creep critical temperature*. These *creep critical temperatures* are presented in Table 6-3 for A992 (Grade 50) steel at different stress levels. These temperatures are evaluated based on the creep test data reported by Morovat et al. [92] for A992 steel at elevated temperatures. For each stress level, the temperature corresponding to the onset of tertiary creep is taken as the *creep critical temperature*. This method of utilizing the *creep critical temperature* to evaluate the extent of creep effects can also be extended to other fire-exposed steel

members such as braces and axially restrained beams, which can experience a high level of compression loading. If the average temperatures in these steel members reach the critical temperature as specified in Table 6-3 for a given stress level, then the creep deformations are more likely to dominate the fire response and need to be considered explicitly through advanced analysis approaches.

Table 6-3: Creep critical temperatures for A992 steel at different stress levels

Stress level %	Critical Temperatures (°C)
20	640
30	585
40	550
50	525
60	500
70	450
80	400

Exposure to non-uniform fire exposure, especially from three sides, was shown to have a significant influence on the extent of creep deformations and the onset of instability in steel columns. When a steel column is subjected to fire exposure from two or three sides, additional stresses and secondary bending moments can develop due to thermal bowing and nonuniform temperature distribution in the cross-section. These additional stresses can induce higher creep deformations which can adversely affect the stability and hence the fire resistance of the column. Thus, in such scenarios, high-temperature creep effects are to be considered explicitly in the fire resistance analysis.

At a structural level, creep deformations can be critical for predicting the onset of progressive collapse in a steel framed building depending on the severity of fire exposure, burning location, and extent of fire spread, as discussed in Section 6.2.3. To identify the level of influence that high-temperature creep has on the onset of instability at a structural level, the extent of creep is again

classified under three categories: ‘minor’, ‘moderate’, and ‘severe’ based on the severity of fire exposure and extent of burning in a single floor (as shown in Table 6-4) and in multiple floors with at least 2 compartments (10% floor area) burning in one floor (as shown in Table 6-5). These recommendations are based on the results of analyses carried out on a braced framed building comprising ten stories and five bays and in which the steel members were provided with 2 h fire rating (based on office occupancy).

Table 6-4: Extent of creep in steel framed buildings based on fire severity and extent of burning on a single floor

Extent of burning on a single floor	Fire severity		
	Low severity ( $T_{\text{peak}} < 800^{\circ}\text{C}$ & duration < 1 h)	Moderate severity ( $800^{\circ}\text{C} < T_{\text{peak}} < 1000^{\circ}\text{C}$ & duration of 1-2 h)	High severity ( $T_{\text{peak}} > 1000^{\circ}\text{C}$ & duration > 2 h)
< 20%	Minor	Minor	Moderate
20 – 40%	Minor	Moderate	Severe
> 40%	Moderate	Severe	Severe

Table 6-5: Extent of creep in steel framed buildings based on fire severity and extent of burning on multiple floors

Extent of burning on multiple floors	Fire severity		
	Low severity ( $T_{\text{peak}} < 800^{\circ}\text{C}$ & duration < 1 h)	Moderate severity ( $800^{\circ}\text{C} < T_{\text{peak}} < 1000^{\circ}\text{C}$ & duration of 1-2 h)	High severity ( $T_{\text{peak}} > 1000^{\circ}\text{C}$ & duration > 2 h)
2 floors or less	Minor	Minor	Moderate
3 to 4 floors	Minor	Moderate	Severe
5 floors or more	Moderate	Severe	Severe

It is evident from Table 6-4 and Table 6-5 that as the extent of fire spread increases either within a single story or to multiple floors, the severity of creep increases even for low to moderate fire severity. These results are obtained for a ten-story steel framed building with steel members having a 2 h fire rating. For other typical steel framed buildings of similar size and fire resistance rating,

the fire severity and extent of burning can be utilized to determine the influence of creep deformations towards the onset of fire-induced collapse.

A summary of the above discussion is presented below under two categories. Since columns are integral to the stability of a structure, the first category presents specific recommendations for steel columns under fire conditions. In the second category, general recommendations for steel framed buildings for tracing fire-induced collapse are provided. For steel columns, the following are scenarios where high-temperature creep strain is to be considered explicitly in the fire resistance analysis.

- When the average sectional temperature in a protected steel column exceeds the *creep critical temperature* as specified in Table 6-3 for A992 steel at different stress levels, transient creep strain highly influences the onset of instability in the column and hence, the predicted fire resistance.
- When the duration of fire exposure exceeds the values specified in Table 6-2 for different standard fire exposure scenarios, creep deformations are significant and can result in an early onset of instability in the column.
- For columns with high slenderness ( $> 50$ ) and/or subjected to high load (stress) levels of 40% or higher, creep effects can be critical.
- When columns are subjected to non-uniform fire exposure (1-, 2-, 3-sides) or when the cooling phase of fire is considered in the fire resistance analysis, high-temperature creep effects on the onset of instability in the column can be significant.

The following are scenarios where transient creep is to be explicitly included in the fire-induced progressive collapse analysis of steel framed buildings.

- Creep effects can be significant when a steel framed building is exposed to severe to very intense fire exposure (peak temperatures exceeding 1000°C and burning for more than 2 h) in 20% of the floor area or more.
- When the extent of fire spread in a single floor of a steel framed building exceeds 20% of the floor area, large creep deformations are likely to occur, and explicit consideration of creep is required.
- Creep effects can be critical when the fire spreads to more than two stories in a steel framed building with at least 10% of the floor area subjected to burning on each floor.

The above-discussed recommendations for the treatment of creep in the fire resistance analysis of steel structures are summarized in Table 6-6 under three categories: ‘*creep-not critical*’, ‘*creep-implicit*’, ‘*creep-explicit*’.

Table 6-6: Treatment of high-temperature creep in fire resistance analysis of steel structures

<b>Creep-not critical</b>	<b>Creep-implicit</b>	<b>Creep-explicit</b>
<ol style="list-style-type: none"> <li>1. When failure of a steel member is evaluated based on strength limit state consideration.</li> <li>2. When the sectional temperatures in a steel member do not exceed 400°C under service stress levels (&lt; 50%).</li> <li>3. When fire scenarios are low to moderate (T &lt; 800°C and duration &lt; 1 h).</li> </ol>	<ol style="list-style-type: none"> <li>1. In unprotected steel members.</li> <li>2. When the average sectional temperatures in a protected steel member do not exceed the <i>creep critical temperature</i> under service stress levels (&lt; 50%).</li> <li>3. For columns with slenderness lower than 50 and lightly loaded (stress level &lt; 40%).</li> <li>4. For steel framed buildings exposed to moderate fire exposure with burning in one or two compartments (&lt; 20% of the floor area).</li> </ol>	<ol style="list-style-type: none"> <li>1. When the temperature and stress levels exceed the values corresponding to the ‘severe’ creep category as specified in Table 6-1.</li> <li>2. For steel columns exposed to fires longer than the times specified in Table 6-2 for a given fire exposure scenario and fire rating.</li> <li>3. When the average sectional temperature in a steel column exceeds the creep critical temperature as specified in Table 6-3.</li> <li>4. For columns with high slenderness (&gt; 50), heavily loaded (&gt; 40%), and/or non-uniform fire exposure.</li> <li>5. When the severity of fire exposure in a steel framed building exceeds the value corresponding to the ‘severe’ creep level as specified in Table 6-4 and Table 6-5.</li> </ol>

#### ***6.4.2 Guidance for identifying critical scenarios for fire-induced collapse***

Steel framed structures may be subjected to fire exposure during their service life, which can cause damage to the structural members to a certain extent. In many scenarios, this damage is local and does not progress to the entire structure if the fire exposure is not severe and contained within a few compartments. Moreover, certain buildings depending on their occupancy, size, and level of fire protection may not develop severe fires that may lead to the progressive collapse of the building. Thus, design for fire-induced progressive collapse may not be critical for all buildings. Moreover, advanced analysis approaches for tracing fire-induced progressive collapse in steel framed buildings, as discussed in Chapter 4, are highly complex and computationally expensive. It is often not practical and economical to design every steel framed building for fire-induced progressive collapse. Only buildings that are at a high-risk level from the perspective of fire hazards should be designed for fire-induced collapse.

GSA [111] and UFC [110] guidance documents provide recommendations for identifying critical buildings for which the design for progressive collapse is needed under ambient temperature conditions. For instance, the GSA guidelines provide recommendations for determining critical buildings based on the number of stories in a building, facility security level (FSL), or through a facility-specific risk assessment. The FSL of a building is determined based on several factors such as occupancy level (and type), building size, symbolism, the likely threat level, etc. For buildings classified under FSL I and II, design for progressive collapse is not recommended irrespective of the number of floors in such buildings. For FSL III and IV buildings, it is recommended to carry out progressive collapse analysis when the number of stories in the building is more than four. However, unoccupied floors such as mechanical penthouses or parking floors are not considered while evaluating the number of stories in a building. The GSA guidelines recommend the design

for progressive collapse for all buildings classified under the FSL V category. The design documents, however, do not provide any recommendations for fire-induced collapse.

The criteria used for identifying high-risk buildings for ambient conditions, such as the GSA guidelines [111] discussed above, can be applied for determining critical scenarios for fire-induced progressive collapse as well. Additionally, in some cases, even if a building is not critical for progressive collapse under ambient conditions, certain characteristics of the building such as the presence of high fuel loads or lack of fire protection systems may increase the risk of a severe fire hazard in the building and hence, needs to be designed for fire-induced progressive collapse. Thus, additional factors which are specific to fire conditions such as the severity of fire exposure and the extent of fire spread that is likely to occur in a building need to be evaluated in identifying scenarios that are critical for fire-induced collapse.

Due to the limited number of studies available on fire-induced progressive collapse and also complex parameters that influence this phenomenon, it is not reasonable to develop any quantitative measure for determining which buildings need to be designed for the fire-induced collapse based on the available data. Instead, a qualitative assessment is recommended to identify buildings that are at high risk of developing severe to intense fires that increase the susceptibility to collapse. A good estimation of the fire conditions that are likely to develop in modern steel framed buildings and occupancies, based on the fuel (fire) loads and fire spread, can aid in determining whether a given fire exposure may result in the progressive collapse of the building. Buildings with a higher fire load density and with plastic and hydrocarbon-based fuels are more likely to develop severe fire exposures compared to the ones with a lower fire load density. Eurocode 1 [77] provides fire load densities for common occupancies ranging from 100 to 1500 MJ/m<sup>2</sup>.

Occupancies such as offices and hotels have moderate fire load densities of 420 and 310 MJ/m<sup>2</sup> [77] respectively, and in such cases, the resulting fire exposure is likely to be medium and thus less probable to induce progressive collapse in the steel framed building. Figure 6.3 shows the time-temperature curve for a compartment in an office building, assuming an opening factor of 0.03 m<sup>1/2</sup> and thermal inertia of 1200 J/m<sup>2</sup>-s<sup>1/2</sup>-K for the lining materials in the compartment. However, when the same office or hotel building is housing additional features (such as a parking garage, storage tanks, etc.) that contribute to increased fuel loads that are not commonly present in similar occupancies, then special consideration is required. E.g., modern hotel buildings have parking stories on the lower floors that can contribute to a significant increase in fuel loads. Another example could involve an office building housing additional fuel storage for backup power generation. The presence of petroleum-based fuel can lead to intense fire scenarios in the building as shown in Figure 6.3. In such scenarios, it is recommended to design the buildings for fire-induced progressive collapse. As such, the designer may assess the availability of fuel in a building and the fire load that may break out in the event of a spill, and if the fire load is high then fire-induced progressive collapse needs to be evaluated in such buildings.

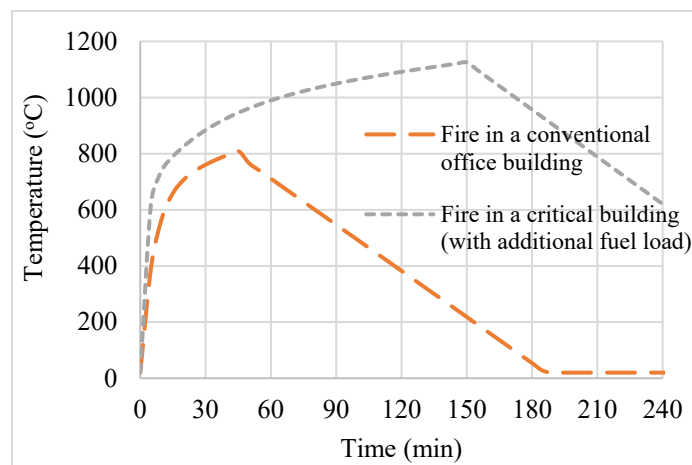


Figure 6.3. Fire exposure scenarios for different fire load densities.

The likelihood of a fully developed fire and the extent of fire spread also depends on the availability of active and passive fire protection systems in a building. Many modern code-complaint buildings are equipped with fire alarms, smoke detectors, and sprinkler systems. In such buildings, the occurrence of a severe fire is rare due to the early detection and suppression of fire spread and hence, design for fire-induced progressive collapse may not be critical. Likewise, buildings with quicker response times also have a lower probability of developing a severe fire. Response time is the expected duration for the first responders to reach the building in the event of fire [137]. Studies indicate that the average response time for building fires in the US is between 9 and 14 min [138]. In some cases, depending on the incident discovery, the time that is taken to dispatch the first responders, the size of the fire event, driving, and traffic conditions at the time of the incident, response times can be longer than the average time. In general, if the response time for a ‘critical’ building is anticipated to be greater than 30 min, then the likelihood of a fully developed fire and fire spreading to multiple compartments (or floors) is high and the design for fire-induced progressive collapse is needed for such buildings. Designers can assess the response time for a particular building from previous data available in that locality or through consultation with the nearest fire department. Further, for buildings with high evacuation times, as presented in Chapter 3 of this thesis, fire-induced progressive collapse analysis is critical for achieving the required fire resistance and allowing complete evacuation to take place.

#### ***6.4.3 Strategies to minimize the onset of fire-induced collapse***

The preliminary guidelines presented in Section 6.4.2 can be applied to assess the vulnerability of a building to undergo fire-induced collapse. This can be done at an early stage of the design process of new buildings or before the rehabilitation/modernization of existing buildings. If a building is found to be in a high-risk category based on the proposed guidelines, suitable design features can

be incorporated to reduce the potential for fire-induced collapse. FEMA 426 [139] specifies structural features for the design against progressive collapse at ambient conditions for extreme loading events such as earthquakes, wind, blasts, and impact. Some of these features include incorporating redundancy in lateral and vertical load resisting systems, use of ductile structural elements, design for load reversals in primary and secondary members, and design for shear failure. These recommendations are beneficial for minimizing the potential of collapse in fire-exposed steel framed buildings as well. However, additional design features such as the design for fire protection to steel members, compartmentation, etc. are needed to minimize the vulnerability of the building to fire hazards. The required fire protection for steel members in buildings is typically evaluated based on prescriptive or simplified approaches, which do not account for several critical factors and hence, may not be sufficient under scenarios that can trigger fire-induced collapse. For high-risk buildings, implementation of performance-based fire design approaches using advanced analysis can yield optimum fire resistance strategies that are unique for a specific building. In the case of high-risk buildings with significant fuel loads, additional strategies such as the installation of reliable fuel containment systems and suppression systems can also be planned to minimize the potential of a severe fire.

Further, studies presented in this thesis clearly show that temperature-induced instabilities in steel columns are the most important factor that triggers fire-induced collapse in steel framed buildings. Even if the columns provided in the building are non-slender as per AISC classifications at room temperatures, they can transform to slender sections at elevated temperatures if the provided slenderness is high, making them susceptible to local buckling. The occurrence of local buckling in steel columns can significantly compromise the load-carrying capacity of the column and thus, precipitate the onset of the fire-induced collapse. For this reason, the following recommendations

are proposed to minimize the occurrence of local buckling in steel columns (and fire-induced collapse). In critical buildings, it is recommended to limit the slenderness of column sections to a certain level. The limit can be established as the lowest slenderness limit that can occur at elevated temperatures. For web and flange of steel columns, the slenderness (for compression limit state) can be limited to 25.4 and 10.1 respectively, which are the least slenderness values that occur at 700°C for Grade 50 steel. Additionally, when columns with slenderness values higher than the proposed limits are utilized in critical buildings, it is recommended to explicitly account for the local buckling effects in the fire-induced progressive collapse analysis.

#### ***6.4.4 Guidance for undertaking advanced analysis for tracing fire-induced progressive collapse***

Buildings with high-risk levels are to be evaluated for fire-induced progressive collapse through advanced analysis. To account for all critical factors influencing the onset of instabilities, advanced analysis at a system level is to be carried out. Advanced analysis at a system level is highly complex and requires significant expertise and experience to implement, and the results obtained are contingent upon the parameters included and the level of complexity adopted in the analysis. For undertaking advanced analysis for tracing the onset of fire-induced instabilities leading to the progressive collapse of a steel framed building, the use of finite element-based programs such as ABAQUS, ANSYS, etc. is required. The fire-induced progressive collapse analysis involves a three-step procedure. The first step involves the determination of fire scenarios that are to be considered for the progressive collapse analysis. At present, in the fire resistance calculations, the fire temperatures are traced using standard or parametric temperature-time relations specified in ASTM E119 [25], ASTM 1529 [27], ISO 834 [28], and Eurocode 1 [77]. Alternatively, for a more realistic evaluation of fire scenarios based on the building characteristics, fuel loads, functions in

a building, available fire protection systems, etc., recommendations provided in the SFPE Handbook [45] can be utilized to obtain design fire scenarios for buildings.

In the second step, thermal analysis of the fire-exposed steel members is to be carried out to obtain the cross-sectional temperatures in each member as a function of fire exposure time. The discretization, boundary conditions, and temperature-dependent thermal properties to be utilized in the thermal model are specified in Chapter 4. The final (third) step involves the structural analysis of the steel framed structure at ambient and elevated temperature conditions. In this step, the load-bearing members in the steel framed building including framing and slab members are discretized using appropriate elements and mesh size, as specified in Section 4.7 for undertaking the structural analysis. The connections between different members and support conditions in the building are modeled through specified joint constraints and boundary conditions.

Two loading sequences are used in the structural analysis. First, the gravity loads, which are obtained as  $1.2 \text{ DL} + 0.5 \text{ LL}$  (where DL and LL represent the dead load and live load respectively), and notional lateral loads, evaluated as 0.2% of gravity loading on that floor, are applied gradually to the steel framed building. Second, sectional temperatures obtained as output from the thermal analysis are applied to the fire-exposed members as predefined temperature fields. Temperature-dependent mechanical property relations for steel and concrete, as specified in Section 4.5, are given as input to the structural model.

When assigning the stress-strain data for steel in the structural analysis, it is to be specified whether transient creep is accounted for implicitly or explicitly. Scenarios, where explicit treatment of creep is needed are determined based on the recommendations provided in Section 6.4.1. The approach for incorporating creep explicitly in the fire-induced progressive collapse analysis is discussed in Chapter 4. Temperature-induced local buckling in fire-exposed steel members is to

be included in the analysis when steel sections with high slenderness ratios are used in the fire compartments (refer to Section 6.4.3). To account for the local buckling effects in the fire-induced progressive collapse analysis, a mixed-element approach, as discussed in Section 4.7, is utilized to discretize the framing members in the building.

The progression of instability in the steel framed structure is to be traced continuously throughout the fire exposure (including the cooling phase) by carrying out either a nonlinear quasi-static analysis or nonlinear dynamic explicit analysis, as discussed in Section 4.3. Flowcharts showing various steps in each of the analysis regimes for evaluating the fire-induced progressive collapse in a steel framed building are presented in Figure 4.2 and Figure 4.3. The appropriate analysis type is chosen based on the parameters to be included in the analysis to obtain a computationally efficient and robust solution.

The response parameters, including stresses and displacements, are to be traced at various points in the structure including all the fire-exposed members, compartments adjoining the fire compartments, at different floor levels, etc. to trace the progression of instabilities in the building. At each time step, these values are used to check for failure at the member or system level based on the limiting criteria specified in Chapter 4. If only members in the fire compartment undergo failure, and this does not progress to system level failure, then only partial or local collapse is said to have occurred in the building. Progressive collapse is said to initiate when the system level failure limits are exceeded. The above-described analysis is to be carried out for a series of probable fire and loading scenarios to determine the robustness of the building against fire-induced collapse. Further, the results from each case can be utilized to develop strategies such as improving the steel sections, connections, fire protection system, etc. The application of the advanced analysis

approach at the system level for tracing the fire-induced progressive collapse of a typical steel framed building is illustrated in Appendix C.

## **6.5 Limitations**

Although the guidelines and approach presented in this chapter can be applied to evaluating the fire-induced progressive collapse of steel framed buildings, there are some limitations, which are listed below.

- The recommendations provided for the treatment of high-temperature creep at a system level are based on the studies carried out on a ten-story braced framed building. Additional studies are needed to determine the effect of creep on other types of framing systems such as moment frames, steel framed buildings with a rigid core, etc. Further, buildings may have different floor layouts, compartment sizes, floor levels, etc. as compared to the building considered in this thesis. Hence, the recommendations provided based on the extent of burning, fire location, etc. are only approximate and cannot be generalized to all buildings.
- The guidelines presented for identifying scenarios critical for fire-induced collapse are based on a qualitative evaluation of different features in the building. However, for better practical applicability, a quantitative measure such as an importance factor can be established for determining the risk associated with buildings based on critical factors that influence fire-induced collapse. Such importance factors have been established for fire hazards in bridges [137] and a similar approach can be adopted for buildings.
- The proposed approach for the explicit treatment of high-temperature creep and local buckling effects in the fire-induced progressive collapse analysis can be applied to 2D steel frames only. This is mainly due to the numerous numerical instabilities that can occur while

carrying out the analysis using the nonlinear quasi-static regime, as well as high computational effort. Further research is needed to implement the effects of transient creep and local buckling in 3D buildings models that include floor slabs and transverse framing with good computational efficiency.

## 6.6 Summary

This chapter presents guidelines for evaluating the fire-induced progressive collapse in steel framed buildings based on the results generated from the parametric studies. The following are key points that summarize the information presented in this chapter.

- The severity of fire exposure including the extent of fire spread, high-temperature creep effects, altering load paths, connections (restraint forces), and temperature-induced local buckling are critical parameters that influence the onset of instabilities leading to the progressive collapse in steel framed buildings under fire conditions.
- The proposed design recommendations can be highly useful for the treatment of creep in the fire resistance analysis at member and system levels. Depending on the extent of transient creep strain that is likely to develop in a fire-exposed steel structure, three alternative scenarios are proposed for incorporating creep in fire resistance analysis (and fire-induced progressive collapse analysis), namely, '*creep-not critical*', '*creep-implicit*', '*creep-explicit*'.
- A qualitative assessment is provided for identifying scenarios critical for the fire-induced collapse based on the availability of fuel loads and the extent of fire spread. Through the guidelines provided, buildings that are at a high-risk level to fire hazard can be determined and designed for fire-induced progressive collapse.

- Through proper design strategies, both from a structural and fire safety perspective, the onset of fire-induced collapse in steel framed buildings can be minimized and the fire performance of critical buildings can be enhanced.
- Advanced analysis at a system level is needed for tracing the fire-induced progressive collapse in critical buildings using the proposed guidelines. Through advanced analysis, the progression of instabilities at member and system levels leading to the progressive collapse of fire-exposed steel framed buildings can be traced with higher accuracy by incorporating critical factors such as specific fire scenarios including fire spread, material models for steel and concrete, high-temperature creep effects, altering load paths, and local buckling in steel members.

### 7 Conclusions

#### 7.1 General

The progressive collapse of buildings is a highly complex and dynamic phenomenon that gets triggered under extreme loading events such as earthquakes, blasts, fires, etc. Fire can occur as a primary event (e.g., electric short circuit) or secondary event (after an earthquake or blast) in buildings and can cause much more damage to the structure. Under severe fire exposure, structural members can experience temperature-induced instabilities leading to the partial or complete collapse of a building. Steel framed buildings are particularly vulnerable to fire-induced collapse due to the low thermal inertia and rapid degradation of strength and stiffness properties of steel with temperature rise. Additionally, steel members are likely to experience high levels of creep deformations and temperature-induced instabilities that can lead to an early onset of failure in structural members. Further, detachment of fire insulation can precipitate the onset of collapse in steel framed buildings.

Significant advances have been made over the past few decades in modeling the collapse mechanisms under extreme loading events such as impact, blast, and earthquakes. However, the fire resistance of steel structures is still evaluated using prescriptive or simplified approaches that do not account for several critical factors that influence the onset of instability in steel structures. Limited studies exist on the system level response of steel framed structures. In addition, very few models specifically trace the fire-induced collapse in steel framed buildings. Even these models do not provide due consideration to critical factors such as fire severity and fire spread, high-temperature creep, altering load paths, and local buckling. To overcome these knowledge gaps,

this dissertation presents a comprehensive study on the performance of steel framed buildings under fire conditions including fire-induced collapse.

Building fires pose a high threat to occupants and first responders and from the perspective of fire safety design in buildings, life safety is given primary importance. For this reason, the first part of this thesis focused on the role of structural stability in emergency evacuation strategies for high-rise buildings. The effect of varying egress parameters in a building on occupant evacuation times under ambient and fire conditions is evaluated. In addition, the influence of incorporating situational awareness in the fire evacuation process is quantified. These evacuation scenarios, in addition to the fire-induced progressive collapse timelines, can provide a more realistic evaluation of the required fire resistance ratings in steel framed buildings.

In the second part of the thesis, extensive numerical studies are carried out to quantify the effect of critical parameters influencing the onset of temperature-induced instabilities leading to the progressive collapse in steel framed buildings. As part of the numerical studies, a finite element-based model is developed in ABAQUS to trace the fire-induced progressive collapse in steel framed buildings. The model accounts for the high-temperature material properties in addition to temperature-induced creep effects, altering load paths, restraints, fire severity, fire spread, and local buckling effects. The validity of the model was established by comparing the response parameters with data available from fire tests carried out at member and system levels. The validated model was applied to carry out a series of parametric studies to quantify the effect of critical factors that influence the onset of fire-induced collapse in steel framed buildings. Results from the parametric study were used to develop guidance for undertaking advanced analysis of the fire-induced collapse and for mitigating the onset of fire-induced collapse in critical buildings.

## 7.2 Key findings

The key conclusions that can be drawn from the information presented in this thesis are as follows.

- The current design philosophy for the fire resistance evaluation of steel framed structures is based on a section or member level approach, without due consideration to the system level behavior of the structure. In addition, from a research perspective, there is a lack of data and understanding on the influence of critical factors including varying fire severities, fire spread, high-temperature creep, and local buckling on the onset of temperature-induced instabilities leading to the progressive collapse in steel framed buildings.
- For achieving the required fire safety in critical buildings, egress strategies and evacuation times are to be considered in conjunction with fire-induced progressive collapse scenarios and timelines. The evacuation times in high-rise buildings are highly influenced by the geometric characteristics of the egress paths including the number of stairways, their location, and width. The location (or placement) of stairways in a high-rise building is found to have the highest influence on the evacuation time. Under fire conditions, evacuation time is the highest when the fire occurs in the lower stories of the building. Incorporating situational awareness during an emergency evacuation can significantly improve the efficiency of evacuation and reduce the evacuation time.
- The proposed numerical model is capable of tracing the system level response of a steel framed building under fire conditions, including the onset of progressive collapse. The model accounts for various critical factors influencing the fire-induced collapse such as varying fire severity and fire spread, high-temperature properties of constituent materials, high-temperature creep, geometric nonlinearity, load redistribution, connection configurations, and local buckling of steel sections. The predictions of the model are in

close agreement with the thermal and structural response measurements from fire tests reported at member and system levels.

- Results generated from the parametric studies on the critical parameters influencing the onset of fire-induced instabilities (and progressive collapse) in steel framed structures infer:
  - The severity of the fire and the extent of fire spread in a building, high-temperature properties including creep, altering load paths, and temperature-induced local buckling effects are the most critical parameters that influence the onset of fire-induced collapse in a steel framed building.
  - Fire-induced collapse is unlikely when the burning is restricted to one compartment in a building. Under severe to very intense fire exposure, progressive collapse is triggered in the following scenarios: one, when the fire spreads to 25% of the floor area with burning on one floor, and the other, when the fire spreads to three stories with 15% of the floor area burning in each floor.
  - Neglecting the effect of high-temperature creep in the fire-induced progressive collapse analysis can result in the underestimation of global failure times. Hence, the full effects of creep need to be accounted for in the fire resistance analysis to obtain conservative failure predictions at member and system levels.
  - Neglecting the effect of temperature-induced local buckling (instabilities) can result in unconservative predictions of the time to collapse. The effect is especially more pronounced when columns of high slenderness are present in the fire-exposed compartments.
- Incorporating high-temperature creep in the progressive collapse analysis is critical for realizing reliable predictions; however, it is quite complex in practice and may not be

necessary for all scenarios. Hence, three recommendations are proposed for including the high-temperature creep effects in the fire resistance analysis (and fire-induced progressive collapse analysis) of steel structures, namely, ‘creep-not critical’, ‘creep-implicit’, and ‘creep-explicit’ based on the extent of creep that is expected to develop in a fire-exposed structure.

- A qualitative assessment is proposed for identifying buildings that are at high risk of a severe fire hazard that increases the susceptibility to fire-induced collapse. The proposed assessment, together with the available guidelines in GSA and UFC design documents for other extreme loading events can be applied to identify critical buildings for which design for progressive collapse is to be carried out.

### **7.3 Research impact**

Fire safety in buildings primarily involves meeting life safety objectives that require buildings to sustain the fire exposure for a given duration for facilitating the safe evacuation of occupants and first responders. During a severe fire incident, when there is a very short time for the occupants to evacuate the fire-damaged structure or for the first responders to undertake firefighting, preventing the onset of instabilities leading to the collapse of the structure becomes critical from the perspective of life safety. The information and guidelines developed as part of this research are to trace the onset of instabilities and mitigate the fire-induced collapse of critical buildings. Through these findings, this research advances fire safety in steel framed buildings.

The fire-induced progressive collapse in buildings is receiving significant attention from building owners, firefighters, and other emergency personnel due to several deaths and injuries of first responders that occurred during such collapses over the last few years. It is desired to develop systems that can predict the real-time response of structures during a fire incident such as the extent

of fire spread, deformations, and impending structural failure. Such information can point to vulnerable areas (or exit routes) in a building and can provide a future projection of the status of the building, which in turn can guide the evacuation process, and firefighting operations. The numerical model presented in this thesis is a first step toward developing such advanced systems for use in critical buildings.

The proposed numerical model can predict the behavior (and impending collapse) of the building under fire exposure provided the reliability of the input parameters such as fire spread scenarios and loading conditions at the time of the fire incident. The critical parameters to be considered in the fire-induced progressive collapse analysis are identified through extensive numerical studies. Furthermore, the guidelines proposed for tracing the onset of fire-induced instabilities and general recommendations for mitigating fire-induced collapse can aid designers to improve the fire resistance design of steel framed structures.

#### **7.4 Recommendations for future research**

While this thesis has advanced the state-of-the-art on the fire-induced progressive collapse of steel framed buildings through comprehensive numerical modeling of the fire response of steel framed buildings, there is still scope for further research in this area. The following are the key recommendations for future research in this area.

- The fire-induced progressive collapse mechanisms in a steel-framed building are quite complex and the numerical analyses presented in this thesis do not capture all possible scenarios in different steel framing systems. Further research is recommended to study the influence of other structural systems including mixed framing configurations (such as a combination of braced frames and moment frames or buildings with shear wall systems).

Other loading and fire scenarios including traveling fire scenarios, combined lateral load (wind) and fire, and post-earthquake fire scenarios can be examined.

- The numerical model can be improved to include the effect of delamination of fire insulation on the onset of instability (and fire-induced collapse) in steel framed structures.
- The approach for incorporating the full effects of high-temperature creep and local buckling was undertaken at a 2D frame level and the entire 3D building was not considered in these analyses. The model can be further extended to include creep and buckling phenomena in 3D building systems while tracing the fire-induced progressive collapse.
- The numerical model developed in this thesis does not specifically account for the effect of connection failures. The model can be extended to incorporate realistic connection models such as the use of component-based models with temperature-dependent axial and rotational stiffness in springs.
- Further experimental studies at a system level can be carried out to generate more data on the load redistributions and collapse mechanisms in steel framed structures.
- The proposed guidelines for identifying critical buildings for fire-induced collapse are preliminary and qualitative based on the limited studies carried out in this thesis. Further research is needed to develop quantitative measures, such as “fire-based importance factors” for critical buildings, which can be incorporated in guidance documents such as GSA or UFC documents.
- Situational awareness tools can be incorporated for developing efficient evacuation strategies during fire incidents.

## **APPENDICES**

## APPENDIX A

### Computation of Evacuation Time using the Hydraulic Model

This Appendix presents the calculations for evaluating the evacuation time of the building described in Chapter 3 using the hydraulic model. The computation of evacuation time is carried out using the following steps. Refer to Chapter 3 for the dimensions of the egress components.

i. Flow capacity of corridors:

Effective width,  $W_{e(\text{corridor})} = 1981 - (2 \times 152) = 1677 \text{ mm}$  (5.5 ft)

Density,  $D = 125 \text{ persons}/245 \text{ m}^2$  (125 persons/2635 ft<sup>2</sup>) corridor area  
 $= 0.51 \text{ persons}/\text{m}^2$  (0.047 persons/ft<sup>2</sup>)

As the density is less than 0.54 persons/m<sup>2</sup> (0.05 persons/ft<sup>2</sup>), all occupants will have a speed (S) of 1.19 m/s (235 ft/min) [45].

The specific flow for corridors is given by:

$F_{s(\text{corridor})} = SD = 0.607 \text{ persons}/\text{s}/\text{m}$  (11.139 persons/min/ft) effective width (governs)

Maximum specific flow,  $F_{sm(\text{corridor})} = 1.3 \text{ persons}/\text{s}/\text{m}$  (24 persons/min/ft) effective width [45]

Calculated flow for the corridors,  $F_{c(\text{corridor})} = F_{s(\text{corridor})} \times W_{e(\text{corridor})} \approx 61 \text{ persons}/\text{min}$

The calculated flow ( $F_{c(\text{corridor})}$ ) is an initial value for the corridors and can be sustained only if the next transition point (stairway doors) can accommodate this flow.

ii. Flow capacity of stairway doors:

Effective width,  $W_{e(\text{door})} = 813 - 305 = 508 \text{ mm}$  (20 in)

Specific flow,  $F_{s(\text{door})} = \frac{F_{s(\text{corridor})}W_{e(\text{corridor})}}{W_{e(\text{door})}} = \frac{0.607 \times 1677}{508}$   
 $= 2 \text{ persons}/\text{s}/\text{m}$  (36.76 persons/min/ft) effective width

The maximum specific flow for doors is given by:

$F_{sm(door)} = 1.3$  persons/s/m (24 persons/min/ft) effective width [45] (governs)

Calculated flow for the doors,  $F_{c(door)} = F_{sm(door)} \times W_{e(door)} \approx 40$  persons/min

As  $F_{c(door)} < F_{c(corridor)}$ , queuing of occupants occurs at the doorway entrance.

The rate of queue buildup is  $61 - 40 = 21$  persons/min

iii. Flow capacity of stairways:

Effective width,  $W_{e(stairs)} = 1118 - 305 = 813$  mm (32 in)

Specific flow,  $F_{s(stairs)} = \frac{F_{s(door)}W_{e(door)}}{W_{e(stairs)}} = \frac{1.3 \times 508}{813}$

= 0.822 persons/s/m (15.04 persons/min/ft) effective width (governs)

$F_{sm(stairs)} = 1.01$  persons/s/m (18.5 persons/min/ft) effective width [45]

Density,  $D = 1.1$  persons/m<sup>2</sup> (0.1 persons/ft<sup>2</sup>)

Speed,  $S = k - akD = 1.08 - 0.266 \times 1.08 \times 1.1 = 0.76$  m/s (149.6 ft/min)

Length of stairways on each floor,  $L_s = 9.67$  m (31.73 ft)

Time to descend from one floor to another is  $\left(\frac{9.67}{0.76}\right) = 0.21$  min (13s)

After 13s, 8 ( $\approx 0.21 \times 40$ ) occupants will be in each stairway to produce a total of 256 (=  $8 \times 32$ ) occupants on all the floors. The remaining 117 (=  $125 - 8$ ) occupants will remain in the queue in front of each stairway.

On each of the floors, merging of stairway flow and stairway entry flow occurs.

Merging flow,  $F_{s(out-stairs)} = \frac{[F_{s(door)}W_{e(door)} + F_{s(in-stairs)}W_{e(in-stairs)}]}{W_{e(in-stairs)}}$   
=  $\frac{(1.3 \times 508) + (0.822 \times 813)}{813} = 1.63$  persons/s/m (30.08 persons/min/ft) effective width

Maximum specific flow,  $F_{sm(stairs)} = 1.01$  persons/s/m (18.5 persons/min/ft) effective width [45] (governs)

iv. Calculation of evacuation time:

Under normal conditions, a duration of 0.5 min is assumed to be required for the flow of occupants to reach the stairway door [45]. This is a conservative estimate as the exit stairways are placed at an average distance of 22.86 m (75 ft) from all the occupants and the occupants are moving at a speed of 1.19 m/s (235 ft/min). At the end of 43s (30s + 13s), 256 occupants will occupy the stairways.

Time taken by the end of the flow to reach the 31<sup>st</sup> floor

$$= 43 + \left(\frac{117}{40}\right) \times 60 + 13 = 231.5 \text{ s}$$

Similarly, the time taken for the flow to reach each of the lower floors can be added to obtain the total time required for all the occupants to exit the building.

$$\text{Evacuation time} = 231.5 + \left[\left(\frac{117}{0.813 \times 1.01}\right) + 13\right] \times 31 = 5052 \text{ s (84.2 min)}$$

**Material Properties at Elevated Temperatures**

This Appendix provides a summary of the high-temperature material property relations used in the numerical model and parametric studies for concrete and steel.

**B.1 Concrete**

The equations presented in this section have been reproduced from Eurocode 2 [125].

***B.1.1 Specific heat***

For siliceous and calcareous aggregates, the specific heat,  $c_p(\theta)$  (J/kg K) is defined as:

$$c_p(\theta) = \begin{cases} 900, & 20^\circ\text{C} \leq \theta \leq 100^\circ\text{C} \\ 900 + (\theta - 100), & 100^\circ\text{C} < \theta \leq 200^\circ\text{C} \\ 1000 + (\theta - 200)/2, & 200^\circ\text{C} < \theta \leq 400^\circ\text{C} \\ 1100, & 400^\circ\text{C} < \theta \leq 1200^\circ\text{C} \end{cases}$$

***B.1.2 Thermal conductivity***

The thermal conductivity,  $\lambda_c$  (W/m K) is determined between the lower and upper limit values defined as follows.

Upper limit: For  $20^\circ\text{C} \leq \theta \leq 1200^\circ\text{C}$ ,

$$\lambda_c = 2 - 0.2451(\theta/100) + 0.0107(\theta/100)^2$$

Lower limit: For  $20^\circ\text{C} \leq \theta \leq 1200^\circ\text{C}$ ,

$$\lambda_c = 1.36 - 0.136(\theta/100) + 0.0057(\theta/100)^2$$

***B.1.3 Thermal expansion***

The thermal strain,  $\varepsilon_{c,th}(\theta)$  of concrete is determined using the following equations with respect to the length at  $20^\circ\text{C}$ .

For siliceous aggregates,

$$\varepsilon_{c,th}(\theta) = -1.8 \times 10^{-4} + 9 \times 10^{-6}\theta + 2.3 \times 10^{-11}\theta^3, \text{ for } 20^\circ\text{C} \leq \theta \leq 700^\circ\text{C}$$

$$\varepsilon_{c,th}(\theta) = 14 \times 10^{-3}, \text{ for } 700^\circ\text{C} < \theta \leq 1200^\circ\text{C}$$

For calcareous aggregates,

$$\varepsilon_{c,th}(\theta) = -1.2 \times 10^{-4} + 6 \times 10^{-6}\theta + 1.4 \times 10^{-11}\theta^3, \text{ for } 20^\circ\text{C} \leq \theta \leq 805^\circ\text{C}$$

$$\varepsilon_{c,th}(\theta) = 12 \times 10^{-3}, \text{ for } 805^\circ\text{C} < \theta \leq 1200^\circ\text{C}$$

#### **B.1.4 Stress-strain relations**

$$\sigma_c(\theta) = \frac{3\varepsilon_c f_{c,\theta}}{\varepsilon_{c1,\theta} \left( 2 + \left( \frac{\varepsilon_c}{\varepsilon_{c1,\theta}} \right)^3 \right)}, \varepsilon_c \leq \varepsilon_{c1,\theta}$$

For  $\varepsilon_{c1,\theta} < \varepsilon_c \leq \varepsilon_{cu1,\theta}$ , EC2 permits the use of either a linear or nonlinear descending branch for numerical purposes. The values of the main parameters used in the stress-strain relations are presented in Table B-1.

Table B-1: Values of main parameters used in the stress-strain relations of concrete

Concrete temperature, $\theta$ (°C)	Siliceous aggregates			Calcareous aggregates		
	$f_{c,\theta}/f_{ck}$	$\varepsilon_{c1,\theta}$	$\varepsilon_{cu1,\theta}$	$f_{c,\theta}/f_{ck}$	$\varepsilon_{c1,\theta}$	$\varepsilon_{cu1,\theta}$
20	1	0.0025	0.0200	1	0.0025	0.0200
100	1	0.0040	0.0225	1	0.0040	0.0225
200	0.95	0.0055	0.0250	0.97	0.0055	0.0250
300	0.85	0.0070	0.0275	0.91	0.0070	0.0275
400	0.75	0.0100	0.0300	0.85	0.0100	0.0300
500	0.6	0.0150	0.0325	0.74	0.0150	0.0325
600	0.45	0.0250	0.0350	0.60	0.0250	0.0350
700	0.3	0.0250	0.0375	0.43	0.0250	0.0375
800	0.15	0.0250	0.0400	0.27	0.0250	0.0400
900	0.08	0.0250	0.0425	0.15	0.0250	0.0425
1000	0.04	0.0250	0.0450	0.06	0.0250	0.0450
1100	0.01	0.0250	0.0475	0.02	0.0250	0.0475
1200	0.00	-	-	0.00	-	-

## B.2 Steel

The thermal and mechanical property relations presented in this section are reproduced from Eurocode 3 [18]. The creep properties are proposed by Venkatachari and Kodur [127].

### B.2.1 Specific heat

The specific heat,  $c_a(\theta_a)$  (J/kg K) of steel is defined as:

$$c_a(\theta_a) = \begin{cases} 425 + 7.73 \times 10^{-1}\theta_a - 1.69 \times 10^{-3}\theta_a^2 + 2.22 \times 10^{-6}\theta_a^3, & 20^\circ\text{C} \leq \theta_a < 600^\circ\text{C} \\ 666 + \frac{13002}{738 - \theta_a}, & 600^\circ\text{C} \leq \theta_a < 735^\circ\text{C} \\ 545 + \frac{17820}{\theta_a - 731}, & 735^\circ\text{C} \leq \theta_a < 900^\circ\text{C} \\ 650, & 900^\circ\text{C} \leq \theta_a \leq 1200^\circ\text{C} \end{cases}$$

### B.2.2 Thermal conductivity

The thermal conductivity,  $\lambda_a$  (W/m K) of steel is determined as follows.

$$\lambda_a = \begin{cases} 54 - 3.33 \times 10^{-2}\theta_a, & 20^\circ\text{C} \leq \theta_a < 800^\circ\text{C} \\ 27.3, & 800^\circ\text{C} \leq \theta_a \leq 1200^\circ\text{C} \end{cases}$$

### B.2.3 Thermal expansion

The relative thermal elongation of steel,  $\Delta l/l$  is determined from the following.

$$\Delta l/l = \begin{cases} 1.2 \times 10^{-5} + 0.4 \times 10^{-8}\theta_a^2 - 2.416 \times 10^{-4}, & 20^\circ\text{C} \leq \theta_a < 750^\circ\text{C} \\ 1.1 \times 10^{-2}, & 750^\circ\text{C} \leq \theta_a \leq 860^\circ\text{C} \\ 2 \times 10^{-5}\theta_a - 6.2 \times 10^{-3}, & 860^\circ\text{C} < \theta_a \leq 1200^\circ\text{C} \end{cases}$$

### B.2.4 Stress-strain relations

The constitutive relations for steel are defined as below.

$$\sigma_s(\theta_a) = \begin{cases} \varepsilon_s E_{s,\theta_a}, & \varepsilon_s \leq \varepsilon_{sp,\theta_a} \\ f_{sp,\theta_a} - c + (b/a) \left[ a^2 - (\varepsilon_{sy,\theta_a} - \varepsilon_s)^2 \right]^{0.5}, & \varepsilon_{sp,\theta_a} < \varepsilon_s < \varepsilon_{sy,\theta_a} \\ f_{sy,\theta_a}, & \varepsilon_{sy,\theta_a} \leq \varepsilon_s \leq \varepsilon_{st,\theta_a} \\ f_{sy,\theta_a} \left[ 1 - (\varepsilon_s - \varepsilon_{st,\theta_a}) / (\varepsilon_{su,\theta_a} - \varepsilon_{st,\theta_a}) \right], & \varepsilon_{st,\theta_a} < \varepsilon_s < \varepsilon_{su,\theta_a} \\ 0, & \varepsilon_s = \varepsilon_{su,\theta_a} \end{cases}$$

Parameters:

$$\varepsilon_{sp,\theta_a} = \frac{f_{sp,\theta_a}}{E_{s,\theta_a}} \quad \varepsilon_{sy,\theta_a} = 0.02 \quad \varepsilon_{st,\theta_a} = 0.15 \quad \varepsilon_{su,\theta_a} = 0.20$$

Functions:

$$a^2 = (\varepsilon_{sy,\theta_a} - \varepsilon_{sp,\theta_a})(\varepsilon_{sy,\theta_a} - \varepsilon_{sp,\theta_a} + c/E_{s,\theta_a})$$

$$b^2 = c(\varepsilon_{sy,\theta_a} - \varepsilon_{sp,\theta_a})E_{s,\theta_a} + c^2$$

$$c = \frac{(f_{sy,\theta_a} - f_{sp,\theta_a})^2}{(\varepsilon_{sy,\theta_a} - \varepsilon_{sp,\theta_a})E_{s,\theta_a} - 2(f_{sy,\theta_a} - f_{sp,\theta_a})}$$

The values of  $f_{sp,\theta_a}$ ,  $f_{sy,\theta_a}$ , and  $E_{s,\theta_a}$  used in the stress-strain relations are presented in Table B-2.

For temperatures below 400°C, the stress-strain relations including the strain-hardening region is used as follows:

$$\sigma_s(\theta_a) = \begin{cases} 50(f_{su,\theta_a} - f_{sy,\theta_a})\varepsilon_s + 2f_{sy,\theta_a} - f_{su,\theta_a}, & 0.02 < \varepsilon_s < 0.04 \\ f_{su,\theta_a}, & 0.04 \leq \varepsilon_s \leq 0.15 \\ f_{su,\theta_a}[1 - 20(\varepsilon_s - 0.15)], & 0.15 < \varepsilon_s < 0.20 \\ 0, & \varepsilon_s \geq 0.20 \end{cases}$$

The ultimate strength,  $f_{su,\theta_a}$  at elevated temperatures is determined by the following.

$$f_{su,\theta_a} = \begin{cases} 1.25f_{sy,\theta_a}, & \theta_a < 300^\circ\text{C} \\ f_{sy,\theta_a}(2 - 0.0025\theta_a), & 300^\circ\text{C} \leq \theta_a < 400^\circ\text{C} \\ f_{su,\theta_a}[1 - 20(\varepsilon_s - 0.15)], & \theta_a \geq 400^\circ\text{C} \end{cases}$$

Table B-2: Values of main parameters used in the stress-strain relations of steel

Steel temperature, $\theta_a$ (°C)	Reduction factors at temperature $\theta_a$ relative to the value of $f_{sy}$ and $E_s$ at 20°C		
	$f_{sy,\theta}/f_{sy}$	$f_{sp,\theta}/f_{sy}$	$E_{s,\theta}/E_s$
20	1	1	1
100	1	1	1
200	1	0.807	0.900
300	1	0.613	0.800
400	1	0.420	0.700
500	0.780	0.360	0.600
600	0.470	0.180	0.310
700	0.230	0.075	0.130
800	0.110	0.050	0.090
900	0.060	0.0375	0.0675
1000	0.040	0.0250	0.0450
1100	0.020	0.0125	0.0225
1200	0	0	0

**Illustration of Fire-Induced Progressive Collapse in a Steel Framed Building using  
Advanced Analysis – Numerical Example**

This appendix presents a working example illustrating the application of the advanced analysis for tracing the fire-induced progressive collapse in a steel framed building. The steel framed building described in Chapter 5 is utilized for this example. The building is subjected to dead and live loads as per ASCE 7-16 [122] provisions for office buildings. In addition, the building is exposed to a design fire scenario, DF 1 that spreads horizontally at an interval of 45 min on floor 1. Figure C.1 shows the fire spread pattern and the design fire exposure scenario used in this example. SFRM-type fire insulation with a rating of 2 h is applied to all steel members.

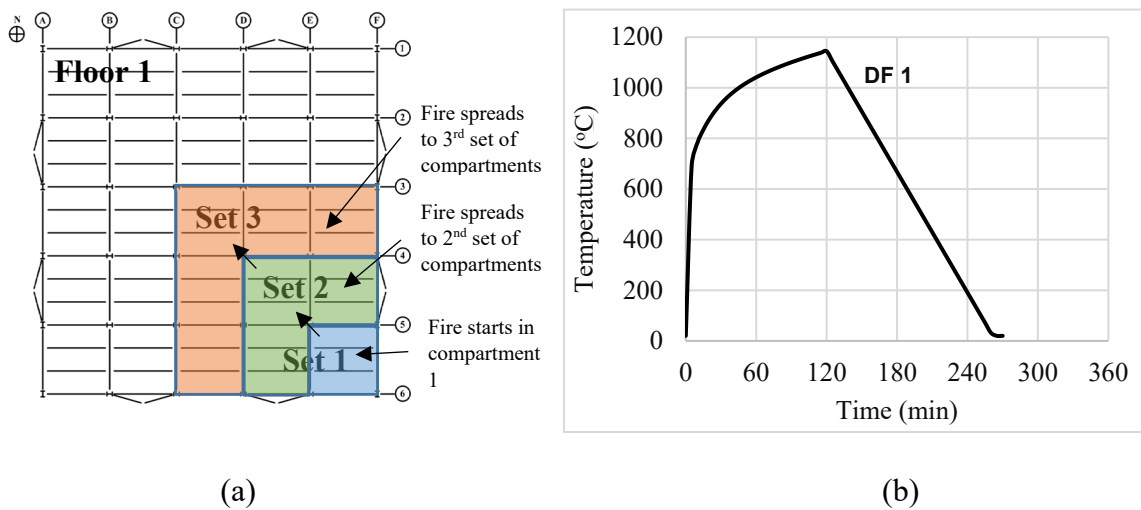


Figure C.1. (a) Fire spread pattern and (b) design fire exposure scenario.

**C.1 Determination of fire temperatures**

At each time step, the fire temperatures in different compartments are established based on the design fire curves shown in Figure C.2. The design fire curve, DF 1 is displaced at a 45 min interval to obtain the temperatures in different sets of compartments as the fire spreads horizontally through floor 1.

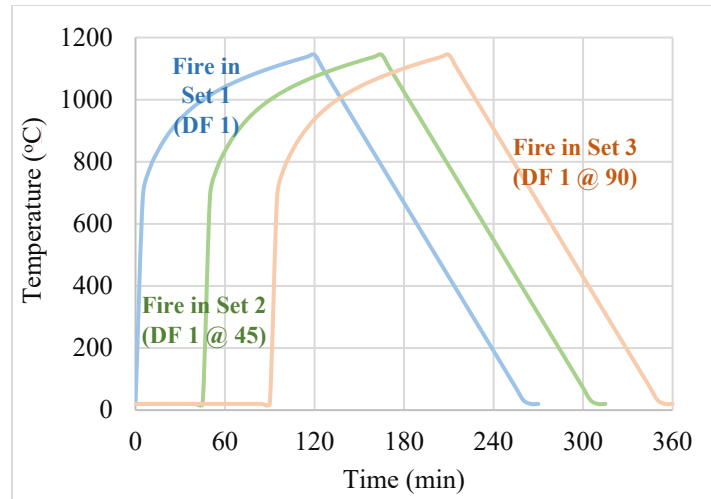


Figure C.2. Time-temperature curves for the design fire exposure scenario with horizontal spread used in the analysis.

## C.2 Thermal analysis

The cross-sectional temperatures of structural members located in the fire-exposed compartments of the building are evaluated using the heat transfer analysis carried out for each member at the mid-section. The fire temperatures and boundary conditions that are to be applied to each member are determined based on the location of the member in the fire-exposed compartment. For example, Figure C.3 shows the fire-exposure conditions for an interior column (E5) and an interior beam (E-5-6). Column E5 and beam E-5-6, which are located at the boundary of compartments in Set 1 and Set 2, are subjected partly to fire temperatures following ‘DF 1’ and partly to fire temperatures following ‘DF 1 @ 45’. The unexposed face of the slab in the composite beam (E-5-6) is subjected to ambient conditions. Figure C.4 and Figure C.5 show the sectional temperatures in these members as a function of fire exposure time. The sectional temperatures are plotted for 5 specific points in the cross-section of each member, which will be utilized to define the thermal loads in the structural model.

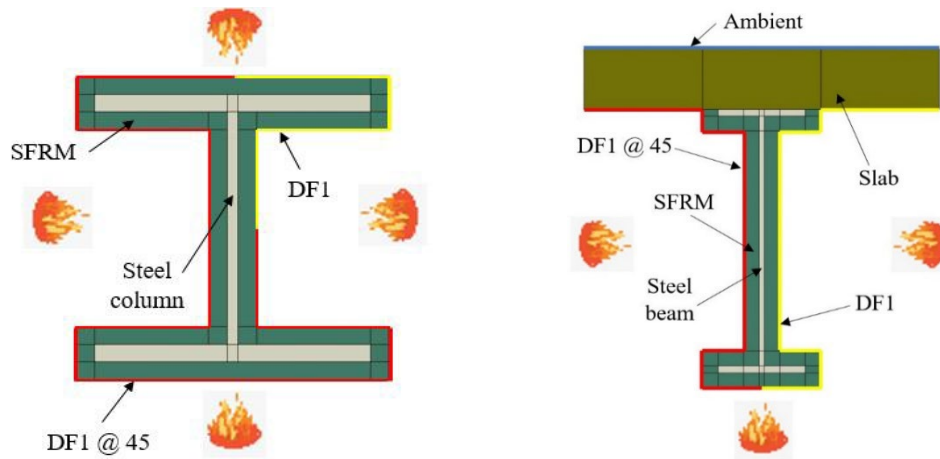


Figure C.3. Fire exposure conditions for (a) an interior column (E5) and (b) an interior beam (E-5-6).

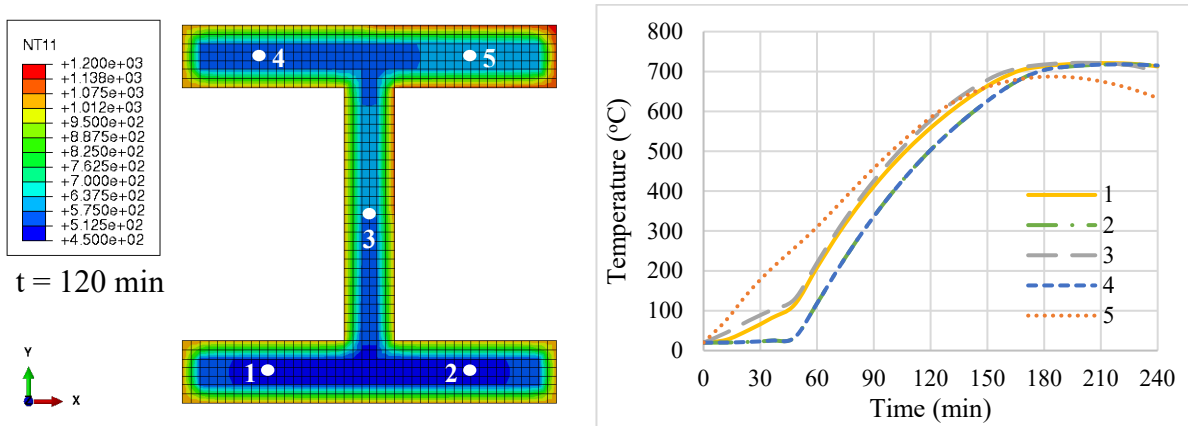


Figure C.4. Sectional temperatures in the interior column E5 as a function of fire exposure time.

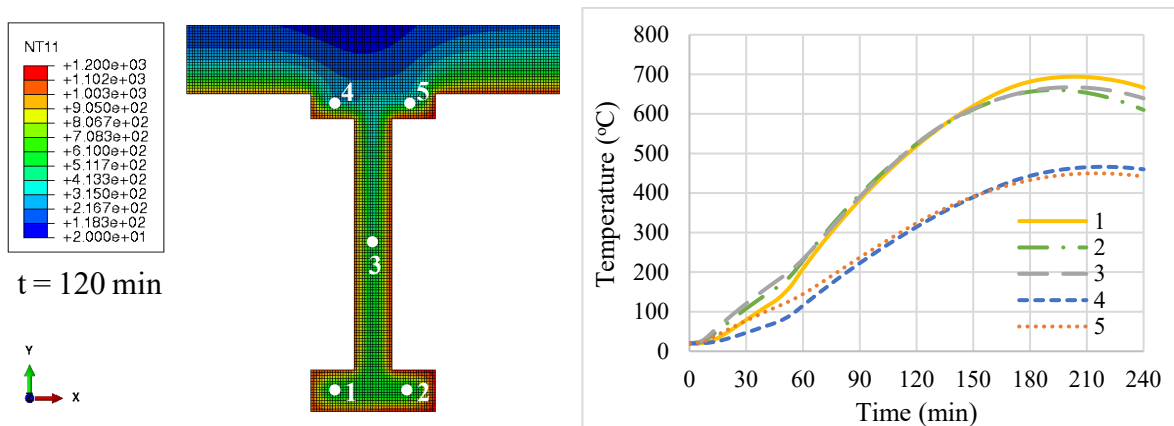


Figure C.5. Sectional temperatures in the interior beam E-5-6 as a function of fire exposure time.

### C.3 Structural analysis

The fire-induced progressive collapse analysis of the steel framed building is carried out using the nonlinear dynamic explicit analysis. The entire building, including the floor slabs and transverse framing, is discretized as discussed in Chapter 4. Two loading sequences are utilized. In the first sequence, the gravity loads, corresponding to  $1.2 \text{ DL} + 1.2 \text{ LL}$  are applied to the structural members. Additionally, system imperfections are incorporated through the application of notional lateral loads at each floor level corresponding to 0.2% of the gravity loads on the corresponding floor. In the second loading sequence, the sectional temperatures obtained from the thermal model are applied to the fire-exposed structural members as predefined fields. The structural response, including the stresses, displacements, and deformed shape of the building is traced continuously throughout the fire exposure time.

Figure C.6 shows the deformed shape of the building at 60 min, 120 min, 140 min, and 154 min of fire exposure. Before 60 min, the deformations measured at various points in the building were minimal. At 60 min, 15 min after the fire has spread to the second set of compartments, the deformations in the structural members become evident in Set 1 and Set 2 compartments. At 120 min, 10 min after the fire has spread to the third set of compartments, column E5 has buckled and the other columns in Set 1 also begin to experience instability. At this stage, the deformations in the floor slabs and beams are also significant. At 140 min, several columns in Set 1 and Set 2 compartments have failed. Additionally, significant deformations can be observed in the higher stories (especially floors 2 and 3). Finally, at 150 min, most of the columns in the fire-exposed compartments have buckled, and global instability sets in. Figure C.7 shows the lateral displacement of the building evaluated at the top story level. Progressive collapse initiates at 154 min according to the rate of lateral displacement criteria for system level failure.

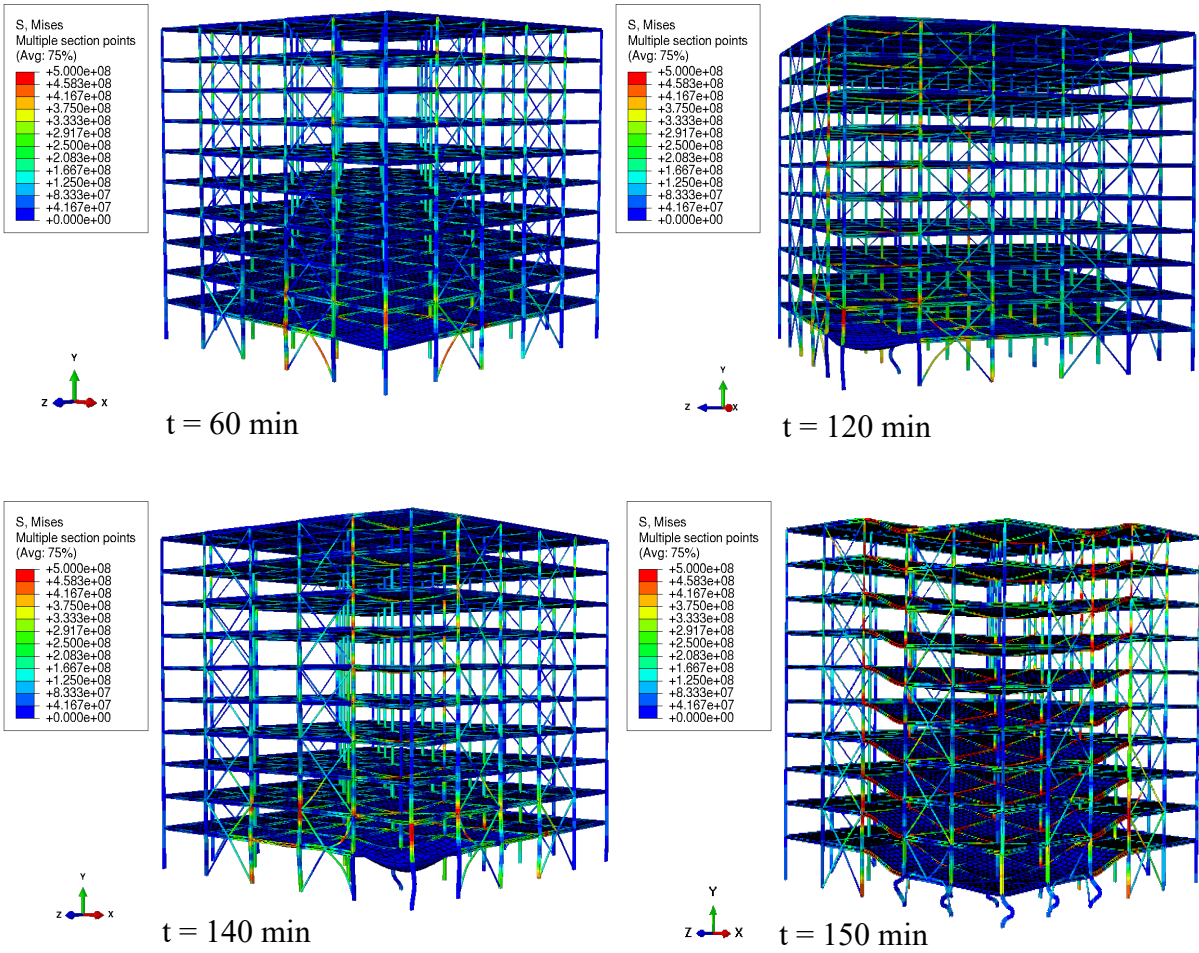


Figure C.6. Deformed shape of the building at different fire exposure times.

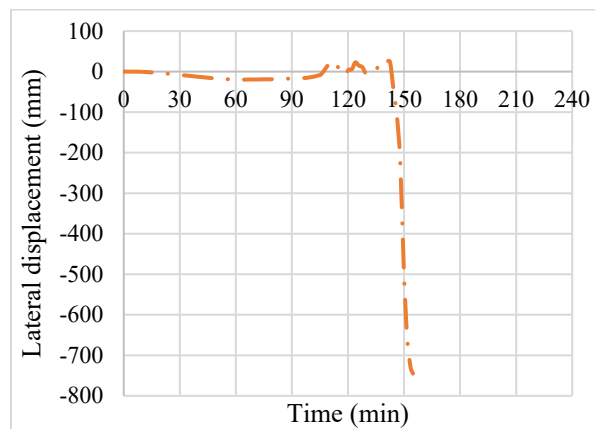


Figure C.7. Lateral displacement at the top story of the building as a function of fire exposure time.

## REFERENCES

## REFERENCES

- [1] V. Kodur, M. Naser, *Structural Fire Engineering*, McGraw Hill Professional, New York, NY, USA, 2020.
- [2] W. Wang, V. Kodur, Chapter 5 - Creep behavior of steels at elevated temperatures, in: *Material Properties of Steel in Fire Conditions*, Academic Press, Cambridge, MA, USA, 2020: pp. 261–343.
- [3] B. Behnam, Fire structural response of the plasco building: A preliminary investigation report, *International Journal of Civil Engineering*. 17 (2019) 563–580.
- [4] C. Bailey, *Case Studies: Historical Fires: Windsor Tower Fire, One Stop Shop in Structural Fire Engineering*. (2021).  
[https://www.911research.wtc7.net/~nin11levi/911research/cache/wtc/analysis/compare/manchester\\_windsortower.html](https://www.911research.wtc7.net/~nin11levi/911research/cache/wtc/analysis/compare/manchester_windsortower.html) (accessed March 17, 2021).
- [5] S. Shyam-Sunder, R.G. Gann, W.L. Grosshandler, H.S. Lew, R.W. Bukowski, F. Sadek, F. Gayle, *Federal Building and Fire Safety Investigation of the World Trade Center Disaster: Final Report of the National Construction Safety Team on the Collapses of the World Trade Center Towers (NIST NCSTAR 1)*, 2005. <https://www.nist.gov/publications/federal-building-and-fire-safety-investigation-world-trade-center-disaster-final-report> (accessed December 3, 2018).
- [6] S. Shyam-Sunder, R.G. Gann, W.L. Grosshandler, H.S. Lew, R.W. Bukowski, F. Sadek, F. Gayle, *Federal Building and Fire Safety Investigation of the World Trade Center Disaster: Final Report of the Collapse of the World Trade Center Building 7 (NIST NCSTAR 1A)*, 2005. <https://nvlpubs.nist.gov/nistpubs/legacy/NCSTAR/ncstar1a.pdf>.
- [7] T. McAllister, G. Corley, R. Hamburger, W. Baker, J. Barnett, R. Gilsanz, R. Smilowitz, J. Milke, J. Fisher, E.M. DePaola, *World Trade Center Building Performance Study: Data collection, Preliminary Observations, and Recommendations (FEMA 403)*, ASCE/FEMA, New York, 2002. <https://www.fema.gov/media-library/assets/documents/3544> (accessed July 3, 2019).
- [8] V.K.R. Kodur, M.M.S. Dwaikat, Effect of high temperature creep on the fire response of restrained steel beams, *Mater Struct*. 43 (2010) 1327–1341. <https://doi.org/10.1617/s11527-010-9583-y>.
- [9] S.E. Quiel, M.E.M. Garlock, M.M.S. Dwaikat, V.K.R. Kodur, Predicting the demand and plastic capacity of axially loaded steel beam–columns with thermal gradients, *Engineering Structures*. 58 (2014) 49–62. <https://doi.org/10.1016/j.engstruct.2013.10.005>.

- [10] E.I. Wellman, A.H. Varma, R. Fike, V. Kodur, Experimental evaluation of thin composite floor assemblies under fire loading, *Journal of Structural Engineering*. 137 (2011) 1002–1016. [https://doi.org/10.1061/\(ASCE\)ST.1943-541X.0000451](https://doi.org/10.1061/(ASCE)ST.1943-541X.0000451).
- [11] A. Agarwal, L. Choe, A.H. Varma, Fire design of steel columns: Effects of thermal gradients, *Journal of Constructional Steel Research*. 93 (2014) 107–118. <http://dx.doi.org/10.1016/j.jcsr.2013.10.023>.
- [12] R. Sun, Z. Huang, I.W. Burgess, Progressive collapse analysis of steel structures under fire conditions, *Engineering Structures*. 34 (2012) 400–413. <https://doi.org/10.1016/j.engstruct.2011.10.009>.
- [13] A. Agarwal, A.H. Varma, Fire induced progressive collapse of steel building structures: The role of interior gravity columns, *Engineering Structures*. 58 (2014) 129–140. <https://doi.org/10.1016/j.engstruct.2013.09.020>.
- [14] J. Jiang, G.-Q. Li, A. Usmani, Effect of Bracing Systems on Fire-Induced Progressive Collapse of Steel Structures Using OpenSees, *Fire Technol*. 51 (2015) 1249–1273. <https://doi.org/10.1007/s10694-014-0451-0>.
- [15] T.T.H. Nguyen, *Composite Framed Buildings under Fire-Induced Progressive Collapse: Computational Analysis and Design Recommendations*, University of Michigan, 2017.
- [16] E. Rackauskaite, P. Kotsovinos, A. Jeffers, G. Rein, Structural analysis of multi-storey steel frames exposed to travelling fires and traditional design fires, *Engineering Structures*. 150 (2017) 271–287. <https://doi.org/10.1016/j.engstruct.2017.06.055>.
- [17] C. Qin, H. Mahmoud, Collapse performance of composite steel frames under fire, *Engineering Structures*. 183 (2019) 662–676. <https://doi.org/10.1016/j.engstruct.2019.01.032>.
- [18] CEN (European Standards Committee), *Eurocode 3-Design of Steel Structures, Part 1-2: General Rules for Structural Fire Design*, EN 1993-1-2, Brussels, Belgium, 2005.
- [19] J.A. Purkiss, L.-Y. Li, *Fire Safety Engineering Design of Structures*, Third Edition, CRC Press, London, UK, 2013.
- [20] K.D. Thompson, *Fire Dynamics*, NIST. (2010). <https://www.nist.gov/el/fire-research-division-73300/firegov-fire-service/fire-dynamics> (accessed August 27, 2018).
- [21] M. Ahrens, B. Evarts, *Fire Loss in the United States During 2019*, National Fire Protection Association (NFPA), Quincy, MA, USA, 2020.
- [22] M.J. Hurley, E.R. Rosenbaum, *The SFPE Guide to Performance-Based Fire Safety Design*, 2nd ed., SFPE, Gaithersburg, MD, USA, 2015.

- [23] M.Z. Naser, V.K.R. Kodur, Cognitive infrastructure - a modern concept for resilient performance under extreme events, *Automation in Construction*. 90 (2018) 253–264. <https://doi.org/10.1016/j.autcon.2018.03.004>.
- [24] N. Daniel, G. Rein, *The fire navigator: forecasting the spread of building fires on the basis of sensor data*, FPE extra issue 3, Society of Fire Protection Engineers (SFPE), Gaithersburg, MD, USA, 2016.
- [25] ASTM (American Society for Testing and Materials), *Standard methods of fire test of building construction and materials*, ASTM E119-19, West Conshohocken, PA, USA, 2019.
- [26] K. Khandelwal, S. El-Tawil, F. Sadek, Progressive collapse analysis of seismically designed steel braced frames, *Journal of Constructional Steel Research*. 65 (2009) 699–708. <https://doi.org/10.1016/j.jcsr.2008.02.007>.
- [27] ASTM (American Society for Testing and Materials), *Standard Test Methods for Determining Effects of Large Hydrocarbon Pool Fires on Structural Members and Assemblies*, ASTM E1529-14a, West Conshohocken, PA, USA, 2014.
- [28] ISO (International Organization for Standardization), *Fire resistance tests-elements of building construction*, ISO-834, Geneva, Switzerland, 1999.
- [29] M.A. Morovat, M.D. Engelhardt, T.A. Helwig, E.M. Taleff, High-Temperature Creep Buckling Phenomenon of Steel Columns Subjected to Fire, *Journal of Structural Fire Engineering*. 5 (2014) 189–202. <https://doi.org/10.1260/2040-2317.5.3.189>.
- [30] V.K. Kodur, E.M. Aziz, Effect of temperature on creep in ASTM A572 high-strength low-alloy steels, *Materials and Structures*. 48 (2015) 1669–1677. <https://doi.org/10.1617/s11527-014-0262-2>.
- [31] G.-Q. Li, C. Zhang, Creep effect on buckling of axially restrained steel columns in real fires, *Journal of Constructional Steel Research*. 71 (2012) 182–188. <https://doi.org/10.1016/j.jcsr.2011.09.006>.
- [32] E.G. Hantouche, K.K. Al Khatib, M.A. Morovat, Modeling creep of steel under transient temperature conditions of fire, *Fire Safety Journal*. 100 (2018) 67–75. <https://doi.org/10.1016/j.firesaf.2018.07.006>.
- [33] V. Kodur, M. Naser, Effect of local instability on capacity of steel beams exposed to fire, *Journal of Constructional Steel Research*. 111 (2015) 31–42. <https://doi.org/10.1016/j.jcsr.2015.03.015>.
- [34] H. Chen, J. Liew, Explosion and fire analysis of steel frames using mixed element approach, *Journal of Engineering Mechanics*. 131 (2005) 606–616. [https://doi.org/10.1061/\(ASCE\)0733-9399\(2005\)131:6\(606\)](https://doi.org/10.1061/(ASCE)0733-9399(2005)131:6(606)).

- [35] M. Seif, T. McAllister, Stability of wide flange structural steel columns at elevated temperatures, *Journal of Constructional Steel Research*. 84 (2013) 17–26.  
<https://doi.org/10.1016/j.jcsr.2013.02.002>.
- [36] ASCE (American Society of Civil Engineers), SFPE (Society of Fire Protection Engineers), Standard Calculation Methods for Structural Fire Protection, SEI/ASCE/SFPE 29-99, Reston, VA, USA, 2003.
- [37] AISC (American Institute of Steel Construction), Specifications for structural steel buildings, ANSI/AISC 360-16, Chicago, IL, USA, 2016.
- [38] H. Shakib, M. Zakersalehi, V. Jahangiri, R. Zamanian, Evaluation of Plasco Building fire-induced progressive collapse, *Structures*. 28 (2020) 205–224.  
<https://doi.org/10.1016/j.istruc.2020.08.058>.
- [39] T. Yarlagadda, H. Hajiloo, L. Jiang, M. Green, A. Usmani, Preliminary modelling of Plasco tower collapse, *Int J High-Rise Build*. 7 (2018) 397–408.  
<http://dx.doi.org/10.21022/IJHRB.2018.7.4.397>.
- [40] R. Angle, D. Barnum, D. Chandler, T. Szamboti, T. Walter, Y. Seyyedi, The plasco building collapse in tehran, *Architects & Engineers for 9/11 Truth*, 2017.
- [41] Z.P. Bažant, Y. Zhou, Why did the world trade center collapse?—Simple analysis, *Journal of Engineering Mechanics*. 128 (2002) 2–6.  
[https://doi.org/10.1061/\(ASCE\)0733-9399\(2002\)128:1\(2\)](https://doi.org/10.1061/(ASCE)0733-9399(2002)128:1(2)).
- [42] G. Flint, A. Usmani, S. Lamont, B. Lane, J. Torero, Structural response of tall buildings to multiple floor fires, *Journal of Structural Engineering*. 133 (2007) 1719–1732.  
[https://doi.org/10.1061/\(ASCE\)0733-9445\(2007\)133:12\(1719\)](https://doi.org/10.1061/(ASCE)0733-9445(2007)133:12(1719)).
- [43] V.K.R. Kodur, Role of fire resistance issues in the first ever collapse of a steel-framed building - WTC 7, CIB World Building Congress, Toronto, Canada, 2004.
- [44] J.J. Beitel, N. Iwankiw, Analysis of needs and existing capabilities for full-scale fire resistance testing, National Institute of Standards and Technology, Gaithersburg, MD, USA, 2008.
- [45] Morgan J Hurley, D.T. Gottuk, J.R. Hall Jr, K. Harada, E.D. Kuligowski, M. Puchovsky, J.M. Watts Jr, C.J. Wieczorek, eds., *SFPE Handbook of Fire Protection Engineering*, 5th ed., Springer, New York, NY, USA, 2015.
- [46] E.D. Kuligowski, Review of 28 Egress Models, National Institute of Standards and Technology (NIST), Gaithersburg, MD, USA, 2004.

- [47] E. Ronchi, E.D. Kuligowski, P.A. Reneke, R.D. Peacock, D. Nilsson, *The Process of Verification and Validation of Building Fire Evacuation Models*, National Institute of Standards and Technology, Gaithersburg, MD, 2013.  
<https://doi.org/10.6028/NIST.TN.1822>.
- [48] E. Ronchi, D. Nilsson, Modelling total evacuation strategies for high-rise buildings, *Building Simulation*. 7 (2014) 73–87. <https://doi.org/10.1007/s12273-013-0132-9>.
- [49] A. Soltanzadeh, M. Alaghmandan, H. Soltanzadeh, Performance evaluation of refuge floors in combination with egress components in high-rise buildings, *Journal of Building Engineering*. 19 (2018) 519–529. <https://doi.org/10.1016/j.jobe.2018.05.029>.
- [50] L. Yang, S.H. Yang, L. Plotnick, How the internet of things technology enhances emergency response operations, *Technological Forecasting and Social Change*. 80 (2013) 1854–1867.  
<https://doi.org/10.1016/j.techfore.2012.07.011>.
- [51] F. Peña-Mora, J. Son, Z. Aziz, Supporting disaster response and recovery through improved situation awareness, *Structural Survey*. 26 (2008) 411–425.  
<https://doi.org/10.1108/02630800810922757>.
- [52] M.M.S. Dwaikat, V.K.R. Kodur, S.E. Quiel, M.E.M. Garlock, Experimental behavior of steel beam–columns subjected to fire-induced thermal gradients, *Journal of Constructional Steel Research*. 67 (2011) 30–38. <https://doi.org/10.1016/j.jcsr.2010.07.007>.
- [53] V. Vimonsatit, K. Tan, Z. Qian, Testing of plate girder web panel loaded in shear at elevated temperature, *Journal of Structural Engineering*. 133 (2007) 815–824.  
[https://doi.org/10.1061/\(ASCE\)0733-9445\(2007\)133:6\(815\)](https://doi.org/10.1061/(ASCE)0733-9445(2007)133:6(815)).
- [54] V. Kodur, R. Fike, Guidelines for improving the standard fire resistance test specifications, in: *Advances in the State of the Art of Fire Testing*, ASTM International, West Conshohocken, PA, USA, 2010.
- [55] D.E. Wainman, B.R. Kirby, Compendium of U.K. standard fire test data on unprotected structural steel–1, Rep. No.RS/RSC/S10328/1/87/B, British Steel Corporation, Rotherham, UK, 1988.
- [56] D.E. Wainman, B.R. Kirby, Compendium of U.K. standard fire test data on unprotected structural steel–2, Rep. No.RS/R/S1199/8/88/B, British Steel Corporation, Rotherham, UK, 1989.
- [57] B. Zhao, J. Kruppa, Fire Resistance of Composite Slabs with Profiled Steel Sheet and Composite Steel Concrete Beams, Part 2: Composite Beams, Final Report, ECSC – agreement No. 7210 SA 509, CTISM, France, 1995.

- [58] E.I. Wellman, A.H. Varma, R. Fike, V. Kodur, Experimental evaluation of thin composite floor assemblies under fire loading, *Journal of Structural Engineering*. 137 (2011) 1002–1016. [https://doi.org/10.1061/\(ASCE\)ST.1943-541X.0000451](https://doi.org/10.1061/(ASCE)ST.1943-541X.0000451).
- [59] SteelConstruction.info, Cardington fire test data, SteelConstruction.Info. (2019). [https://www.steelconstruction.info/Cardington\\_fire\\_test\\_data](https://www.steelconstruction.info/Cardington_fire_test_data) (accessed May 10, 2019).
- [60] Y.C. Wang, V.K.R. Kodur, Research Toward Use of Unprotected Steel Structures, *Journal of Structural Engineering*. 126 (2000) 1442–1450. [https://doi.org/10.1061/\(ASCE\)0733-9445\(2000\)126:12\(1442\)](https://doi.org/10.1061/(ASCE)0733-9445(2000)126:12(1442)).
- [61] C.G. Bailey, T. Lennon, D.B. Moore, The behaviour of full-scale steel-framed buildings subjected to compartment fires, *The Structural Engineer*. 77 (1999) 15–21.
- [62] B. Kirby, Large Scale Fire Tests: The British Steel European Collaborative Research Programme On The Bre 8-storey Frame, *Fire Safety Science*. 5 (1997) 1129–1140. <https://doi.org/10.3801/IAFSS.FSS.5-1129>.
- [63] G.M. Newman, J.T. Robinson, C.G. Bailey, Fire safe design: A new approach to multi-storey steel-framed buildings, Steel Construction Institute Ascot, London, UK, 2000.
- [64] J. Zhao, Z. Shen, Experimental studies of the behaviour of unprotected steel frames in fire, *Journal of Constructional Steel Research*. 50 (1999) 137–150. [https://doi.org/10.1016/S0143-974X\(98\)00246-6](https://doi.org/10.1016/S0143-974X(98)00246-6).
- [65] K.-C. Yang, H.-H. Lee, O. Chan, Experimental study of fire-resistant steel H-columns at elevated temperature, *Journal of Constructional Steel Research*. 62 (2006) 544–553. <https://doi.org/10.1016/j.jcsr.2005.09.008>.
- [66] J.R. Liew, L. Tang, T. Holmaas, Y. Choo, Advanced analysis for the assessment of steel frames in fire, *Journal of Constructional Steel Research*. 47 (1998) 19–45. [https://doi.org/10.1016/S0143-974X\(98\)80004-7](https://doi.org/10.1016/S0143-974X(98)80004-7).
- [67] H.M. Ali, P.E. Senseny, R.L. Alpert, Lateral displacement and collapse of single-story steel frames in uncontrolled fires, *Engineering Structures*. 26 (2004) 593–607. <https://doi.org/10.1016/j.engstruct.2003.12.007>.
- [68] J.C. Rodrigues, I.C. Neves, J. Valente, Experimental research on the critical temperature of compressed steel elements with restrained thermal elongation, *Fire Safety Journal*. 35 (2000) 77–98. [http://dx.doi.org/10.1016/S0379-7112\(00\)00018-7](http://dx.doi.org/10.1016/S0379-7112(00)00018-7).
- [69] Y. Dong, K. Prasad, Experimental study on the behavior of full-scale composite steel frames under furnace loading, *Journal of Structural Engineering*. 135 (2009) 1278–1289. [https://doi.org/10.1061/\(ASCE\)0733-9445\(2009\)135:10\(1278\)](https://doi.org/10.1061/(ASCE)0733-9445(2009)135:10(1278)).

- [70] Y. Dong, E. Zhu, K. Prasad, Thermal and structural response of two-storey two-bay composite steel frames under furnace loading, *Fire Safety Journal*. 44 (2009) 439–450. <http://dx.doi.org/10.1016/j.firesaf.2008.09.005>.
- [71] Dong Yu-Li, Peng Xing-Qian, Fang Yuan-Yuan, Zhang Da-Shan, Behavior of Sway Two-Bay, Two-Story Composite Steel Frames in Fire, *Journal of Structural Engineering*. 142 (2016) 04015119. [https://doi.org/10.1061/\(ASCE\)ST.1943-541X.0001369](https://doi.org/10.1061/(ASCE)ST.1943-541X.0001369).
- [72] R. Sun, Z. Huang, I.W. Burgess, The collapse behaviour of braced steel frames exposed to fire, *Journal of Constructional Steel Research*. 72 (2012) 130–142. <https://doi.org/10.1016/j.jcsr.2011.11.008>.
- [73] D. Lange, C. Röben, A. Usmani, Tall building collapse mechanisms initiated by fire: Mechanisms and design methodology, *Engineering Structures*. 36 (2012) 90–103. <https://doi.org/10.1016/j.engstruct.2011.10.003>.
- [74] T. Gernay, A. Gamba, Progressive collapse triggered by fire induced column loss: Detrimental effect of thermal forces, *Engineering Structures*. 172 (2018) 483–496. <https://doi.org/10.1016/j.engstruct.2018.06.060>.
- [75] A. Usmani, C. Roben, A. Al-Remal, A very simple method for assessing tall building safety in major fires, *International Journal of Steel Structures*. 9 (2009) 17–28. <https://doi.org/10.1007/BF03249476>.
- [76] E. Rackauskaite, C. Hamel, A. Law, G. Rein, Improved formulation of travelling fires and application to concrete and steel structures, *Structures*. 3 (2015) 250–260. <https://doi.org/10.1016/j.istruc.2015.06.001>.
- [77] CEN (European Standards Committee), Eurocode 1: Actions on structures - Part 1-2: General actions - Actions on structures exposed to fire, EN 1991-1-2, Brussels, Belgium, 2002.
- [78] SFPE (Society of Fire Protection Engineers), Calculating Fire Exposures to Structures, S.01, Gaithersburg, MD, USA, 2011.
- [79] H. Nguyen, A.E. Jeffers, V. Kodur, Computational simulation of steel moment frame to resist progressive collapse in fire, *Journal of Structural Fire Engineering*. 7 (2016) 286–305. <https://doi.org/10.1108/JSFE-12-2016-020>.
- [80] K. Poh, Stress-strain-temperature relationship for structural steel, *Journal of Materials in Civil Engineering*. 13 (2001) 371–379. [https://doi.org/10.1061/\(ASCE\)0899-1561\(2001\)13:5\(371\)](https://doi.org/10.1061/(ASCE)0899-1561(2001)13:5(371)).
- [81] Y. Anderberg, Modelling steel behaviour, *Fire Safety Journal*. 13 (1988) 17–26. [https://doi.org/10.1016/0379-7112\(88\)90029-X](https://doi.org/10.1016/0379-7112(88)90029-X).

- [82] G. Williams-Leir, Creep of structural steel in fire: Analytical expressions, *Fire and Materials*. 7 (1983) 73–78. <https://doi.org/10.1002/fam.810070205>.
- [83] J.L. Rempe, D.L. Knudson, High temperature thermal properties for metals used in LWR vessels, *Journal of Nuclear Materials*. 372 (2008) 350–357. <https://doi.org/10.1016/j.jnucmat.2007.03.268>.
- [84] D.P. Bentz, K. Prasad, Thermal Performance of Fire Resistive Materials: I. Characterization with Respect to Thermal Performance Models | NIST, (2007). <https://doi.org/10.6028/NIST.IR.7401>.
- [85] Y.S. Touloukian, D.P. DeWitt, *Thermal Radiative Properties - Nonmetallic Solids*, Springer, New York, NY, USA, 1972.
- [86] R.W. Powell, R.P. Tye, High alloy steels for use as a thermal conductivity standard, *British Journal of Applied Physics*. 11 (1960) 195.
- [87] Yawata Iron and Steel Co. Ltd., WEL-TEN 80, Data sheets for WEL-TEN 80 steel, Japan, 1969.
- [88] V. Kodur, M. Dwaikat, R. Fike, High-temperature properties of steel for fire resistance modeling of structures, *Journal of Materials in Civil Engineering*. 22 (2010) 423–434. [https://doi.org/10.1061/\(ASCE\)MT.1943-5533.0000041](https://doi.org/10.1061/(ASCE)MT.1943-5533.0000041).
- [89] M.F. Ashby, H. Shercliff, D. Cebon, *Materials: Engineering, Science, Processing and Design*, 4th ed., Butterworth-Heinemann, Oxford, UK, 2018.
- [90] M. Fujimoto, F. Furumura, T. Ave, Y. Shinohara, Primary creep of structural steel (SS 41) at high temperatures, *Transactions of the Architectural Institute of Japan*. 296 (1980) 145–157.
- [91] J. Brnic, G. Turkalj, M. Canadija, D. Lanc, Creep behavior of high-strength low-alloy steel at elevated temperatures, *Materials Science and Engineering: A*. 499 (2009) 23–27. <https://doi.org/10.1016/j.msea.2007.08.102>.
- [92] M.A. Morovat, J.W. Lee, M.D. Engelhardt, E.M. Taleff, T.A. Helwig, V.A. Segrest, Creep properties of ASTM A992 steel at elevated temperatures, in: *Trans Tech Publ*, 2012: pp. 786–792.
- [93] J. Lee, *Elevated-Temperature Properties of ASTM A992 Steel for Structural-Fire Engineering Analysis*, The University of Texas at Austin, Austin, TX, USA, 2012.
- [94] T.Z. Harmathy, A Comprehensive Creep Model, *Journal of Basic Engineering*. 89 (1967) 496–502. <https://doi.org/10.1115/1.3609648>.

- [95] B.A. Fields, R.J. Fields, Elevated Temperature Deformation of Structural Steel: Report NISTIR 88-3899, NIST, Gaithersburg, MD, USA, 1989.
- [96] W. Wang, B. Liu, V. Kodur, Effect of temperature on strength and elastic modulus of high-strength steel, *Journal of Materials in Civil Engineering*. 25 (2013) 174–182. [https://doi.org/10.1061/\(ASCE\)MT.1943-5533.0000600](https://doi.org/10.1061/(ASCE)MT.1943-5533.0000600).
- [97] W. Wang, K. Wang, V. Kodur, B. Wang, Mechanical properties of high-strength Q690 steel at elevated temperature, *Journal of Materials in Civil Engineering*. 30 (2018) 04018062. [https://doi.org/10.1061/\(ASCE\)MT.1943-5533.0002244](https://doi.org/10.1061/(ASCE)MT.1943-5533.0002244).
- [98] V. Kodur, A. Shakya, Effect of temperature on thermal properties of spray applied fire resistive materials, *Fire Safety Journal*. 61 (2013) 314–323. <https://doi.org/10.1016/j.firesaf.2013.09.011>.
- [99] A. Arablouei, V. Kodur, Modeling delamination of fire insulation from steel structures subjected to blast loading, *Engineering Structures*. 116 (2016) 56–69. <https://doi.org/10.1016/j.engstruct.2016.02.042>.
- [100] W.-Y. Wang, G.-Q. Li, V. Kodur, Approach for modeling fire insulation damage in steel columns, *Journal of Structural Engineering*. 139 (2013) 491–503. [https://doi.org/10.1061/\(ASCE\)ST.1943-541X.0000688](https://doi.org/10.1061/(ASCE)ST.1943-541X.0000688).
- [101] N.L. Braxtan, S.P. Pessiki, Postearthquake fire performance of sprayed fire-resistive material on steel moment frames, *Journal of Structural Engineering*. 137 (2011) 946–953. [https://doi.org/10.1061/\(ASCE\)ST.1943-541X.0000441](https://doi.org/10.1061/(ASCE)ST.1943-541X.0000441).
- [102] A. Arablouei, V. Kodur, Effect of fire insulation delamination on structural performance of steel structures during fire following an earthquake or an explosion, *Fire Safety Journal*. 84 (2016) 40–49. <https://doi.org/10.1016/j.firesaf.2016.07.001>.
- [103] AISC (American Institute of Steel Construction), *Steel construction manual*, 15th ed., AISC, Chicago, IL, USA, 2017.
- [104] B. Uy, M. Bradford, Local buckling of cold formed steel in composite structural elements at elevated temperatures, *Journal of Constructional Steel Research*. 34 (1995) 53–73. [https://doi.org/10.1016/0143-974X\(94\)00021-9](https://doi.org/10.1016/0143-974X(94)00021-9).
- [105] A. Heidarpour, M.A. Bradford, Local buckling and slenderness limits for steel webs under combined bending, compression and shear at elevated temperatures, *Thin-Walled Structures*. 46 (2008) 128–146. <https://doi.org/10.1016/j.tws.2007.08.014>.
- [106] ICC (International Code Council), *International Building Code, IBC 2021*, Country Club Hills, IL, USA, 2021. <https://codes.iccsafe.org/public/document/toc/542/> (accessed June 25, 2018).

- [107] NFPA (National Fire Protection Association), Building Construction and Safety Code, 2021st ed., NFPA 5000, Quincy, MA, USA, 2021.
- [108] UL (Underwriters Laboratories), Fire Tests of Building Construction and Materials, 14th ed., UL 263, Bensenville, IL, USA, 2011.
- [109] CEN (European Standards Committee), Eurocode 4: Design of composite steel and concrete structures – Part 1-2: General rules - Structural fire design, EN 1994-1-2, Brussels, Belgium, 2005.
- [110] UFC (Unified Facilities Criteria), Design of Buildings to Resist Progressive Collapse, With Change 3, UFC 4-023-03, Washington D.C., USA, 2016.
- [111] GSA (General Service Administration), Alternate Path Analysis & Design Guidelines for Progressive Collapse Resistance, U.S. General Services Administration, Washington D.C., USA, 2013.
- [112] M. Kobes, I. Helsloot, B. de Vries, J.G. Post, Building safety and human behaviour in fire: A literature review, *Fire Safety Journal*. 45 (2010) 1–11. <https://doi.org/10.1016/j.firesaf.2009.08.005>.
- [113] Thunderhead Engineering, Pathfinder 2018.3.0730 Version Technical Reference, Manhattan, KS, USA, 2018.
- [114] S.M.V. Gwynne, E.D. Kuligowski, M.J. Kinsey, L.M. Hulse, Modelling and influencing human behaviour in fire, *Fire and Materials*. 41 (2018) 412–430. <https://doi.org/10.1002/fam.2391>.
- [115] E. Ronchi, D. Nilsson, Fire evacuation in high-rise buildings: a review of human behaviour and modelling research, *Fire Science Reviews*. 2 (2013) 7. <https://doi.org/10.1186/2193-0414-2-7>.
- [116] Block 162, Floor Plans, Block 162. (2018). <http://www.block162.com/stacking-plan/> (accessed June 25, 2018).
- [117] Thunderhead Engineering, Pathfinder 2018.3.0730 Version Verification and Validation, Thunderhead Engineering, Manhattan, KS, USA, 2018.
- [118] E. Ronchi, P. Colonna, J. Capote, D. Alvear, N. Berloco, A. Cuesta, The evaluation of different evacuation models for assessing road tunnel safety analysis, *Tunnelling and Underground Space Technology*. 30 (2012) 74–84. <https://doi.org/10.1016/j.tust.2012.02.008>.
- [119] E. Ronchi, Testing the predictive capabilities of evacuation models for tunnel fire safety analysis, *Safety Science*. 59 (2013) 141–153. <https://doi.org/10.1016/j.ssci.2013.05.008>.

- [120] R. Lovreglio, E. Ronchi, G. Maragkos, T. Beji, B. Merci, A dynamic approach for the impact of a toxic gas dispersion hazard considering human behaviour and dispersion modelling, *Journal of Hazardous Materials*. 318 (2016) 758–771.  
<https://doi.org/10.1016/j.jhazmat.2016.06.015>.
- [121] NFPA (National Fire Protection Association), *Life Safety Code*, 2021st ed., NFPA 101, Quincy, MA, USA, 2021.
- [122] ASCE (American Society of Civil Engineers), *Minimum Design Loads and Associated Criteria for Buildings and Other Structures*, ASCE/SEI 7-16, New York, NY, USA, 2016.
- [123] SIMULIA User Assistance, *ABAQUS: Analysis*, Dassault Systèmes, Simulia Corporation, Providence, RI, USA, 2020.
- [124] Isolatek International, *CAFCO 300 HS ISOLATEK Type 300 HS*, (2020).  
<https://www.isolatek.com/construction/commercial-products/commercial-density/cafco-300-hs-isolatek-type-300-hs/> (accessed September 9, 2020).
- [125] CEN (European Standards Committee), *Eurocode 2-Design of Concrete Structures, Part 1-2: General Rules for Structural Fire Design*, EN 1992-1-2, Brussels, Belgium, 2004.
- [126] N. Torić, R.R. Sun, I.W. Burgess, Development of a creep-free stress-strain law for fire analysis of steel structures, *Fire and Materials*. 40 (2016) 896–912.  
<https://doi.org/10.1002/fam.2347>.
- [127] S. Venkatachari, V. Kodur, Effect of transient creep on fire induced instability in steel framed structures, *Journal of Constructional Steel Research*. 181 (2021) 106618.  
<https://doi.org/10.1016/j.jcsr.2021.106618>.
- [128] V. Kodur, S. Alogla, S. Venkatachari, Guidance for treatment of high-temperature creep in fire resistance analysis of concrete structures, *Fire Technology*. 57 (2021) 1167–1197.  
<https://doi.org/10.1007/s10694-020-01039-0>.
- [129] BSI (British Standards Institution), *Fire tests on building materials and structures – Part 20: Method for determination of the fire resistance of elements of construction (general principles)*, BS 476-20, London, UK, 1987.
- [130] E.M. Aziz, V.K. Kodur, J.D. Glassman, M.E.M. Garlock, Behavior of steel bridge girders under fire conditions, *Journal of Constructional Steel Research*. 106 (2015) 11–22.  
<https://doi.org/10.1016/j.jcsr.2014.12.001>.
- [131] X. Liang, Q. Shen, S.K. Ghosh, *Assessing ability of seismic structural systems to withstand progressive collapse: Design and progressive collapse analysis of steel braced frame buildings*, Report - S K Ghosh Associates, Inc., Palatine, IL, USA, 2006.

- [132] V. Kodur, M. Naser, P. Pakala, A. Varma, Modeling the response of composite beam–slab assemblies exposed to fire, *Journal of Constructional Steel Research*. 80 (2013) 163–173. <http://dx.doi.org/10.1016/j.jcsr.2012.09.005>.
- [133] J.D. Glassman, M.E.M. Garlock, E.M. Aziz, V.K. Kodur, Modeling parameters for predicting the postbuckling shear strength of steel plate girders, *Journal of Constructional Steel Research*. 121 (2016) 136–143. <https://doi.org/10.1016/j.jcsr.2016.01.004>.
- [134] A. Reis, N. Lopes, P.V. Real, Numerical study of steel plate girders under shear loading at elevated temperatures, *Journal of Constructional Steel Research*. 117 (2016) 1–12. <https://doi.org/10.1016/j.jcsr.2015.10.001>.
- [135] C. Couto, P.V. Real, N. Lopes, B. Zhao, Effective width method to account for the local buckling of steel thin plates at elevated temperatures, *Thin-Walled Structures*. 84 (2014) 134–149. <https://doi.org/10.1016/j.tws.2014.06.003>.
- [136] S.E. Quiel, M.E. Garlock, Calculating the buckling strength of steel plates exposed to fire, *Thin-Walled Structures*. 48 (2010) 684–695. <https://doi.org/10.1016/j.tws.2010.04.001>.
- [137] V. Kodur, M. Naser, Importance factor for design of bridges against fire hazard, *Engineering Structures*. 54 (2013) 207–220. <https://doi.org/10.1016/j.engstruct.2013.03.048>.
- [138] J.D. Flynn, Fire Service Performance Measures, Fire Analysis and Research Division, National Fire Protection Association, Quincy, MA, USA, 2009.
- [139] Reference Manual to Mitigate Potential Terrorist Attacks against Buildings, 2nd ed., BIPS 06/FEMA 426, Washington D.C., USA, 2011.